

AD A 122840



FRANK J. SEILER RESEARCH LABORATORY

FJSRL-TR-82-0004

SEPTEMBER 1982

**ELECTROCHEMICAL SURVEY OF
SELECTED CATIONS AND
ELECTRODE MATERIALS IN
DIALKYLIMIDAZOLIUM CHLORO-
ALUMINATE MELTS**

Bernard J. Piersma

John S. Wilkes

APPROVED FOR PUBLIC RELEASE;
DISTRIBUTION UNLIMITED.

PROJECT 2303

AIR FORCE SYSTEMS COMMAND

UNITED STATES AIR FORCE

82 12 27 046



FJSRL-TR-82-0004

This document was prepared by the Electrochemistry Division, Directorate of Chemical Sciences, Frank J. Seiler Research Laboratory, United States Air Force Academy, CO. The research was conducted under Project Work Unit number 2303-F2-10. John S. Wilkes was the project scientist.

When U.S. Government drawings, specifications or other data are used for any purpose other than a definitely related government procurement operation, the government thereby incurs no responsibility nor any obligation whatsoever, and the fact that the government may have formulated, furnished or in any way supplied the said drawings, specifications or other data is not to be regarded by implication or otherwise, as in any manner licensing the holder or any other person or corporation or conveying any rights or permission to manufacture, use or sell any patented invention that may in any way be related thereto.

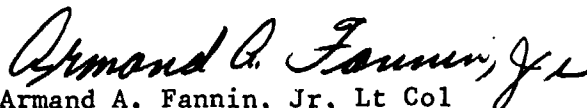
Inquiries concerning the technical content of this document should be addressed to the Frank J. Seiler Research Laboratory (AFSC), FJSRL/NC, USAF Academy, CO 80840. Phone AC 303 472-2655.

This report has been reviewed by the Commander and is releasable to the National Technical Information Service (NTIS). At NTIS it will be available to the general public, including foreign nations.

This technical report has been reviewed and is approved for publication.



John S. Wilkes
Project Scientist



Armand A. Fannin, Jr, Lt Col
Director, Chemical Sciences



William D. Siuru, Jr., Colonel
Commander

Copies of this report should not be returned unless return is required by security considerations, contractual obligations, or notice on a specific document.

Printed in the United States of America. Qualified requestors may obtain additional copies from the Defense Documentation Center. All others should apply to:

National Technical Information Service
6285 Port Royal Road
Springfield, Virginia 22161

SECURITY CLASSIFICATION OF THIS PAGE (When Data Entered)

REPORT DOCUMENTATION PAGE		READ INSTRUCTIONS BEFORE COMPLETING FORM
1. REPORT NUMBER FJSRL-TR-82-0004	2. GOVT ACCESSION NO. ADA122840	3. RECIPIENT'S CATALOG NUMBER
4. TITLE (and Subtitle) Electrochemical Survey of Selected Cations and Electrode Materials in Dialkylimidazolium Chloroaluminate Melts		5. TYPE OF REPORT & PERIOD COVERED Interim, 9/81 - 2/82
		6. PERFORMING ORG. REPORT NUMBER FJSRL-TR-82-0004
7. AUTHOR(s) Dr. Bernard J. Piersma Dr. John S. Wilkes		8. CONTRACT OR GRANT NUMBER(S)
9. PERFORMING ORGANIZATION NAME AND ADDRESS Frank J. Seiler Research Laboratory (AFSC) FJSRL/NC USAF Academy, CO 80840		10. PROGRAM ELEMENT, PROJECT, TASK AREA & WORK UNIT NUMBERS 2303-F2-10
11. CONTROLLING OFFICE NAME AND ADDRESS Frank J. Seiler Research Laboratory (AFSC) FJSRL/NC USAF Academy, CO 80840		12. REPORT DATE September 1982
		13. NUMBER OF PAGES 137
14. MONITORING AGENCY NAME & ADDRESS (if different from Controlling Office)		15. SECURITY CLASS. (of this report) UNCLASSIFIED
		15a. DECLASSIFICATION/DOWNGRADING SCHEDULE
16. DISTRIBUTION STATEMENT (of this Report) Approved for public release; distribution unlimited.		
17. DISTRIBUTION STATEMENT (of the abstract entered in Block 20, if different from Report)		
18. SUPPLEMENTARY NOTES		
19. KEY WORDS (Continue on reverse side if necessary and identify by block number) room temperature molten salts dialkylimidazolium chloroaluminate electrochemistry		
20. ABSTRACT (Continue on reverse side if necessary and identify by block number) Room temperature chloroaluminate melts of 7 dialkylimidazolium chlorides were prepared and studied using cyclic voltammetry in basic (excess organic) and acidic (excess $AlCl_3$) regions. 1-methyl-3-ethyl imidazolium chloride was selected for further electrochemical studies. Twenty-one electrode materials were studied for stability in the melts. Initial studies were performed to identify and characterize the redox and metal deposition behaviors of 25 cations (primarily chloride salts of transition metal ions).		

**ELECTROCHEMICAL SURVEY OF SELECTED CATIONS AND ELECTRODE MATERIALS
IN DIALKYLIMIDAZOLIUM CHLOROALUMINATE MELTS**

By

B. J. Piersma

J. S. Wilkes

Accession for	
NTIS GRA&I	<input checked="" type="checkbox"/>
DTIC TAB	<input type="checkbox"/>
Unannounced	<input type="checkbox"/>
Justification	
By	
Distribution	
Avail. and/or	
Special	
Dist.	SA-100

A

SEPTEMBER 1982

Approved for public release; distribution unlimited.

Directorate of Chemical Sciences
The Frank J. Seiler Research Laboratory
Air Force Systems Command



TABLE OF CONTENTS

Summary.	ii
Preface.	iii
Introduction	1
Experimental	1
Results and Discussions.	3
Conclusions.	18
References	20
Tables	21
Abbreviations and Symbols.	41
Illustrations.	42

SUMMARY

Room temperature chloroaluminate melts of 7 dialkylimidazolium chlorides were prepared and studied using cyclic voltammetry in basic (excess organic) and acidic (excess AlCl_3) regions. 1-methyl-3-ethylimidazolium chloride was selected for further electrochemical studies. Twenty-one electrode materials were studied for stability in the melts. Initial studies were performed to identify and characterize the redox and metal deposition behavior of 25 cations (primarily chloride salts of transition metal ions).

PREFACE

The work described in this report is part of the research performed in the Electrochemistry Task at FJSRL by Dr. Piersma, a visiting professor from Houghton College, Houghton, New York, under the University Resident Research Program of the Air Force Office of Scientific Research.

INTRODUCTION

Room temperature (20°C) melts of 1,3-dialkylimidazolium chlorides with aluminum chloride were recently discovered in this laboratory⁽¹⁾. Their relatively wide electrochemical windows (about 2.5 V), high conductivities (equivalent to the best non-aqueous electrolyte systems at similar temperatures) and wide range of Lewis acidity make these melts of particular interest as electrolytes for high energy density batteries. This report summarizes our preliminary electrochemical studies of 7 melt systems and the examination of 21 electrode materials with initial work in identifying and characterizing redox behavior of 25 cations in 1-methyl-3-ethylimidazolium chloroaluminate melts. The purpose of the survey was to screen candidates for cathodes that could be used in secondary battery cells employing the new low melting molten salts.

EXPERIMENTAL

Aluminum chloride (Fluka AG) was purified and the dialkylimidazolium chlorides were synthesized and recrystallized following procedures established in this laboratory⁽¹⁾. All melts were prepared by slowly adding AlCl_3 to the dialkylimidazolium chloride. Melts were made and all experiments performed under a dry argon atmosphere in a Vacuum Atmospheres Corp. controlled environment system. Cations were, in most cases, added as chloride salts (Alfa Products) without further purification. TiCl_4 was vacuum distilled to remove TiOCl_2 . Oxychloride was removed from MoCl_5 by heating the salt, inside the dry box, for 2 weeks at 80°C. Titrations of the melts with TiCl_4 following the method of Osteryoung, et. al.⁽²⁾ indicated oxide levels on the order of 3-5 mM with a maximum of 5 mM oxide in our melts.

Pure metal electrodes were made by coiling wires (approx. 26 gauge) in the dry box after they had been polished with silicon carbide paper (various grades). A PAR/EGG hanging drop electrode was used as the Hg electrode.

Pt-group-metal alloys of Ti and Ta (Materials Research Corp) were sealed in teflon and the ends polished inside the dry box with silicon carbide paper. A polished glassy carbon disk sealed in pyrex glass (geometric area 0.196 cm^2) was used for comparative cyclic voltammetric studies. A W rod, 0.071 cm^2 geometric cross-sectional area was sealed in glass and polished for the studies of W. Other electrochemical analyses were made with a Pine Instrument Co. glassy carbon rotating disk electrode (geometric area = 0.459 cm^2). The temperature was $25 \pm 1 \text{ }^\circ\text{C}$ unless otherwise indicated.

A simple, single-compartment pyrex glass cell (35 mm i.d. x 75 mm high) with a teflon cover, containing a large (7.5 cm^2 geometric area) W foil electrode as counter electrode, was used for CV (cyclic voltammetric) studies. Sweep rates were 50 mV/sec unless otherwise stated. In the figures, where the initial point and sweep direction is not obvious, they are indicated by an "X" and arrow respectively. Other electrochemical measurements were performed in a two-compartment pyrex glass cell with the anode and cathode compartments separated by a fine porosity glass frit. The reference electrode for all measurements was a coiled Al wire (Alfa) immersed in 0.6 MeEtImCl (methylethylimidazolium chloride) melt contained in a separate pyrex glass tube (11 mm i.d.) with a fine porosity glass frit. Al wires were cleaned in aqueous 5% HF/15% HNO_3 for 5 seconds (to remove oxide) and rinsed with absolute ethanol just prior to being placed in the dry box.

A PAR/EGG model 173 potentiostat was used with a PAR/EGG model 165 universal programmer and a Houston Omnigraphic model 2000 X-Y recorder for CV measurements. Dana model 5900 digital multimeters were used to measure potential and current, and a Hewlet Packard model 7100 BM strip chart recorder was used to record steady-state currents. A Pine Instrument Co. electrode rotator was used for RDE (rotating disk electrode) studies. Steady state currents were measured at a rotation rate of 1000 RPM. A PAR/EGG model 174A polarographic analyzer was used for analyses of melts for oxides by titration with TiCl_4 .

After a series of measurements with a given melt system was completed, the cell and electrodes were removed from the dry box and thoroughly rinsed with distilled H_2O (approx. 30 rinses). All glassware and W electrodes were then placed in a drying oven for a minimum of 12 hours before being returned to the dry box. The glassy carbon electrodes were wiped dry with Kimwipes and returned to the dry box. In the CV survey of cations, a given salt was dissolved in basic melt (mole fraction $AlCl_3 = 0.40$, denoted "0.4 melt" hereafter), CV scans run, and then $AlCl_3$ was added to the system to give 0.6 melt (mole fraction $AlCl_3 = 0.60$, denoted "0.6 melt" hereafter). Following the CV studies in acidic melt, the cell and electrodes were removed from the dry box and cleaned. When the CV current peak heights changed with cycling, a situation occasionally observed (particularly in basic melts), results are reported for the initial cycle. In these cases, the working electrode was removed from the cell and cleaned with a Kimwipe for each measurement. This allowed good reproducibility in peak currents and peak potentials.

RESULTS AND DISCUSSION

Electrochemical Windows

Seven melt systems were surveyed using cyclic voltammetry and the results for electrochemical windows are summarized in Table I. The electrochemical window is arbitrarily defined as the potential range for which the current, measured at a sweep rate $v = 50$ mV/sec, is less than or equal to $5 \mu A$ on the glassy carbon electrode ($A = 0.196$ cm²). Figures 1-7 permit comparisons of the CV behavior in the different melts. We observe that the 1,3-diBuImCl chloroaluminate melt exhibited the widest electrochemical window of the melts studied. The results are easily compared from the following:

Electrochemical Windows

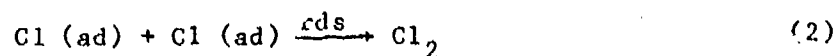
Organic Chloride	0.4 (basic) Melt	0.6 (acidic) Melt
1,3-diMeImCl	2.65V	2.44V
1,3-MeEtImCl	2.57	2.40
1,3-MePrImCl	2.70	2.60
1,3-MeBuImCl	2.60	2.53
1,3-diBuImCl	2.82	2.65
1,2,3-tri MeImCl	-	2.30
1,2-diMe-3-EtImCl	2.30	2.19

(See Table I for explanations)

Except for minor differences in the CV's, which are likely due to impurities formed during syntheses of the organic species, the processes which limit the electrochemical windows in the different melt systems appear to be similar.

The melts having the 1-methyl-3-ethylimidazolium cation appear to behave typically of the series of imidazolium-based melts. However, the MeEtIm melts had the most favorable combination of physical properties and ease of preparation, so most further studies were done in the MeEtIm system. All experiments in this report were done in MeEtIm melts except those measurements of potential windows described above. In the basic melts, the anodic limit is oxidation of Cl^- . Fig. 8 demonstrates that as the anodic potential limit is increased, the reduction peak on the reverse sweep (between 0.3 and 0.6 V) gets larger. The effect of changing the sweep rate, when the anodic limit is held constant at 1.5 V, is seen in Fig. 9. From Fig. 10, in which the cathodic sweep is held for 15 sec at different potentials after an anodic sweep to 1.5 V, we conclude that oxidation of the melt occurs at potentials greater than about +1.0 V. When the cathodic sweep is held at 1.05 V (where no appreciable oxidation or reduction occurs) for varying times (Fig. 11) after

an anodic sweep to 1.50 V, we observe the diffusion of chlorine away from the electrode. A linear plot of $i_{p,c}$ for chlorine reduction vs $t^{-1/2}$, for the data derived from Fig. 11 (cf. Fig. 12) suggests that at moderate sweep rates the current is controlled by linear diffusion of Cl_2 away from the electrode. Steady state potentiostatic measurements on the anodic process at a glassy carbon RDE (1000 RPM) in 0.4 melt give a good Tafel slope over three orders of magnitude of current (Fig. 13), with the limiting anodic process being kinetic, not diffusion, controlled. The Tafel slope of RT/F is consistent with the following process for Cl^- oxidation:



Thus, at least on glassy carbon, combination of chlorine atoms on the electrode surface appears to be the rate limiting step at the anodic limit of the melts studied.

The quantity of chlorine that can be reduced in a cathodic sweep is controlled by diffusion of Cl_2 away from the electrode. From Fig. 12, we see that linear diffusion conditions hold for up to about 200 sec. From CV measurements on Cl_2 reduction, we note that only one reduction peak is observed and $(dE_{p,c} / d \log i_{p,c}) = -0.52V$ which implies mixed kinetic and diffusion control.

The cathodic limit in basic melts is determined by reduction of the indazolium ion. Variation in the cathodic limit of the several melt systems may indicate that the ring substituents have some influence on the reduction potential. We should note that a reduction process actually begins about 0.5V before the melt limit and the product of reduction remains on the electrode. Reoxidation of the cathodic product occurs at about +0.4V and the current for that oxidation increases as the cathodic limit is extended. Further identification of the limiting cathodic process in basic melt has not been done.

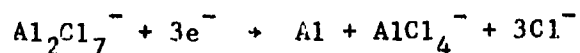
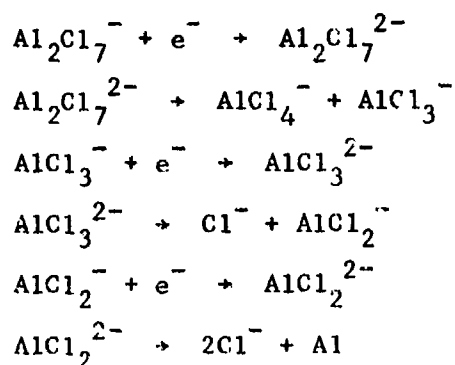
In acidic melts, the cathodic limit is determined by Al deposition. Repeated cycling at the cathodic limit (Fig. 15) results in some Al remaining on the electrode. Under the proper conditions, e.g., after several cycles in Fig. 15, three steps can be distinguished in the reoxidation of the deposited Al, perhaps relating to the three electron transfers necessary, i.e.,



Steady state potentiostatic measurements in 0.6 MeEtImCl melt at glassy C are represented in Fig. 16. The Tafel region beginning at -1.9V has a slope of $-2RT/F$, suggesting that for Al^{3+} reduction, the first electron transfer is the rate limiting step, thus:



A second Tafel region, with a slope of $-RT/F$, is observed between -0.9V and -1.1V. This process has not been identified and is not apparent from the cyclic voltammograms. It may be related to reduction of the dialkylimidazolium ion, however, no anodic process connected with such a reduction is observed in acidic melts. We conclude that Al deposition is the primary reduction process in acidic melts and the electrochemical-window-limiting process. A reasonable mechanism for the reduction of Al_2Cl_7^- to Al is:



The limiting anodic process in acidic melts has not been determined. No reducible chlorine can be observed from oxidation at the anodic limit in

acidic melts. The variation in anodic limits for the different melts and the lack of evidence of chlorine reduction lead us to favor oxidation of the dialkylimidazolium ion as the electrochemical-window-limiting process at the anodic limit in acidic melts.

Electrochemical Windows in Ternary Melts

Several organic solvents were added to MeEtImCl melts in order to modify physical properties (viscosity and conductivity). These ternary melts were screened using CV and the results are seen in Figs. 17-21, and summarized in Table II. Nitrobenzene and nitromethane are reduced about one volt anodic to the cathodic melt limit. *m*-Xylene appears unreactive in basic melt, but is reduced in acidic melt about 0.2V anodic to Al deposition. Acetonitrile is reduced in basic melt about 0.2V anodic to the cathodic limit. Propionitrile is unreactive in the melts and in acidic melt appears to increase the overpotential for Al deposition by nearly half a volt. The alkylnitriles give a two-phase system in acidic melt in the range 5% < [alkylnitrile] < 50% (w/w).

Stability of Electrode Materials

Twenty-one electrode materials (selected partly on the basis of availability) were surveyed using CV in 0.4 (basic) and 0.6 (acidic) MeEtImCl melts. The open circuit potentials and approximate electrochemical windows are summarized in Tables III and IV. Representative voltammograms are presented in Figs. 22-43. As expected, electrodes which have lower electrocatalytic activity tend to have wider electrochemical windows. In the following we shall briefly point out significant features of the voltammograms for the materials studied.

Silver (Fig. 22)

Anodic dissolution of silver occurs at open circuit in both basic and acidic melts, and is the limiting anodic process. The limiting cathodic process in acidic melt appears to be reduction of the MeEtIm ion, rather than

aluminum deposition.

Aluminum (Fig. 23)

Dissolution of Al occurs at open circuit in both basic and acidic melts and is the limiting anodic process. Al has a window of about 1.00V in basic melt, before reduction of the MeEtIm ion occurs. In acidic melts, Al dissolution and deposition are in equilibrium.

Copper (Fig. 24)

Copper dissolution occurs at open circuit in both basic and acidic melts. A limiting cathodic process occurs at Cu in acidic melt before Al deposition.

Iron (Fig. 25)

Iron dissolution occurs at open circuit in both basic and acidic melts. The limiting cathodic process in acidic melt occurs prior to Al deposition.

Nickel (Fig. 26)

Nickel dissolution occurs at open circuit in both basic and acidic melts as the limiting anodic process. Reduction of the MeEtIm ion occurs about 0.2V anodic to Al deposition in acidic melt on Ni.

Lead (Fig. 27)

As with most of the materials, dissolution of lead occurs in both basic and acidic melts as the limiting anodic process. In acidic melt, there is no evidence of Al deposition on lead.

Platinum (Fig. 29)

In basic melt, the limiting anodic process is oxidation of Cl^- to produce Cl_2 . The open circuit in basic melt is approximately the cathodic limit. In acidic melt, there is reduction of the MeEtIm ion about 0.6V anodic to Al deposition on Pt. The processes occurring at the cathodic limits of both melts merit further study.

Tantalum (Fig. 30)

Al deposition is apparent in acidic melt for the first cycle on Ta, however, no peak for reoxidation of Al is observed and successive sweeps show

large cathodic currents anodic to Al deposition.

Tantalum/Platinum Group Metal Alloys (Figs. 30-32)

Ta/20% Ru has the widest electrochemical window for any of the electrodes examined in basic melt. The behavior at both anodic and cathodic limits shows a gradual increase in current, not the marked increase that characterizes the limits at most other electrodes. In acidic melts, the alloys show cathodic behavior similar to Ta, i.e., Al deposition is evident only on the first potential cycle and not on successive cycles.

Titanium/Platinum Group Metal Alloys (Figs. 33-39)

There appears to be significant dissolution of all the Ti alloys in both basic and acidic melts. The dissolution process appears to increase significantly as the amount of Pt in the Ti/Pt alloys is increased. For all the Ti alloys studied in acidic melt, Al deposition is observed only at Ti/5% Pt.

Tungsten (Figs. 40 and 41)

The anodic limit on tungsten in basic melt is chlorine evolution. In acidic melt, tungsten has the widest electrochemical window of the electrode materials studied. The limiting cathodic process in acidic melt is Al deposition, with essentially reversible reoxidation of the Al deposit on the anodic sweep.

Gold (Fig. 42)

The overpotential for chlorine evolution in basic melt appears to be reduced by about 0.5V on Au. A limiting cathodic process in acidic melt occurs about 0.7V anodic to Al deposition. The open circuit in acidic melt occurs near the anodic limit which is probably dissolution of the Au electrode.

Mercury (Fig. 43)

Dissolution of Hg occurs at open circuit in both basic and acidic melts. Two reduction peaks following the anodic limit suggest that Hg is oxidized to the Hg²⁺ state.

The electrode materials which give the widest electrochemical windows are most suitable for further studies in these melt systems. The three materials with the widest windows are summarized as follows:

ELECTROCHEMICAL WINDOW

ELECTRODE	0.4 MELT	0.6 MELT
Glassy carbon	2.60V	2.40V
Tungsten	1.70	2.48
Ta/20% Ru	2.95	2.40

CV Analyses of Cations

To select cations that would undergo suitable redox reactions as battery cathodes, we used cyclic voltammetry to survey a variety of transition metal salts. The following results are all for MeEtImCl melts using a polished glassy carbon working electrode. We have studied the chloride salts of 22 cations, plus sulfur, CrO_3 , $\text{K}_2\text{Cr}_2\text{O}_7$ and ferrocene. The open circuit potentials are summarized in Table V for melts containing approximately 30 mM concentration for each species. Table VI reports the colors generated by the various species in basic and acidic melts. Some observations relating to colors in the melts are relevant:

(a) All of the species examined were soluble in basic melts while four salts, AgCl , PbCl_2 , SnCl_2 and ZnCl_2 were insoluble in acidic melts. These four salts became insoluble (white precipitates) at or near the neutral melt composition. In basic melts, with excess chloride ions, the cations probably are present as chloride complexes, e.g., FeCl_4^- , thus explaining the solubilities of all the salts studied. In acidic melts which have no free chloride ions, the chloride salts of Ag^+ , Pb^{2+} , Sn^{2+} and Zn^{2+} become insoluble. It has been reported that anodic dissolution of these metals in acidic melts results in soluble species.⁽³⁾

(b) In several instances, notably with Cu^{2+} , Fe^{3+} , the several molybdenum species, S_2Cl_2 , W^{6+} and ferrocene, species which were lightly

colored in basic melts turned very dark in acidic melts. For these cases, we have observed chemical reaction of the cation with the acidic melt (e.g., we noted a decrease of the reduction current peak with time). Kinetic studies (following the change in limiting cathodic current at a RDE with time) for Fe^{3+} and Cu^{2+} indicate that the reaction is 2nd order in the cation. The 2nd order rate constant for Fe^{3+} at 30°C is $k \sim 5.9 \times 10^{-5}$ L/mole-sec, and for Cu^{2+} is 5.1×10^{-4} l/mole sec.

(c) Ti^{4+} was an exception, being bright yellow in basic melt but colorless in acidic melt.

(d) Cr^{3+} in acidic melts and Ta^{5+} in basic melts and acidic melts gave cloudy solutions which may indicate a reaction with the melt.

(e) Ferrocene appears, in some respects, to be unaffected by change in chloride ion concentration, e.g., identical open circuit potentials and identical peak potentials for oxidation and reduction are obtained in basic and acidic melts, yet gives a pronounced color change in going from basic to acidic melt. We also observed chemical reaction of ferrocene with both basic and acidic melts.

The CV responses of the 26 species studied are illustrated in Figs. 44-82. Parameters obtained from CV studies with variation of sweep rates from 1-500 mV/sec are tabulated in Table VII for basic melt and Table VIII for acidic melt. It should be noted that these parameters are derived from our survey studies and should be used in that light, i.e., as suggestive since the results are for only one concentration of each species in a single melt composition at glassy carbon and for only one temperature. The terms used in Tables VII and VIII are defined as follows:

$$E_{p/2} = (E_{p,a} + E_{p,c})/2$$

where $E_{p,a}$ is the potential at the anodic current peak maximum and $E_{p,c}$ is the potential at the cathodic current peak maximum. When multiple peaks are present (particularly in acidic melts) $E_{p/2}$ is given for the most

anodic redox couple. In general, $E_p/2$ was found to be independent of potential sweep rate (v).

$$\Delta E_p = E_{p,a} - E_{p,c}$$

$$= \frac{59}{n} \text{ mV for a reversible process}$$

The values reported are for $v = 50$ mV/sec.

$E_{dep.}$

The potential, at $v = 50$ mV/sec, at which deposition of metal by reduction of the cation begins.

$E_{reoxid.}$

The potential, at $v = 50$ mV/sec, at the anodic current maximum for reoxidation of deposited metal, after the cathodic sweep is reversed.

$E_{Al reoxid.}$

The potential, at $v = 50$ mV/sec, at the anodic current maximum for reoxidation of Al (which was deposited on the cathodic sweep), after the cathodic sweep is reversed.

$i_{p,a}$

The current (in μ amps) at the maximum of the anodic current peak.

$i_{p,c}$

The current (in μ amps) at the maximum of the cathodic current peak.

$$\frac{d(E_p/2 - E_p)}{d \log i}$$

$$= \frac{2.3RT}{\alpha F} \text{ if the process is kinetically controlled.}$$

$$\frac{i_{p,a}}{i_{p,c}}$$

equal to unity and independent of v for reversible processes.

$$\frac{dE_p}{d \log v}$$

$$= \frac{30}{\alpha n} \text{ if the process is kinetically controlled}$$

$$\frac{d\left(\frac{i_{p,a}}{i_{p,c}}\right)}{dv}$$

>0 suggests that a chemical reaction precedes a reversible charge transfer.

$$\frac{d\left(\frac{i_{p,a}}{i_{p,c}}\right)}{dv}$$

<0 suggests that a chemical reaction follows areversible charge transfer.

Discussion of Cyclic Voltammograms

Silver (Fig. 44)

In basic melts, Ag^+ (present as a chloride complex) is reduced and deposited on the glassy C cathode at -0.90V . The Ag is reoxidized at $+0.12\text{V}$. AgCl is insoluble in acidic melt.

Cobalt (Fig. 45)

Co^{2+} exhibits no electrochemical activity in basic melt. In acidic melt, cobalt deposition begins at 0.48V . Apparently the overpotential for Al deposition is lowered by about 0.35V on the deposited Co.

Chromium (Figs. 46-48)

The behavior of CrO_3 and $\text{K}_2\text{Cr}_2\text{O}_7$ are essentially the same, and very different from the CV behavior of Cr^{3+} . In acidic melt, no electrochemical processes are observed for Cr^{3+} . In basic melt, Cr^{3+} exhibits two irreversible reductions and two oxidation peaks are observed on the reverse sweep. For CrO_3 and $\text{K}_2\text{Cr}_2\text{O}_7$, one very large reduction peak is observed with no subsequent oxidation. Metal deposition (assumed to be chromium) is also observed in basic melt with both CrO_3 and $\text{K}_2\text{Cr}_2\text{O}_7$ and again, no subsequent oxidation is seen. In acidic melt the voltammograms are more complicated with 5 reduction peaks and 4 oxidation peaks in addition to the usual processes at the melt limits.

Copper (Figs. 49 and 50)

Cu^{2+} has an apparently quasi-reversible oxidation-reduction couple in both basic and acidic melts and copper deposition is observed in both basic and acidic melts. As previously mentioned, Cu^{2+} is observed to chemically react with the acidic melt. The second order rate constant for this process is $k \sim 5 \times 10^{-4}$ L/mole sec. Cu^{2+} has been studied in more detail and the results are presented in another report.

Iron (Figs. 51-54)

In basic melt iron (both Fe^{2+} and Fe^{3+}) has a quasi-reversible redox

couple. As expected, Fe^{2+} has essentially no reduction until after oxidation and Fe^{3+} has essentially no oxidation until after reduction. No iron deposition is observed in basic melts. In acidic melts a pronounced irreversibility is observed in the redox behavior of both Fe^{2+} and Fe^{3+} . Iron is co-deposited from acidic melts with Al at the cathodic melt limit. Fe^{3+} reacts chemically with acidic melt and the second order rate constant at 30°C is $k \sim 6 \times 10^{-5}$ L/mole sec. The chemical reaction in which the cation is reduced by the melt appears to be similar for Cu^{2+} and Fe^{3+} (i.e., both are 2nd order). More detailed studies of Fe^{3+} are presented in another report.

Ferrocene (Figs. 55 and 56)

Ferrocene is the only species which has the same open circuit potentials and same $E_{p/2}$ in basic and acidic melts, suggesting that ferrocene is not complexed with Cl^- in basic melt. The redox process for ferrocene is reversible and the same peak potentials are observed in basic and acidic melts. Ferrocene reacts chemically in both basic and acidic melts. In basic melt, ferrocene is oxidized and a reduction peak at -0.87V (which shows no subsequent oxidation) appears and increases with time (cf. Fig. 56a). In acidic melt, ferrocene is chemically reduced and an oxidation peak at $+0.82\text{V}$ (no subsequent reduction is observed) develops with time (cf. Fig. 56b).

Mercury (Figs. 57-58)

In basic melt, Hg^{2+} undergoes cathodic deposition at -1.4V . The reoxidation of the deposited Hg has a large overpotential and two oxidation steps can be observed, with anodic peaks at -0.22V and 0.19V . In acidic melt, Hg^{2+} is reduced stepwise, with cathodic peaks evident at about 0.96V and 0.72V . Reduction of Hg^{2+} does not appear to follow the usual deposition behavior. The reduced Hg is oxidized in a single observable step at about 1.13V . Al deposition in acidic melt has a slightly lower overpotential (about 50mV less) on the mercury deposit, but reoxidation of Al occurs at about 0.1V

more cathodic than in acidic melt in the absence of Hg^{2+} .

Lithium (Fig. 59)

In basic melt no reduction is observed until the cathodic limit of the melt, however, the process at the limit does not appear to be the same as in the melt alone. On the anodic sweep there is a small oxidation peak at -0.75V . In acidic melt there appears to be co-deposition of Li with Al.

Manganese (Fig. 60)

In basic melt, Mn^{2+} has an irreversible cathodic peak at -1.53V , and an anodic peak at 0.46V . In acidic melt, Mn co-deposition occurs with Al. The overpotential for reoxidation of Al is significantly increased in the presence of manganese.

Molybdenum (Fig. 61-70)

In basic melt, the 5 molybdenum species studied (Mo^{3+} , Mo^{4+} , Mo^{5+} , MoO_2Cl_2 and $[\text{Et}_4\text{N}][\text{MoCl}_6]$) all exhibit perhaps quasi-irreversible redox couple with an average $E_{p/2} = 0.32 \pm 0.05\text{V}$. The large irreversible cathodic peak at about -0.55V has been clearly shown to be the oxychloride impurity in the molybdenum compounds (cf. Fig. 65 for example). The irreversible cathodic peak disappears when the Mo salt is heated at 80°C to remove the volatile oxychloride. The material collected from the sublimation process produces the -0.55V peak when added to the melt. In MoO_2Cl_2 , the reversible redox couple is observed only after the oxychloride is reduced (see Fig. 67). With the Mo^{3+} , reduction (in the redox couple) is observed only after oxidation. The similarities observed suggest that the redox couple involves the Mo^{4+} to Mo^{3+} process, with Mo^{5+} being reduced to Mo^{4+} by the melt.

In acidic melt the electrochemistry is much more complicated. The irreversible oxychloride reduction peak at about 1.1V is obvious in all the salts except the MoCl_5 salt specifically treated to remove the oxychloride. In general the redox couple (except for the MoO_2Cl_2) consists of two cathodic peaks and two anodic peaks in acidic melt. Further detail can be observed in

the voltammograms depending on sweep rate and sweep limits, and these are tabulated in Table IX for acidic melt. Molybdenum compounds provide an interesting area for further study, particularly since the $E_{p/2}$ for Mo^{5+} is close to the anodic melt limit in acidic melt.

Nickel (Fig. 71)

No electrochemical behavior is observed for Ni^{2+} in basic melt. Ni^{2+} is electrodeposited from acidic melt at about 0.64V and it appears that the overpotential for Al deposition is reduced by about 0.6V on the deposited Ni surface.

Lead (Fig. 72)

Lead chloride is insoluble in acidic melt. In basic melt, Pb^{2+} undergoes electrodeposition beginning at about -1.1V. The reduction is stepwise since, under the right sweep conditions, two cathodic peaks can be observed.

Sulfur (Figs. 73-76)

We examined 3 sulfur species, elemental sulfur, S_2Cl_2 and Na_2S in 0.4, 0.5, and 0.6 melts. No electrochemical activity was observed for Na_2S in any of the melts due to the lack of solubility of Na_2S . Sulfur and S_2Cl_2 gave very similar CV behavior, that is, in 0.4 (basic) melt they show irreversible reduction with no oxidation. In 0.6 melt, they both exhibit apparently the same redox couple, which is also irreversible. A significant observation in acidic melt is that Al deposition occurs at about -0.4V in the presence of sulfur or S_2Cl_2 , i.e., nearly 300 mV cathodic to Al deposition in the pure melt. Thus it appears that the sulfur species on the electrode increases the overpotential for Al deposition by about 300 mV, hence extending the melt limit by about 300 mV. In neutral (0.5) melt, an additional cathodic process is observed with S_2Cl_2 and an additional anodic process is observed with sulfur.

Tin (Fig. 77)

$SnCl_2$ is insoluble in acidic melt. Sn^{2+} has a quasi-reversible redox

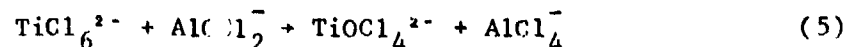
couple with $E_{p/2} = -0.86V$ and a large irreversible anodic peak at about $+0.50V$ in basic melt.

Tantalum (Fig. 78)

In basic melt, Ta^{5+} has a quasi-reversible redox couple with $E_{p/2} = -0.31V$. A large irreversible reduction begins at about $-1.4V$ and may be associated with an oxychloride impurity, however, this has not been established. In acidic melt, the quasi-reversible redox couple is missing. Ta appears to be co-deposited with Al.

Titanium (Figs. 79 and 80)

A quasi-reversible redox couple is obtained with Ti^{4+} in basic melt with $E_{p/2} = -0.12V$. A second cathodic peak, due to irreversible $TiOCl_2$ reduction is observed at $-0.6V$. The $TiOCl_2$ peak increases with time due to reaction of oxychloride impurity in the melt with Ti^{4+} .



To estimate the amount of Ti^{4+} present in our $TiCl_4$ as $TiOCl_2$ we ran a CV in DMF and the results are shown in Fig. 80. Assuming that the DMF contained no oxide which could react with $TiCl_4$, we estimate the amount of $TiOCl_2$ in the sample as nearly 50%.

In acidic melt the CV behavior is more complex and, in fact, not well reproducible.

Tungsten (Fig. 81)

In basic melt W^{6+} has a reversible redox couple with $E_{p/2} \sim 0.625$, which is the most anodic couple observed in basic melt for all the species studied. A second, irreversible cathodic peak, likely due to reduction of oxychloride impurity is seen at about $-0.68V$. There appears to be some oxidation of the product from reduction of the (assumed) oxychloride. In acidic melt the CV for W^{6+} is very complex with no evident reversible redox behavior and 5 cathodic peaks in addition to Al deposition with W co-deposition and 10 anodic peaks in addition to the anodic melt limit. Detailed studies of

W⁶⁺ are being continued, especially for basic and neutral melt.

Zinc (Fig. 85)

ZnCl₂ is insoluble in acidic melt. Zn²⁺ shows no electrochemical CV behavior in basic melt.

CONCLUSIONS

Based on our cyclic voltammetric studies and other physical properties, specifically melting point, conductivity and viscosity (which are not discussed in this report), 1-methyl-3-ethylimidazolium chloride was selected as the best dialkylimidazolium chloride for detailed analyses in chloroaluminate melts. Of the electrode materials studied in the melt, 3 electrodes, glassy carbon, tungsten and tantalum/20% ruthenium all y gave the widest electrochemical windows. In selecting cations that may be useful as battery cathode reactions, we can initially examine the E_{p/2} values which are summarized as follows:

Relative E _{p/2} Values			
Species	0.4 (basic) melt	Species	0.6 (acidic) melt
anodic limit	+1.00V	anodic limit	+2.35V
W ⁶⁺	0.62	Fe ³⁺	2.22
Mo ⁵⁺	0.31	Mo ⁵⁺	2.07
Fe ³⁺	0.30	Cu ²⁺	1.98
Cu ²⁺	0.24	Sulfur	1.75
Ti ⁴⁺	-0.11	S ₂ Cl ₂	1.68
Ta ⁵⁺	-0.31	W ⁶⁺	1.62
Cr ³⁺	-0.58	Ti ⁴⁺	1.07
Sn ²⁺	-0.86	Ta ⁵⁺	0.77

For the purpose of comparison the relative E_{p/2} values in the melts are similar to E° values in aqueous solutions. For the cations studied, Fe³⁺ gives the most anodic redox behavior in acidic melt and W⁶⁺ gives the most anodic redox behavior in basic melt. The parameters derived from cyclic voltammetric studies of the cations are useful but should not be used without

other supporting data for mechanism interpretation, hence we did not include mechanism discussions in this report. We are extending the electrochemical studies for selected ions, namely Fe^{3+} , Cu^{2+} , W^{6+} and sulfur, using steady state potentiostatic and other techniques and these will be presented in future reports.

REFERENCES

1. Wilkes, J. S.; Levisky, J. A.; Wilson, R. A.; Passey, C. L., Inorg. Chem., 1982, 21, 1263 .
2. Stojek, Z.; Linga, H.; Osteryoung, R. A., J. Electroanal. Chem. 1981, 119, 365.
3. Hussey, C. L., private communication.

TABLE I

ELECTROCHEMICAL WINDOWS* OF DIAALKYLIMIDAZOLIUM CHLOROALUMINATE MELTS

IMIDAZOLIUM CHLORIDE	BASIC MELT (0.4)	ACIDIC MELT (0.6)
1,3-Dimethyl ⁽¹⁾	0.90 to -1.75 V	2.40 to -0.04 V
1-Methyl-3-Ethyl	0.97 to -1.60	2.35 to -0.05
1-Methyl-3-Propyl	1.00 to -1.70	2.40 to -0.20
1-Methyl-3-Butyl	1.00 to -1.60	2.45 to -0.08
1,3-Dibutyl	0.97 to -1.85 ⁽²⁾	2.50 to -0.15
1,2,3-Trimethyl	(3)	2.40 to +0.10
1,2-Dimethyl-3-Ethyl	0.86 to -1.50	2.07 to -0.12

* The window is defined as the potential region, with reference to an Al wire in 0.6 MeEtImCl acidic melt, measured at $v = 50$ mv/sec, for which $i \leq 5 \mu\text{A}$.

(1) All compositions of melt required heating to $\sim 50^\circ\text{C}$.

(2) Basic and neutral melts required heating to $\sim 60^\circ\text{C}$.

(3) Melting point $> 70^\circ\text{C}$.

TABLE II

ELECTROCHEMICAL WINDOWS IN TERNARY MELTS

ORGANIC SOLVENT	0.4 MeEtImCl Melt	0.6 MeEtImCl Melt
10% (w/w) Nitrobenzene	0.96 to -0.46 V	2.47 to 1.09 V
10% (w/w) Nitromethane	0.94 to -0.67 V	2.43 to 0.80 V
10% (w/w) m-xylene	0.98 to -1.60 V	1.66 to 0.18 V
33% (w/w) Acetonitrile	0.90 to -1.35 V	*
15% (w/w) Propionitrile	0.91 to -1.57 V	(1.45 to -0.75 V)*
5% (w/w) Propionitrile (binary melt)	0.91 to -1.57 V 0.97 to -1.60 V	2.30 to -0.50 V 2.35 to -0.05 V

* 2 Phases present

TABLE III
ELECTROCHEMICAL RESPONSE OF ELECTRODE MATERIALS IN BASIC MELT*

ELECTRODE	OPEN CIRCUIT POTENTIAL	ELECTROCHEMICAL WINDOW
Ag	-0.35	-0.35 to -0.70
Al	-1.35	-1.10 to -2.05
Glassy Carbon	+0.25	+1.00 to -1.60
Cu	-0.63	None
Fe	-0.44	-0.40 to -0.70
Ni	-0.35	-0.25 to -0.55
Pb	-0.76	None
Pt	-0.18	+0.90 to -0.15
Ta	-0.23	0.40 to -1.00
Ta/20% Ir	-0.25	0.80 to -1.50
Ta/20% Pt	-0.37	-0.1 to -0.80
Ta/20% Ru	-0.27	+1.25 to -1.70
Ti/20% Ir	-0.18	-0.15 to -0.30
Ti/5% Pt	-0.34	-0.20 to -0.70
Ti/10% Pt	-0.31	-0.20 to -0.45
Ti/20% Pt	-0.44	None
Ti/30% Pt	-0.25	None
Ti/20% Ru	-0.27	+0.25 to -2.00
W	+0.30	+0.85 to -0.80
Au	+0.15	+0.30 to -0.55
Hg	-0.36	-0.35 to -1.05

* 0.4 mole fraction $AlCl_3$ in $AlCl_3$ -MeEtImCl

TABLE IV
ELECTROCHEMICAL RESPONSE OF ELECTRODE MATERIALS IN ACIDIC MELT^{*}

ELECTRODE	OPEN CIRCUIT POTENTIAL	ELECTROCHEMICAL WINDOW
Ag	+0.70	+0.70 to 0.15
Al	0.000	None
Glassy Carbon	1.35	+2.35 to -0.005
Cu	0.65	0.60 to +0.10
Fe	0.71	None
Ni	0.93	1.00 to 0.00
Pb	0.36	0.30 to 0.00
Pt	1.33	2.00 to 0.70
Ta	1.14	1.90 to 0.50
Ta/20% Ir	0.85	1.95 to -0.05
Ta/20% Pt	0.54	1.05 to 0.30
Ta/20% Ru	1.19	2.30 to -0.10
Ti/20% Ir	1.11	1.20 to 0.70
Ti/5% Pt	1.08	1.30 to 0.00
Ti/10% Pt	1.07	1.10 to 0.60
Ti/20% Pt	1.03	None
Ti/30% Pt	1.09	None
Ti/20% Ru	1.04	None
W	0.78	2.40 to -0.075
Au	1.94	1.95 to 0.80
Hg	0.99	1.00 to 0.03

* 0.6 mole fraction AlCl_3 in $\text{AlCl}_3\text{-MeEtImCl}$

TABLE V
OPEN CIRCUIT POTENTIALS OF CATIONS

SPECIES	0.4 BASIC MELT	0.6 ACIDIC MELT
Melt	0.25 V	1.35 V
Ag ⁺	0.86	insoluble
Co ²⁺	0.26	1.20
Cr ³⁺	0.00	0.80
CrO ₃	0.84	1.73
K ₂ Cr ₂ O ₇	0.84	1.78
Cu ²⁺	0.28	1.90
Fe ²⁺	0.18	1.86
Fe ³⁺	0.30	1.98
Ferrocene	0.10	0.10
Hg ²⁺	0.32	1.30
Li ⁺	0.30	1.20
Mn ²⁺	0.27	1.55
Mo ³⁺	0.00	1.30
Mo ⁴⁺	0.25	1.75
Mo ⁵⁺ (oxide-free)	0.84	2.10
MoO ₂ Cl ₂	0.33	1.98
[Et ₄ N][MoCl ₆]	0.50	1.70
Na ₂ S	0.32	0.66
Ni ²⁺	0.33	1.00
Pb ²⁺	0.15	insoluble
sulfur	0.70	1.10
S ₂ Cl ₂	0.65	1.80
Sr ²⁺	-0.11	insoluble
Ta ⁵⁺	0.25	0.74
Ti ⁴⁺	0.24	1.19
W ⁶⁺	0.0	1.48
Zn ²⁺	0.20	insoluble

glassy carbon indicating electrode

Reference is Al in 0.6 MeEtImCl Melt

All species as chlorides unless otherwise indicated

TABLE VI

COLORS OF CATIONS IN MELTS

SPECIES	0.4 BASIC MELT	0.6 ACIDIC MELT
Melt	Clear, colorless	Clear, slightly yellow
Ag^+	Pale green-yellow*	White precipitate
Co^{2+}	Robin's egg blue	Medium blue
Cr^{3+}	Bright violet	Cloudy, light violet
CrO_3	Yellow	Orange-yellow
$\text{K}_2\text{Cr}_2\text{O}_7$	Yellow	Orange-yellow
Cu^{2+}	Pale yellow	Dark orange
Fe^{2+}	Pale yellow	Bright yellow
Fe^{3+}	Pale yellow	Dark green
Ferrocene	Yellow	Turns dark green on standing
Hg^{2+}	Clear, colorless	Clear, colorless
Li^+	Clear, colorless	Clear, colorless
Mn^{2+}	Clear, colorless	Clear, colorless
Mo^{3+}	Violet	Dark non-distinct
Mo^{4+}	Dark yellow orange	Dark green
Mo^{5+} (oxide-free)	Bright yellow	Dark non-distinct
MoO_2Cl_2	Pale yellow	Dark red-brown
$[\text{Et}_4\text{N}]^+[\text{MoCl}_6]^-$	Bright yellow	Dark orange-brown
Na_2S	Clear, colorless	Clear, slightly yellow
Ni^{2+}	Deep blue	Bright yellow
Pb^{2+}	Clear, colorless	White precipitate
Sulfur	Clear, colorless	Clear, yellow
S_2Cl_2	Clear, colorless	Dark brown
Sn^{2+}	Clear, colorless	White precipitate
Ta^{5+}	Cloudy (white)	Cloudy (white)
Ti^{4+}	Bright yellow	Clear, colorless
W^{6+}	Bright orange*	Dark red-brown
Zn^{2+}	Pale yellow-green	White precipitate

* Lime-green in 0.5 melt.

TABLE VII

CV PARAMETERS FOR CATIONS IN 0.4 MELT

SPECIES	$E_{p/2}$	ΔE_p^*	$\frac{i_{p,c}}{i_{p,c}}$	$E_{dep.}$	$E_{reoxid.}$	$E_{p,c}$	$i_{p,c}^*$
Ag ⁺	-	-	-	-0.90	0.12	-	-
Co ²⁺	-	-	-	-	-	-	-
Cr ³⁺	-0.586 ⁽¹⁾	915	0.4	-	-	-1.035	15
CrO ₃	-	-	-	-2.17	-	-0.33	265
K ₂ Cr ₂ O ₇	-	-	-	-2.20	-	-0.30	68
Cu ²⁺	0.240	156	1.0	-1.20 ⁽²⁾	-0.30 ⁽³⁾	0.16	33
Fe ²⁺	0.265	137	1.1	-	-	0.20	45
Fe ³⁺	0.300	123	0.9	-	-	0.24	44
Ferric ene	0.400	112	1.4	-	-	0.345	44
Ag ²⁺	-	-	-	-1.40	-0.24 ⁽⁴⁾	-	-
Li ⁺	-	-	-	-1.60	-0.74 ⁽⁵⁾	-	-
Mn ²⁺	-	-	-	-	-	-1.53	24
Mo ⁴⁺	0.270	75	1.0	-	-	0.235	11
Mo ⁵⁺	0.315	101	0.9	-	-	0.26	32

TABLE VII (CONTINUED)

SPECIES	$E_{p/2}$	ΔE_p^*	$\frac{i_{p,d}}{i_{p,c}}$	$E_{den.}$	$E_{reoxid.}$	$E_{p,c}$	$i_{p,c}^*$
MoO_2Cl_2	$0.370^{(6)}$	77	2.1	-	-	0.20	9
$[Et_4N][MoCl_6]$	0.290	77	0.9	-	-	0.25	10
Ni^{2+}	-	-	-	-	-	-	-
Pb^{2+}	-	-	-	$-1.10^{(7)}$	$-0.67^{(8)}$	-	-
Sulfur	-	-	-	-	-	-0.63	141
S_2Cl_2	-	-	-	-	-	-1.07	178
Sn^{2+}	$-0.860^{(9)}$	310	$0.8^{(10)}$	-	-	-1.03	86
Ta^{5+}	-0.310	118	0.8	-	-	-0.36	39
Ti^{4+}	-0.115	108	1.6	-	-	-0.16	13
Ti^{4+} (1td sweep)	-0.120	100	1.0	-	-	-0.17	18
W^{6+} (1st couple)	0.625	118	0.8	-	-	0.565	40
W^{6+} (2nd couple)	-0.620	125	0.7	-	-	-0.68	38
Zn^{2+}	-	-	-	-	-	-	-

* at $v = 50$ mV/sec

TABLE VII (CONTINUED)

SPECIES	$\frac{-d(E_p/2 - E_{p,c})}{d \log i_{p,c}}$	$\frac{-dE_{p,c}}{d \log v}$	$\frac{d(E_{p,a} - E_p/2)}{d \log i_{p,a}}$	$\frac{dE_{p,a}}{d \log v}$	$\frac{i_{p,c}}{v^{1/2}}$	$\frac{i_{p,a}}{v^{1/2}}$	$\frac{d(i_{p,a}/i_{p,c})}{d \log v}$
Ag ⁺	-	-	-	-	-	-	-
Co ²⁺	-	-	-	-	-	-	-
Cr ³⁺	120	60	<120	-	-	-	-
CrO ₃	-	-	-	-	-	-	-
K ₂ Cr ₂ O ₇	-	-	-	-	-	-	-
Cu ²⁺	60	30	60	30	-	-	-
Fe ²⁺	60	30	60	30	-	-	-
Fe ³⁺	60	30	60	30	-	-	-
Ferrocene	60	30	60	30	Const	f(v)	~ 0
Hg ²⁺	-	-	-	-	-	-	-
Li ⁺	-	-	-	-	-	-	-
Mn ²⁺	-	-	-	-	-	-	-
Mo ⁴⁺	60	30	30	15	f(v)	f(v)	0
Mo ⁵⁺	60	30	60	30	Const	f(v)	-0.1

TABLE VII (CONTINUED)

SPECIES	$\frac{d(E_{p/2} - E_{p,c})}{d \log i_{p,c}}$	$\frac{dE_{p,c}}{d \log v}$	$\frac{d(E_{p,a} - E_{p/2})}{d \log i_{p,a}}$	$\frac{dE_{p,a}}{d \log v}$	$\frac{i_{p,c}}{v^{1/2}}$	$\frac{i_{p,a}}{i/2}$	$\frac{d(i_{p,a}/i_{p,c})}{d \log v}$
MoO_2Cl_2	0	0	0	0	f(v)	Const	0.3
$[\text{Et}_4\text{N}][\text{MoCl}_6]$	30	15	30	15	Const	Const	0
Ni^{2+}	-	-	-	-	-	-	-
Pb^{2+}	-	-	-	-	-	-	-
Sulfur	-	-	-	-	-	-	-
S_2Cl_2	-	-	-	-	-	-	-
Sn^{2+}	120	60	0	0	f(v)	Const	0
Ta^{5+}	120	60	120	60	Const	f(v)	-0.08
Ti^{4+}	60	30	60	30	Const	f(v)	-0.3
Ti^{4+} (1td. sweep)	60	30	60	15	f(v)	f(v)	-0.16
W^{6+} (1st couple)	120	60	120	60	Const	f(v)	-0.06
W^{6+} (2nd couple)	120	60	120	60	f(v)	f(v)	0
Zn^{2+}	-	-	-	-	-	-	-

FOOTNOTES FOR TABLE VII

- (1) The anodic peak potential is dependent on cathodic sweep limit and becomes more anodic as the sweep limit is made more cathodic; e.g., with a sweep limit of $-1.0V$, $E_{p,a} = 0.17V$, for a limit of $-1.8V$, $E_{p,a} = +0.04V$. The anodic peak is a broad peak and develops a second peak as the sweep limit is made more cathodic, e.g., with a limit of $-1.8V$, the 2nd peak has $E_{p,a} = +0.42V$.
- (2) E_{dep} is dependent on v , being more cathodic as v increases. After initial deposition of Cu, a reduction peak occurs on subsequent sweeps with a peak potential identical to the initial deposition potential of the cathodic sweep, indicating that the overpotential for Cu deposition on the deposited Cu is less than on glassy carbon.
- (3) E_{reoxid} is dependent on cathodic sweep limit and on v , being more cathodic as the sweep limit is made more cathodic or as v is increased.
- (4) The reoxidation of deposited Hg occurs in two steps with peaks at -0.24 and $+0.40V$. The potential of the -0.24 peak is independent of cathodic sweep limit and of v , however the other peak is very sensitive to both. The relative heights of the two peaks are dependent on both cathodic sweep limit and v .
- (5) The current for reoxidation is very small, being less than 1% of the deposition current.
- (6) The oxychloride is readily reduced but shows no related oxidation peak. After the oxychloride is reduced, a redox couple appears as indicated. This couple is not seen if the cathodic sweep is stopped short of the oxychloride reduction ($\sim -0.2V$).
- (7) Depending on v and cathodic sweep limits, the deposition of Pb appears to occur stepwise with cathodic peaks at -1.20 and $-1.50V$.

FOOTNOTES FOR TABLE VII (CONTINUED)

- (8) E_{reoxid} is dependent on cathodic sweep limit, being more anodic as the sweep limit is made more cathodic. When the cathodic limit is negative to -1.1V , a second anodic peak (much broader than the 1st peak) occurs at $\sim +0.5\text{V}$. The second peak is dependent on cathodic sweep limit, being more anodic as the sweep limit is more cathodic.
- (9) Sn^{2+} shows an oxidation peak at $\sim +0.53\text{V}$, but the product is apparently not reduced, i.e., there is no evidence of a cathodic peak.
- (10) The $i_{\text{p,a}}/i_{\text{p,c}}$ is very dependent on v , e.g., at $v = 5$, $i_{\text{p,a}}/i_{\text{p,c}} = 0.5$; at $v = 500$, $i_{\text{p,a}}/i_{\text{p,c}} = 2.3$. The current peaks increase significantly with cycling.

TABLE VIII

CV PARAMETERS FOR CATIONS IN 0.6 MELT

SPECIES	$E_{p/2}$	ΔE_p^*	$\frac{i_{p,a}}{i_{p,c}}$	E_{dep}	E_{reoxid}	$E_{Al\ reoxid}$	$E_{p,c}$	$i_{p,c}^*$
Co^{2+}	-	-	-	0.48 ⁽¹⁾	1.32	0.78 ⁽²⁾	-	-
Cr^{3+}	-	-	-	-	-	0.15	-	-
CrO_3	1.56	1160	0.8	-	-	0.08	0.98	23
$K_2Cr_2O_7$	1.56	1180	1.2	-	-	0.09	0.97	24
Cu^{2+}	1.98	107	1.2	0.50 ⁽³⁾	1.35	0.85	1.92	55
Fe^{2+}	2.00	485	1.6	0.05	0.92	0.85 ⁽⁴⁾	1.765	18
Fe^{3+}	2.22	335	1.9	0.05	0.93	0.87 ⁽⁴⁾	2.025	23
Ferrocene	0.41	110	1.3	-	-	0.07	0.35	106
Hg^{2+}	-	-	-	0.80 ⁽⁵⁾	1.08	0.02	0.96	-
Li^+	-	-	-	Co-dep with Al	0.41	0.22	-	-
Mn^{2+}	-	-	-	Co-dep with Al	0.75	0.55	-	-
Mo^{4+}	2.02	80	1.2	-	-	0.22	1.98	40
Mo^{5+}	2.06 ⁽⁶⁾	75	1.2	-	-	0.22	1.925	21

TABLE VIII (CONTINUED)

SPECIES	$E_{p/2}$	ΔE_p^*	$\frac{i_{p,a}}{i_{p,c}}$	E_{dep}	E_{reoxid}	$E_{Al\ reoxid}$	$E_{p,c}$	$i_{p,c}^*$
MoO_2Cl_2	2.07(7)	97	1.3	-	-	0.22	2.02	74
$[Et_4N][MoCl_6]$	1.97(8)	67	2.6	-	-	0.22	1.925	19
Ni^{2+}	-	-	-	0.64(9)	1.44	1.05	-	-
Sulfur	1.75	740	3.3	-	-	0.21	1.45	160
S_2Cl_2	1.68	810	1.2	-	-	0.12	1.30	66
Ta^{5+}	0.77	885(10)	0.6	Co-dep with Al	0.39	0.22	0.32	70
Ti^{4+}	1.08	550(11)	0.4	0.04	0.57	0.145	0.80	26
W^{6+}	1.62	320(12)	1.1	Co-dep	0.02(13)	0.02	1.45	49.5

* at $v = 50$ mv/s

Table VIII (continued)

SPECIES	$-\frac{d(E_{p/2} - E_{p,c})}{d \log i_{p,c}}$	$\frac{-dE_{p,c}}{d \log v}$	$\frac{d(E_{p,a} - E_{p/2})}{d \log v}$	$\frac{dE_{p,a}}{d \log v}$	$\frac{i_{p,c}}{v^{1/2}}$	$\frac{i_{p,a}}{v^{1/2}}$	$d\left(\frac{i_{p,a}}{i_{p,c}}\right)$ $\frac{d \log v}{v}$
Co ²⁺	-	-	-	-	-	-	-
Cr ³⁺	-	-	-	-	-	-	-
CrO ₃	-	-	-	-	-	-	-
K ₂ Cr ₂ O ₇	-	-	-	-	-	-	-
Cu ²⁺	30	60	30	60	f(v)	f(v)	0.12
Fe ²⁺	30	60	30	60	f(v)	f(v)	~0
Fe ³⁺	30	60	30	60	f(v)	f(v)	~0
Ferrocene	60	30	60	30	Const	Const	~0
Hg ²⁺	-	-	-	-	-	-	-
Li ⁺	-	-	-	-	-	-	-
Mn ²⁺	-	-	-	-	-	-	-
Mo ⁴⁺	30	15	30	15	f(v)	f(v)	~0
Mo ⁵⁺	30 ⁽¹⁴⁾	15	30 ⁽¹⁴⁾	15	f(v)	f(v)	~0

Table VIII (continued)

SPECIES	$-\frac{d(E_{p/2} - E_{p,c})}{d \log i_{p,c}}$	$-\frac{dE_{p,c}}{d \log v}$	$\frac{d(E_{p,a} - E_{p/2})}{d \log v}$	$\frac{dE_{p,a}}{d \log v}$	$\frac{i_{p,c}}{v^{1/2}}$	$\frac{i_{p,a}}{v^{1/2}}$	$\frac{d(\frac{i_{p,a}}{i_{p,c}})}{d \log v}$
MoO ₂ Cl ₂	60	15	30	15	f(v)	f(v)	~0
[Et ₄ N][MoCl ₆]	30	15	0	0	f(v)	Const	0.65
Ni ²⁺	-	-	-	-	-	-	-
Sulfur	60	120	120	60	Const	f(v)	~0
S ₂ Cl ₂	120	120	120	60	Const	f(v)	~0
Ta ⁵⁺	60	30	60	30	f(v)	f(v)	~0
Ti ⁴⁺	(15)	-	-	-	-	-	-
W ⁶⁺	60	30	60	15	f(v)	f(v)	0.5

FOOTNOTES FOR TABLE VIII

1. Co^{2+} deposits on the deposited Al layer at +0.55V on the anodic sweep.
2. In pure acidic melt, Al is deposited at -0.075V and is reoxidized on the anodic sweep at +0.22V.
3. Al is co-deposited with Cu (as seen by separate oxidation peaks on the anodic sweep before an Al deposition peak is obtained). Al deposition is shifted anodically to +0.25V.
4. The potential for reoxidation of Al on the reverse sweep is dependent on the cathodic sweep limit. As the limit is made more cathodic the reoxidation potential is shifted cathodically to a limiting value of +0.55V.
5. Hg deposition is preceded by an irreversible reduction with a peak at 0.96V, probably $\text{Hg}^{2+} + e \rightarrow \text{Hg}^+$. The Hg deposition potential is very dependent on sweep rate, but the reoxidation potential is independent of v.
6. Mo^{5+} exhibits 2 reduction peaks about equal in magnitude. When the cathodic sweep is limited to potentials positive to +0.8V, the anodic peak splits into 3 peaks.
7. A large irreversible reduction peak associated with the oxychloride species occurs at +1.06V.
8. This Mo complex exhibits 2 reduction peaks and 3 oxidation peaks.
9. Al deposition is shifted anodically, apparently being reduced on deposited Ni at +0.5v.
10. Ta^{5+} has 3 cathodic peaks and 2 anodic peaks. Data given is for the first cathodic and first anodic peaks.
11. Ti^{4+} peak potentials and peak currents are not reproducible and change significantly with cycling.
12. W^{6+} has a very complex CV in acidic melt with 5 cathodic peaks and 10 anodic peaks. Another major peak is irreversible, probably associated with an oxy-chloride with $E_{p,c} = 0.865\text{V}$.

13. The anodic peaks for reoxidation are significantly smaller than the metal deposition peak.
14. Tafel slopes shift to 60 mV when analyses are made for full sweep cycles.
15. No reproducibility could be obtained.

TABLE IX

MOLYBDENUM COMPOUNDS IN ACIDIC MELT $v = 50 \text{ mV/Sec}$

PEAK POTENTIAL/RELATIVE PEAK HEIGHT

SPECIES	CATHODIC SWEEP	
Mo^{5+} (purified)	+1.775/8	(1) +0.290/0.6 +0.140/0.4
Mo^{5+}	+1.78/28	+1.11/48 0.25/2 0.12/2
Mo^{4+}	1.99/17	1.74/5(2) 1.06/51 0.24/0.5 - +2.36/5 (2)
Mo^{3+}	1.96/5	1.74/3 1.125/19 0.41/7 0.06/0.5
MoO_2Cl_2	2.02/48	1.77/1.5 1.11/24 0.27/10 0.10/3
$[\text{Et}_4\text{N}][\text{MoCl}_6]$	1.75/9	1.04-1.12/0.2(3) 0.24/0.8 0.05/1.8

- (1) Peak develops with time (exposure to oxygen) at +1.1V. Can also be seen by adding material sublimed from MoCl_5 .
- (2) Not present when sweep is limited on cathodic side +0 potentials positive to +1.2V.
- (3) Peak increases significantly with time, e.g., after 48 hours it becomes the primary peak.

TABLE IX (CONTINUED)

MOLYBDENUM COMPOUNDS IN ACIDIC MELT

PEAK POTENTIAL/RELATIVE PEAK HEIGHT

SPECIES	ANODIC SWEEP						
Mo ⁵⁺ (purified)	+2.05/24 ⁽¹⁾	*	-	-			
Mo ⁵⁺	2.10/103	1.84/17	1.35/2	0.52/1	-	+2.25/0.5	
Mo ⁴⁺	2.08/80	1.79/36	-	-	-	+1.86/7† ⁽²⁾	+2.45/4 †
Mo ³⁺	2.07/30	1.80/8	1.21/3	0.84/0.5	0.61/2 ⁽³⁾	+1.93 ⁽⁴⁾	+2.22/0.1
MoO ₂ Cl ₂	2.11/68	1.83/2	1.35/1	-	(5)	1.92/4	
[Et ₄ N][MoCl ₆]	1.99/21 ⁽⁶⁾	1.75/0.5 ⁽⁷⁾	-	-	-		

* Peak develops with time (as oxychloride peak develops) at ~ +1.81V.

† Peak not present if sweep is initially limited to cathodic potentials positive to +1.1V.

(1) At slower sweep rates and when cathodic sweep is limited to +0.8V, peak is resolved into 3 peaks with: +2.11/15, +1.97/47, +1.86/7.

(2) Peak is only present if, after oxychloride is reduced, the sweep is limited to potentials positive to +1.1V.

(3) Peak is associated with oxidation of Al deposited from melt.

(4) Peak is resolved at slower sweep rates.

(5) When cathodic limit is extended to Al deposition (-0.10V), 4 oxidation peaks between 0.0 and 0.5V are observed.

(6) If cathodic sweep is limited to -1.0V, peak can be resolved into 2 peaks: +1.98/30, +1.91/25.

(7) Peak becomes significantly larger as oxychloride peak develops.

ABBREVIATIONS AND SYMBOLS

CV	cyclic voltammetry
$E_{p,a}$	potential (in volts) of anodic current peak
$E_{p,c}$	potential (in volts) of cathodic current peak
$E_{p/2} =$	$(E_{p,a} + E_{p,c})/2$
$\Delta E_p =$	$E_{p,a} - E_{p,c}$ (in mV)
E_{dep}	potential ($v = 50$ mV/sec) at which metal deposition by reduction of the cation begins.
E_{reoxid}	potential ($v = 50$ mV/sec) at the anodic current peak for reoxidation of the deposited metal.
$E_{Al\ reoxid}$	potential ($v = 50$ mV/sec) at the anodic current peak for reoxidation of Al.
$i_{p,a}$	current (in μ Amps) at the anodic current peak.
$i_{p,c}$	current (in μ Amps) at the cathodic current peak.
v	sweep rate (in mV/sec) for CV measurements.

ILLUSTRATIONS

- Fig 1 CV of 1,3-dimethylimidazolium chloroaluminate melts. (a) basic melt; (b) acidic melt.
- Fig 2 CV of 1-methyl-3-ethylimidazolium chloroaluminate melts. (a) basic melt; (b) acidic melt.
- Fig 3 CV of 1-methyl-3-propylimidazolium chloroaluminate melts. (a) basic melt; (b) acidic melt.
- Fig 4 CV of 1-methyl-3-butylimidazolium chloroaluminate melts. (a) basic melt; (b) acidic melt.
- Fig 5 CV of 1,3-dibutylimidazolium chloroaluminate melts. (a) basic melt; (b) acidic melt.
- Fig 6 CV of acidic 1,2,3-trimethylimidazolium chloroaluminate melt.
- Fig 7 CV of 1,2-dimethyl-3-ethylimidazolium chloroaluminate melts. (a) basic melt; (b) acidic melt.
- Fig 8 Influence of anodic potential limit on chlorine formation in 0.4 MeEtImCl melt. Sweep rate = 100 mV/sec.
- Fig 9 Effect of sweep rate on chlorine formation and subsequent reduction in 0.4 MeEtImCl melt. Anodic limit = 1.50 V. 1. 2 mV/sec, 2. 5 mV/sec, 3. 10 mV/sec, 4. 20 mV/sec, 5. 50 mV/sec, 6. 100 mV/sec, 7. 200 mV/sec, 8. 500 mV/sec.
- Fig 10 Effect of holding cathodic sweep at different potentials on chlorine reduction in acidic MeEtIm melt. 1. continuous sweep. Held for 1 sec at different potentials: 2. 1.270 V, 3. 1.150 V, 4. 1.050 V, 5. 0.942 V, 6. 0.845 V.
- Fig 11 Effect of holding cathodic sweep at 1.05V for varying times after anodic sweep to 1.50 V. 1. 1.0 sec, 2. 5 sec, 3. 10 sec, 4. 15 sec, 5. 30 sec, 6. 60 sec, 7. 120 sec, 8. 180 sec, 9. 300 sec, 10. 600 sec.

- Fig 12 i_p for chlorine reduction vs $t^{-1/2}$ where t is the time (in sec) the cathodic sweep is held at +1.05V after sweep to 1.50 V.
- Fig 13 E vs log i at anodic limit in 0.4 MeEtImCl melt.
- Fig 14 i vs $\omega^{1/2}$ for Cl^- oxidation in 0.4 MeEtImCl melt.
- Fig 15 Effect of cycling at cathodic limit in 0.66 MeEtImCl melt. Numbers indicate nth cycle.
- Fig 16 E vs log i at cathodic limit in 0.6 MeEtImCl melt.
- Fig 17 CV of nitrobenzene in MeEtImCl melt. (a) 10% (w/w) nitrobenzene in 0.4 melt. (b) 10% (w/w) Nitrobenzene in 0.6 melt.
- Fig 18 CV of Nitromethane in MeEtImCl melt. (a) 10% (w/w) Nitromethane in 0.4 melt. (b) 10% (w/w) Nitromethane in 0.6 melt.
- Fig 19 CV of m-xylene in MeEtImCl melt. (a) 10% (w/w) m-xylene in 0.4 melt. (b) 10% (w/w) m-xylene in 0.6 melt
- Fig 20 CV of 33% (w/w) Acetonitrile in 0.5 MeEtImCl melt
- Fig 21 CV of Propionitrile in MeEtImCl melt
(a) 15% (w/w) propionitrile in 0.4 melt
(b) 5% (w/w) propionitrile in 0.6 melt
- Fig 22 CV on Ag in MeEtImCl melts. (a) basic melt. (b) acidic melt (two scans with different cathodic limits: 1. 0.075 V, 2. 0.050 V)
- Fig 23 CV on Al in MeEtImCl melts. (a) basic melt. (b) acidic melt
- Fig 24 CV on Cu in MeEtImCl melts. (a) basic melt, (b) acidic melt
- Fig 25 CV on Fe in MeEtImCl melts. (a) basic melt, (b) acidic melt
- Fig 26 CV on Ni in MeEtImCl melts. (a) basic melt; (b) acidic melt.
- Fig 27 CV on Pb in MeEtImCl melts. (a) basic melt; (b) acidic melt.
- Fig 28 CV on Pt in MeEtImCl melts. (a) basic melt; (b) acidic melt (two different sweep limits).
- Fig 29 CV on Ta in MeEtImCl melts. (a) basic melt; (b) acidic melt (two successive scans; 1. first, 2. second).

- Fig 30 CV on Ta/20% Ir in MeEtImCl melts. (a) basic melt; (b) acidic melt.
- Fig 31 CV on Ta/20% Pt in MeEtImCl melts. (a) basic melt; (b) acidic melt.
- Fig 32 CV on Ta/20% Ru in MeEtImCl melts. (a) basic melt; (b) acidic melt.
- Fig 33 CV on Ti/20% Ir in MeEtImCl melts. (a) basic melt; (b) acidic melt.
- Fig 34 CV on Ti/5% Pt in MeEtImCl melts. (a) basic melt; (b) acidic melt.
- Fig 35 CV on Ti/10% Pt in MeEtImCl melts. (a) basic melt; (b) acidic melt.
- Fig 36 CV on Ti/20% Pt in MeEtImCl melts. (a) basic melt; (b) acidic melt.
- Fig 37 CV on Ti/30% Pt in MeEtImCl melts. (a) basic melt; (b) acidic melt.
- Fig 38 CV on Ti/30% Pt in basic MeEtImCl melt; expanded CV at higher i.
- Fig 39 CV on Ti/20% Ru in MeEtImCl melts. (a) basic melt; (b) acidic melt.
- Fig 40 CV on W in MeEtImCl melts. (a) basic melt; (b) acidic melt (two sweeps at cathodic end).
- Fig 41 Further details of CV on W in basic melt.
- Fig 42 CV on Au in MeEtImCl melts. (a) basic melt; (b) acidic melt (four scans).
- Fig 43 CV on Hg in MeEtImCl melts. (a) basic melt; (b) acidic melt.
- Fig 44 CV of Ag⁺ in 0.4 melt.
- Fig 45 CV of Co²⁺. (a) 0.4 melt. (b) 0.6 melt (1. three scans with successively lower cathodic limits, 2. cathodic limit = 0.25 V).
- Fig 46 CV of Cr³⁺. (a) 0.4 melt with varying cathodic limits, 1. -1.0 V, 2. -1.4 V, 3. -1.8 V; (b) 0.6 melt
- Fig 47 CV of CrO₃. (a) 0.4 melt; (b) 0.6 melt
- Fig 48 CV of K₂Cr₂O₇. (a) 0.4 melt; (b) 0.6 melt
- Fig 49 CV of Cu²⁺. (a) 0.4 melt; (b) 0.6 melt
- Fig 50 CV of Cu²⁺ in 0.4 melt showing effect of cycling. Numbers indicate nth scan.
- Fig 51 CV of Fe²⁺. (a) 0.4 melt; (b) 0.6 melt
- Fig 52 CV of Fe³⁺. (a) 0.4 melt; (b) 0.6 melt. Sweep rate = 100 mV/sec.

- Fig 53 (a) CV of Fe^{3+} in 0.5 melt (slightly basic). (b) Detail at cathodic limit for Fe^{2+} in 0.6 melt. Two cathodic limits: 1. 0.10 V, 2. 0.20 V.
- Fig 54 CV of $\text{Fe}^{2+} + \text{Fe}^{3+}$ in 0.6 melt
- Fig 55 CV of ferrocene. (a) 0.4 melt; (b) 0.6 melt (two scans taken several minutes apart, 1. first, 2. second).
- Fig 56 (a) CV of ferrocene in 0.4 melt showing effect of chemical reaction with melt, curve taken 3 hours after curve in 55(a). (b) CV of ferrocene in 0.6 melt after 12 hours on a clean electrode.
- Fig 57 CV of Hg^{2+} . (a) 0.4 melt; (b) 0.6 melt (1. sweep started at 0.30 V and swept anodic first, 2. sweep started at 1.3 V and swept cathodic first).
- Fig 58 CV of Hg^{2+} in 0.4 melt with cathodic sweep limited to avoid appreciable Hg deposition.
- Fig 59 CV of Li^+ . (a) 0.4 melt; (b) 0.6 melt (three scans swept to different cathodic limits: 1. 0 V, 2. -0.05 V, 3. -0.10 V).
- Fig 60 CV of Mn^{2+} . (a) 0.4 melt; (b) 0.6 melt
- Fig 61 CV of Mo^{3+} . (a) 0.4 melt; (b) 0.6 melt. Sweep rate = 100 mV/sec.
- Fig 62 CV of Mo^{4+} . (a) 0.4 melt; (b) 0.6 melt
- Fig 63 CV of Mo^{5+} . (a) 0.4 melt; (b) 0.6 melt
- Fig 64 (a) CV of oxide-free Mo^{5+} in 0.6 melt; (b) Details for Mo^{5+} in anodic region in 0.6 melt at $v = 5$ mV/sec.
- Fig 65 (a) CV of oxide-free Mo^{5+} in 0.6 melt; (b) CV when substance (oxy-chloride) sublimed from MoCl_5 is added to melt
- Fig 66 CV of MoO_2Cl_2 . (a) 0.4 melt; (b) 0.6 melt
- Fig 67 Detail of MoO_2Cl_2 in 0.4 melt. (a) Clean electrode, sweep limited to -0.2V; (b) Trace taken after reduction of oxide peak

- Fig 68 Detail of MoO_2Cl_2 in 0.6 melt. (a) Sweep limits: 2.5V to 1.0V; (b) Sweepo limits: 2.5V to 0.2V
- Fig 69 CV of $[\text{Et}_4\text{N}][\text{MoCl}_6]$. (a) 0.4 melt; (b) 0.6 melt
- Fig 70 Details of $[\text{Et}_4\text{N}][\text{MoCl}_6]$ in 0.6 melt. (a) 2.2 to 1.2V, $v = 10$ mV/sec; (b) 0.7 to -0.15V
- Fig 71 CV of Ni^{2+} . (a) 0.4 melt; (b) 0.6 melt
- Fig 72 CV of Pb^{2+} in 0.4 melt. (a) 0.85 to -1.5V; (b) 0.85 to -1.85V
- Fig 73 CV of sulfur. (a) 0.4 melt; (b) 0.6 melt
- Fig 74 (a) CV of sulfur in 0.5 melt; (b) CV of S_2Cl_2 in 0.5 melt
- Fig 75 CV of S_2Cl_2 . (a) 0.4 melt; (b) 0.6 melt
- Fig 76 S_2Cl_2 in 0.6 melt showing Al deposition at -0.4V
- Fig 77 CV of Sn^{2+} in 0.4 melt
- Fig 78 CV of Ta^{5+} . (a) 0.4 melt; (b) 0.6 melt (two sweeps).
- Fig 79 CV of Ti^{4+} . (a) 0.4 melt; (b) 0.6 melt
- Fig 80 CV of Ti^{4+} in DMF. (a) background in DMF; (b) with TiCl_4
- Fig 81 CV of W^{6+} . (a) 0.4 melt; (b) 0.6 melt
- Fig 82 CV of Zn^{2+} in 0.4 melt

FIG 1(a) CV OF 0.4 dMeImCl MELT

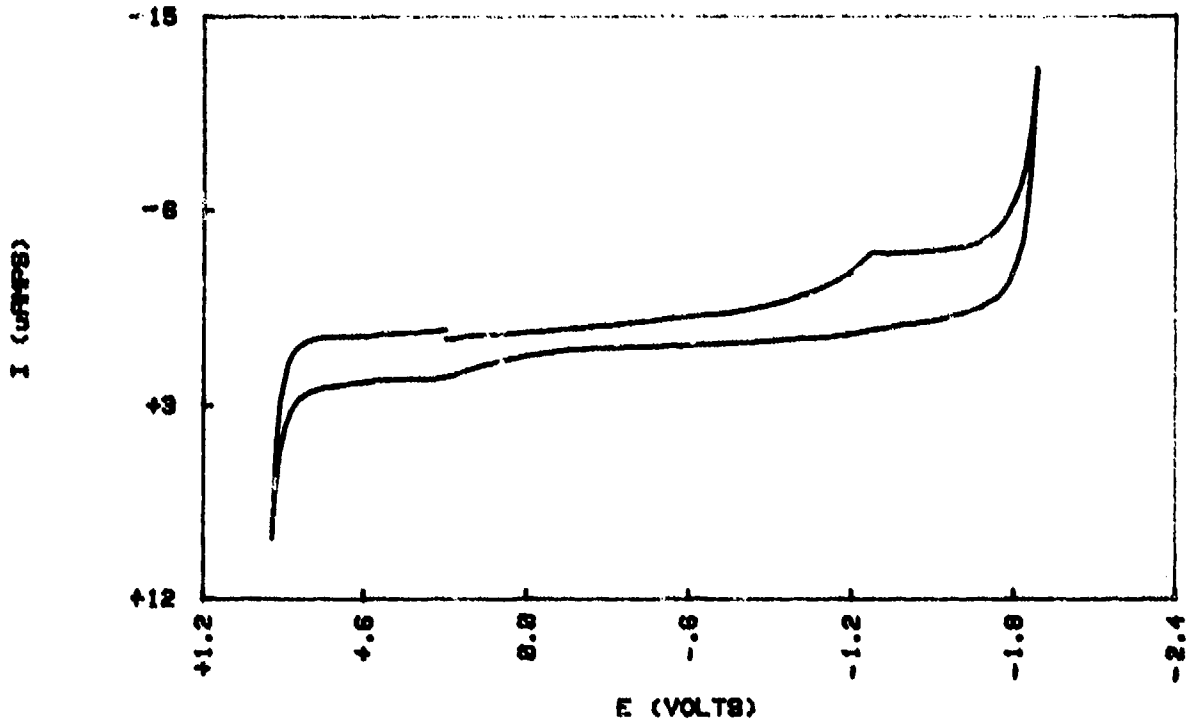


FIG 1(b) CV OF 0.6 dMeImCl MELT

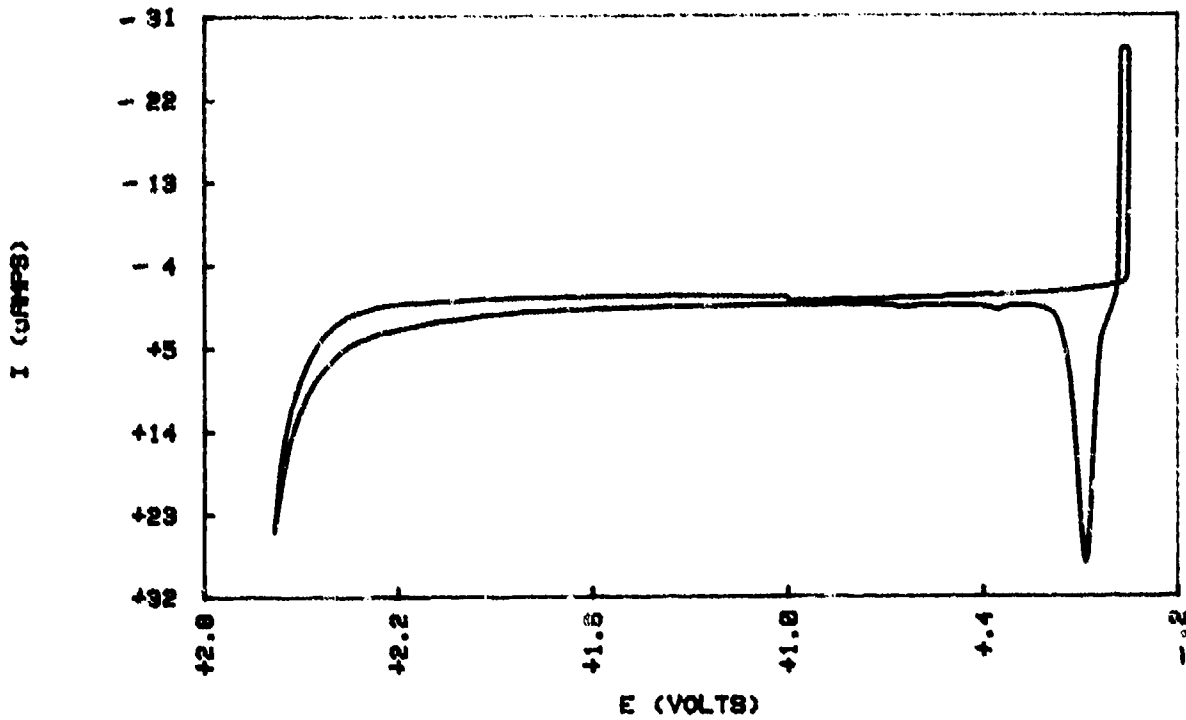


FIG 2(a) CV OF 3.4 MeEtImCl MELT

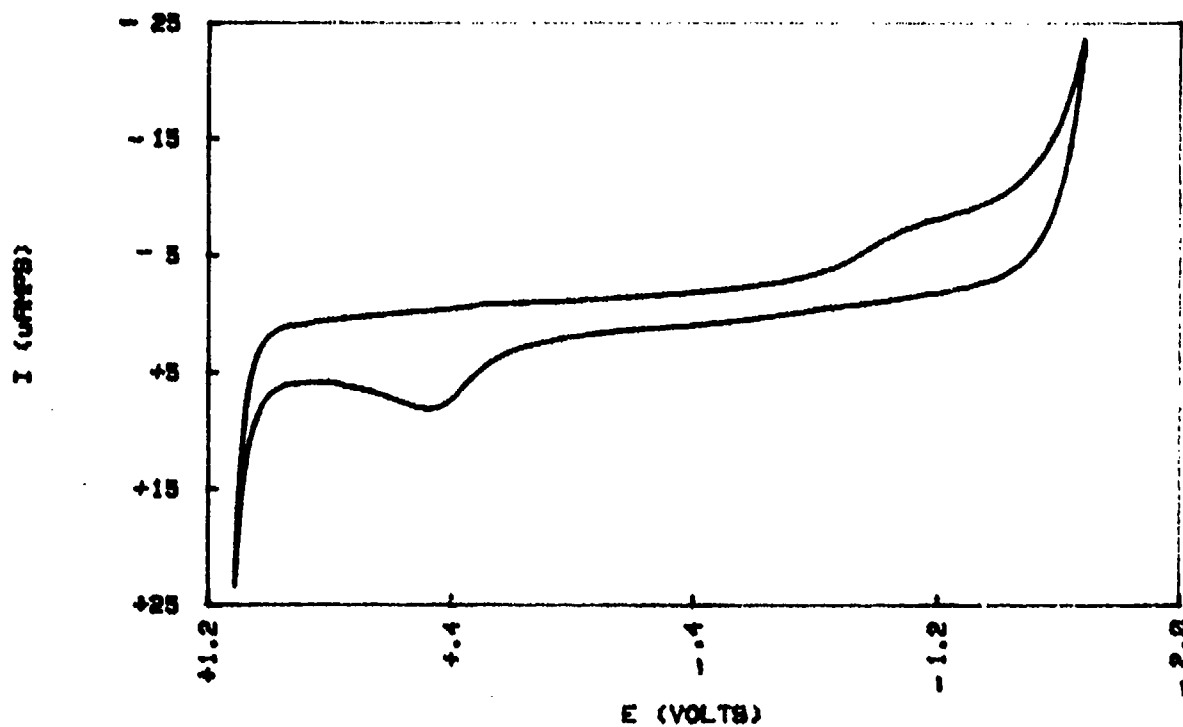


FIG 2(b) CV OF 8.6 MeEtImCl MELT

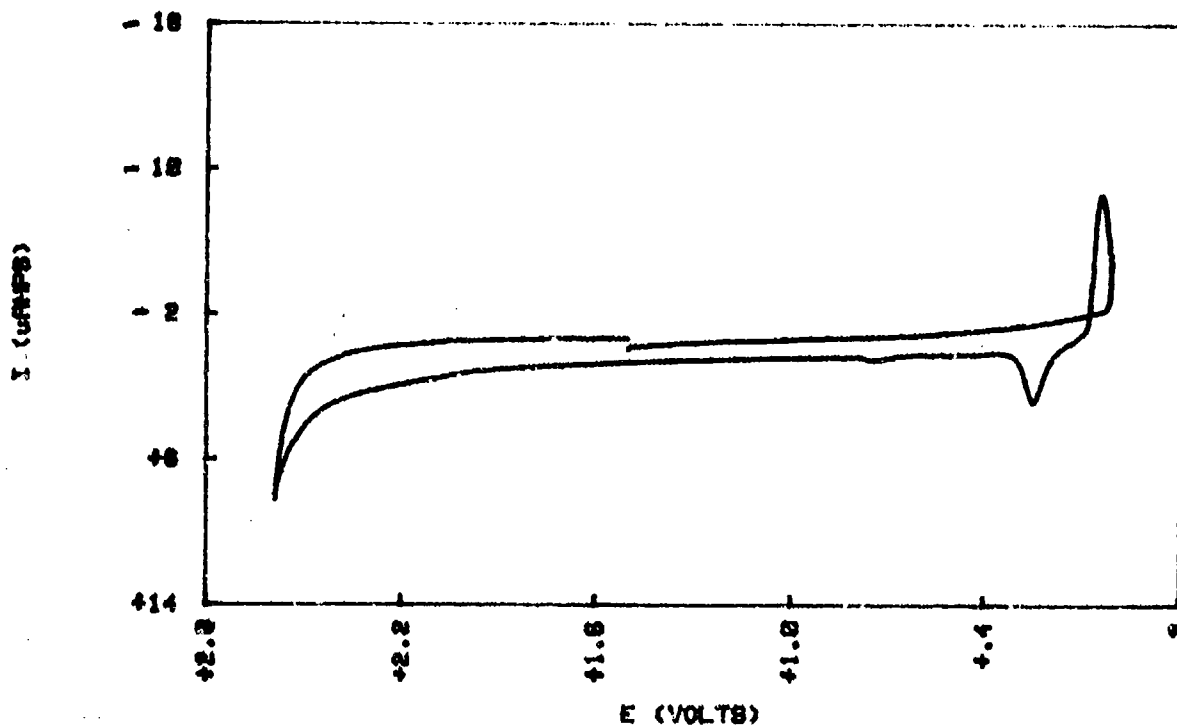


FIG 3(a) CV OF 0.4 MePrImCl MELT

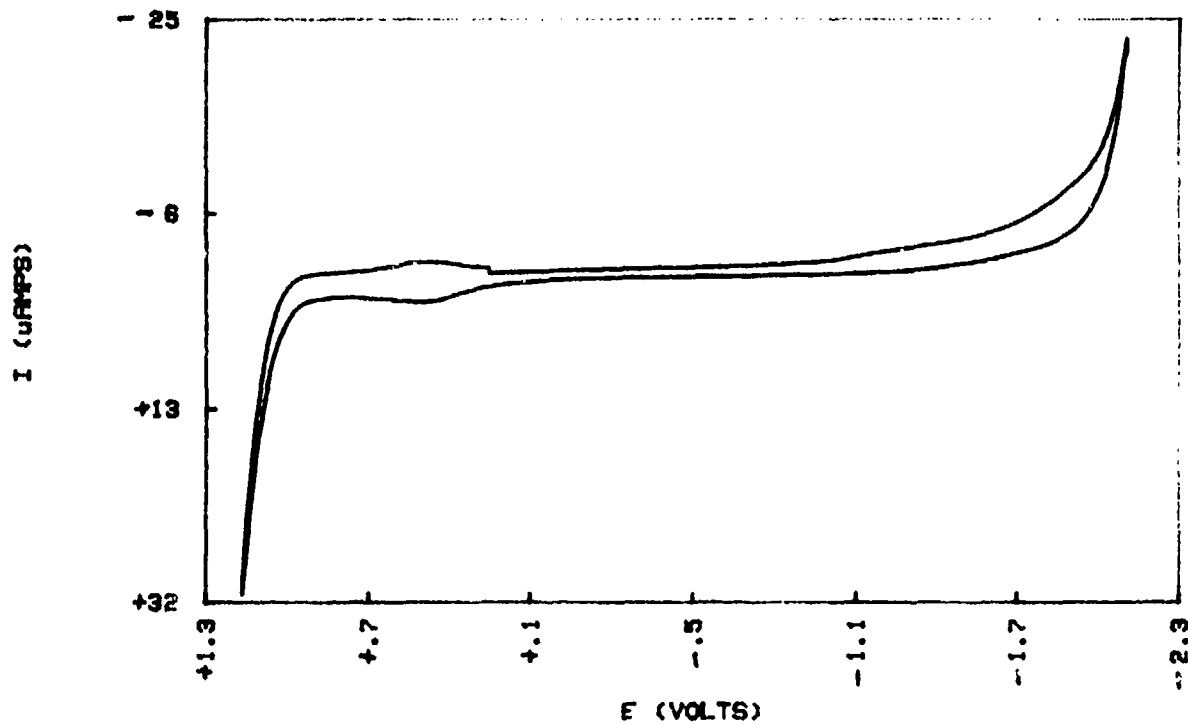


FIG 3(b) CV OF 0.6 MePrImCl MELT

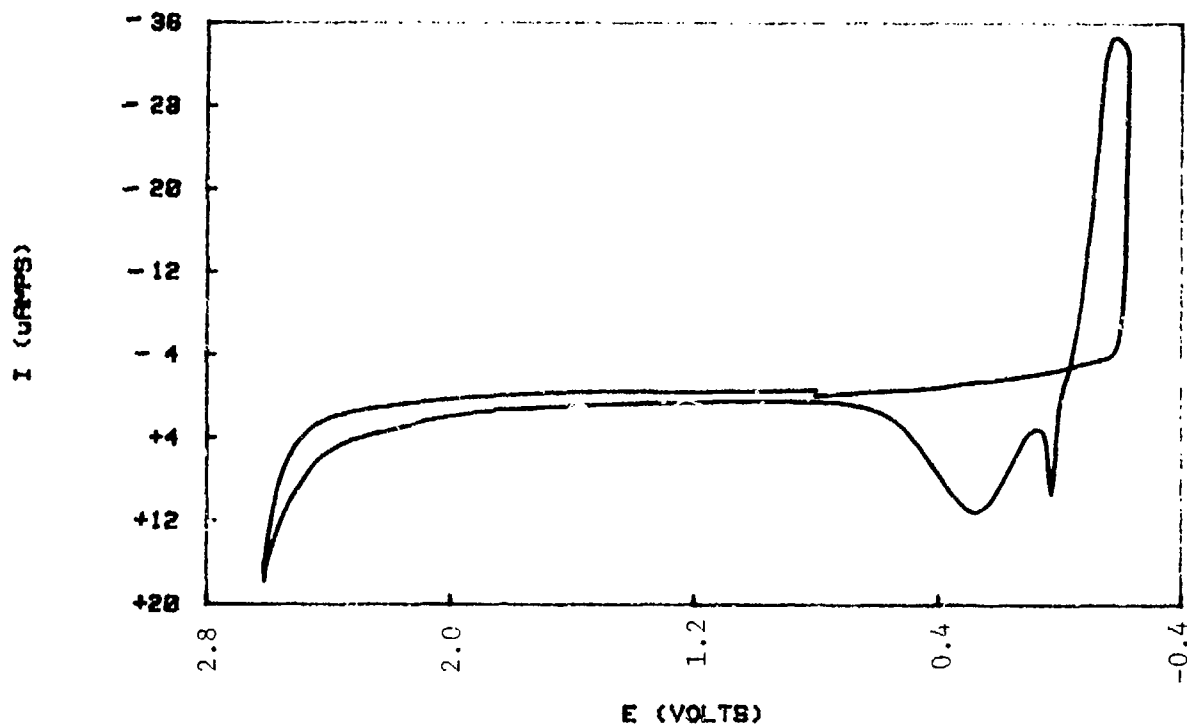


FIG 4(a) 0.4 MeBuImCl MELT

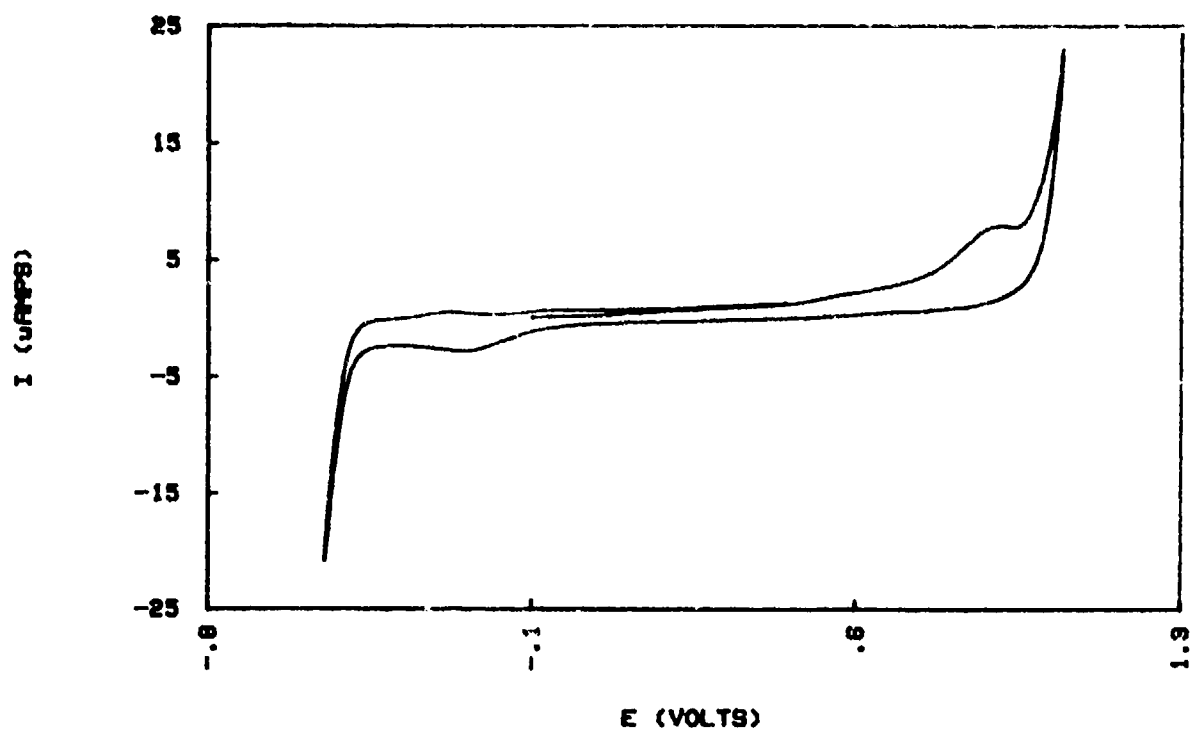


FIG 4(b) CV OF 0.8 MeBuImCl MELT

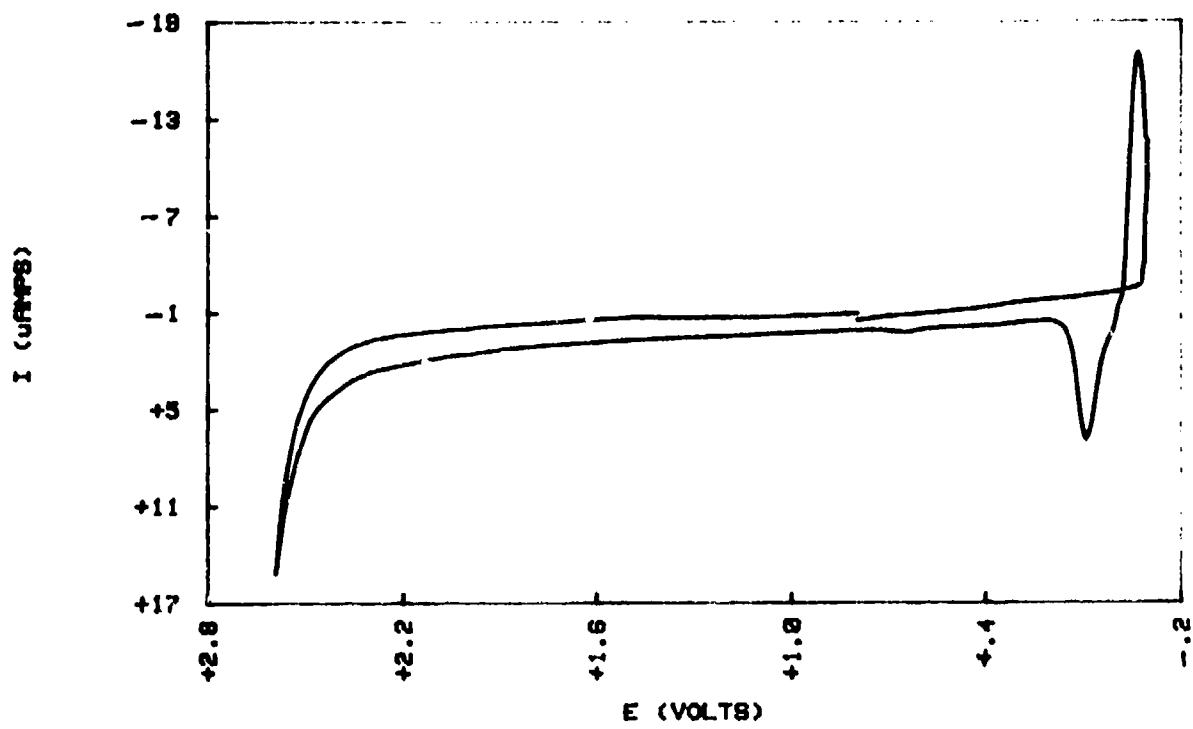


FIG 5(a) CV OF 0.4 d1BuImCl MELT

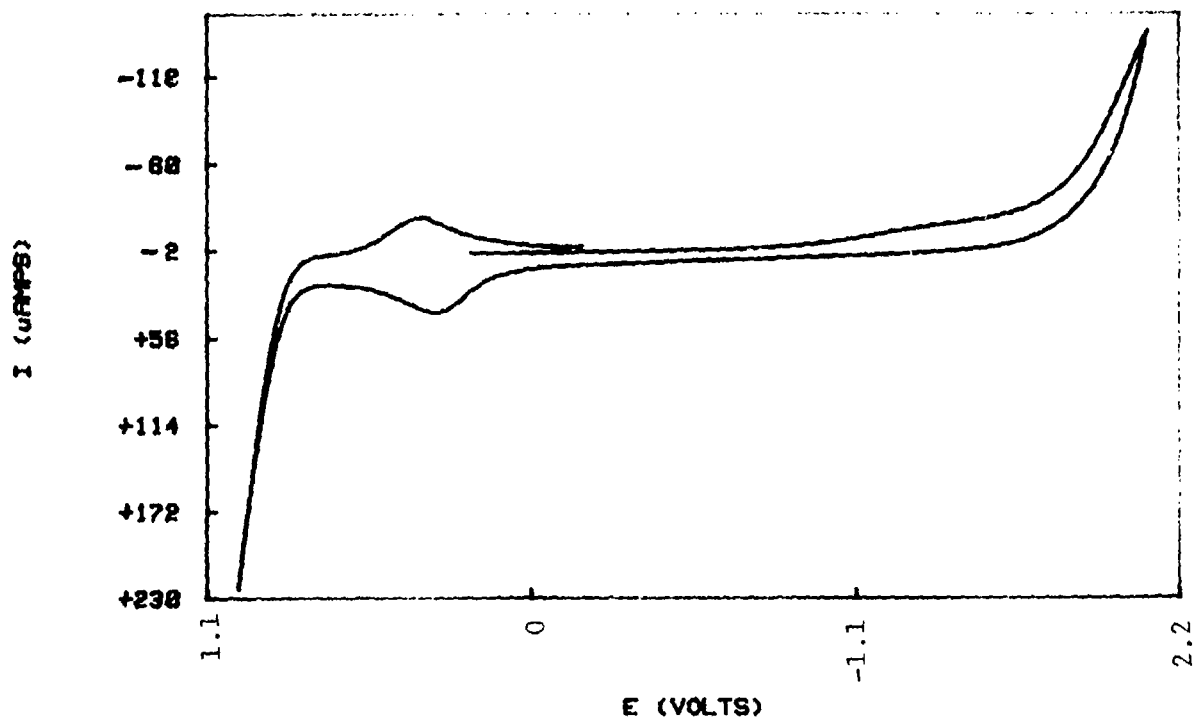


FIG 5(b) CV OF 0.6 d1BuImCl MELT

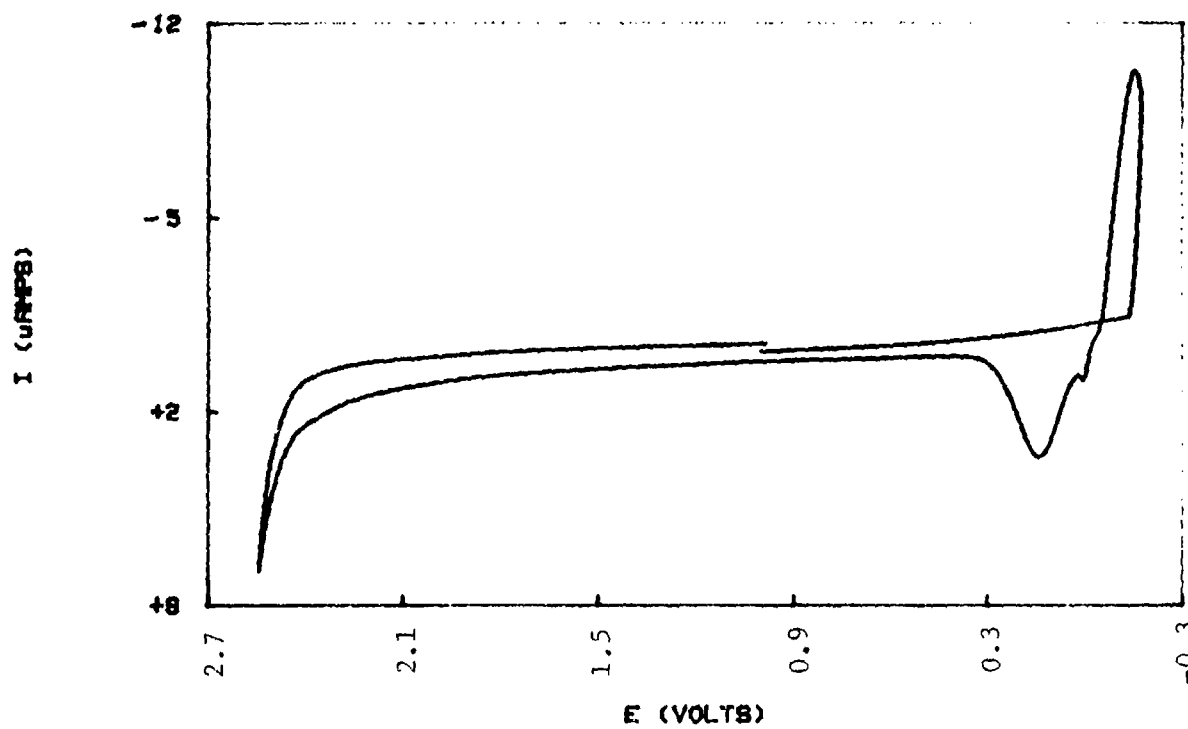


FIG 8 CV OF TiMe_2ZnCl MELT

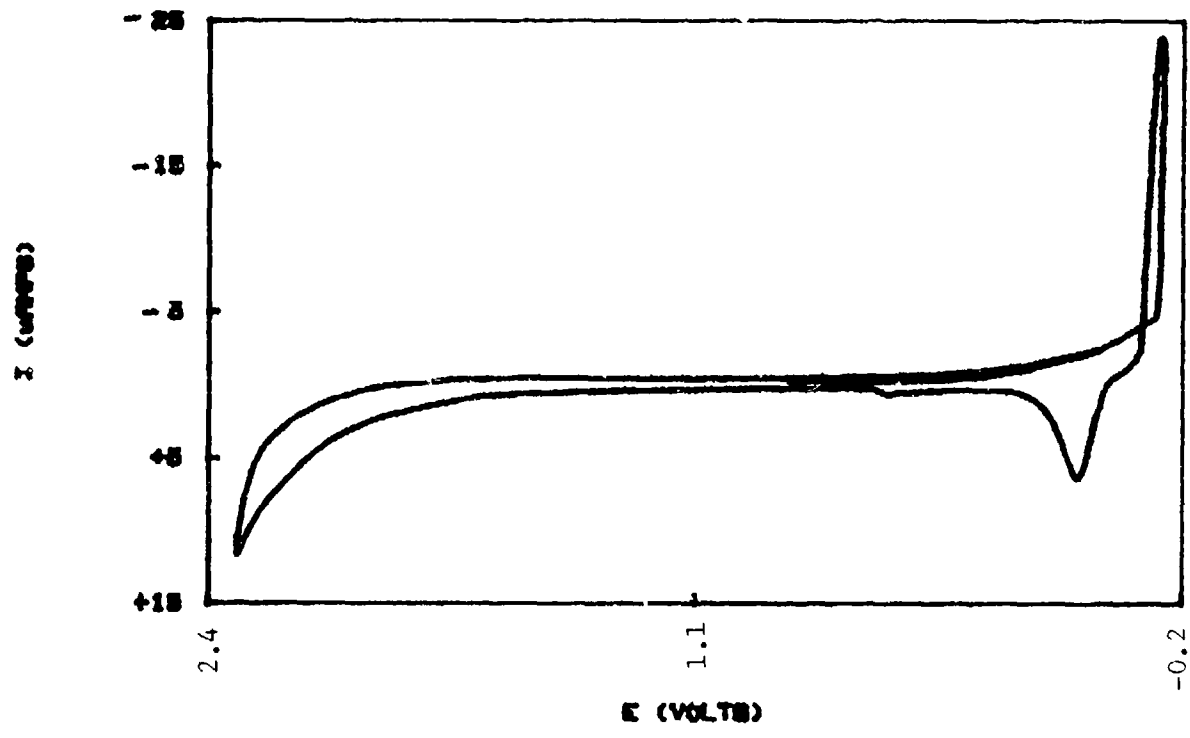


FIG 7(a) CV OF 0.4 dImeEtImCl MELT

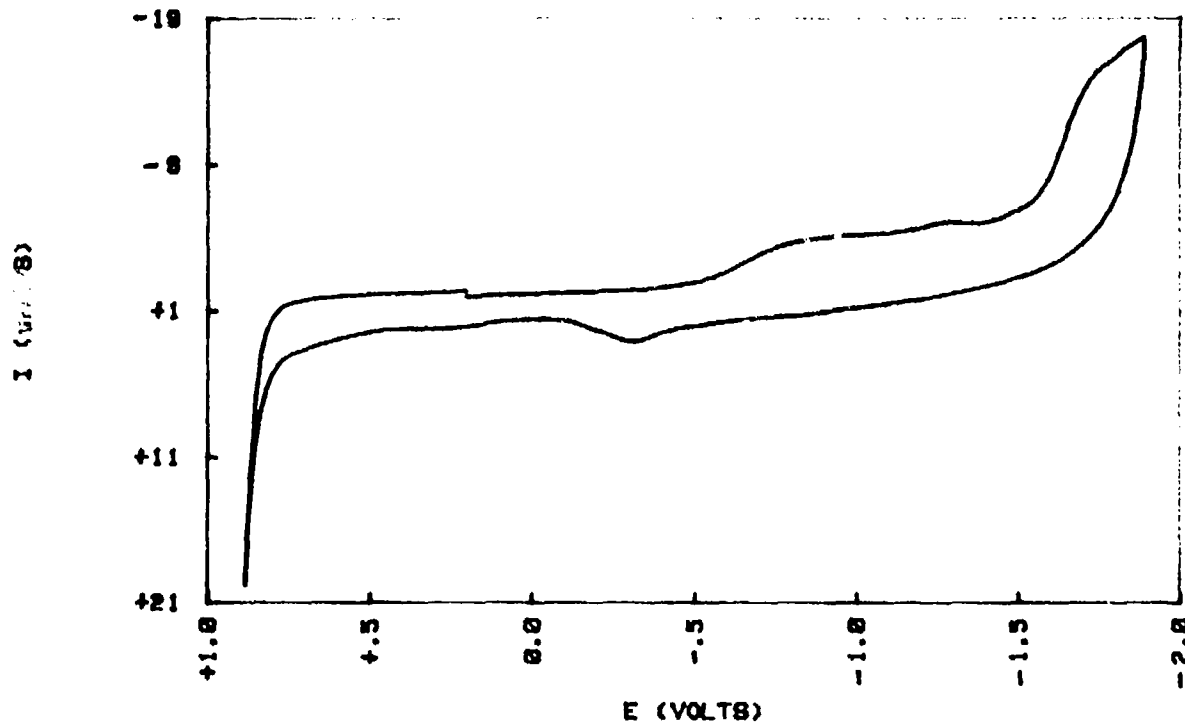


FIG 7(b) CV OF 0.6 dImeEtImCl MELT

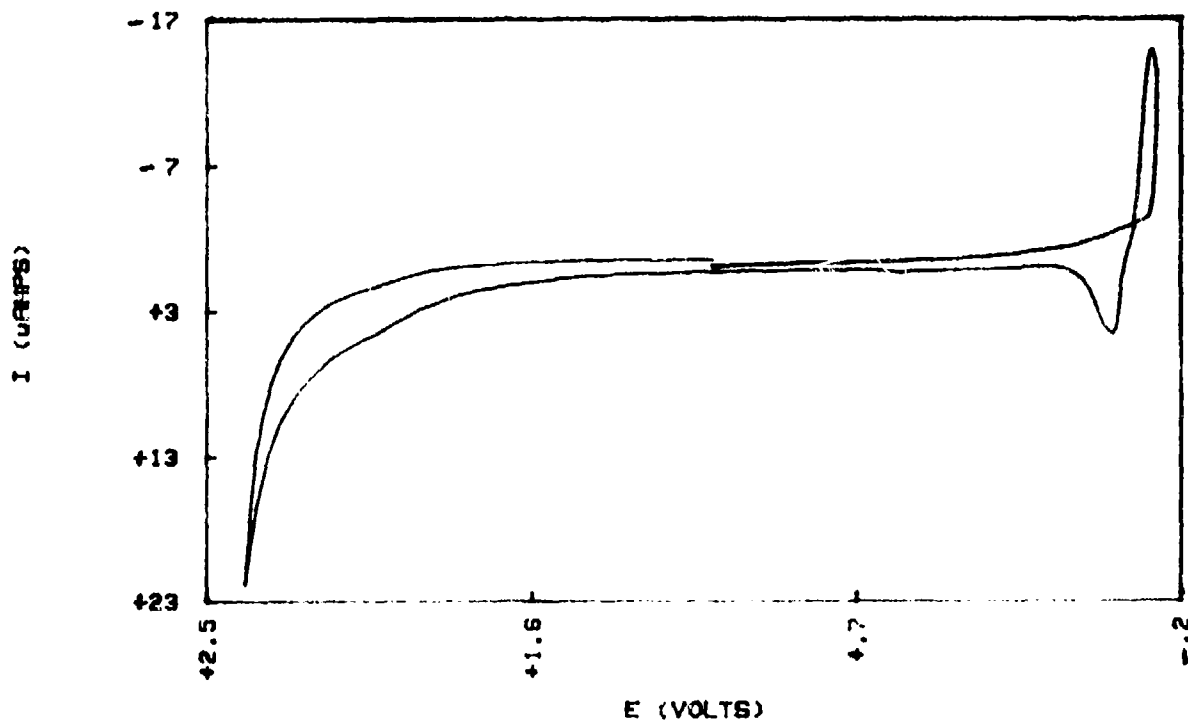


FIG 8 INFLUENCE OF ANODIC POTENTIAL LIMIT ON CHLORINE FORMATION

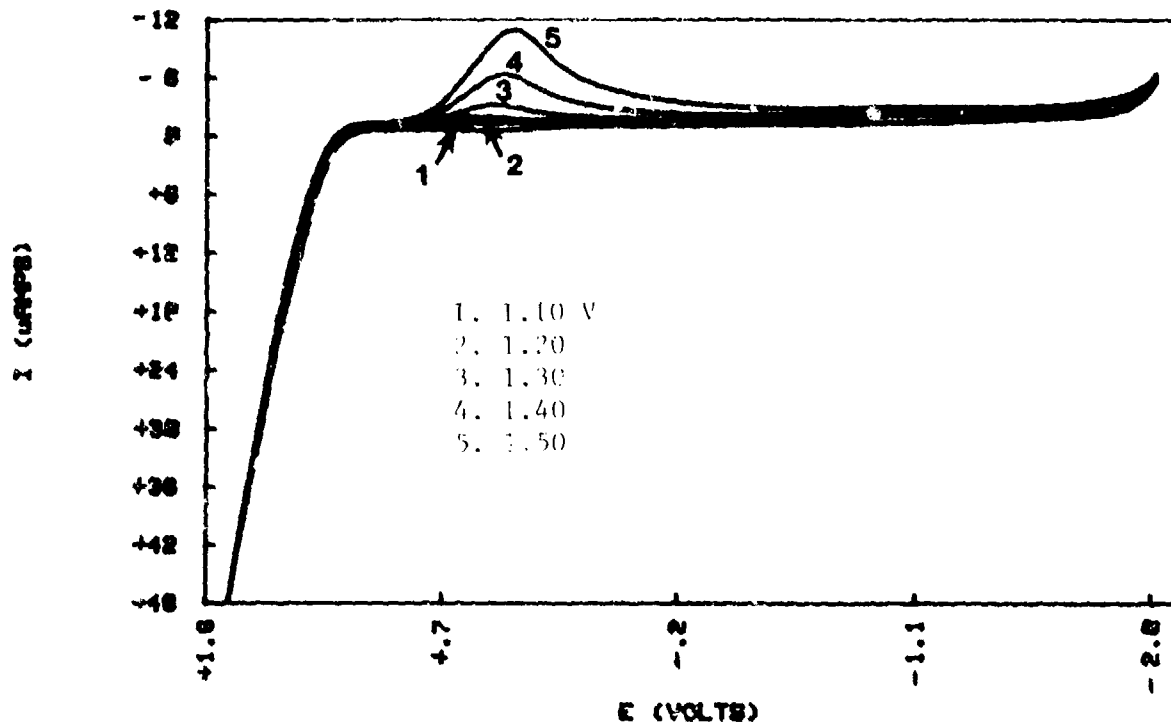


FIG 9 EFFECTS OF SWEEP RATE AT ANODIC LIMIT IN 0.4 M NaEtI₂ MELT

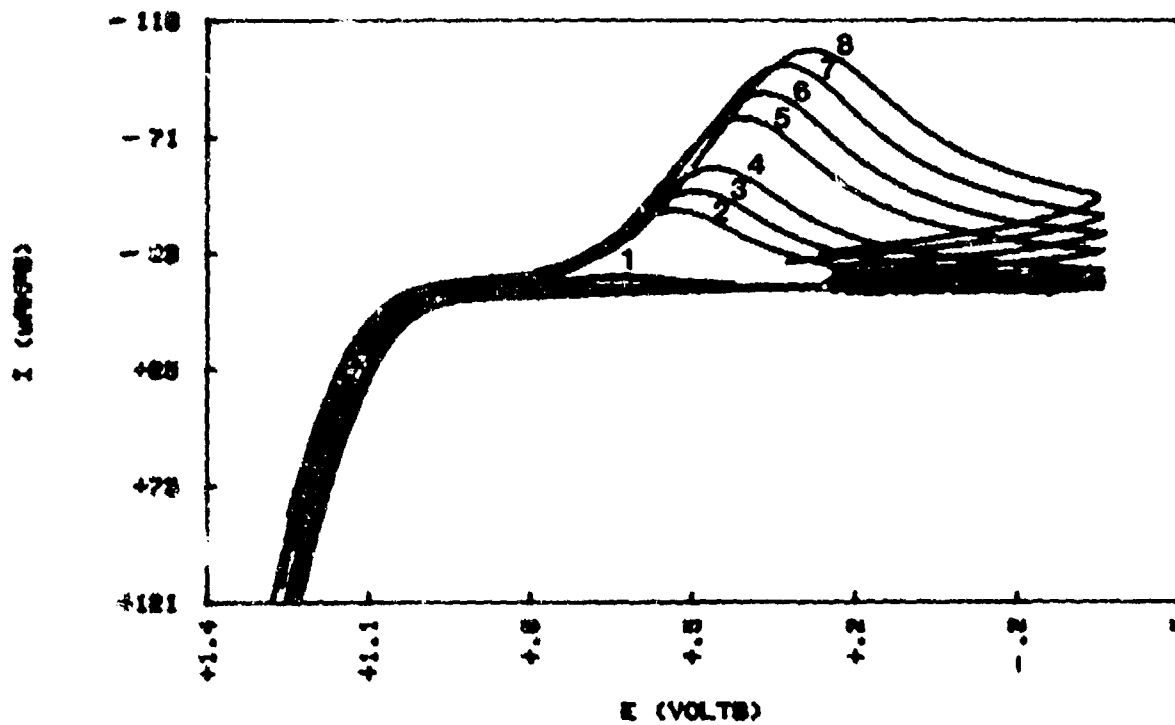


FIG 10 EFFECTS OF STOPPING SWEEP AT DIFFERENT POTENTIALS ON CHLORINE REDUCTION

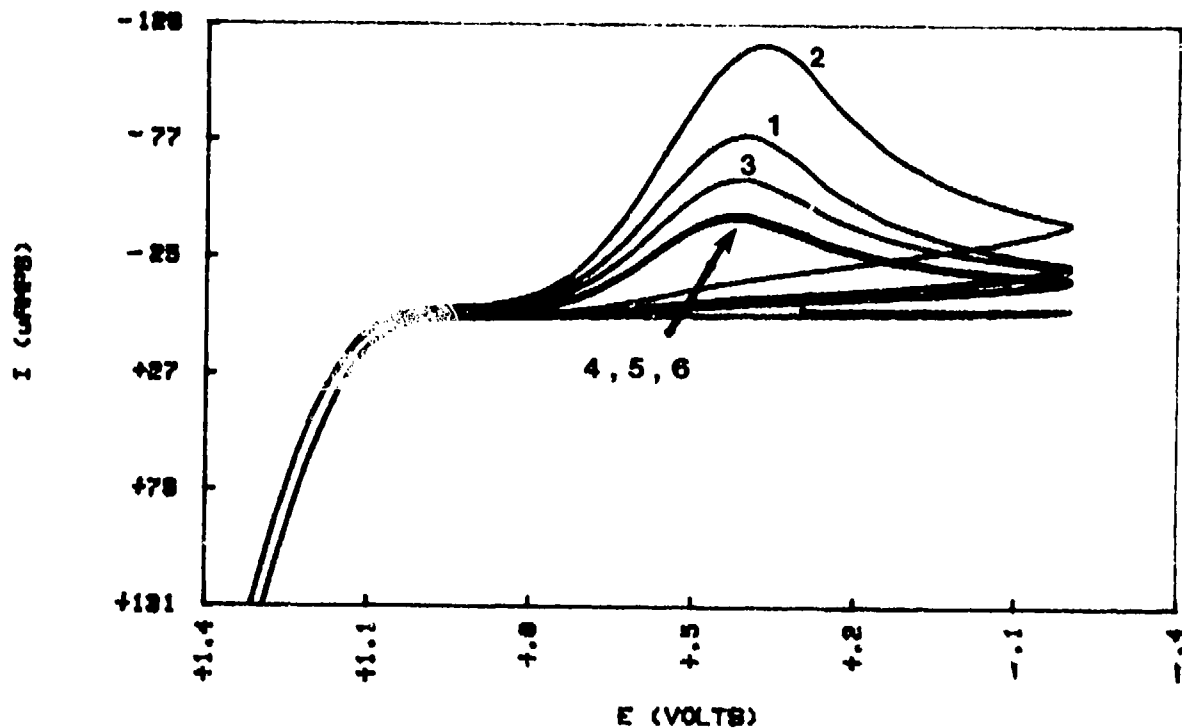


FIG 11 EFFECT OF HOLDING CATHODIC SWEEP AT 1.85V AT VARYING TIMES

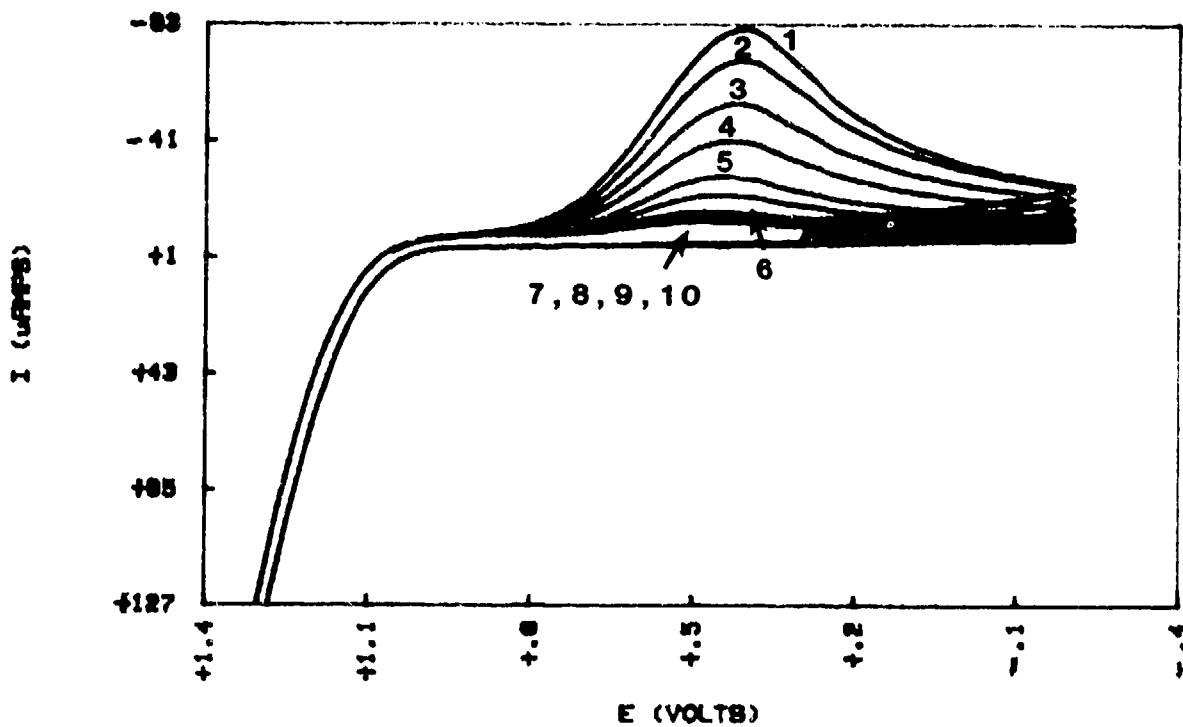


FIG 12 i_p VS $t^{-1/2}$ FOR 0.4 MELT

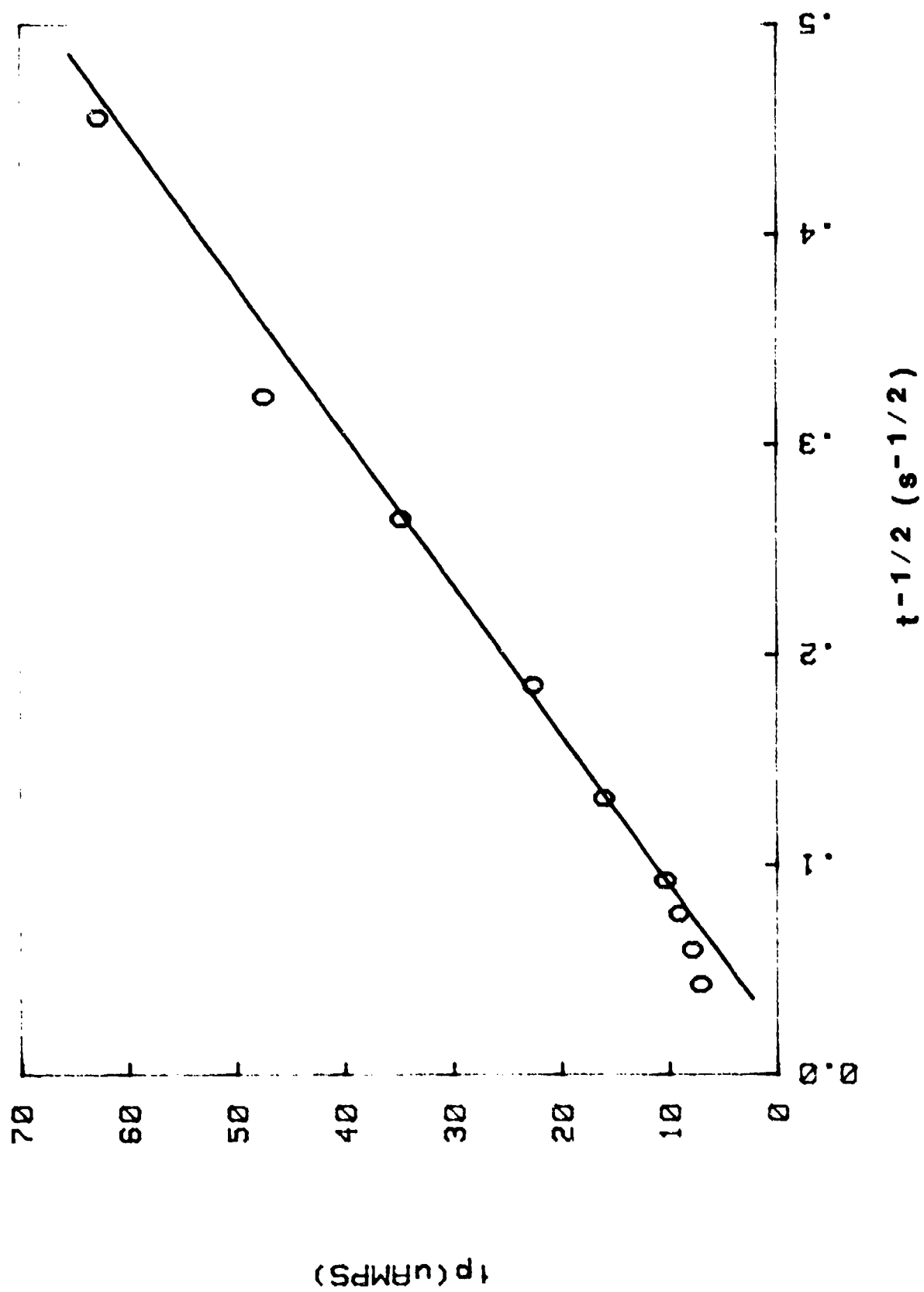


FIG 13 E VS log i FOR Ø.4 MELT

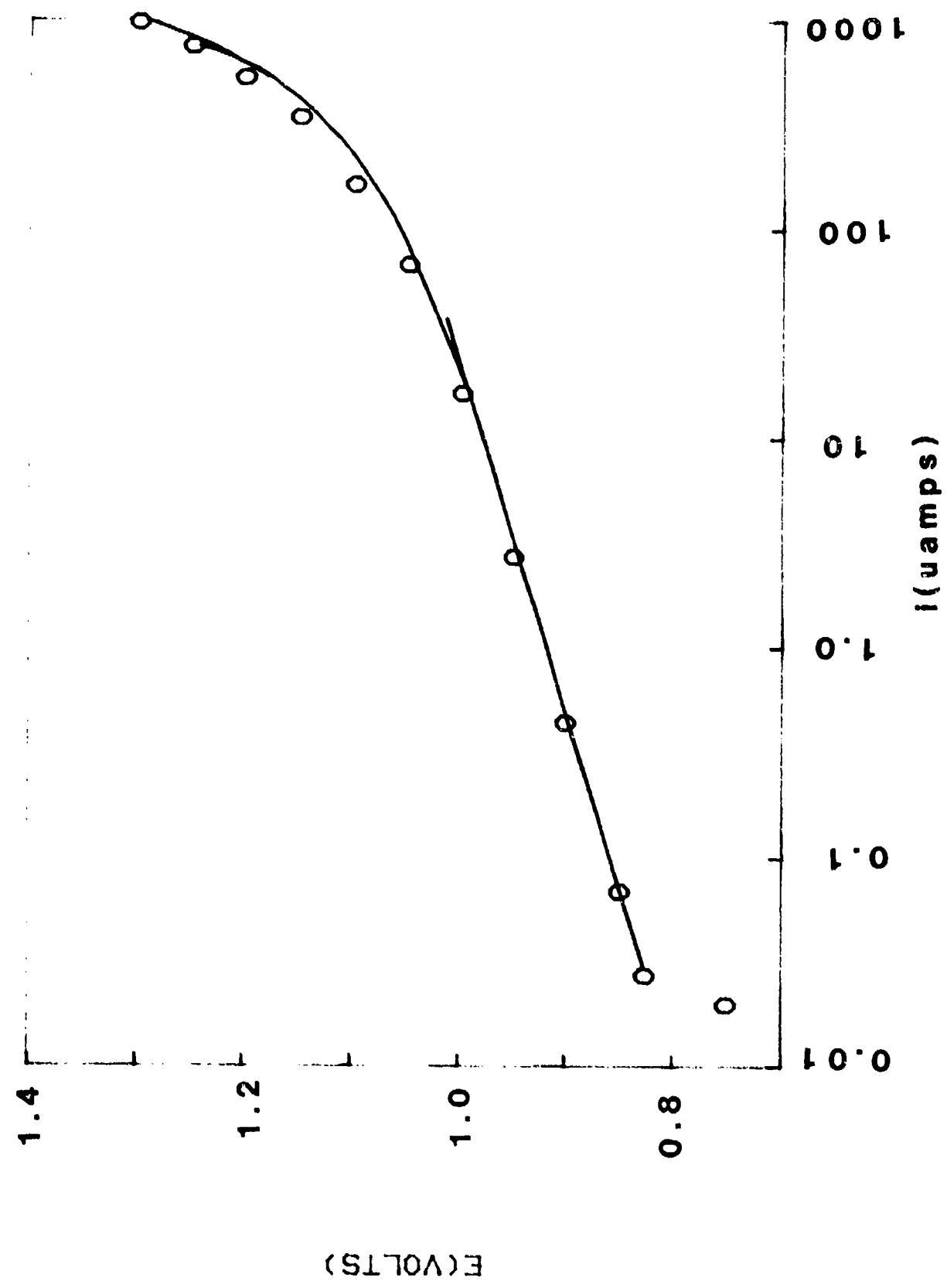


FIG 14 i VS $W(1/2)$ FOR 0.4 MELT

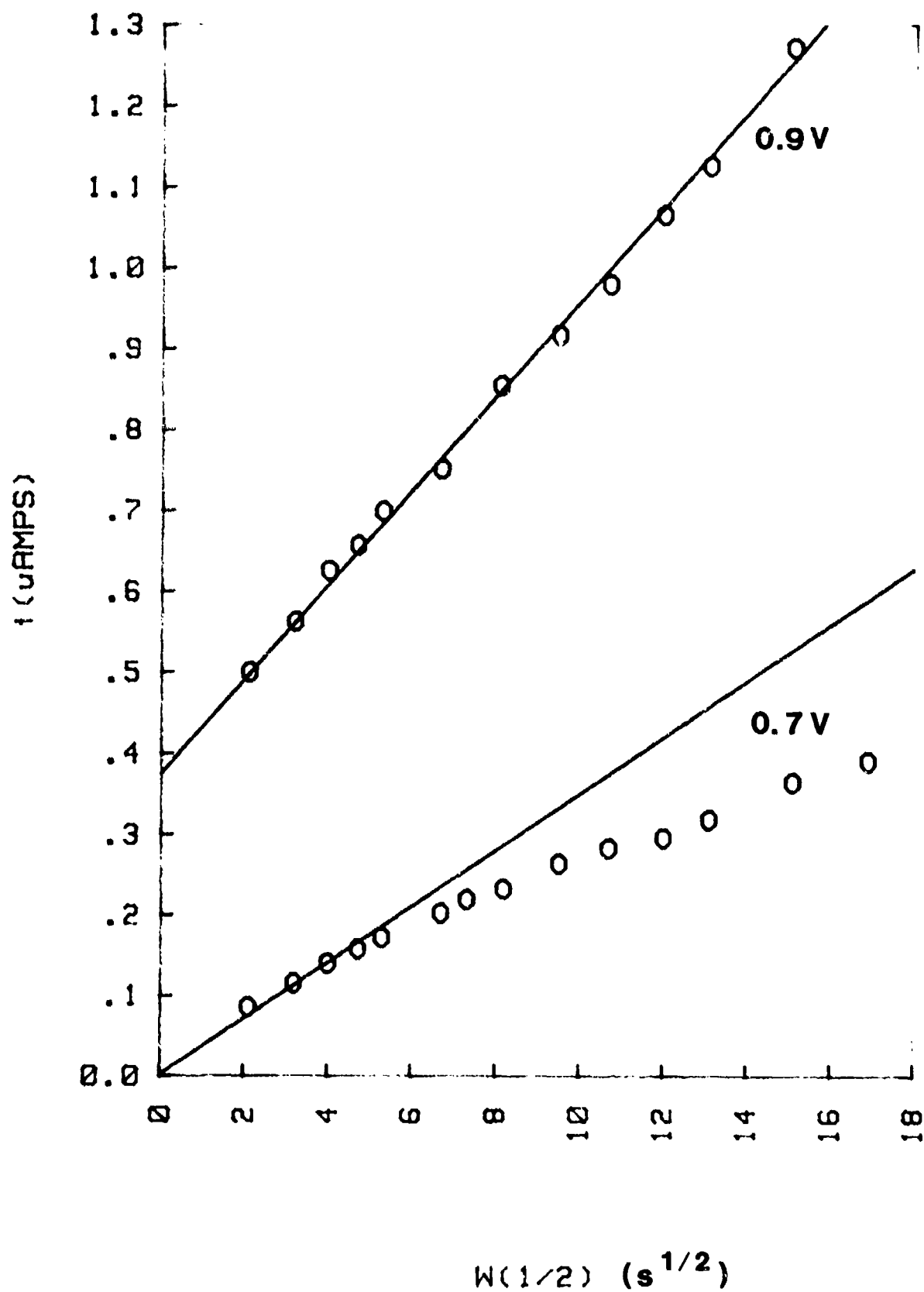


FIG 15 EFFECT OF CYCLING IN 0.6 MeEtImCl MELT

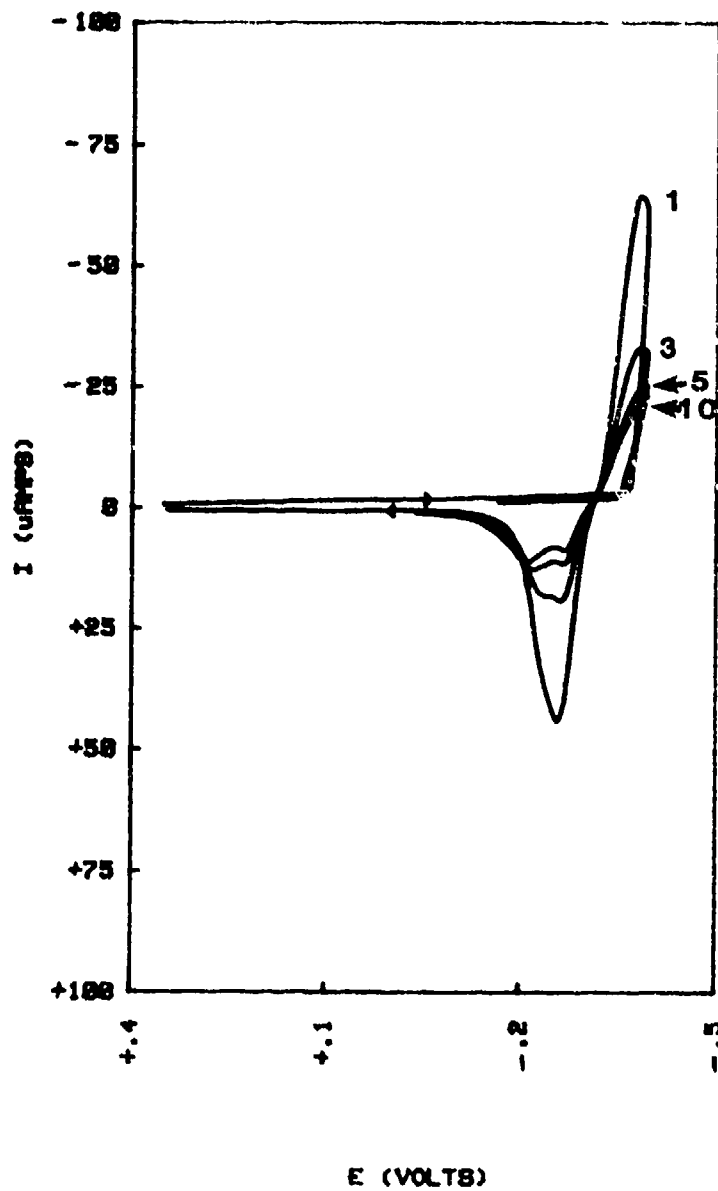


FIG 16 STEADY-STATE E VS log i FOR Ø.6 MELT

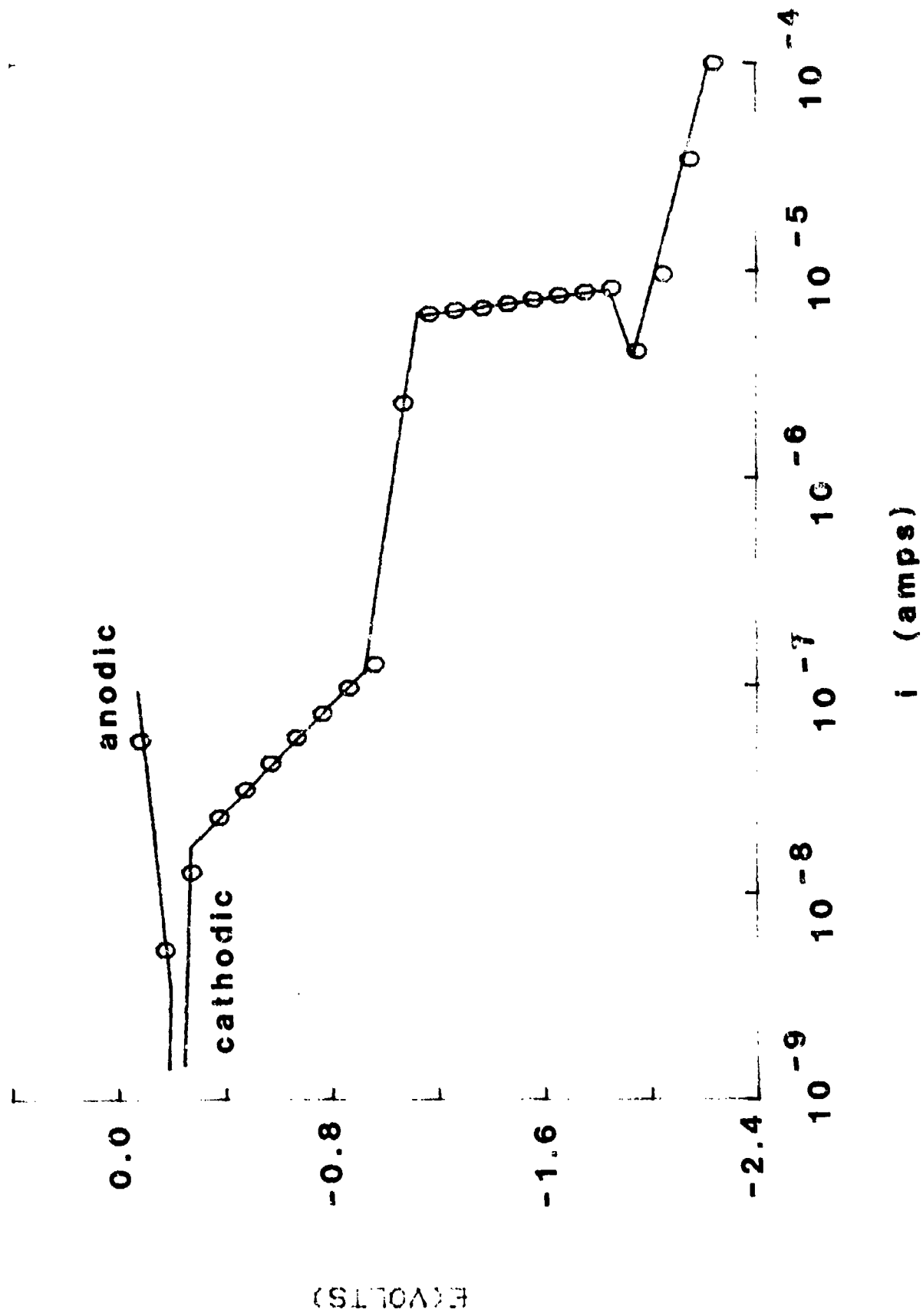


FIG. 17(a) CV OF NITROBENZENE IN 0.4 MeEtImCl MELT

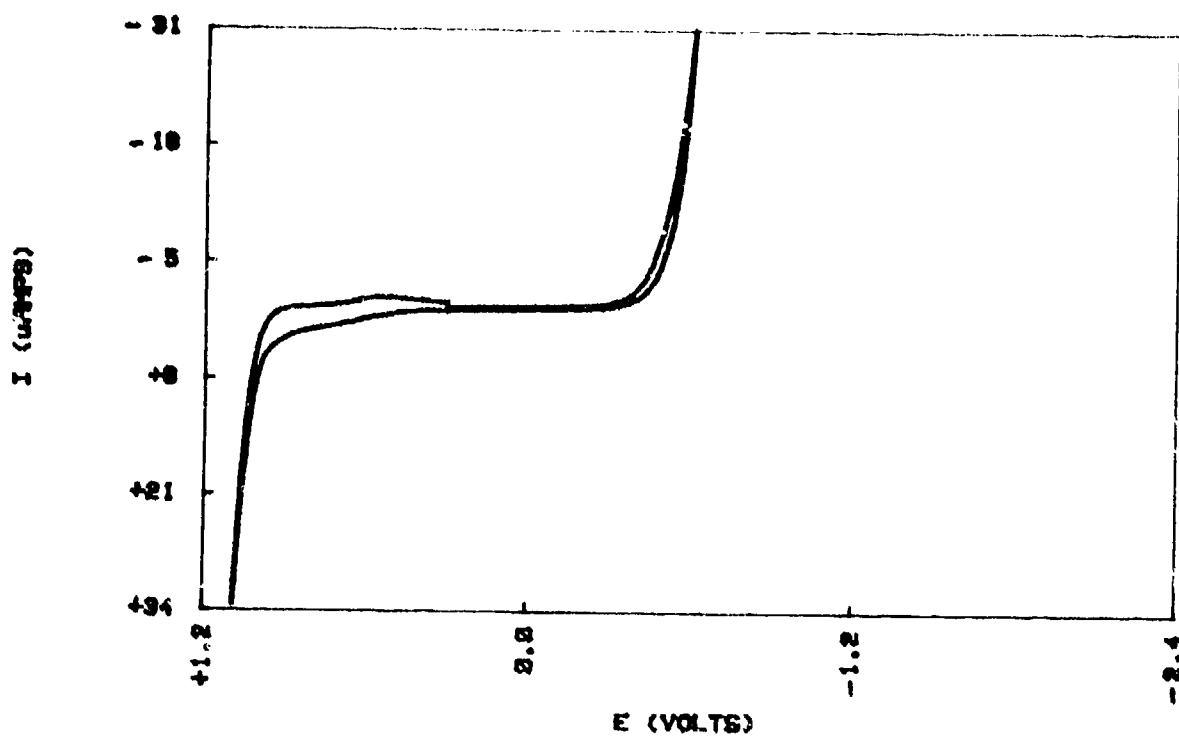


FIG 17(b) CV OF NITROBENZENE IN 0.6 MeEtImCl MELT

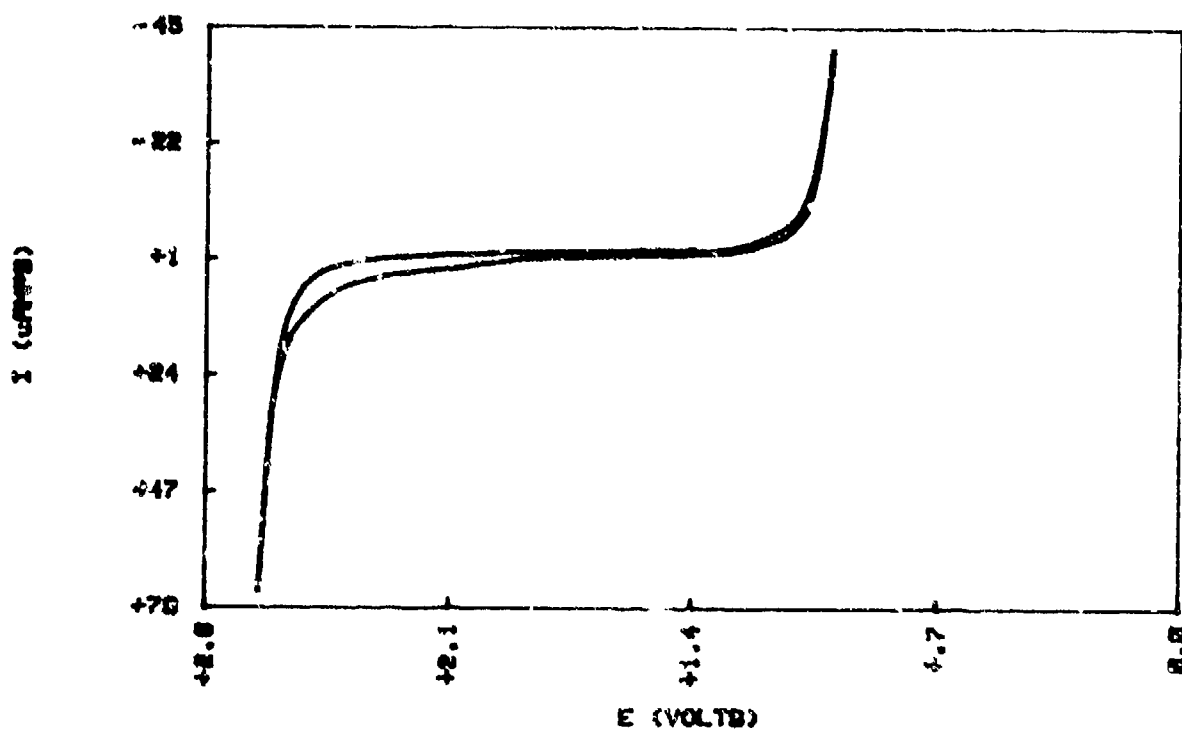


FIG 18 (a) CV OF NITROMETHANE IN 0.4 M₀EtImCl MELT

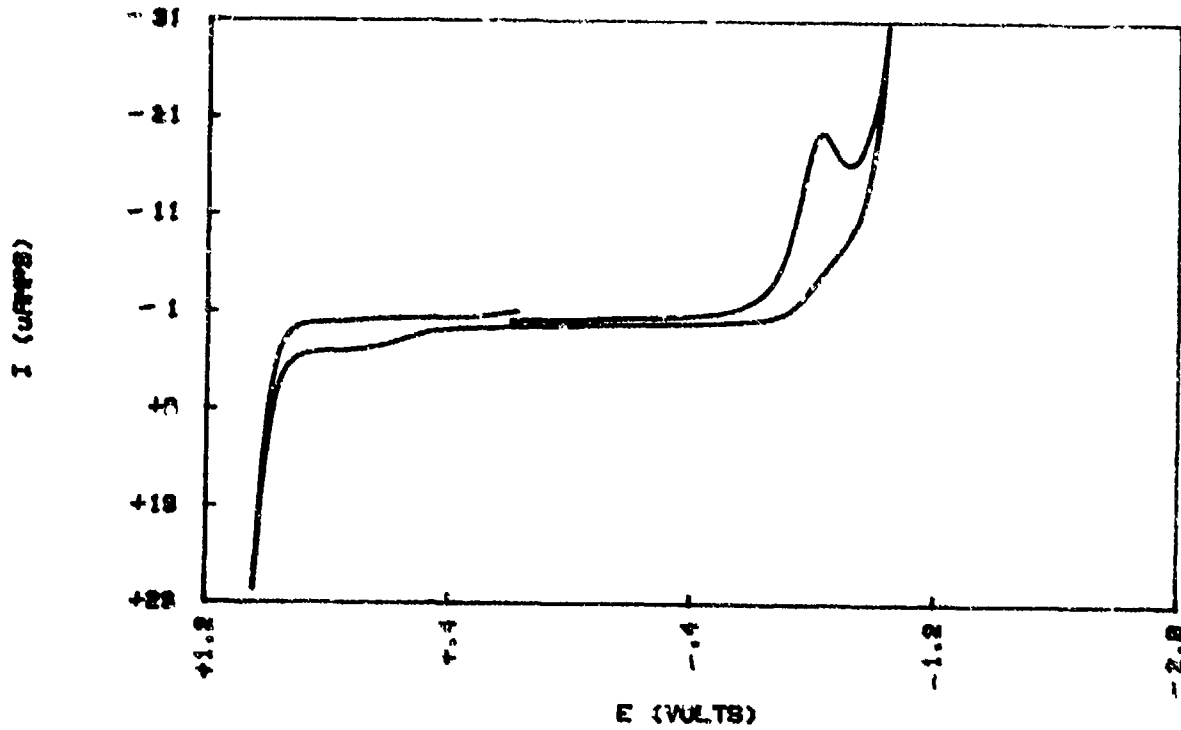


FIG 18 (b) CV OF NITROMETHANE IN 0.6 M₀EtImCl MELT

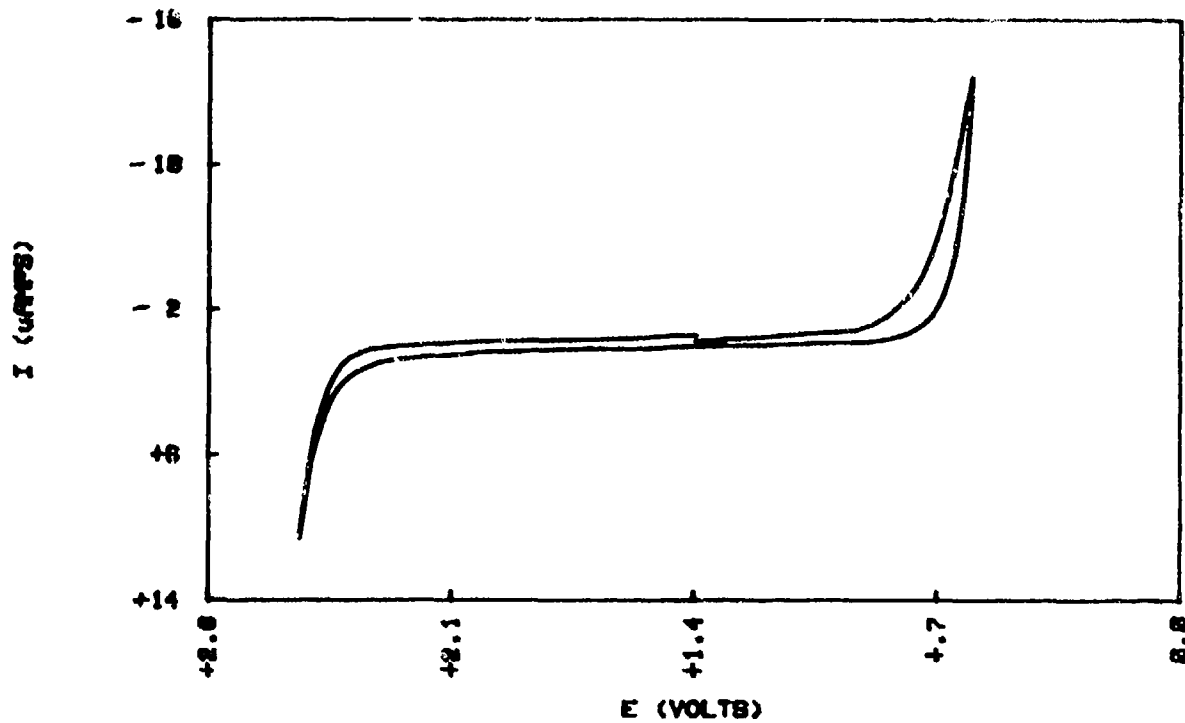


FIG 19 (a) CV OF M-XYLENE IN 0.4 MeEtImCl MELT

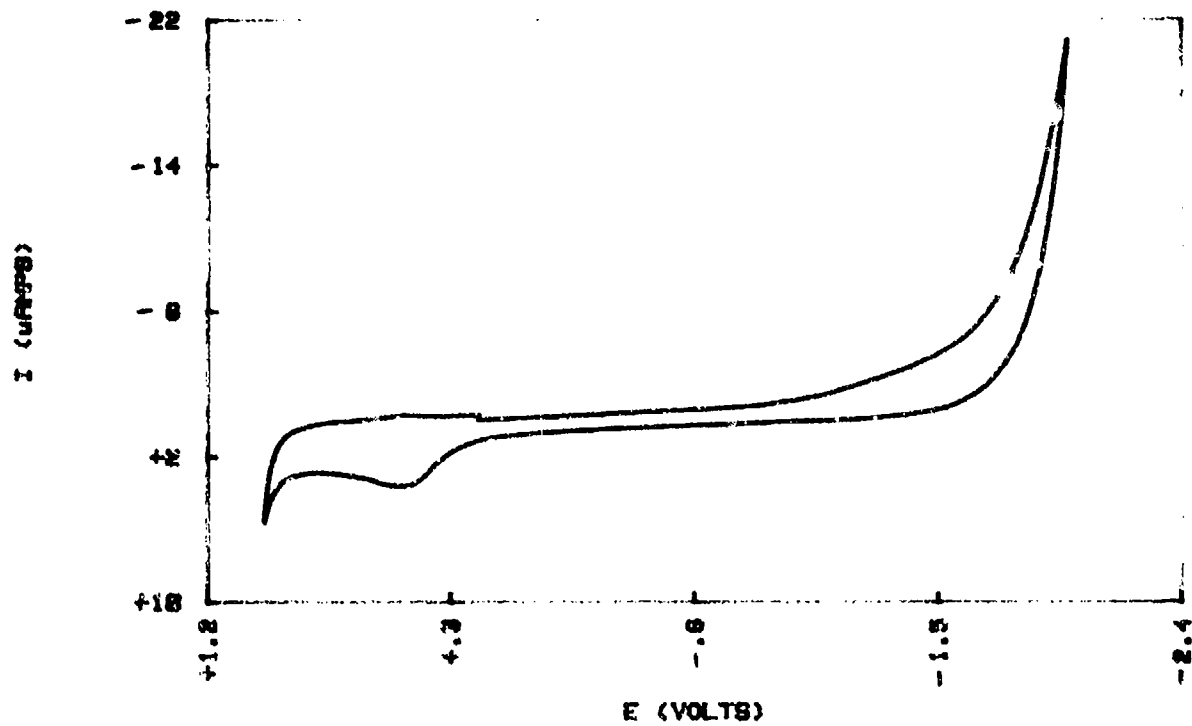


FIG 19(b) CV OF M-XYLENE IN 0.6 MeEtImCl MELT

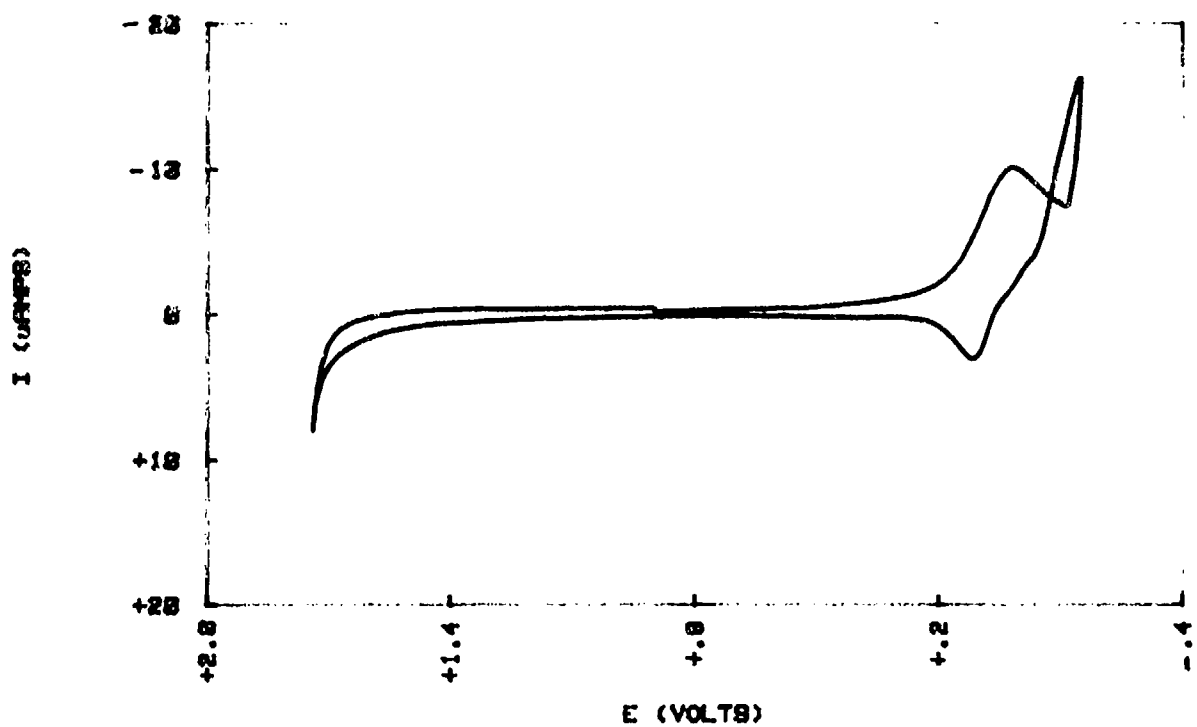


FIG 20 CV OF 33% ACETONITRILE IN 0.5 MeEtImCl MELT

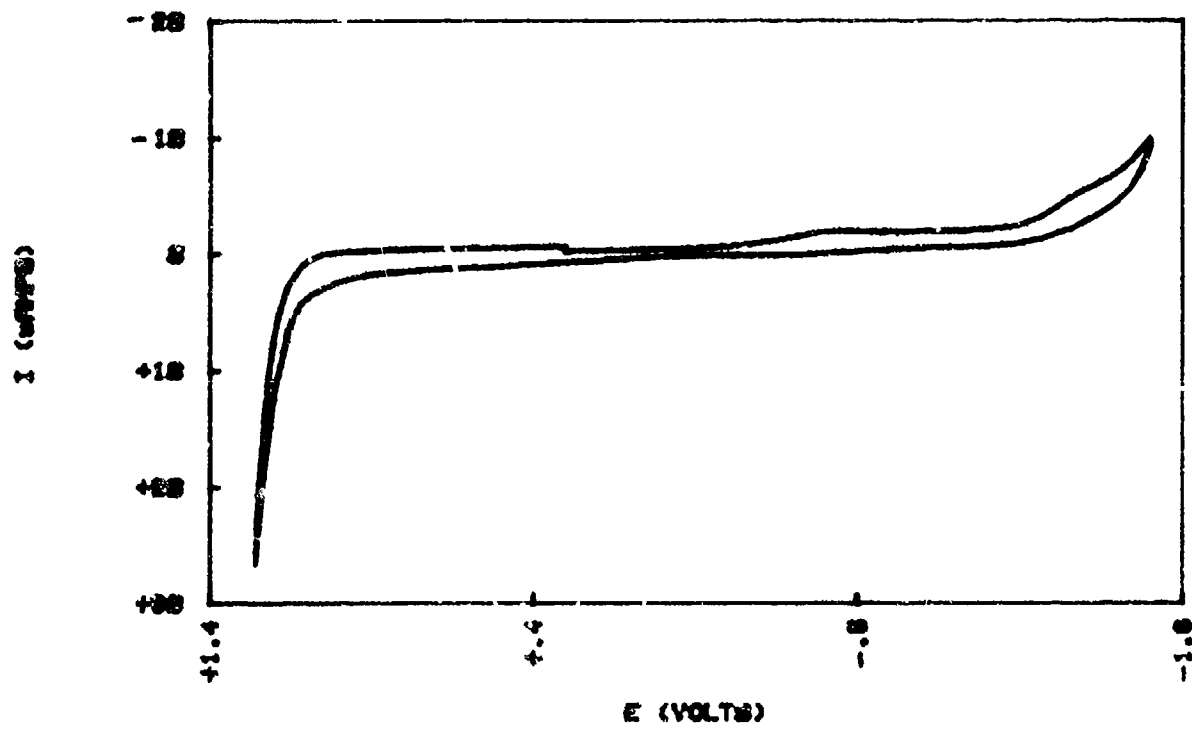


FIG 21 (a) CV OF PROPIONITRILE IN 8.4 MeEtImCl MELT

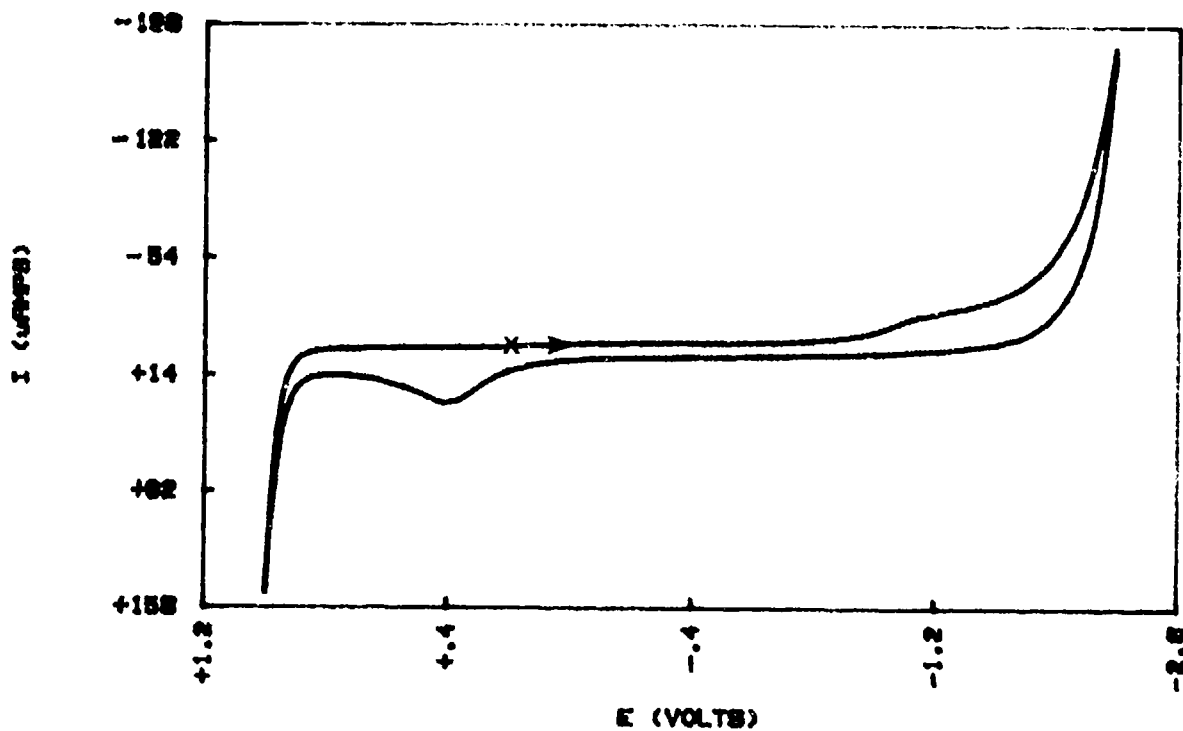


FIG 21 (b) CV OF PROPIONITRILE IN 9.8 MeEtImCl MELT

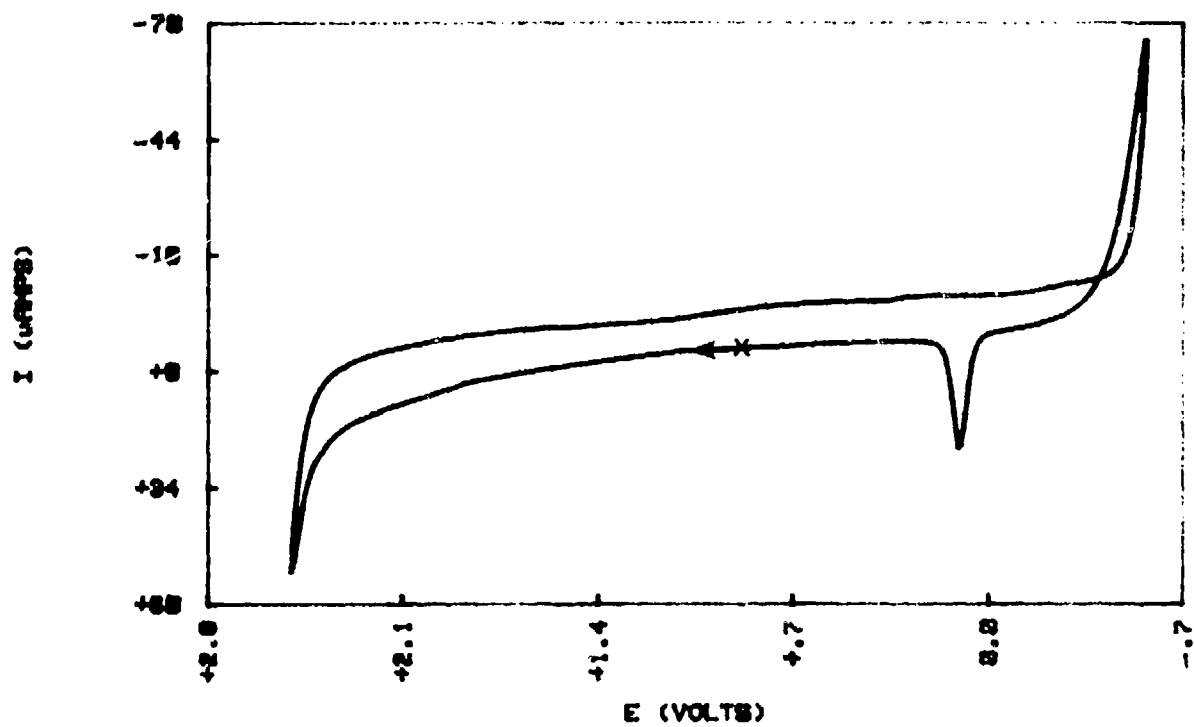


FIG 22(a) CV OF Ag IN BASIC MELT

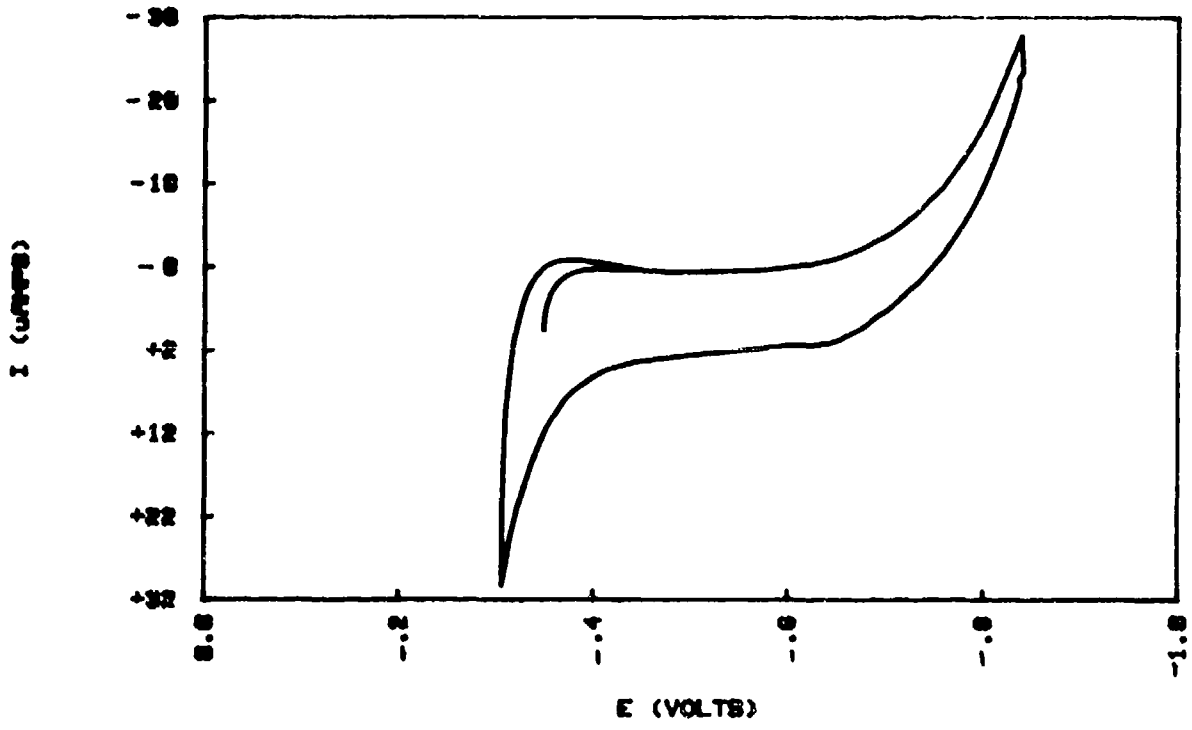


FIG 22(b) CV OF Pg IN ACIDIC MELT

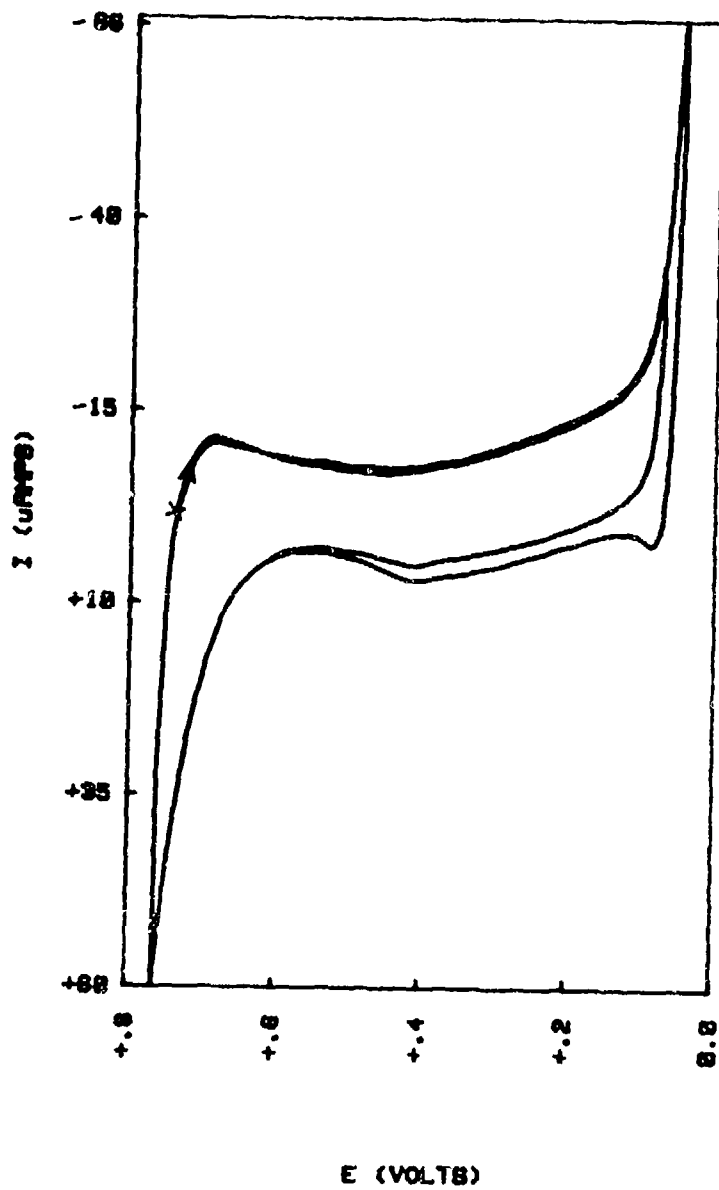


FIG 23 (a) CV OF R1 IN NaBIC MELT

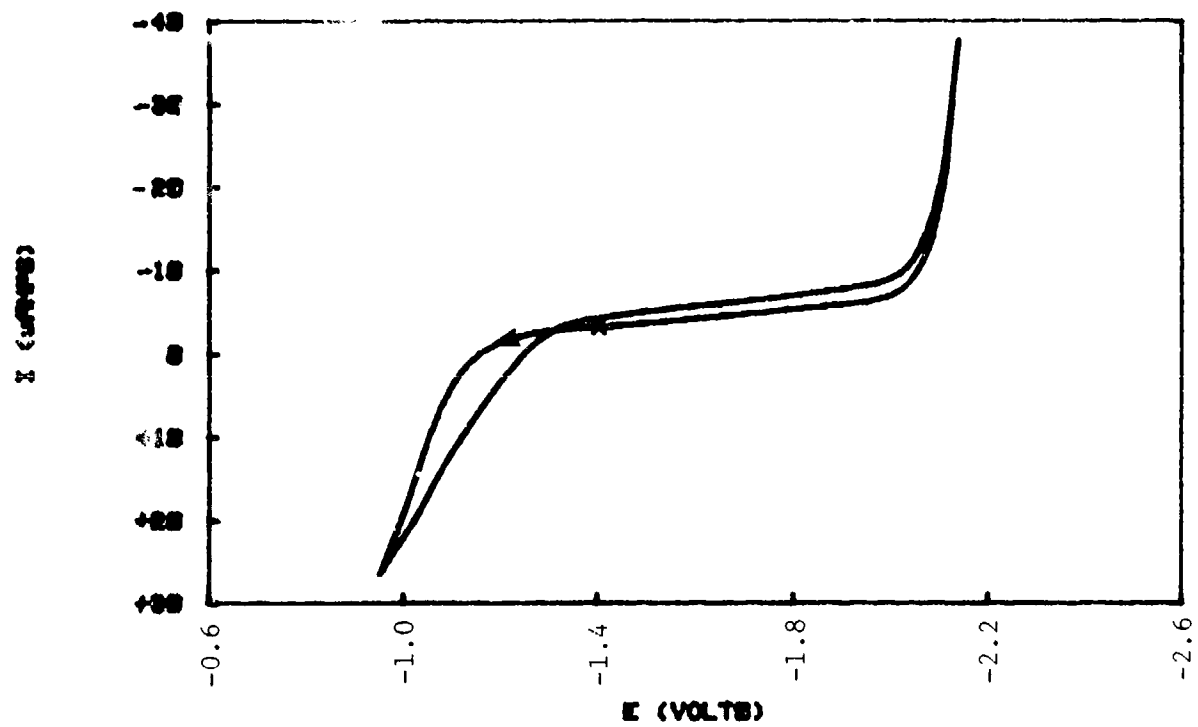


FIG 23(b) CV OF Pt IN ACIDIC MELT

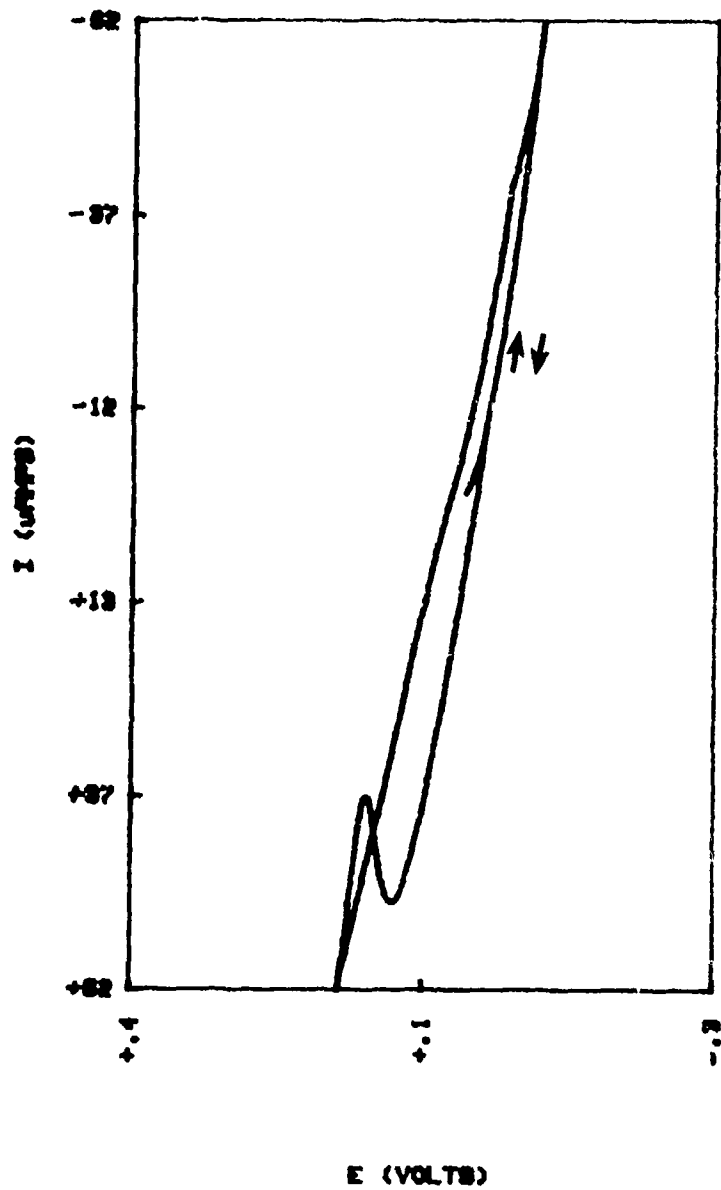


FIG 24 (b) CV OF CU IN ACIDIC MELT

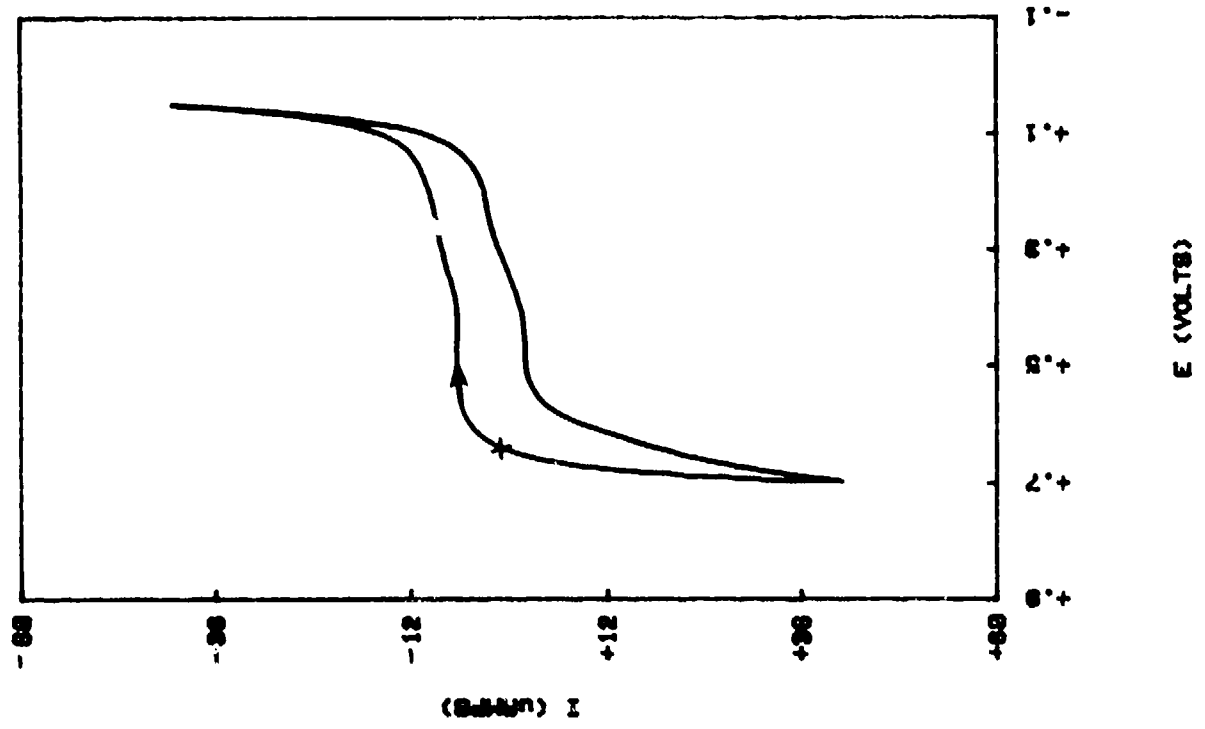


FIG 24 (a) CV OF CU IN BASIC MELT

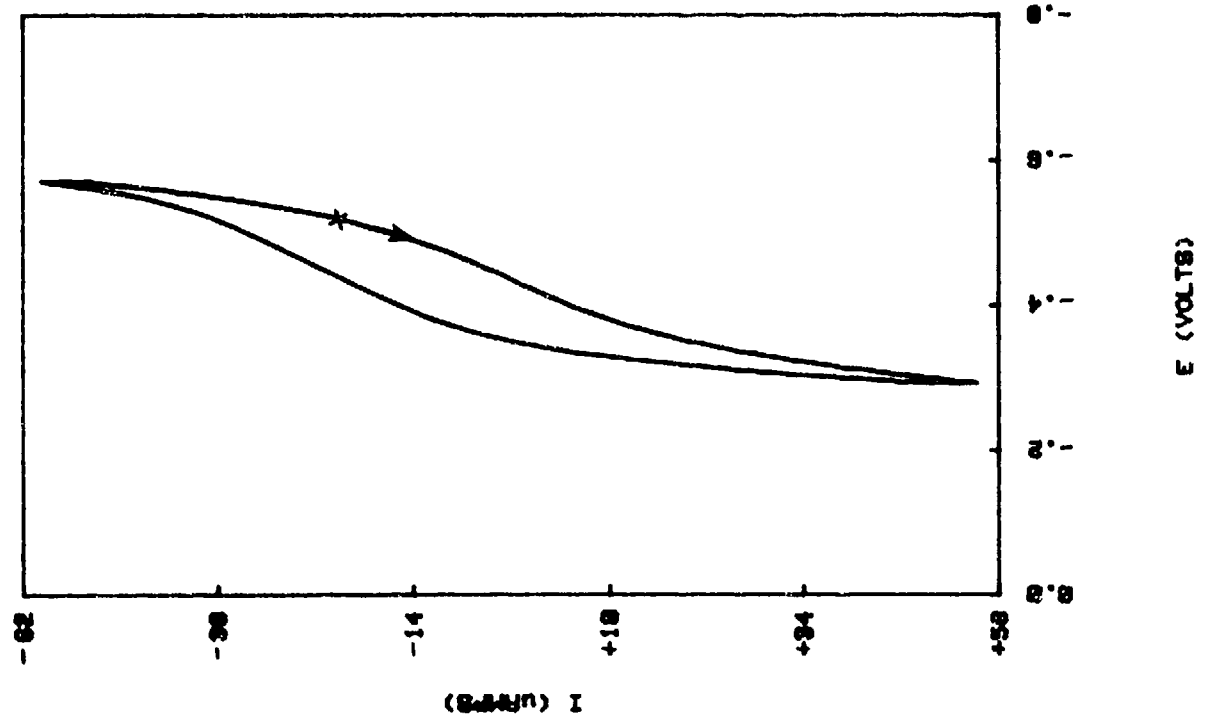


FIG 25 (b) CV OF Fe IN ACIDIC MELT

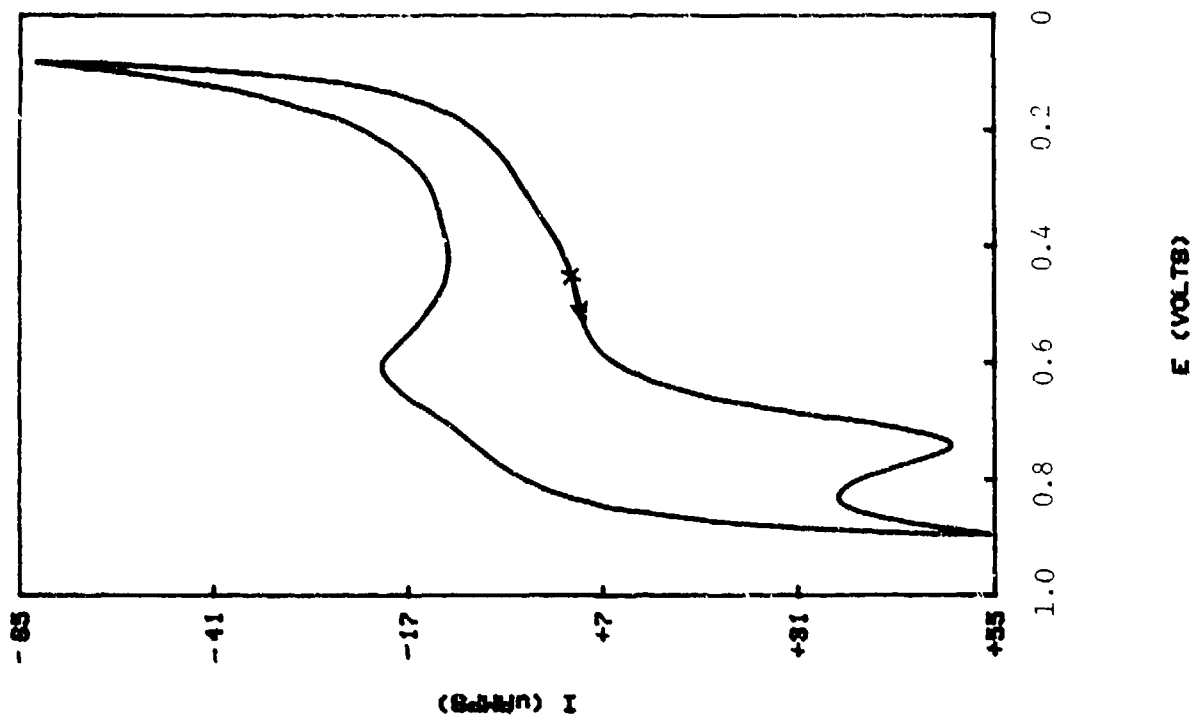


FIG 25 (a) CV OF Fe IN BASIC MELT

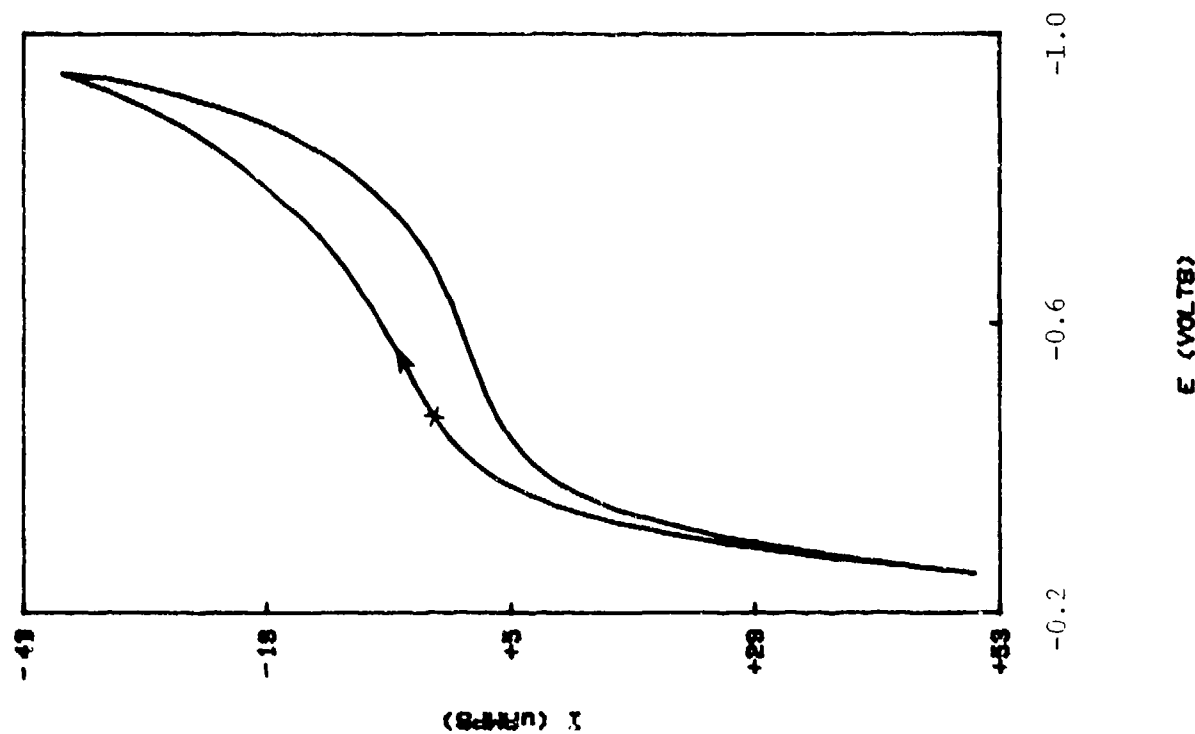


FIG 26 (a) CV OF NI IN BASIC MELT

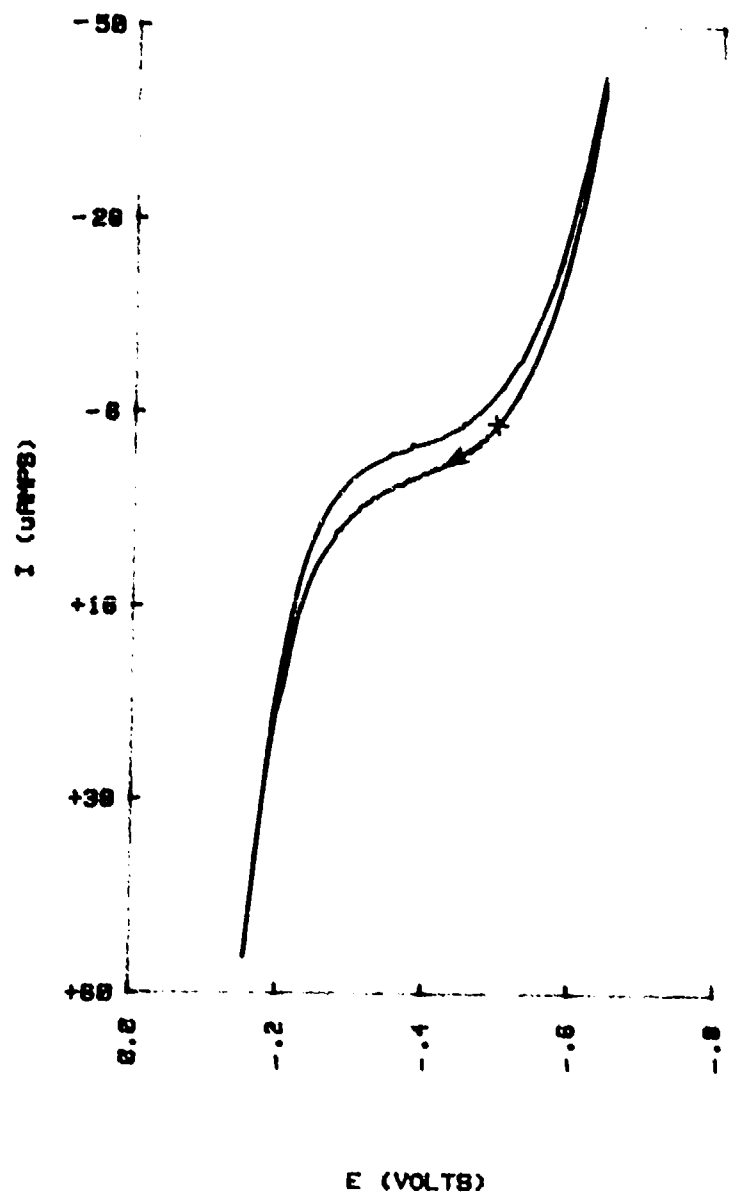


FIG 26 (b) CV OF N1 IN ACIDIC MELT

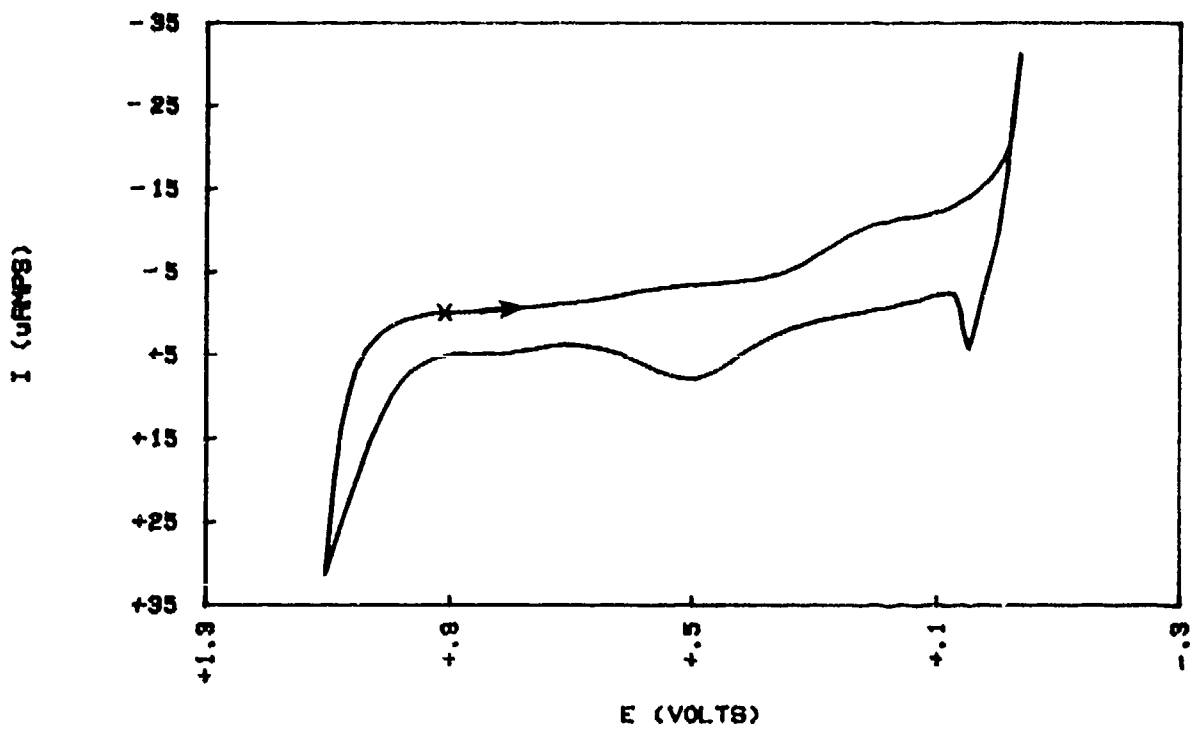


FIG 27(b) CV OF Pb IN BRASIC MELT

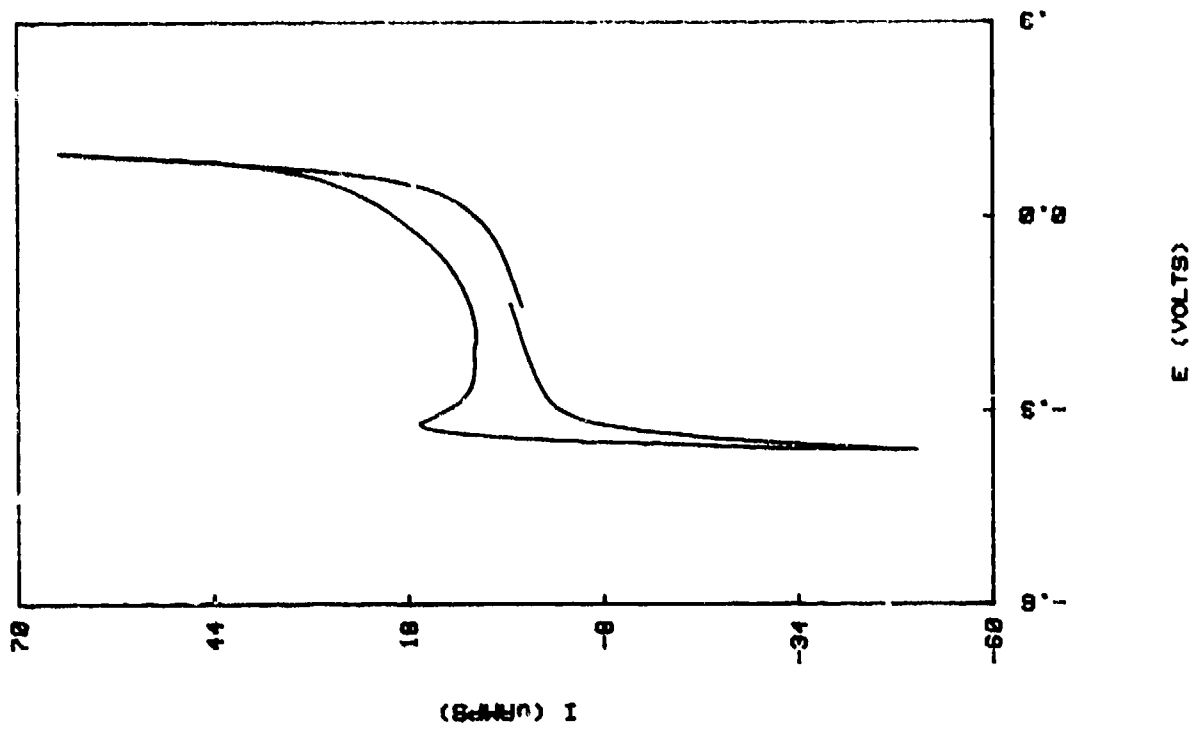


FIG 27 (a) CV OF Pb IN BRASIC MELT

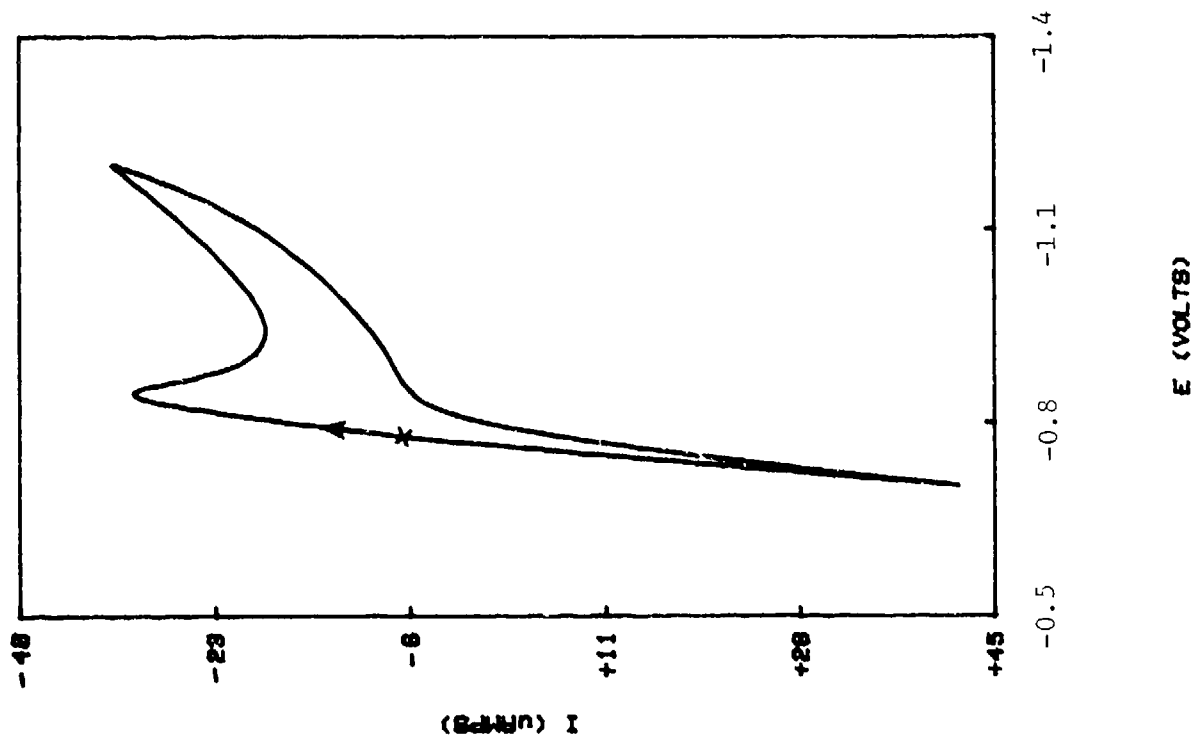


FIG 28 (a) CV OF Pt IN BASIC MELT

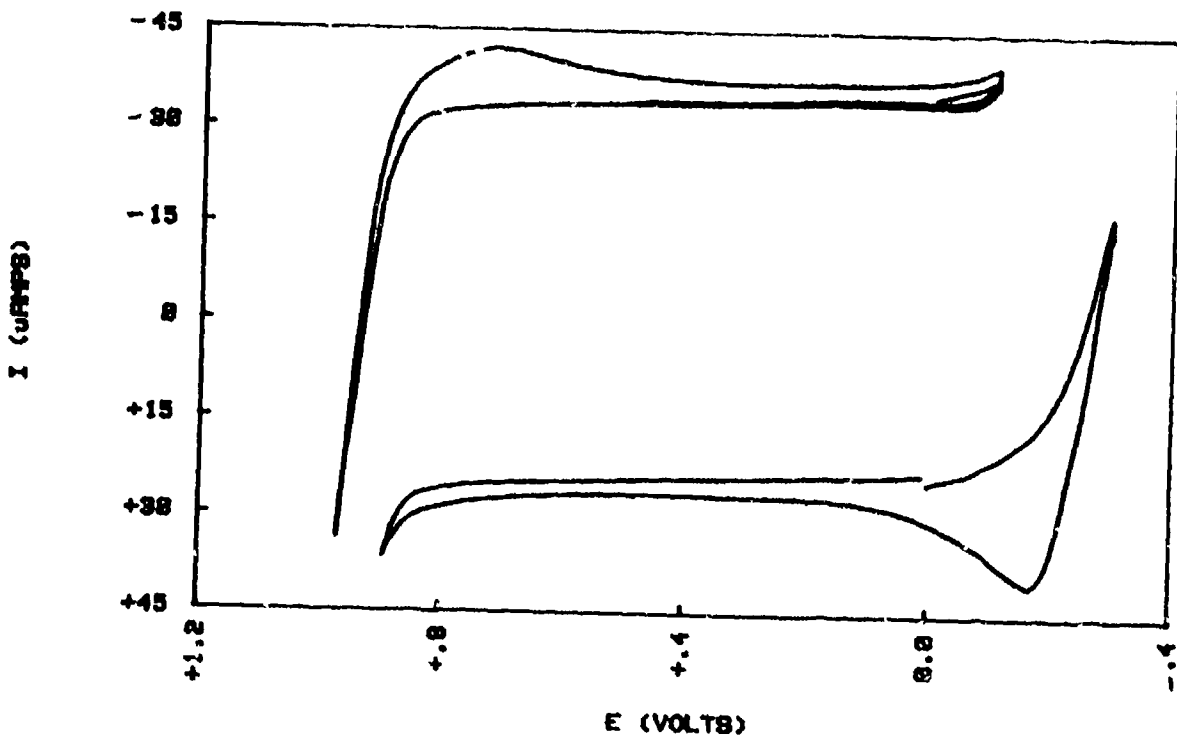


FIG 28 (b) CV OF Pt IN ACIDIC MELT

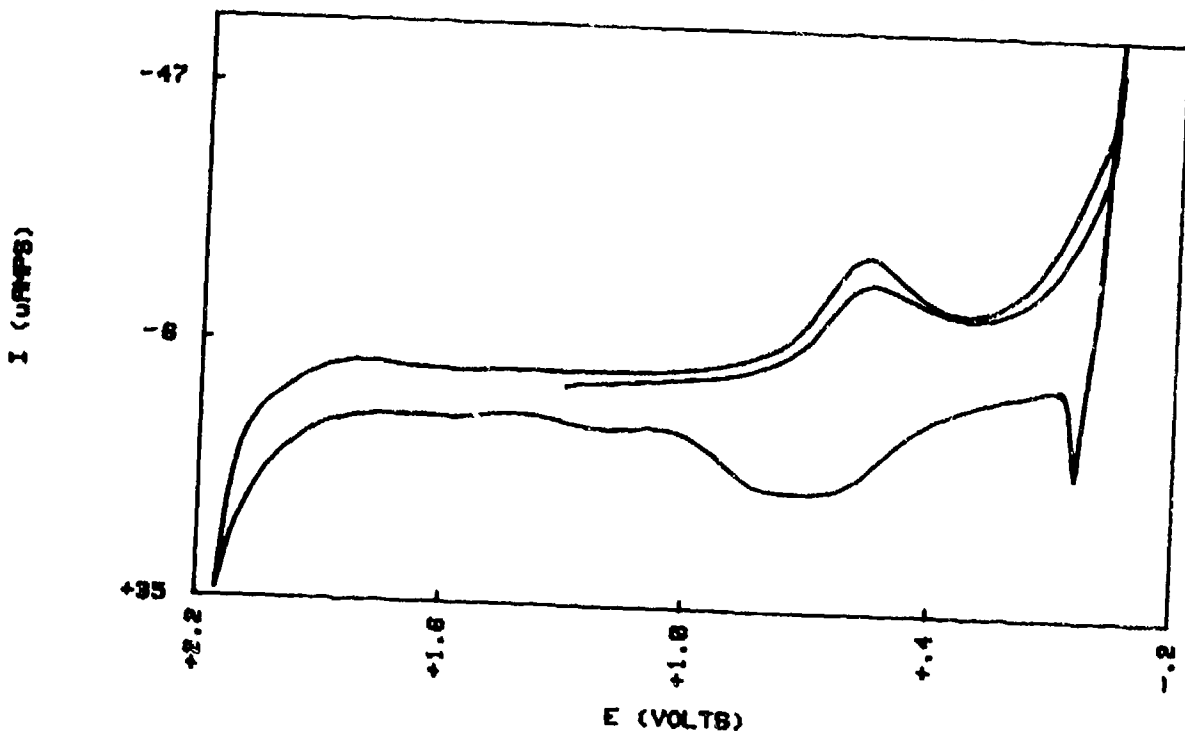


FIG 29 (a) CV OF Ta IN BASIC MELT

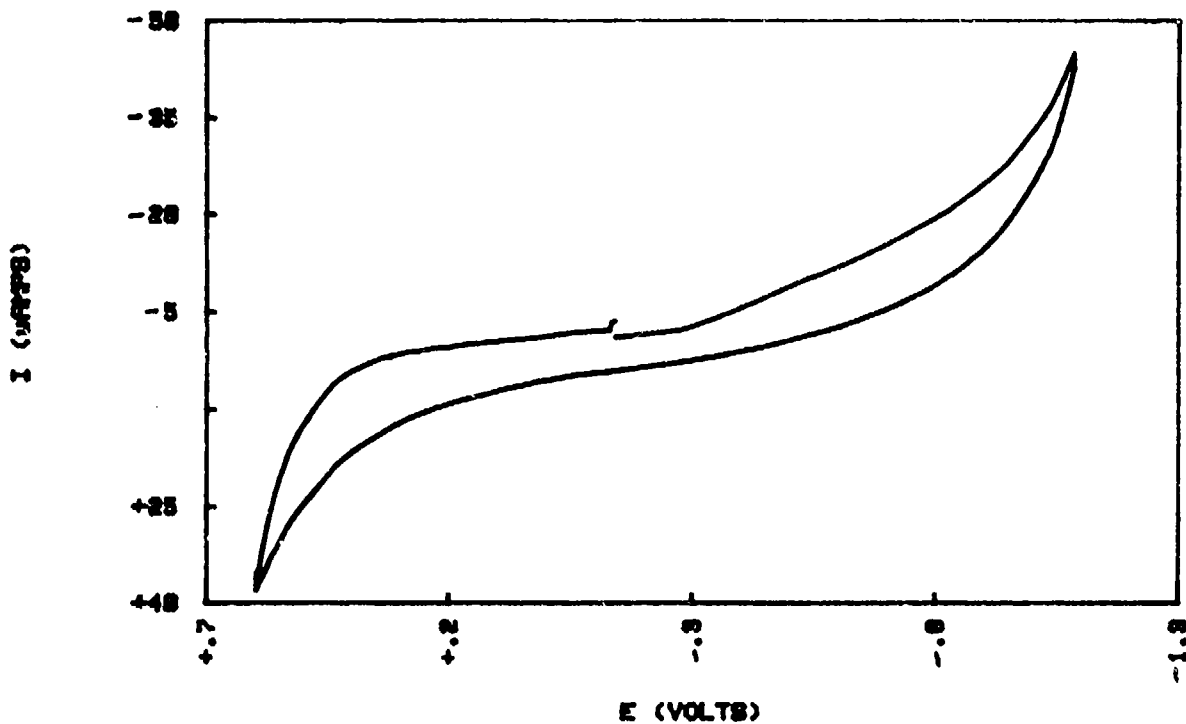


FIG 29 (b) CV OF Ta IN ACIDIC MELT

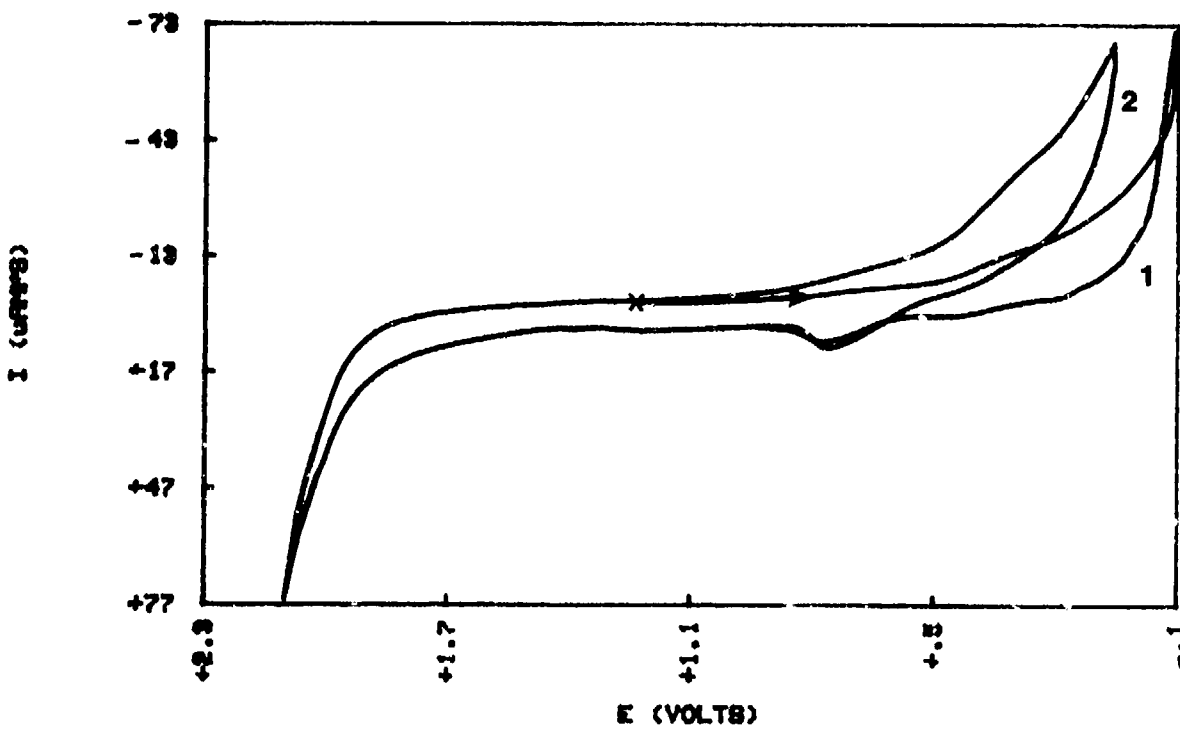


FIG 30(a) CV OF Ta/28XIr IN BASIC MELT

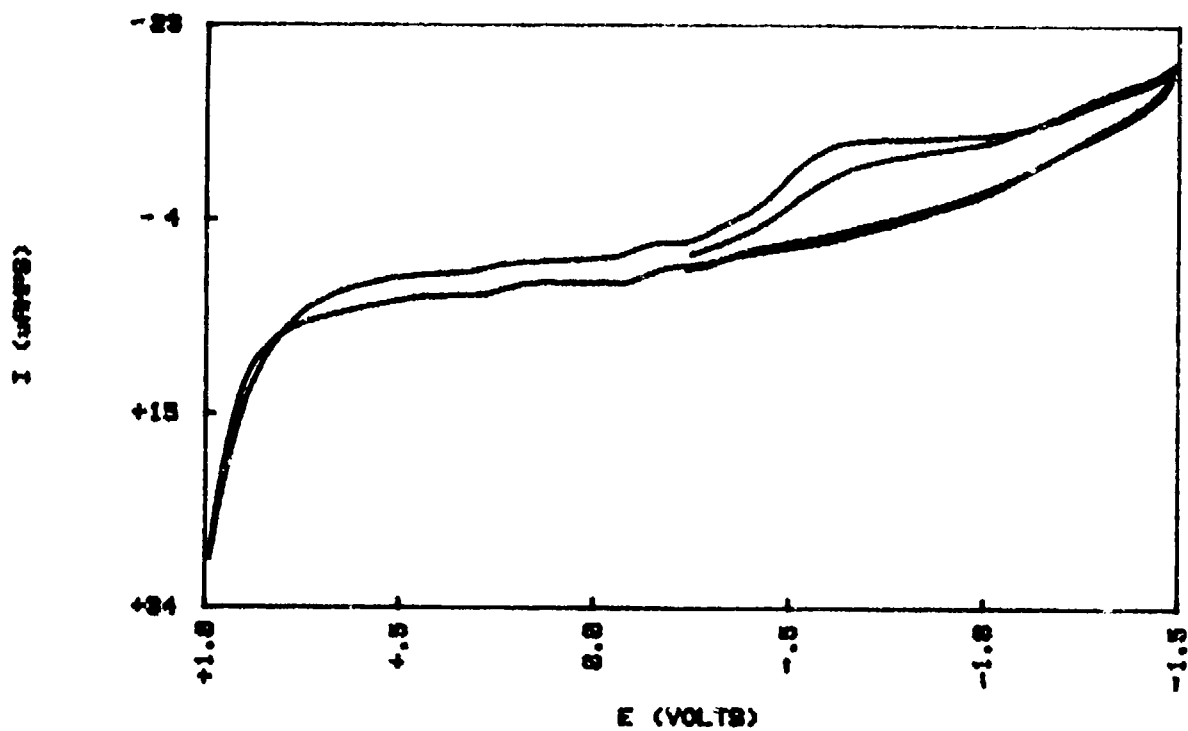


FIG 30(b) CV OF Ta/28XIr IN ACIDIC MELT

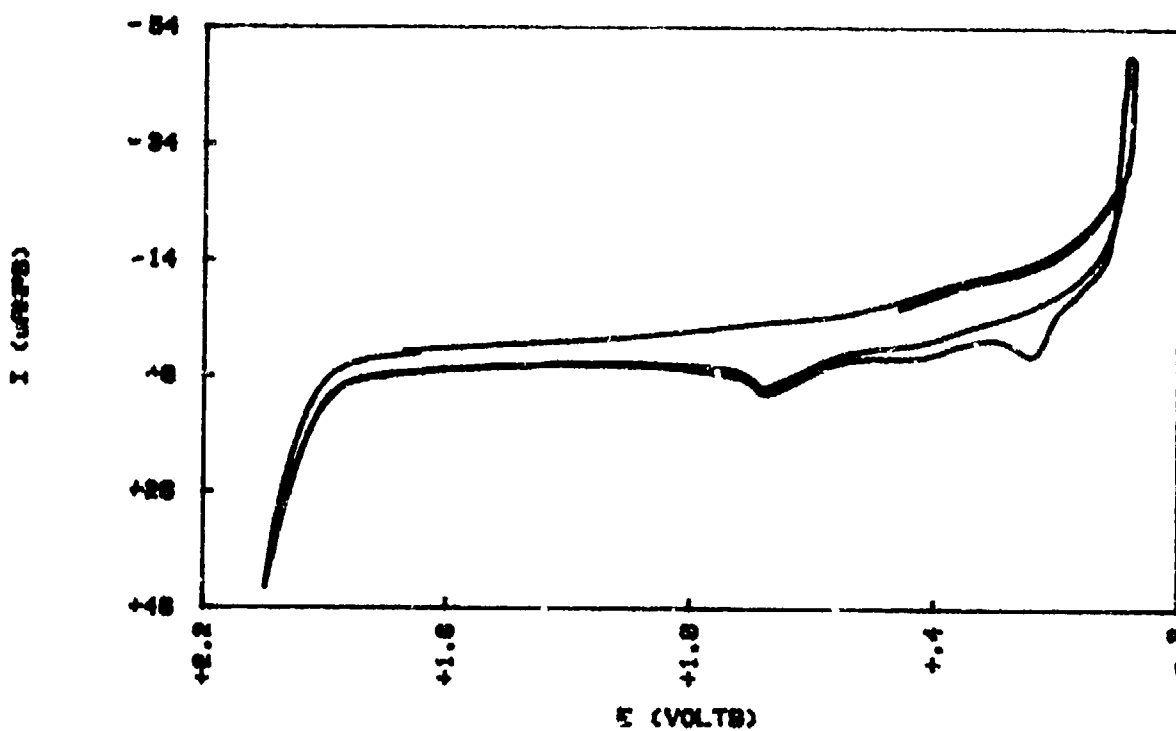


FIG 31 (a) CV OF Ta/200Pt IN BASIC MELT

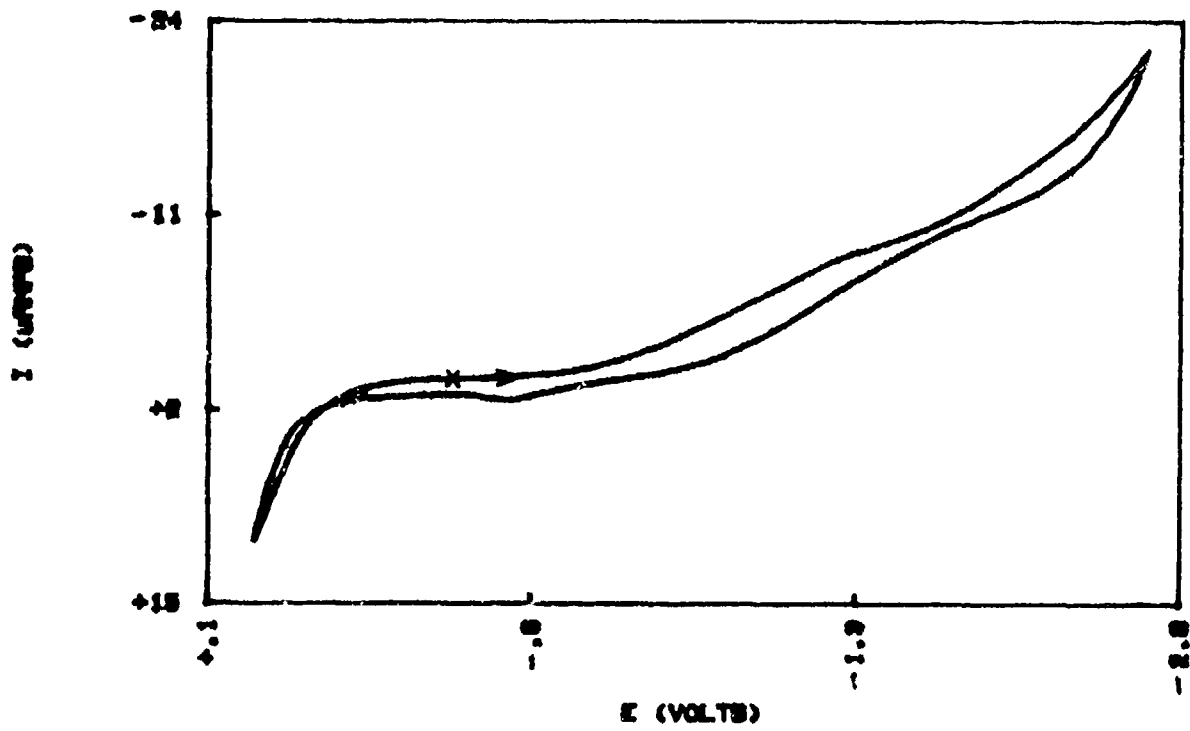


FIG 31 (b) CV OF Ta/200Pt IN ACIDIC MELT

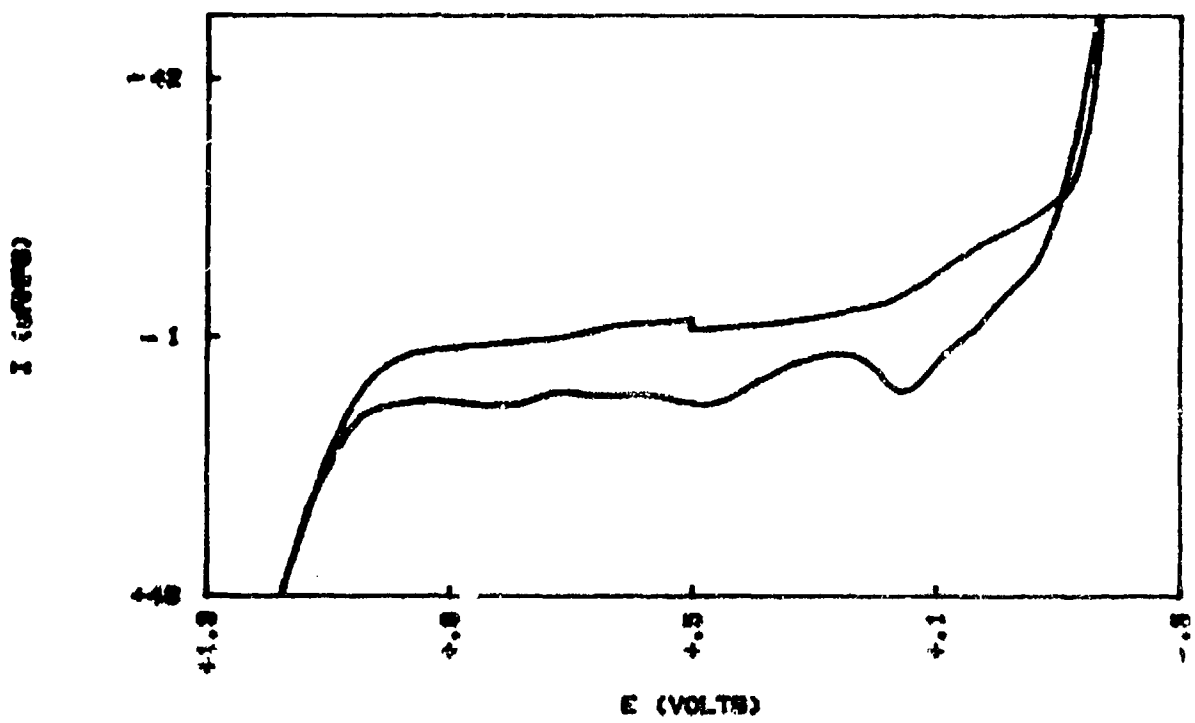


FIG 32 (a) CV OF Ta/200Ru IN BASIC MELT

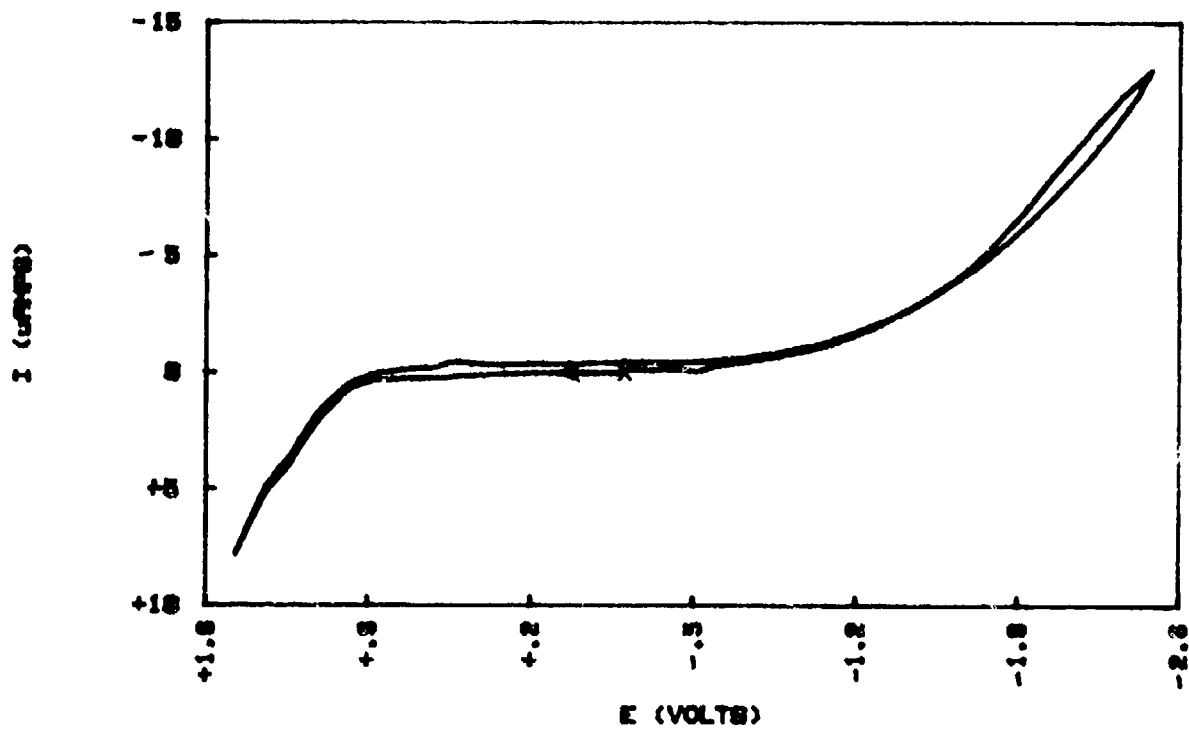


FIG 32 (b) CV OF Ta/200Ru IN ACIDIC MELT

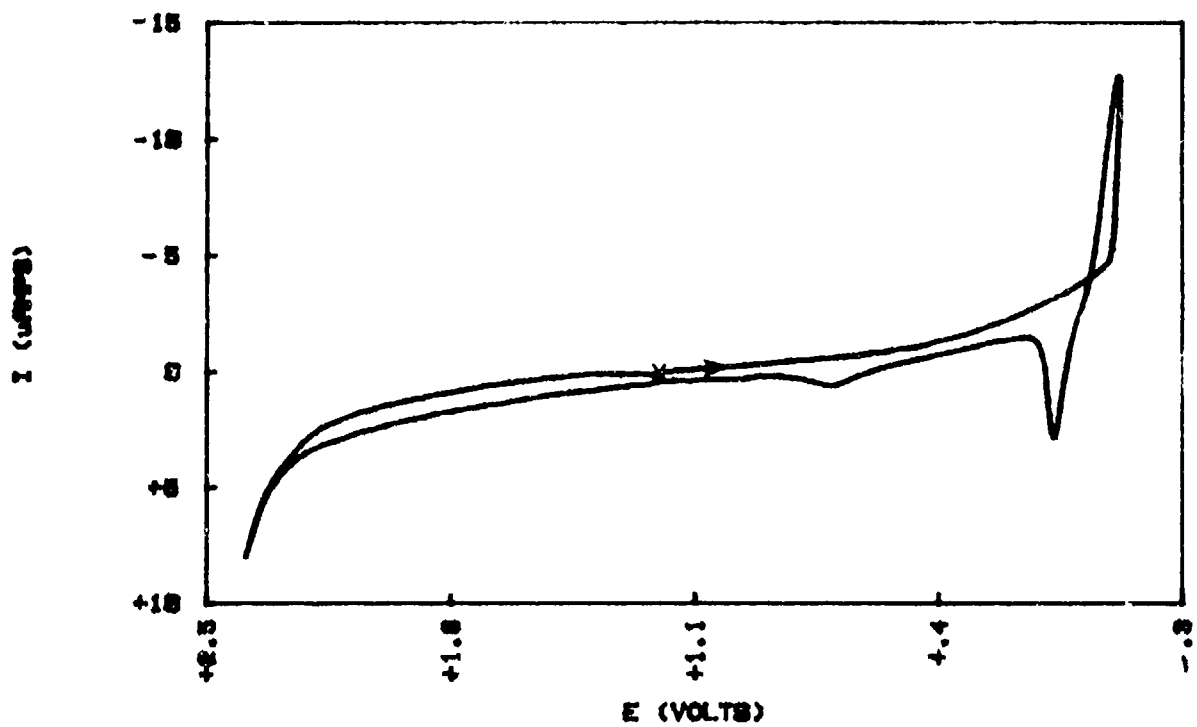


FIG 33 (a) CV OF T1/2001P IN BASIC MELT

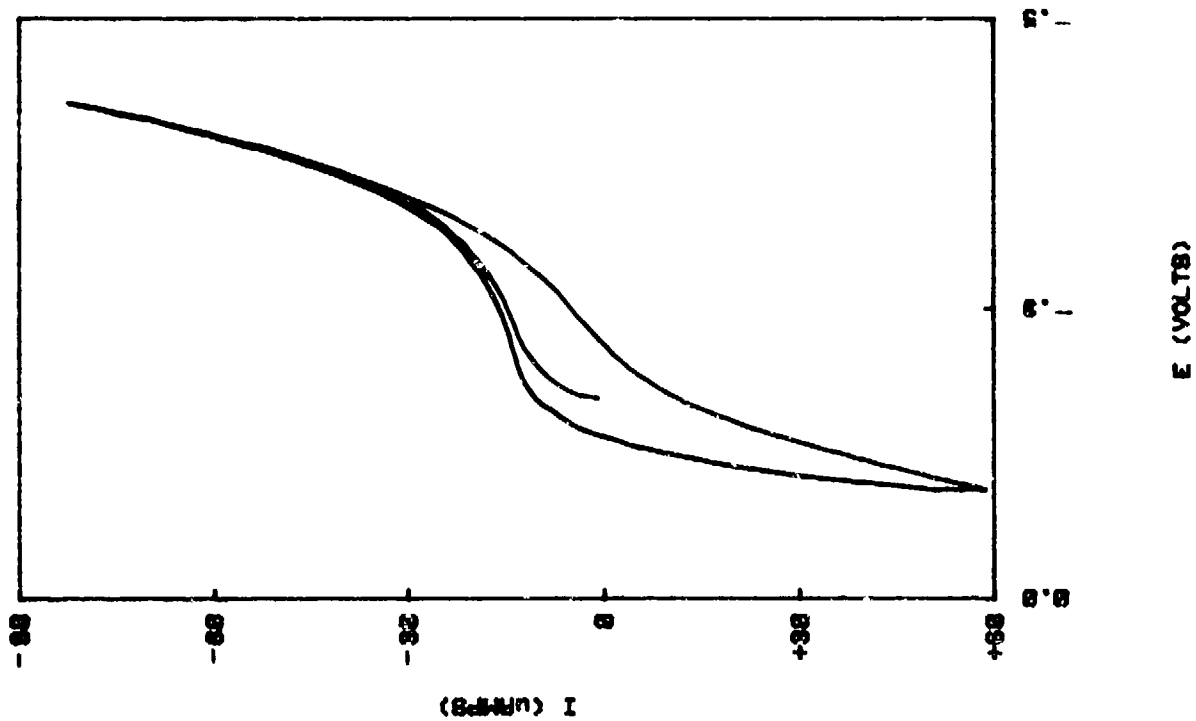


FIG 33 (b) CV OF T1/2001P IN ACIDIC MELT

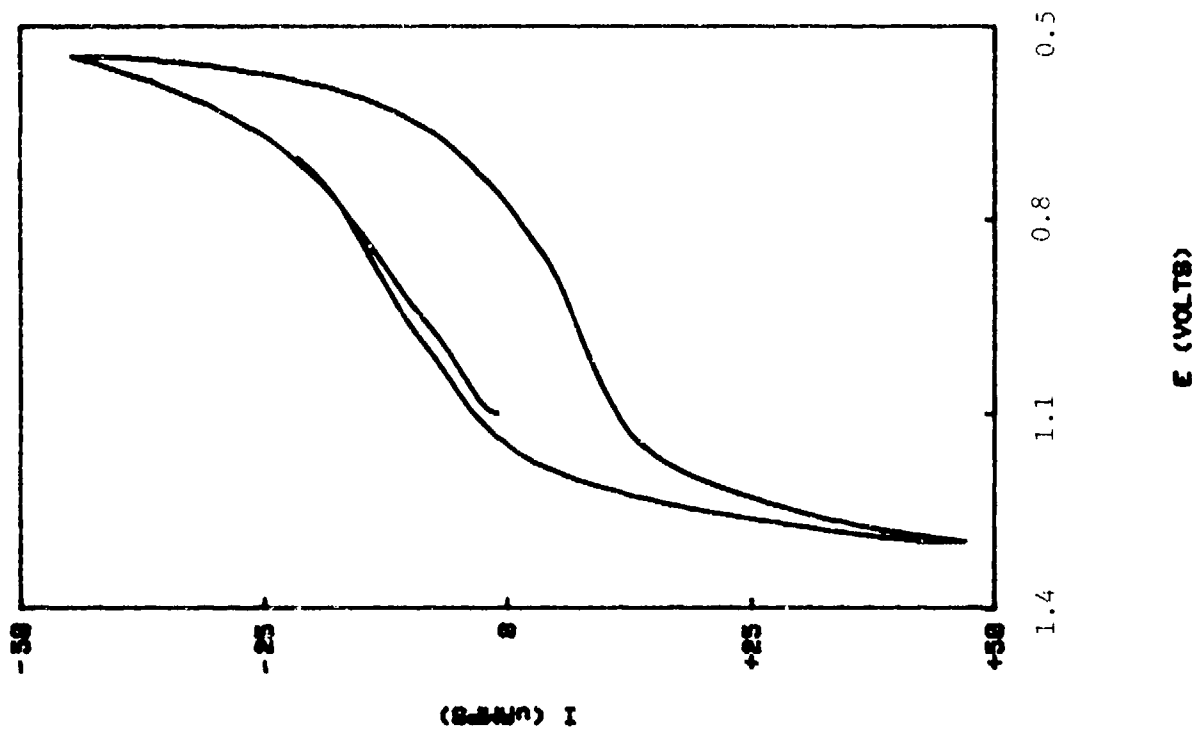


FIG 34 (a) CV OF Ti/5XPt IN BRBIC MELT

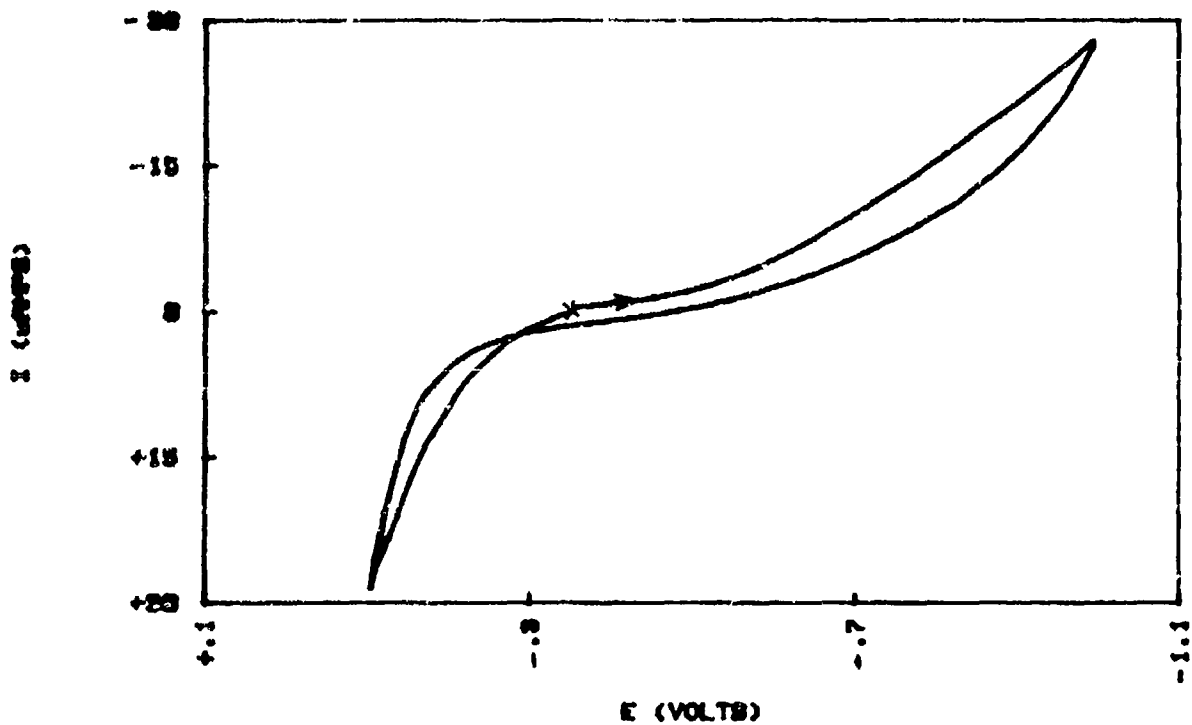


FIG 34 (b) CV OF T1/SAP₆ IN ACIDIC MELT

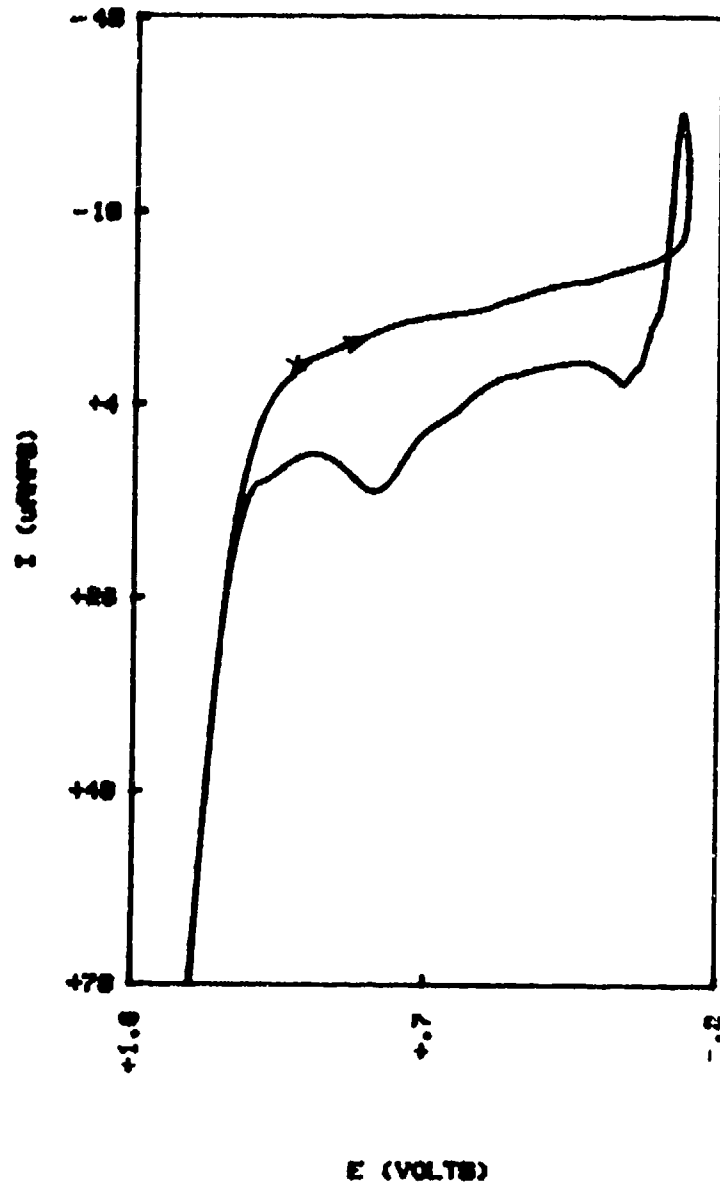


FIG 35 (a) CV OF T1/18xPt IN BASIC MELT

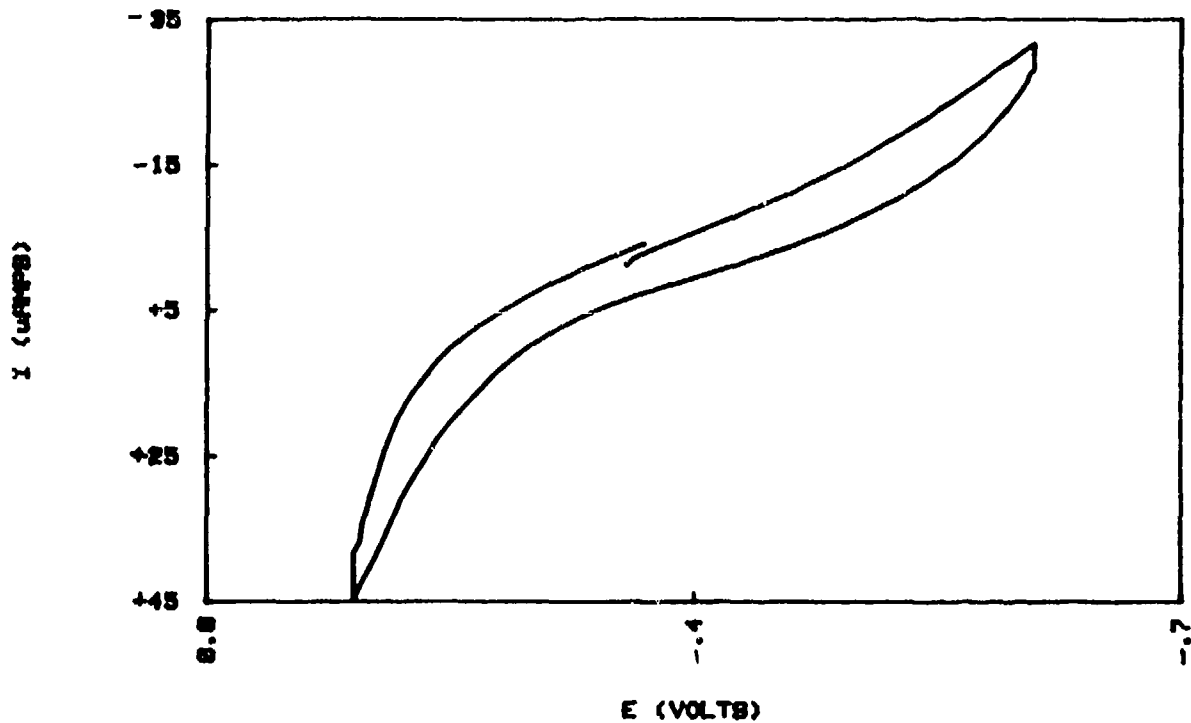


FIG 35 (b) CV OF T1/10X% IN ACIDIC MELT

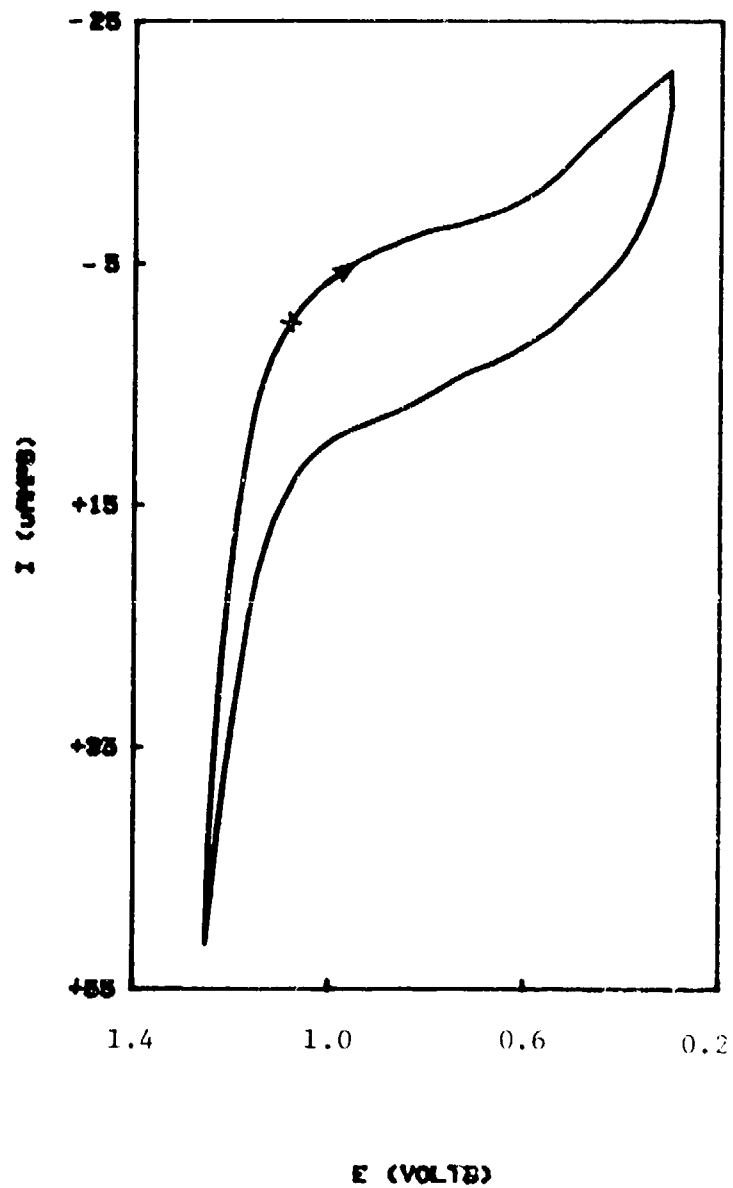


FIG 36 (a) CV OF T1/2800Pt IN BASIC MELT

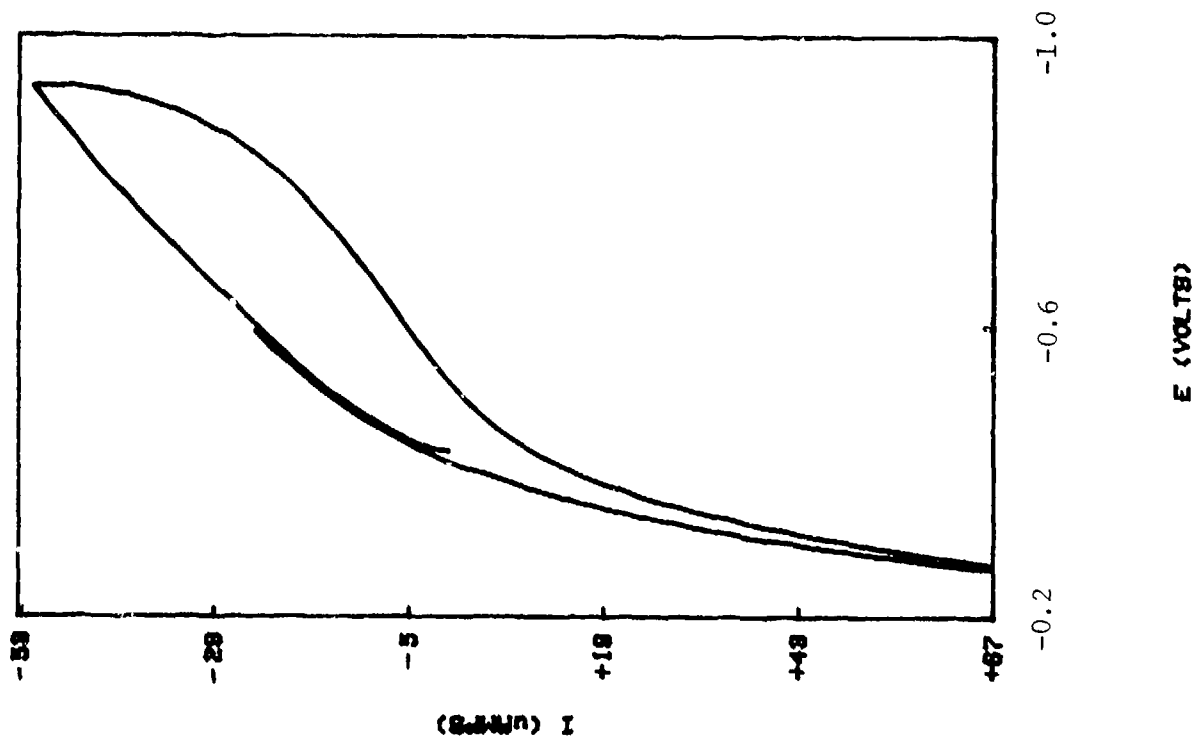


FIG 36 (b) CV OF T1/2800Pt IN ACIDIC MELT

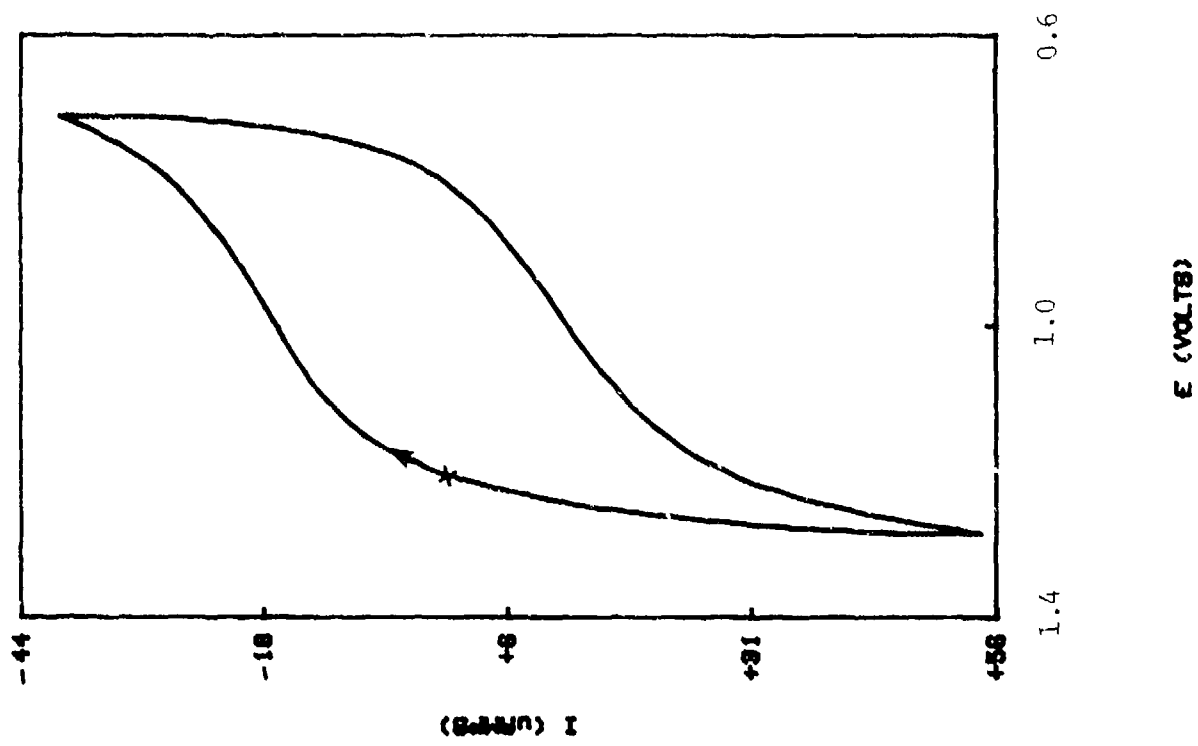


FIG 37 (a) CV OF T1/200Pt IN BASIC MELT

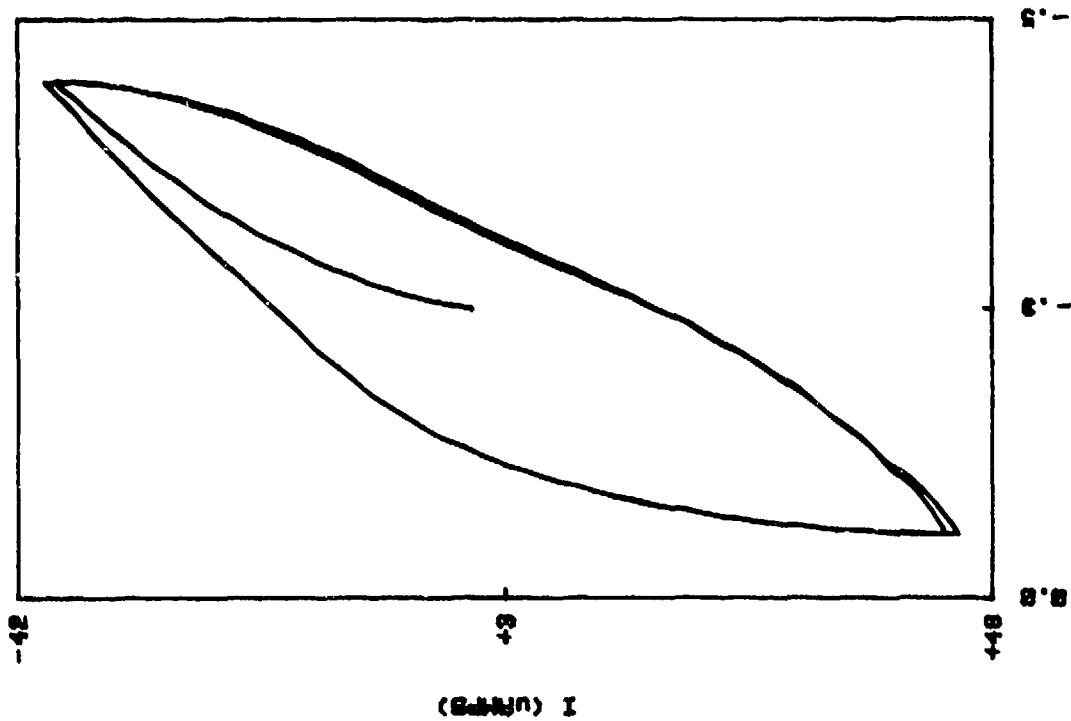


FIG 37 (b) CV OF T1/200Pt IN ACIDIC MELT

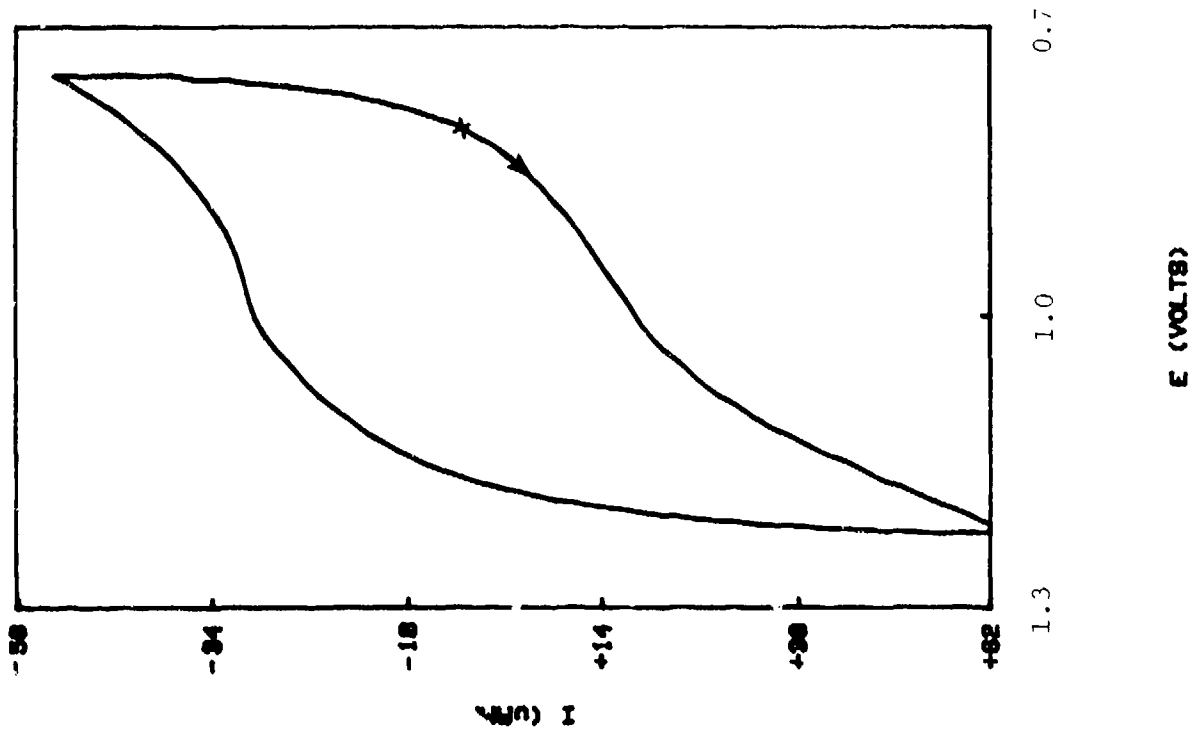


FIG 38 CV OF Ti/30X% IN BASIC MELT

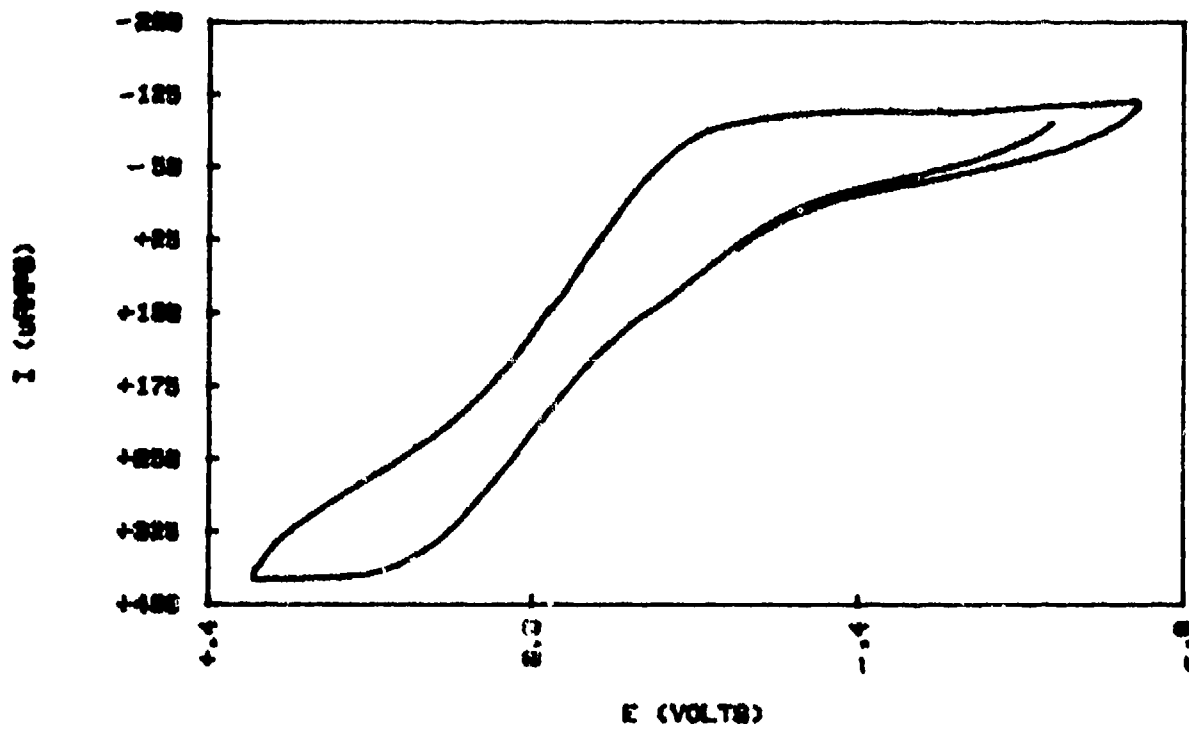


FIG 39 (a) CV OF $Ti/ZrRu$ IN BASIC MELT

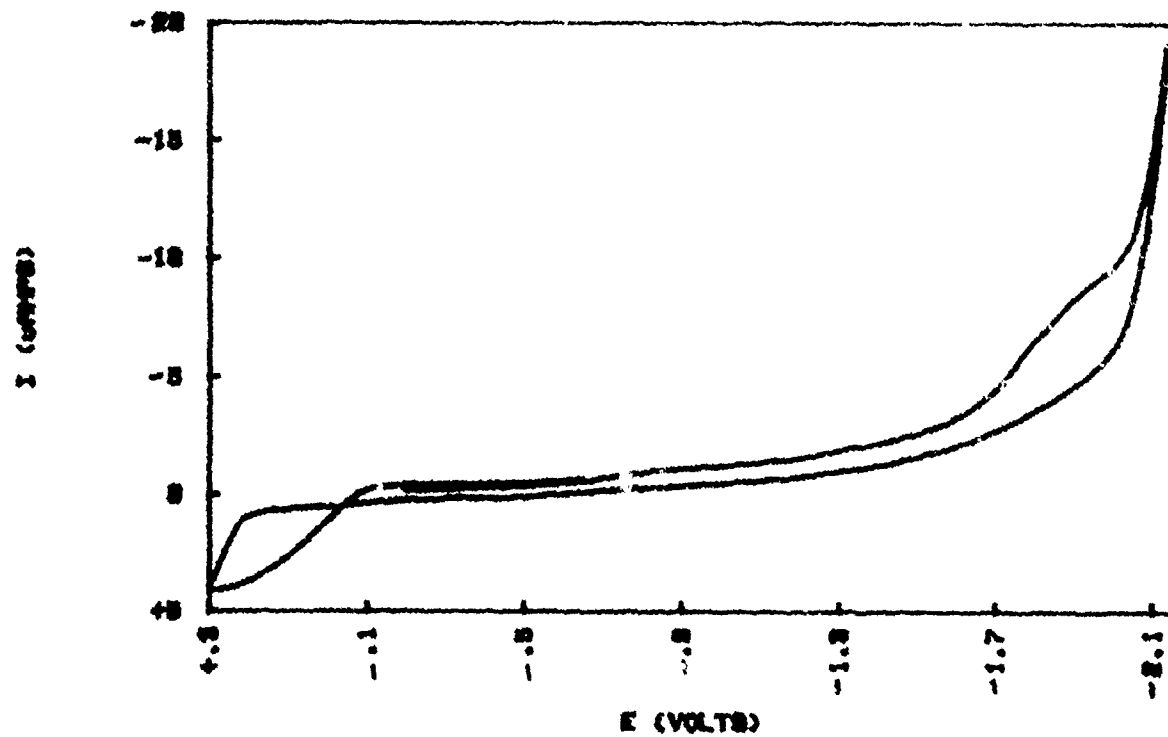


FIG 39 (b) CV OF $Ti/ZrRu$ IN ACIDIC MELT

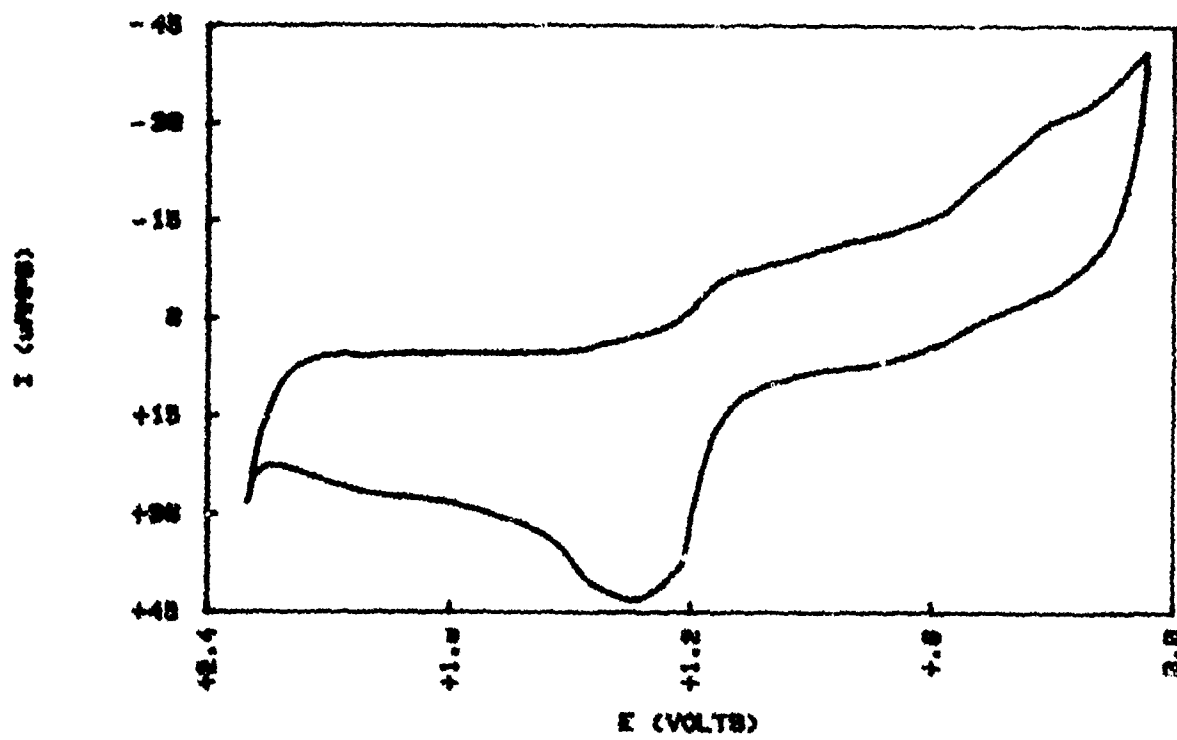
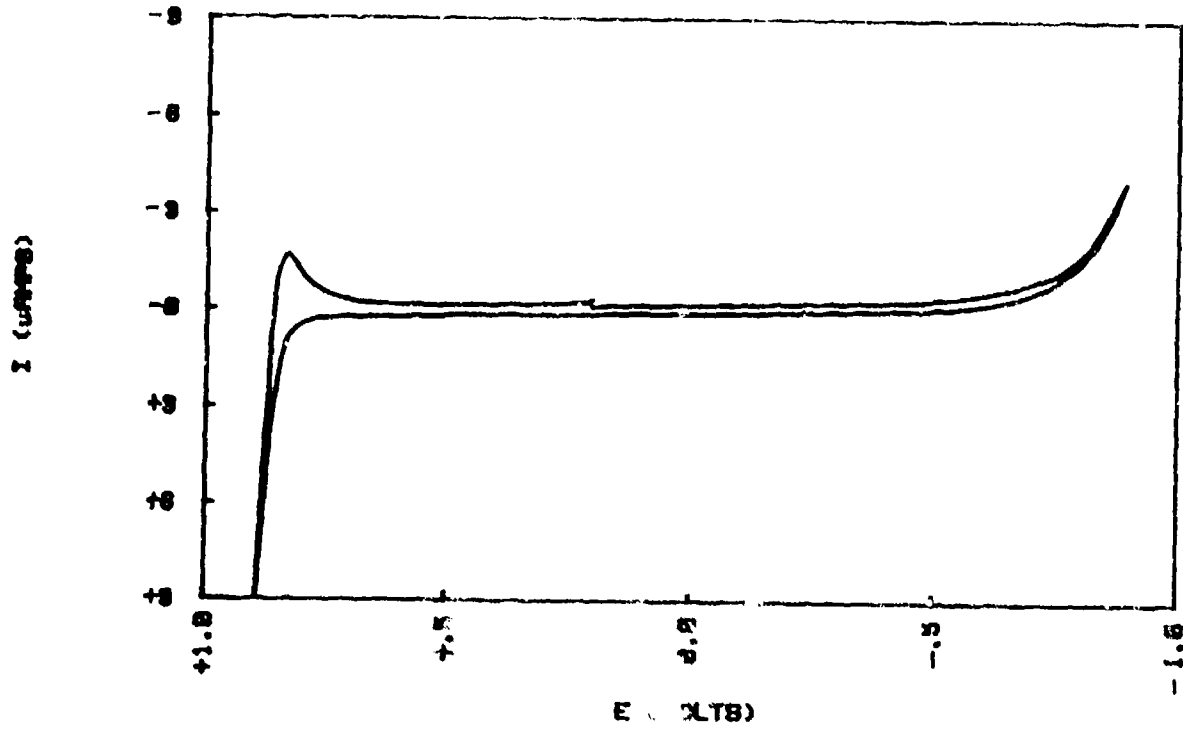


FIG 40(a) CV OF W IN BASIC MELT



40 (b) CV OF W IN ACIDIC MELT

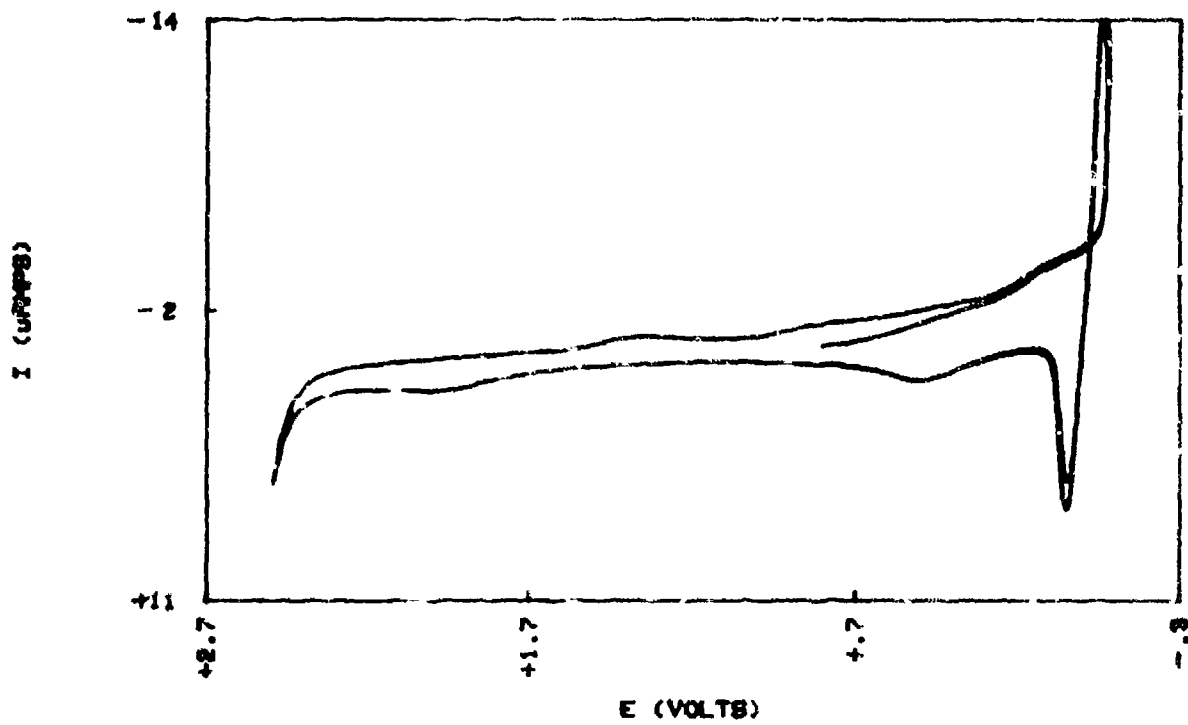


FIG 42 (a) CV OF Au IN BASIC MELT

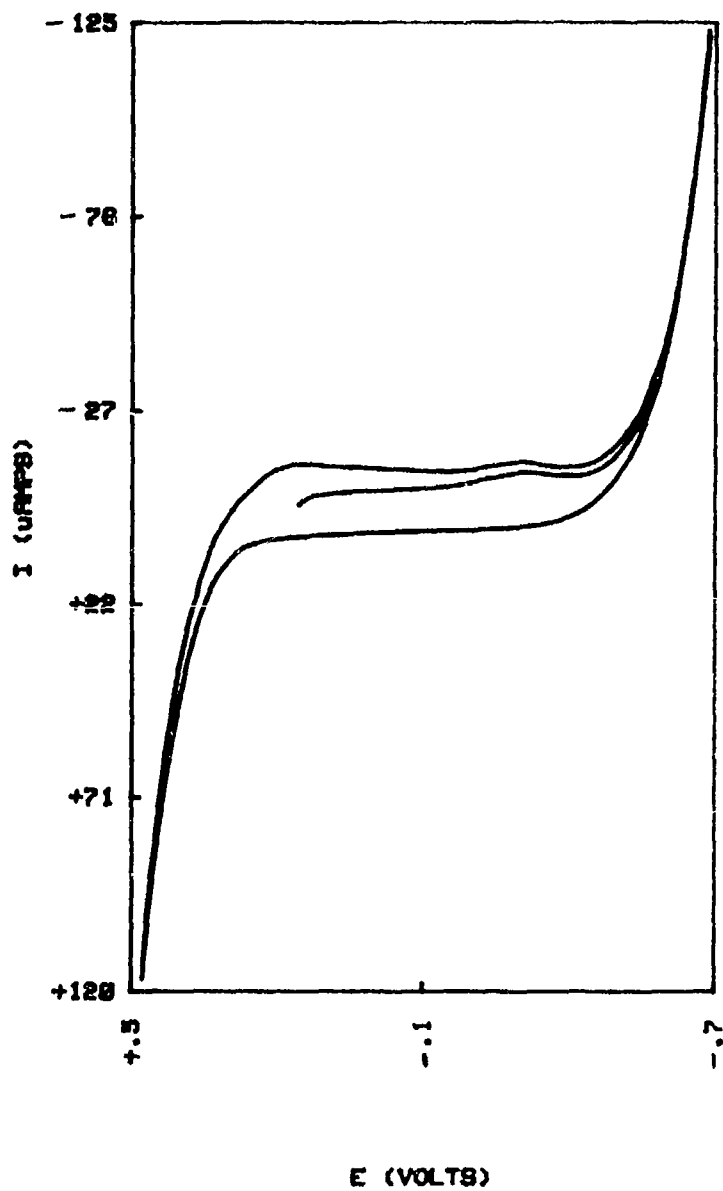


FIG 42 (b) CV OF Ru IN ACIDIC MELT

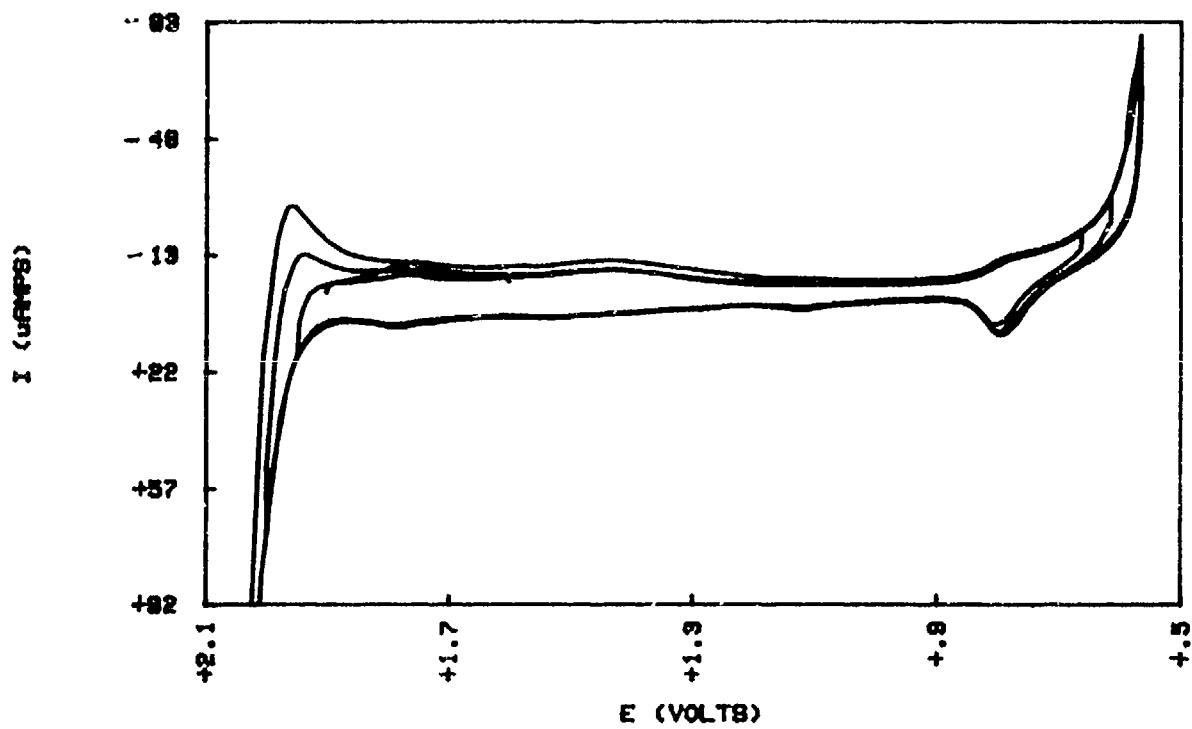


FIG 43 (a) CV OF Hg IN BASIC MELT

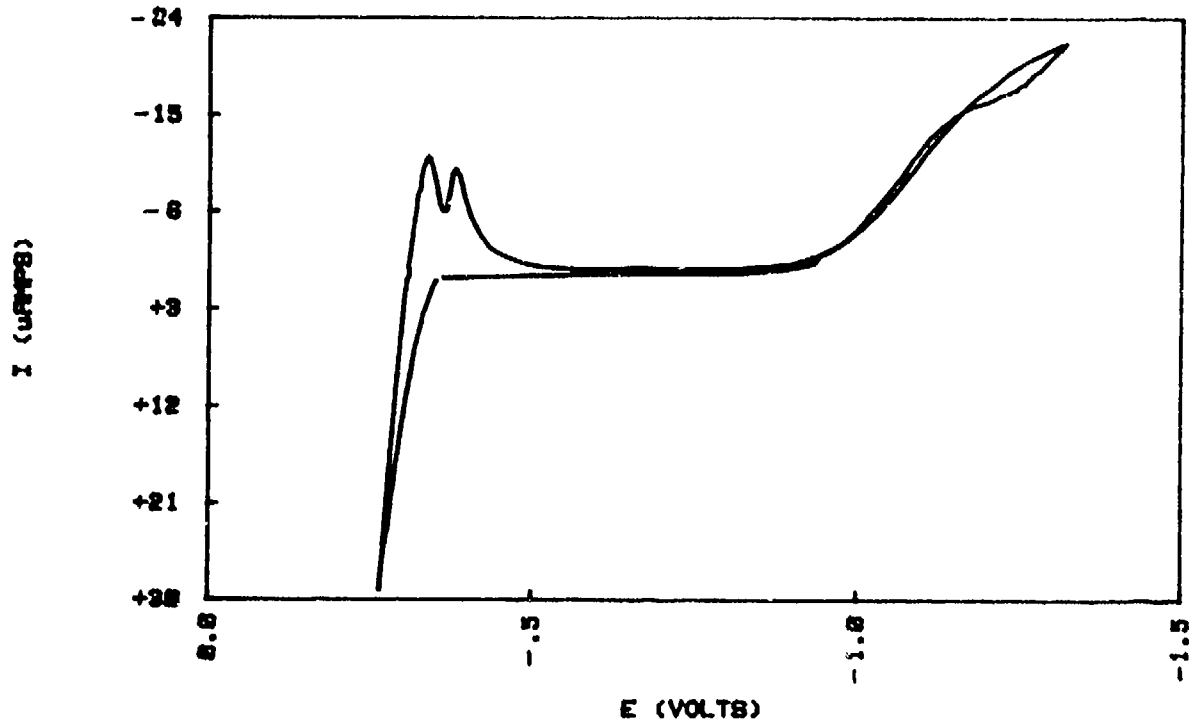


FIG 43 (b) CV OF Hg IN ACIDIC MELT

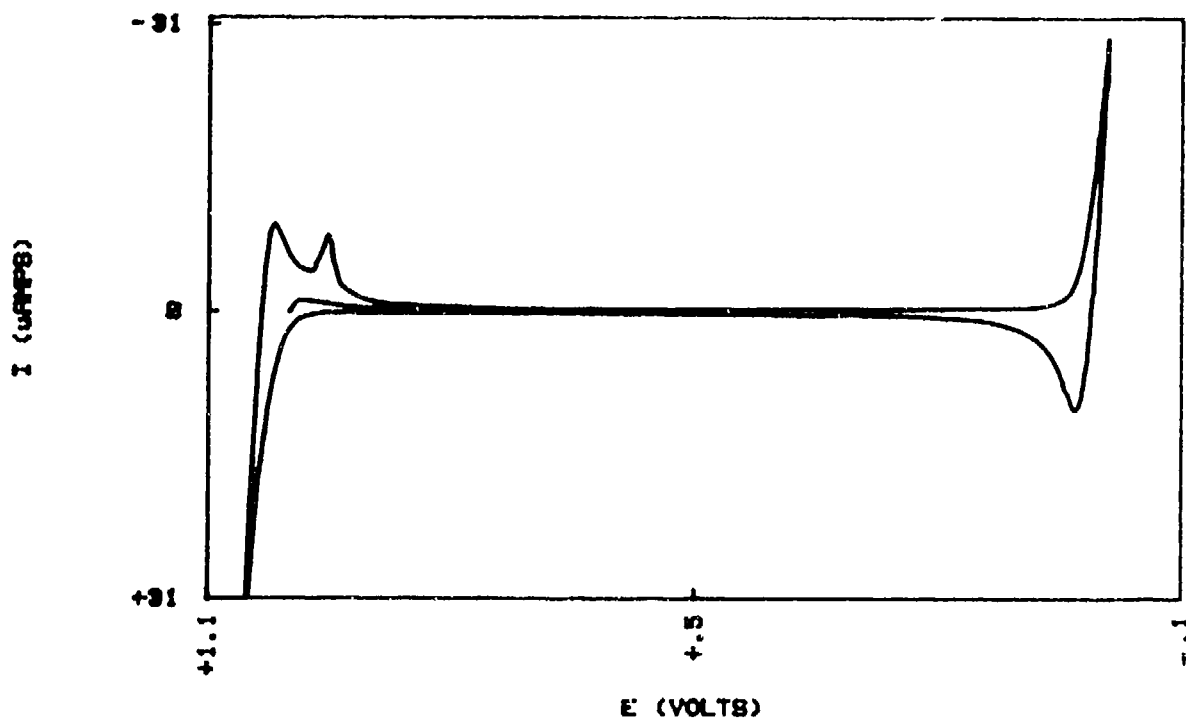


FIG 44 (a) CV OF $Pg(I)$ IN 0.4 MELT

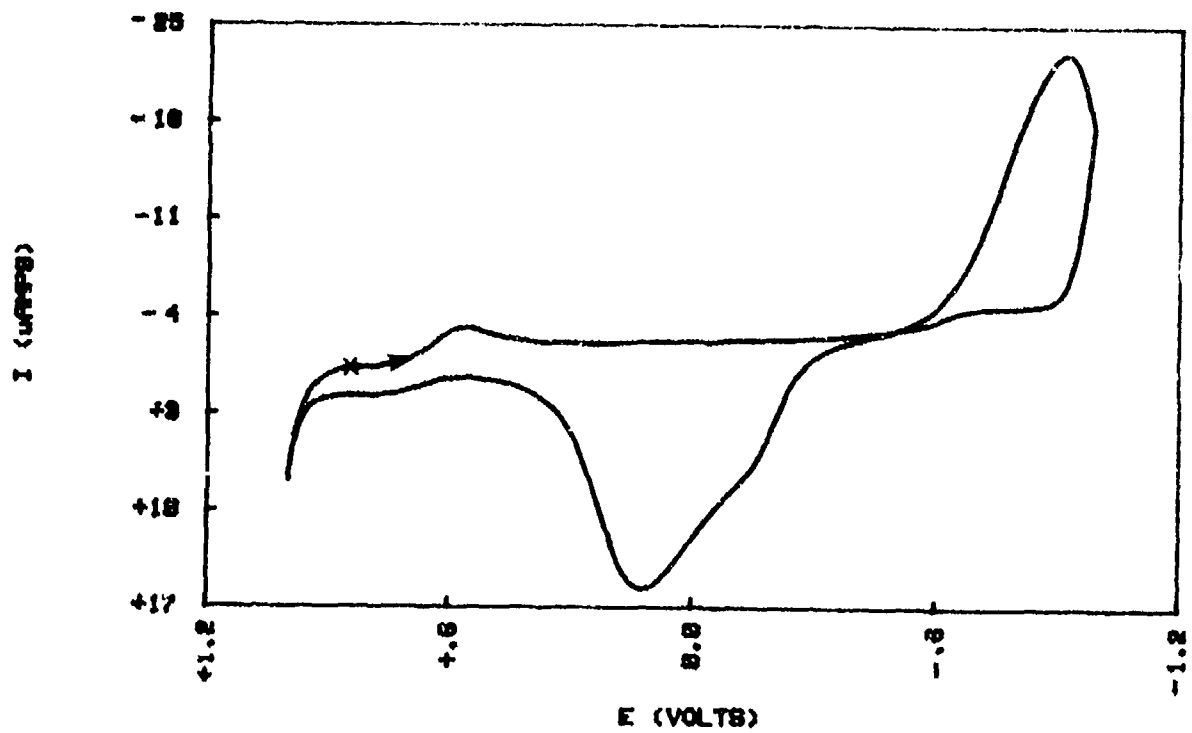


FIG 44 (b) CV OF $Pg(I)$ IN 0.4 MELT

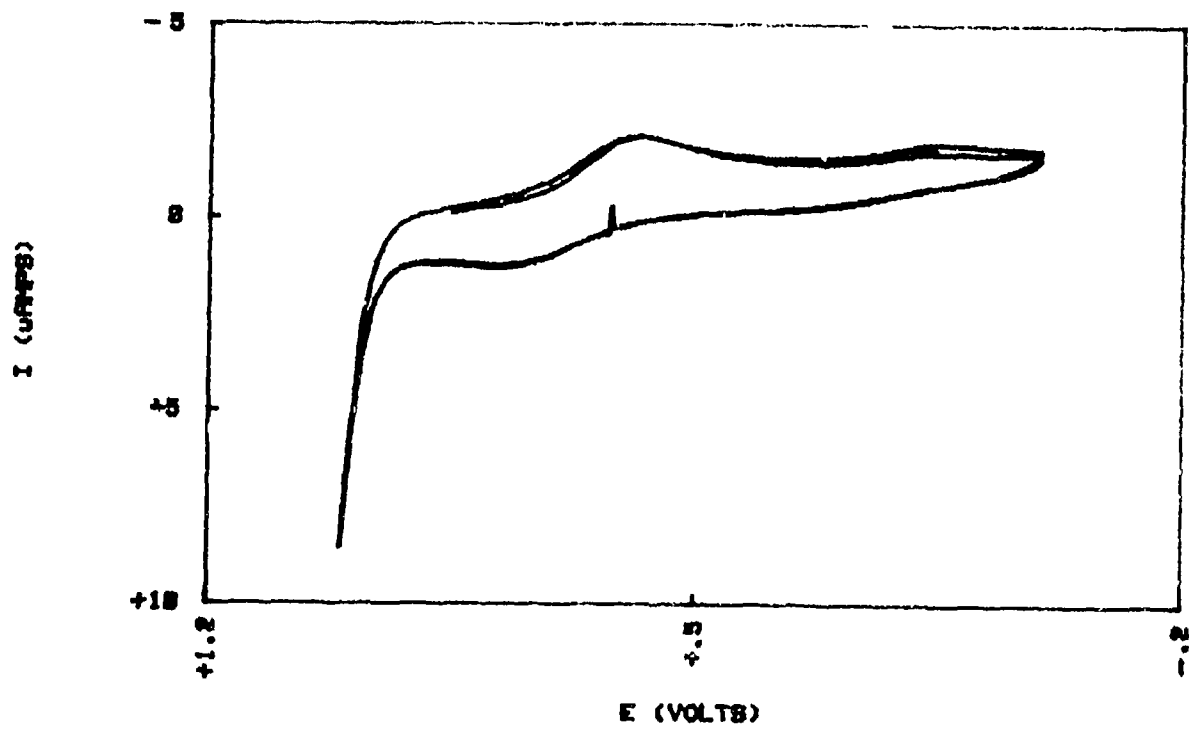


FIG 45 (a) CV OF Co(II) IN 8.4 MELT

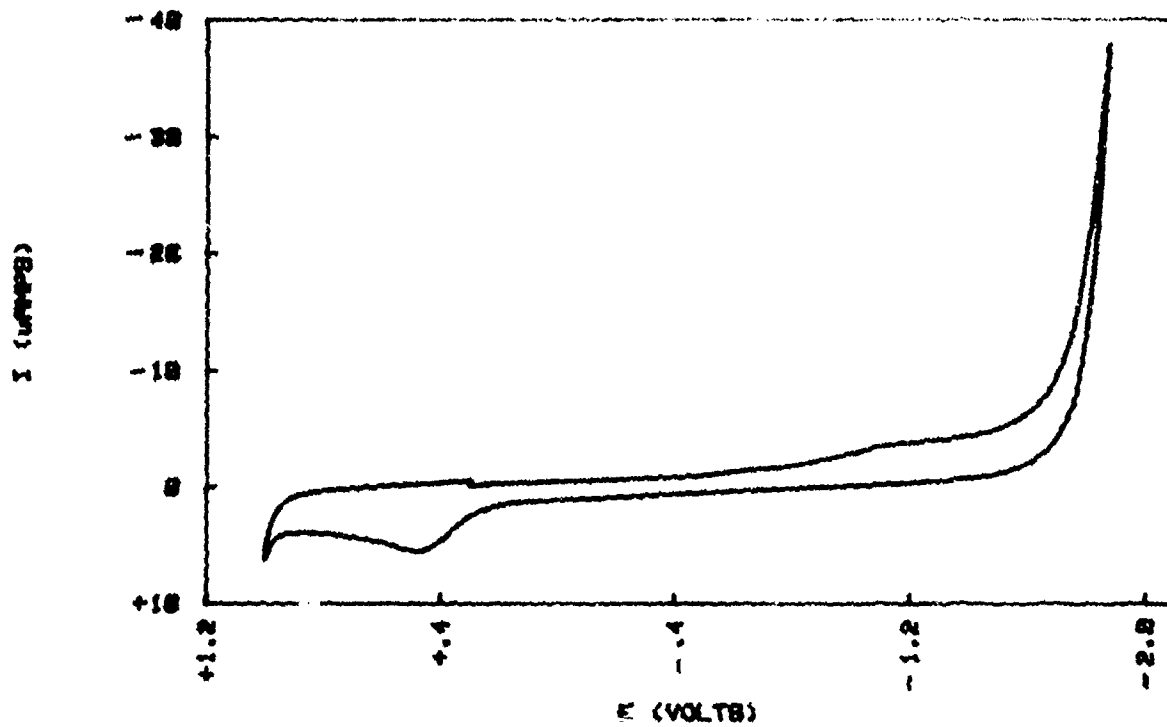


FIG 45 (b) CV OF Co(II) IN 8.8 MELT

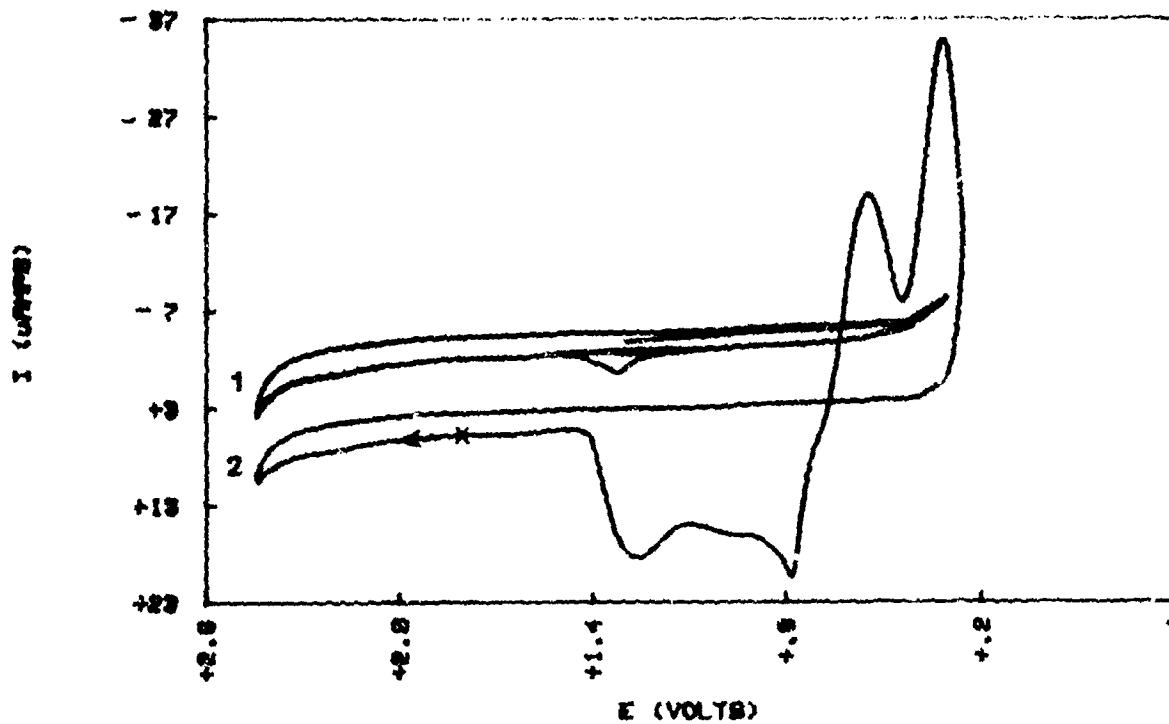


FIG 46 (a) CV OF Cr(III) IN 8.4 MELT

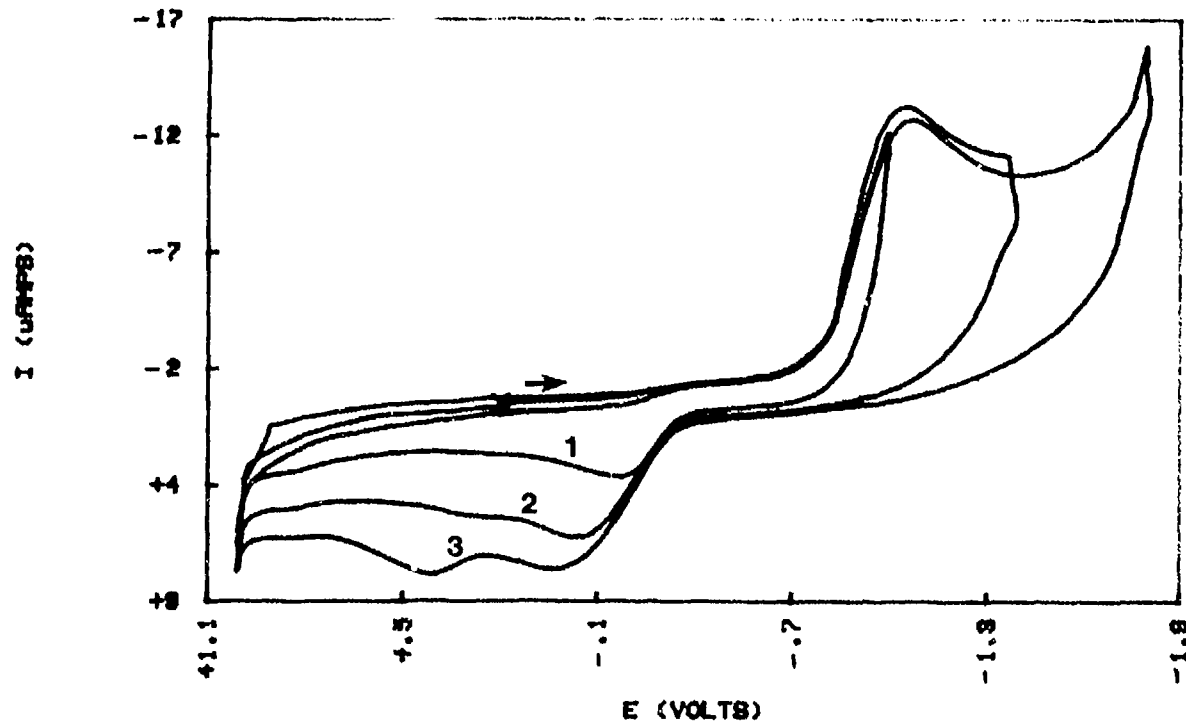


FIG 46 (b) CV OF Cr(III) IN 8.6 MELT

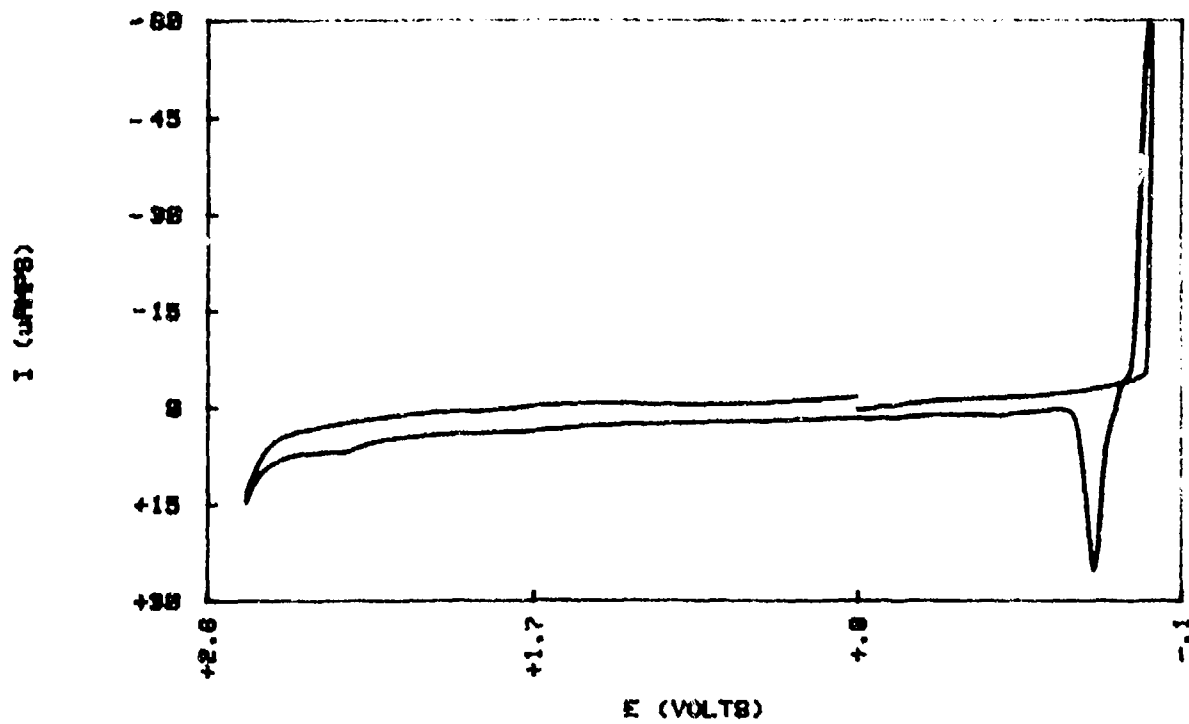


FIG 47 (a) CV OF CrO3 IN 0.4 MELT

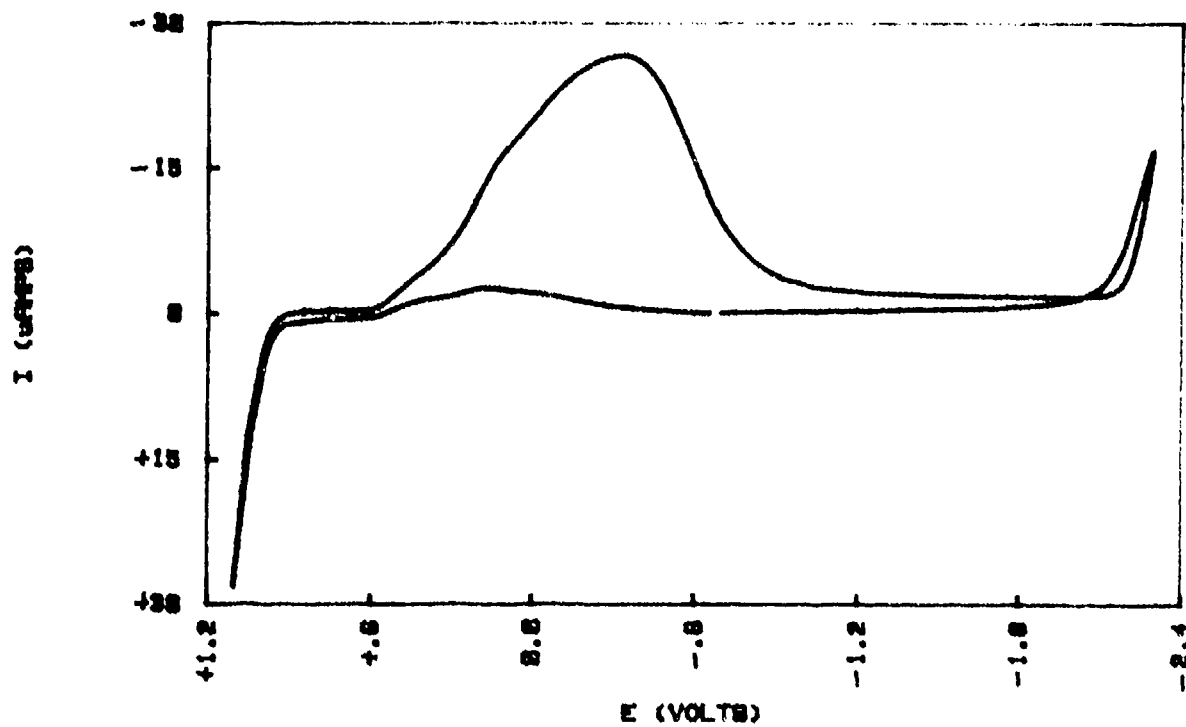


FIG 47 (b) CV OF CrO3 IN 0.8 MELT

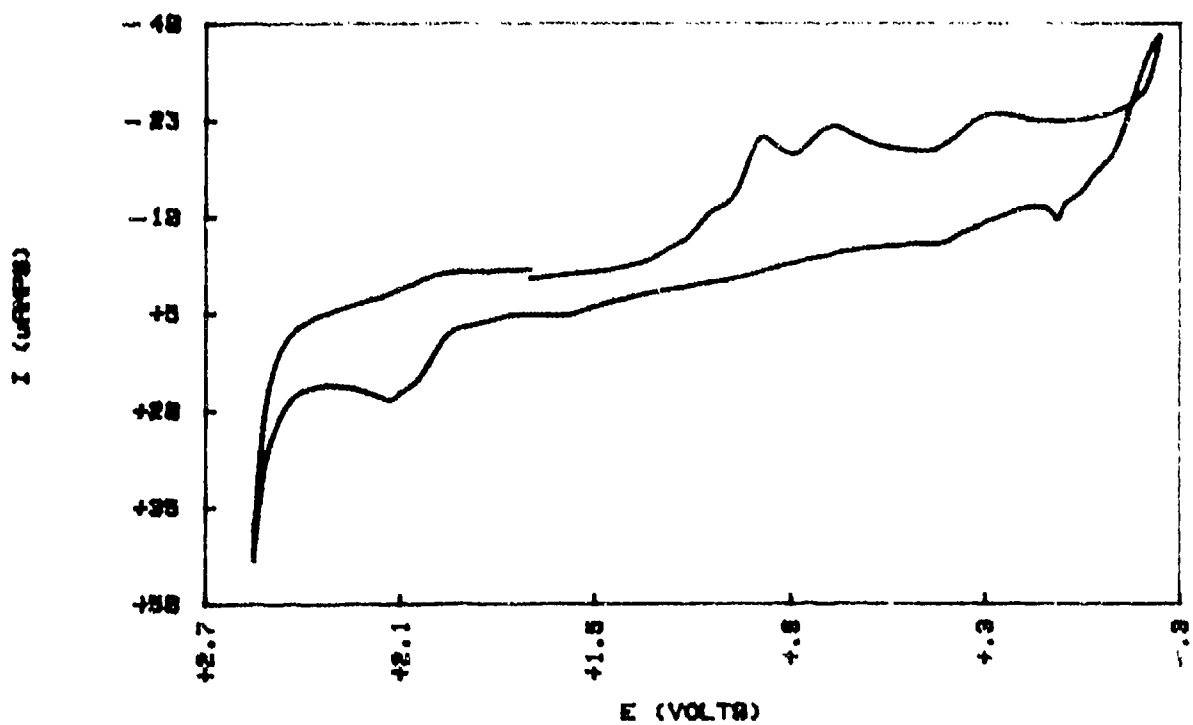


FIG 48 (a) CV OF K₂Cr₂O₇ IN 8.4 MELT

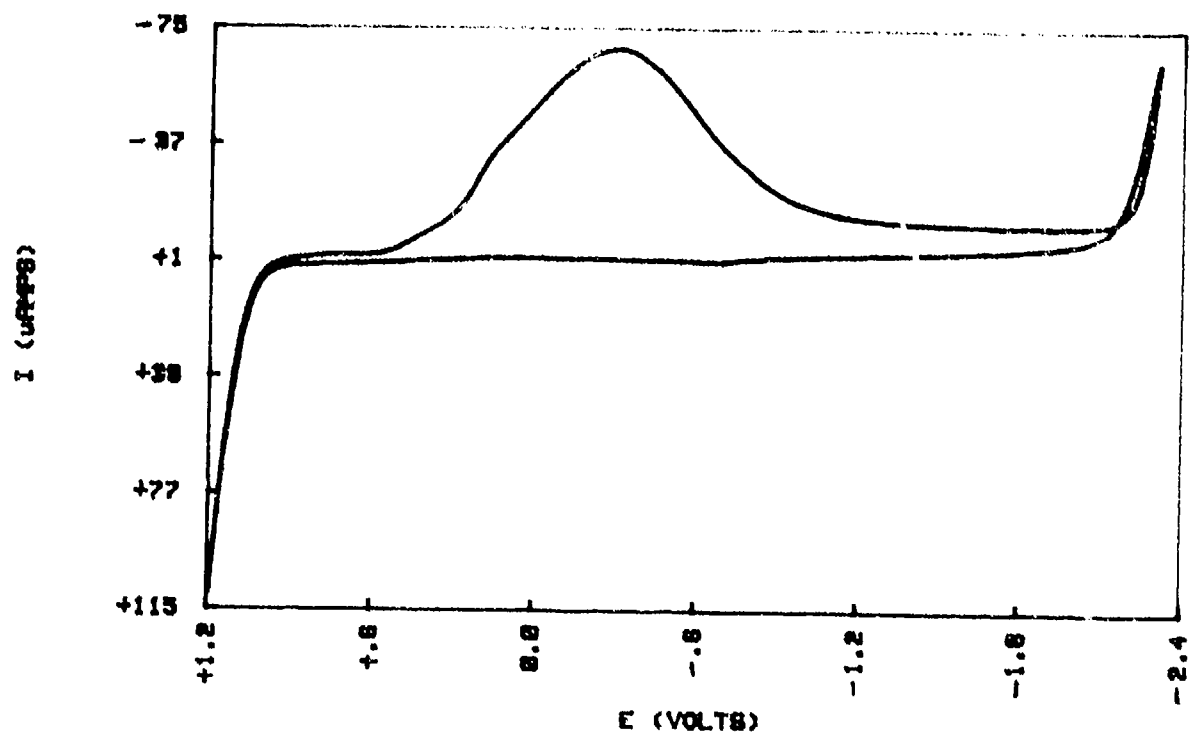


FIG 48 (b) CV OF K₂Cr₂O₇ IN 8.8 MELT

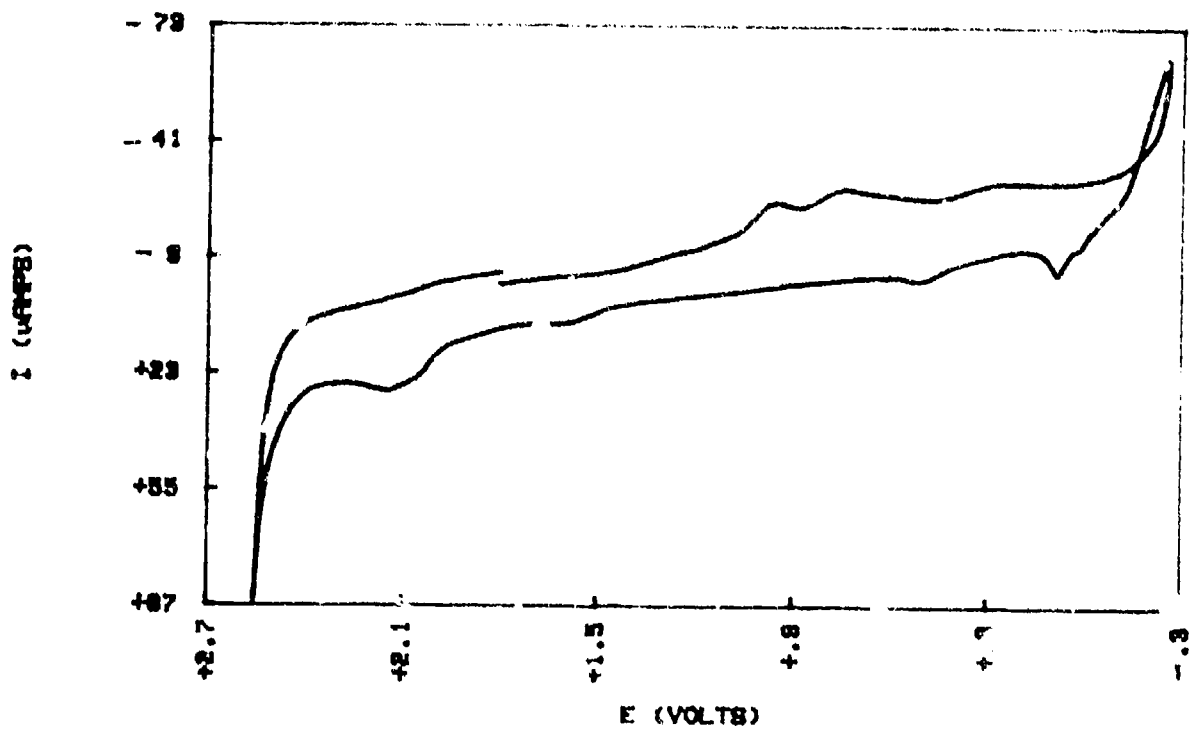


FIG 49 (a) CV OF Cu(II) IN 8.4 MELT

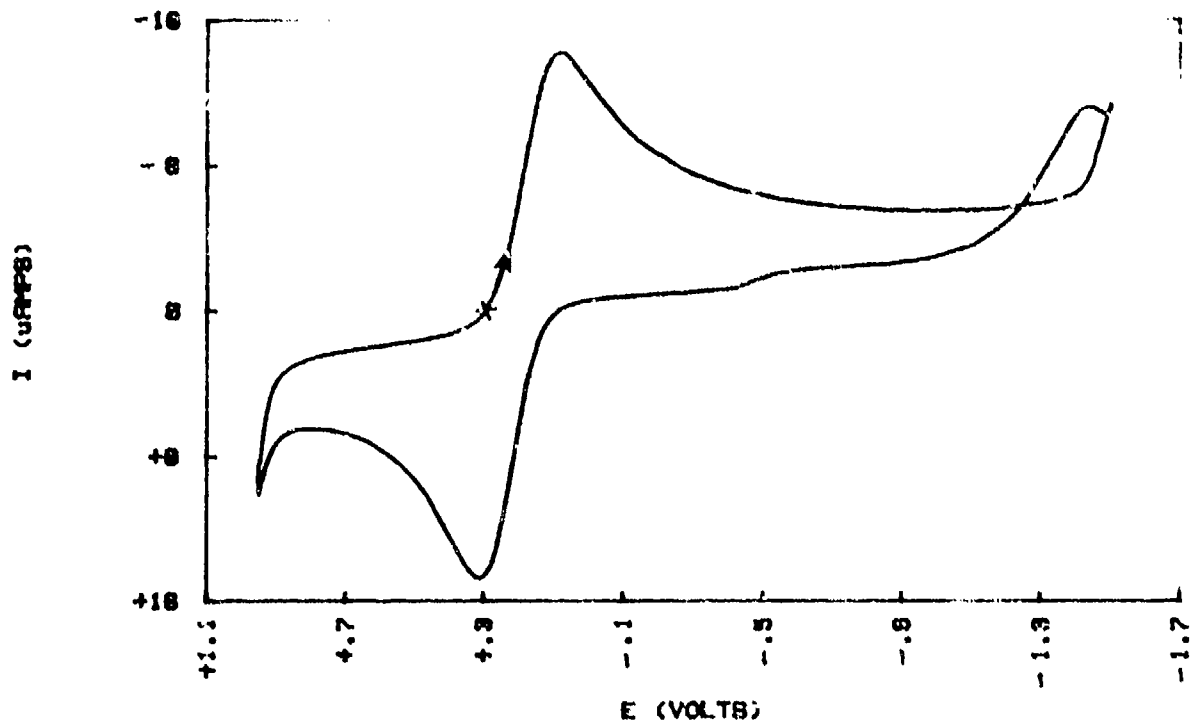


FIG 49 (b) CV OF Cu(II) IN 8.6 MELT

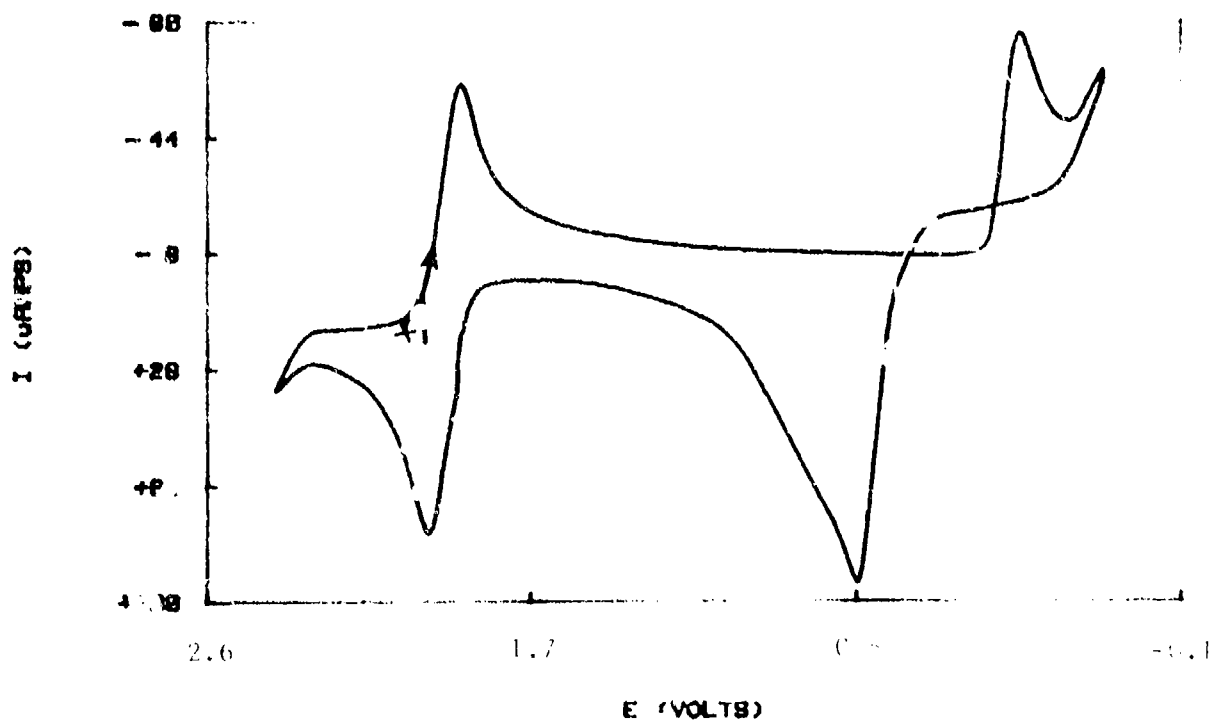


FIG 50 CV OF Cu(II) IN B.4 MELT

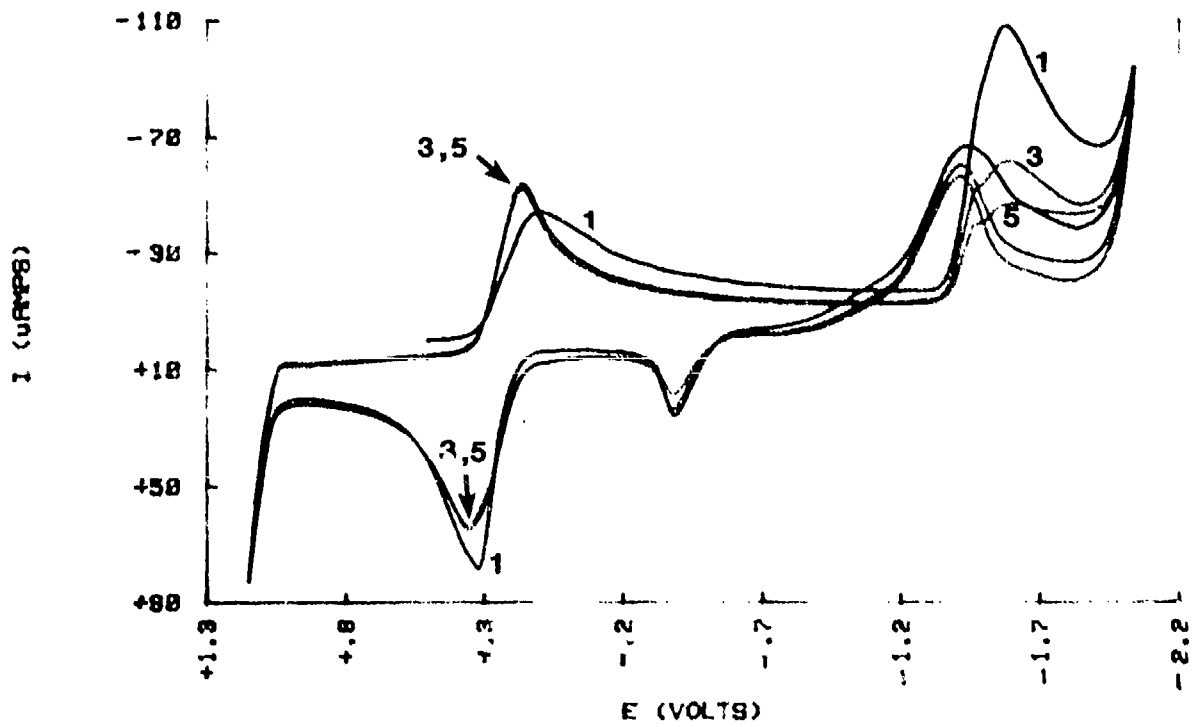


FIG 51 (a) CV OF Fe(II) IN 0.4 MELT

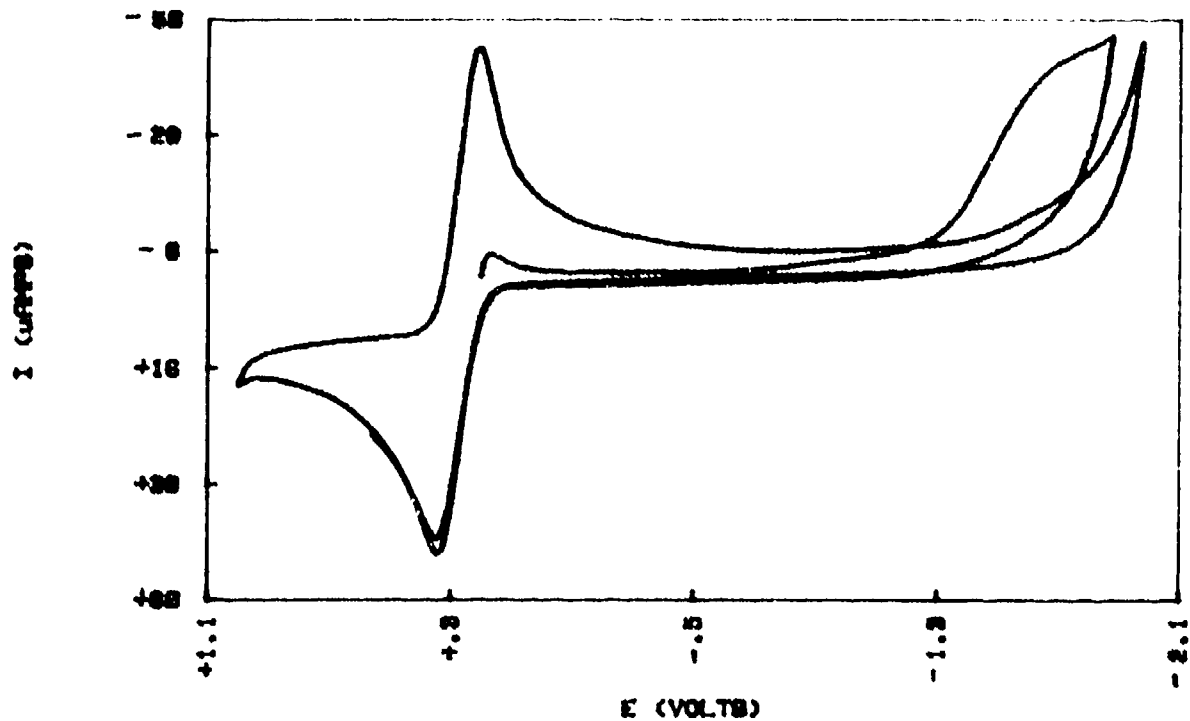


FIG 51 (b) CV OF Fe(II) IN 0.8 MELT

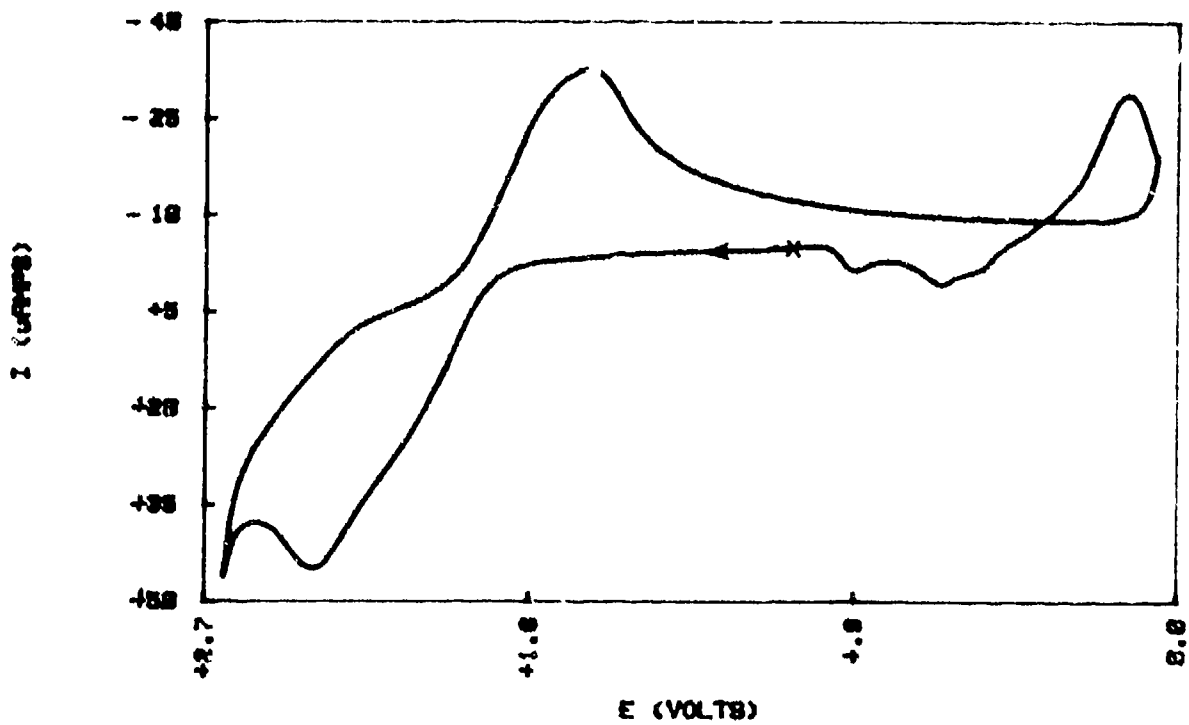


FIG 52 (a) CV OF Fe(III) IN B.4 MELT

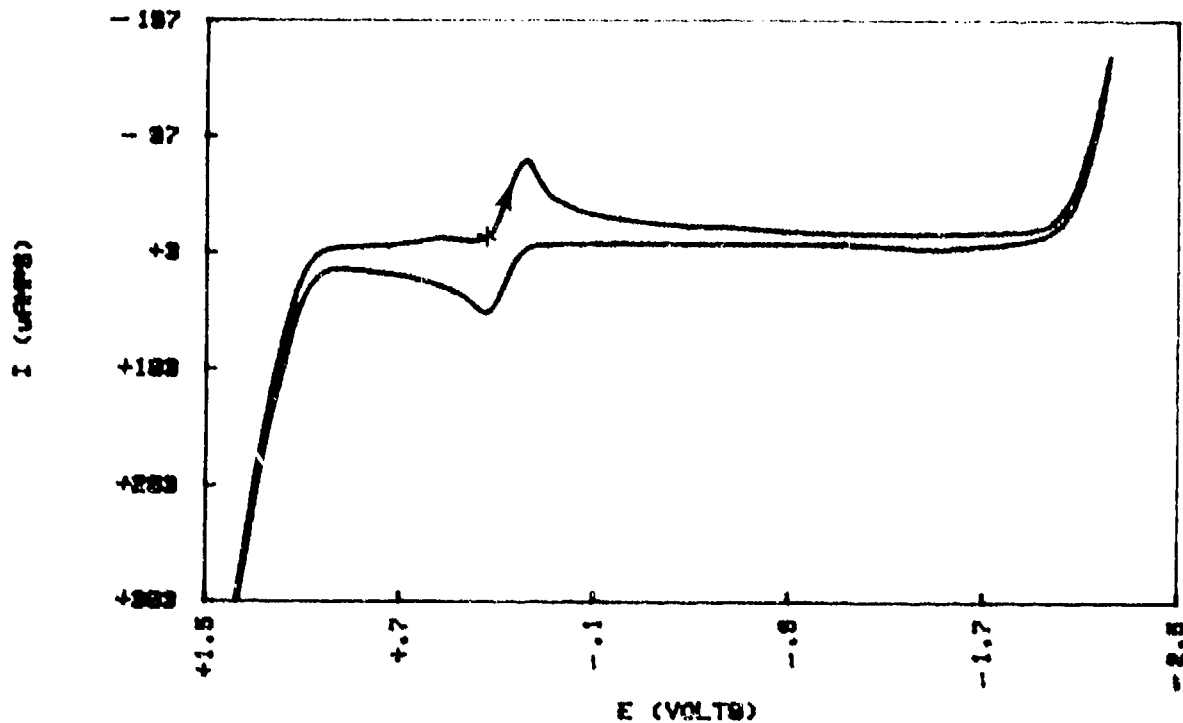


FIG 52 (b) CV OF Fe(III) IN B.8 MELT

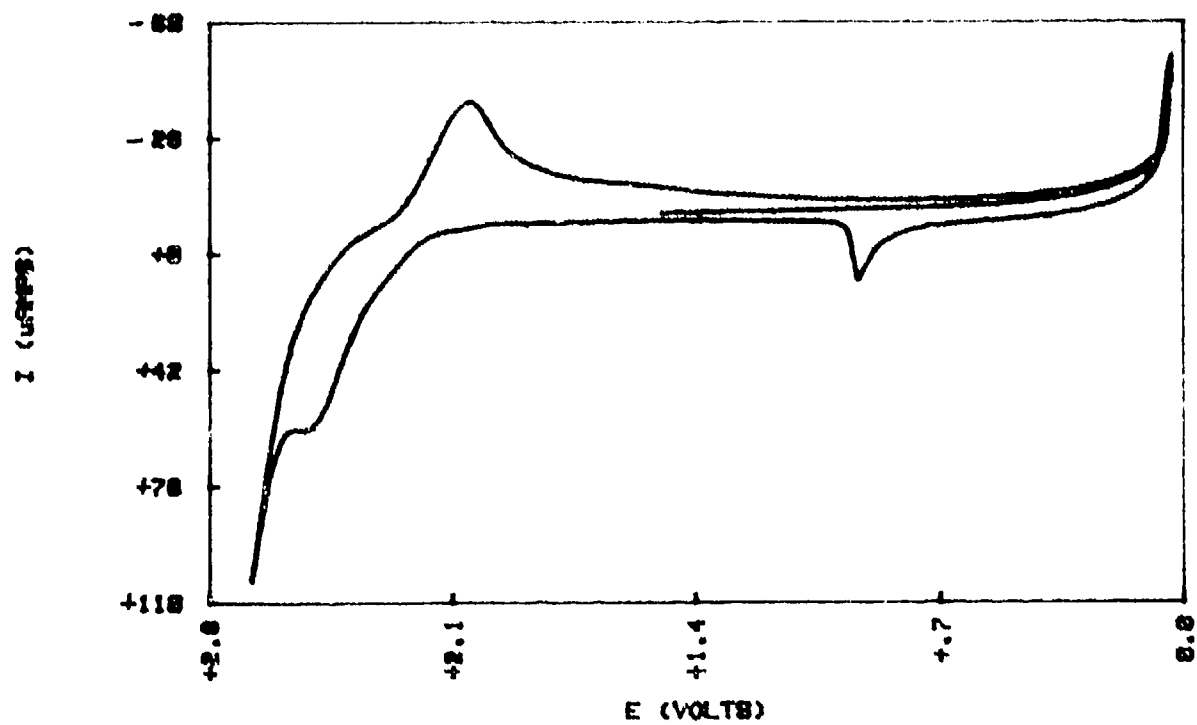


FIG 53 (a) CV OF Fe(III) IN 0.5 MELT

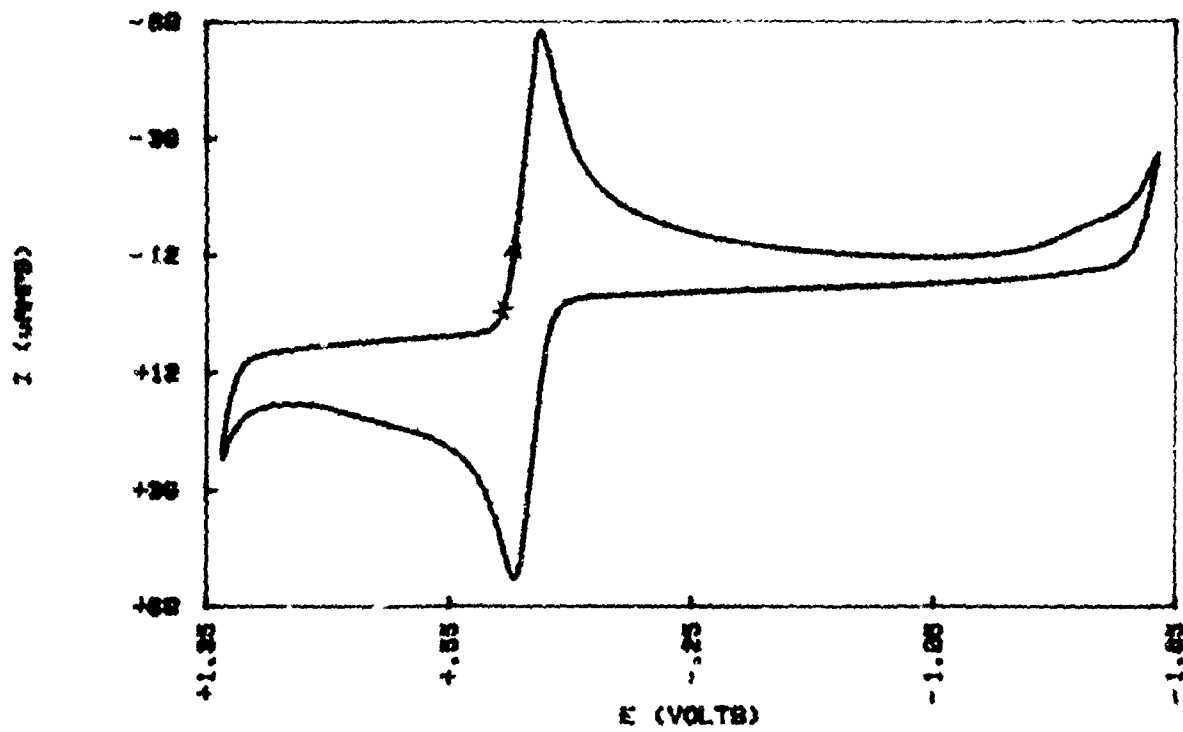


FIG 53 (b) CV OF Fe(II) IN 0.6 MELT

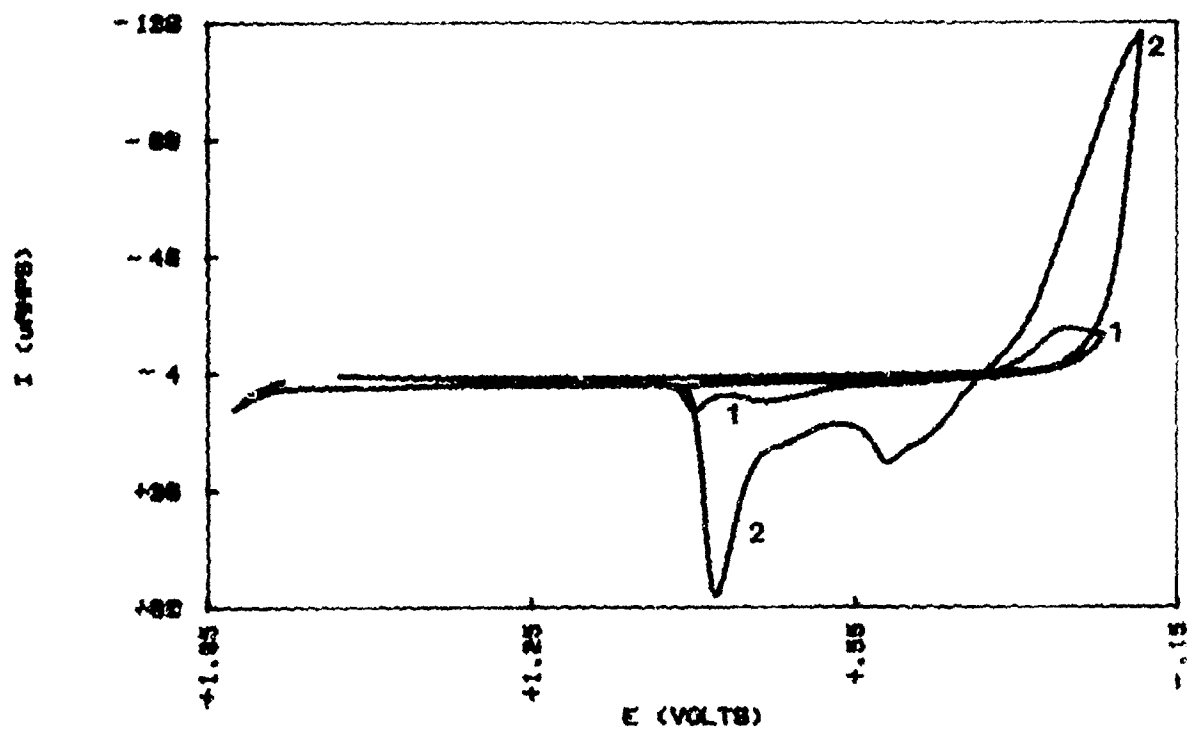


FIG 54 CV OF Fe(II) AND Fe(III) IN 0.6 MELT

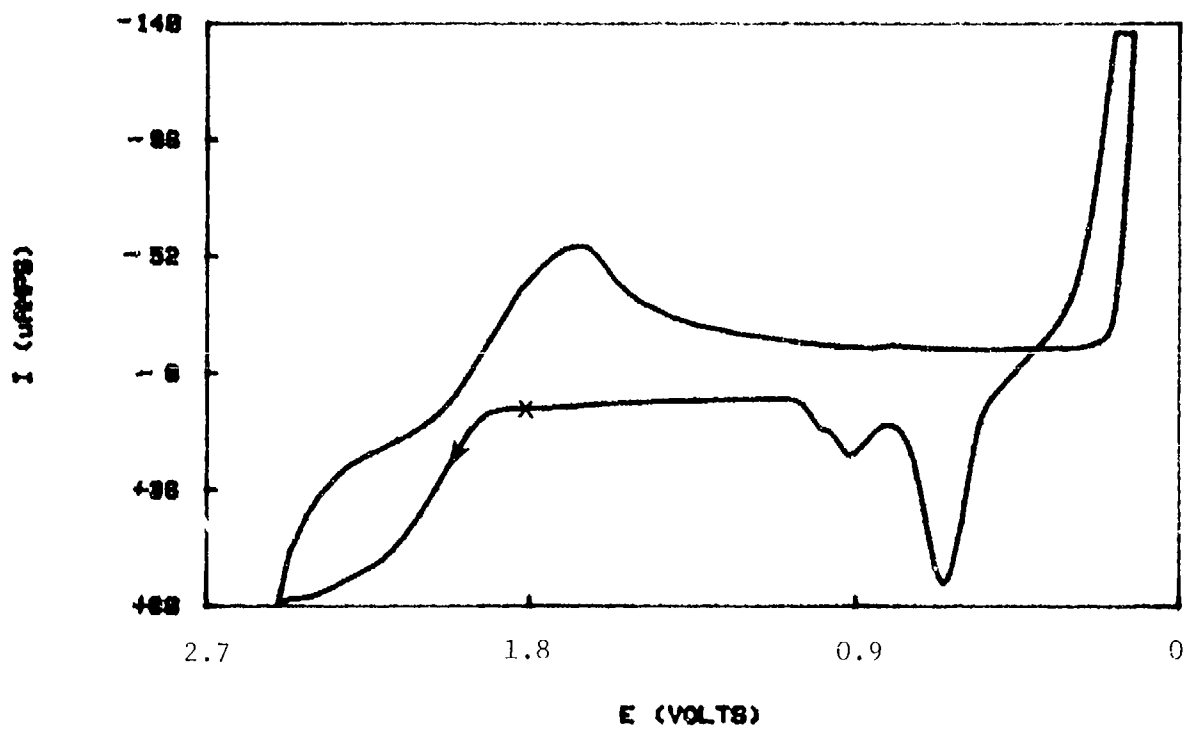


FIG 55(a) CV OF FERROCENE IN 0.4 MELT

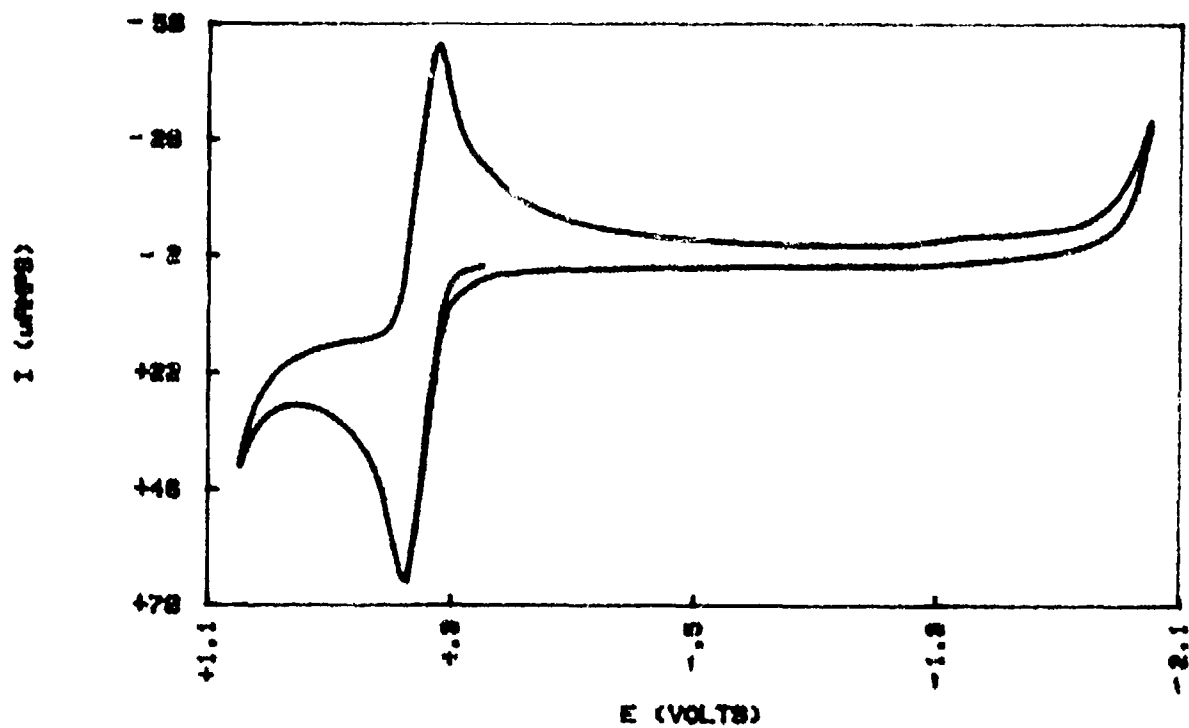


FIG 55(b) CV OF FERROCENE IN 0.6 MELT

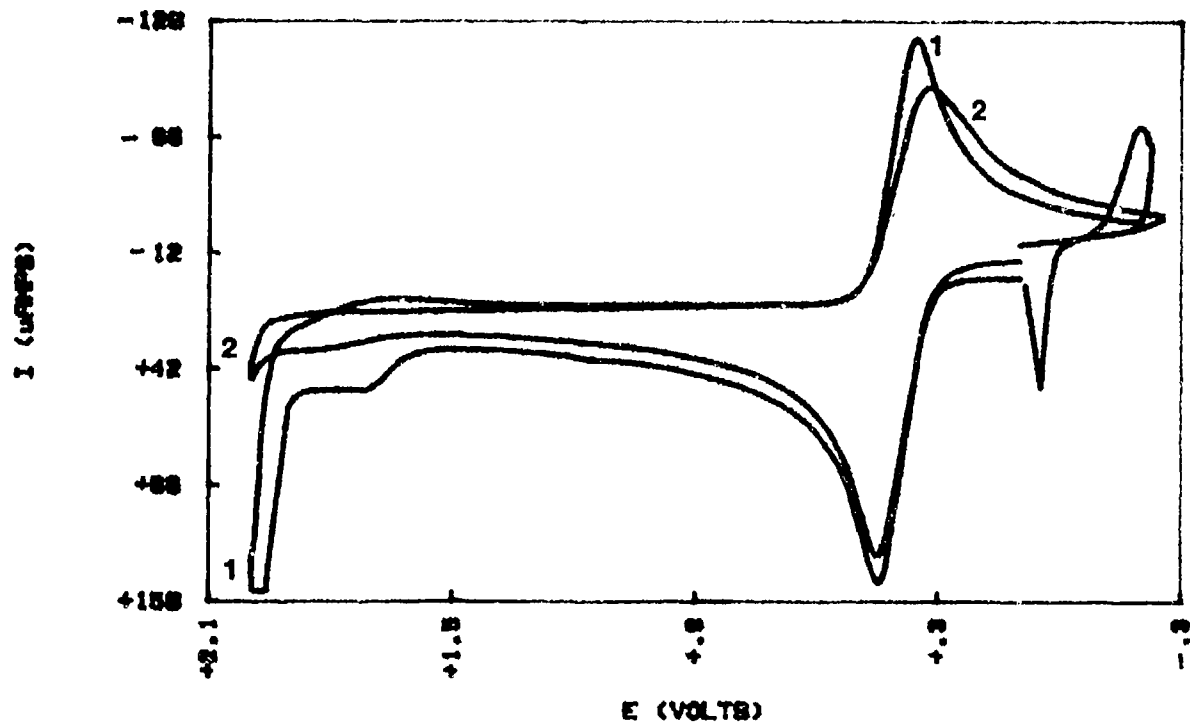


FIG 56 (a) CV OF FERROCENE IN 0.4 MELT

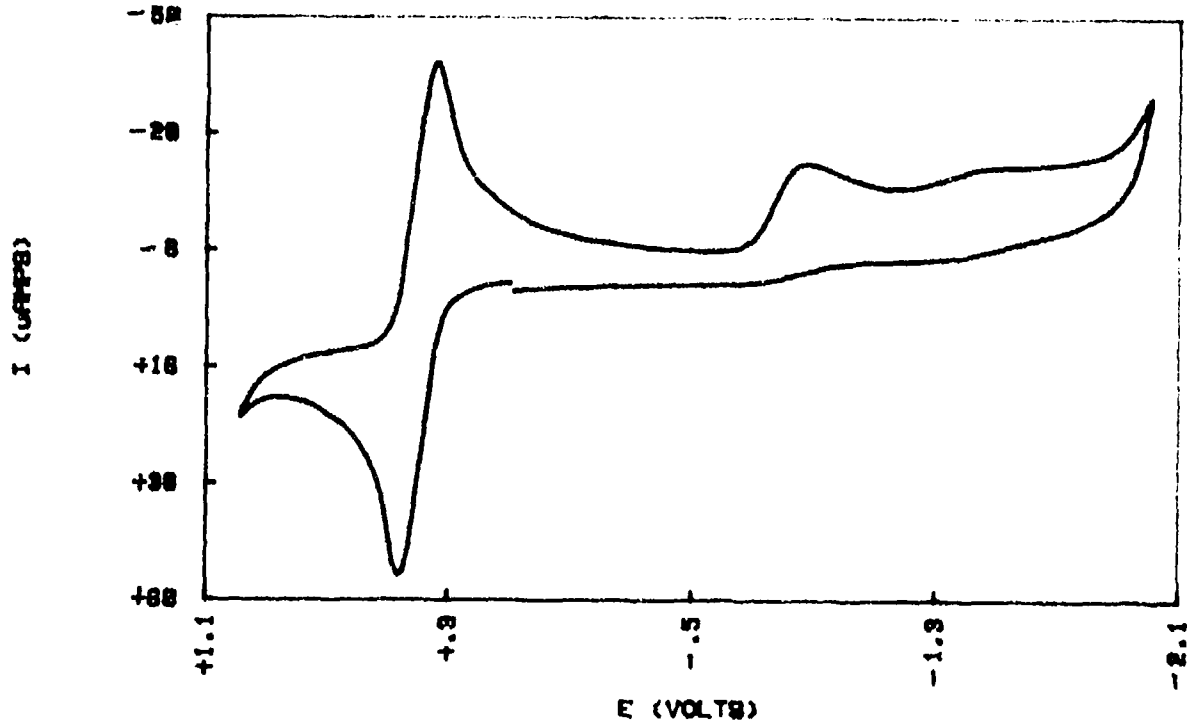


FIG 56 (b) CV OF FERROCENE IN 0.6 MELT

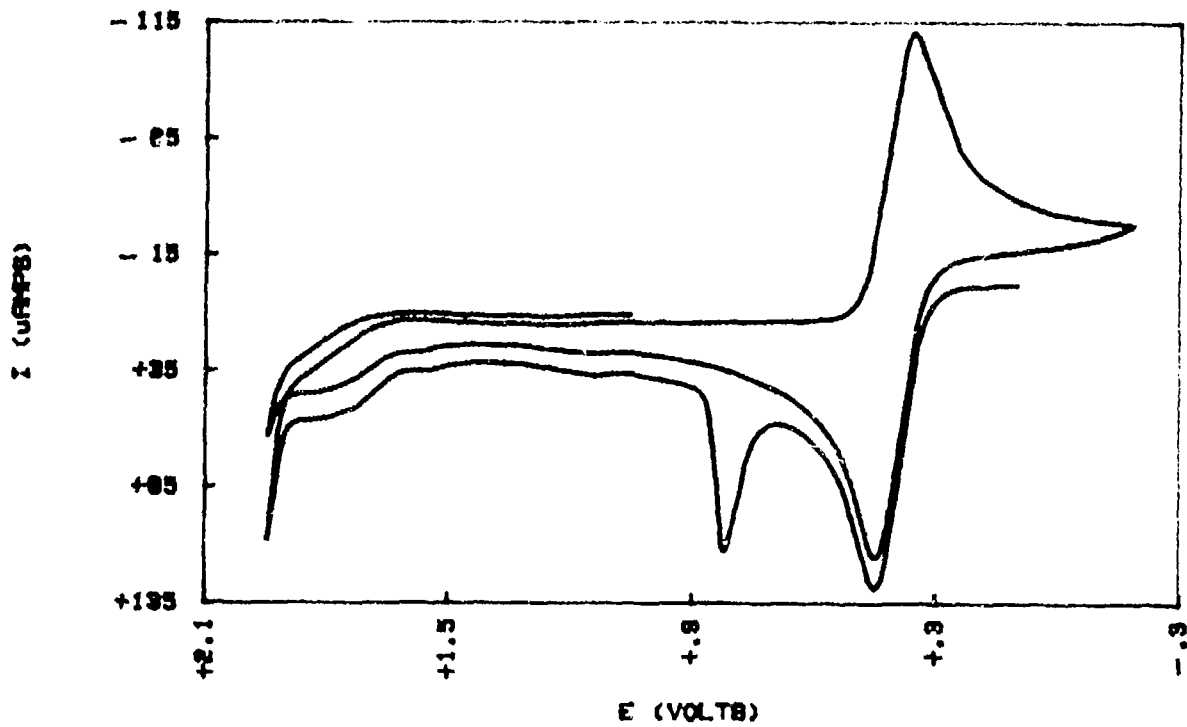


FIG 57 (a) CV OF Hg(II) IN 0.4 MELT

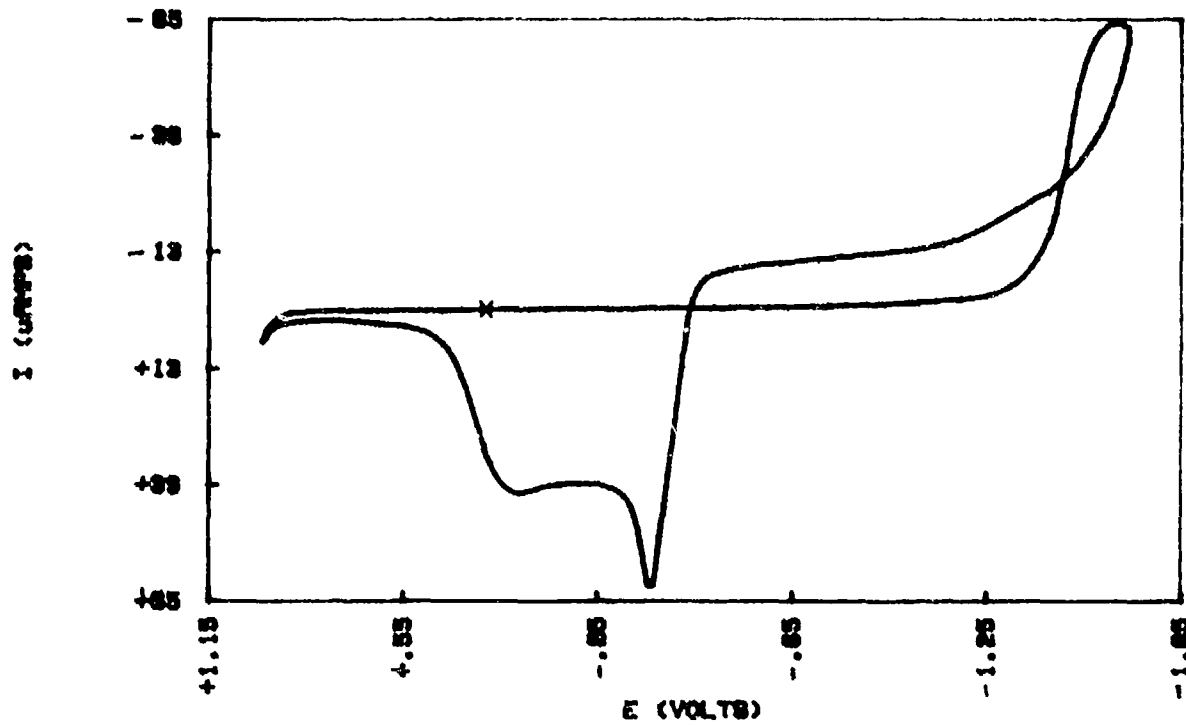


FIG 57 (b) CV OF Hg(II) IN 0.6 MELT

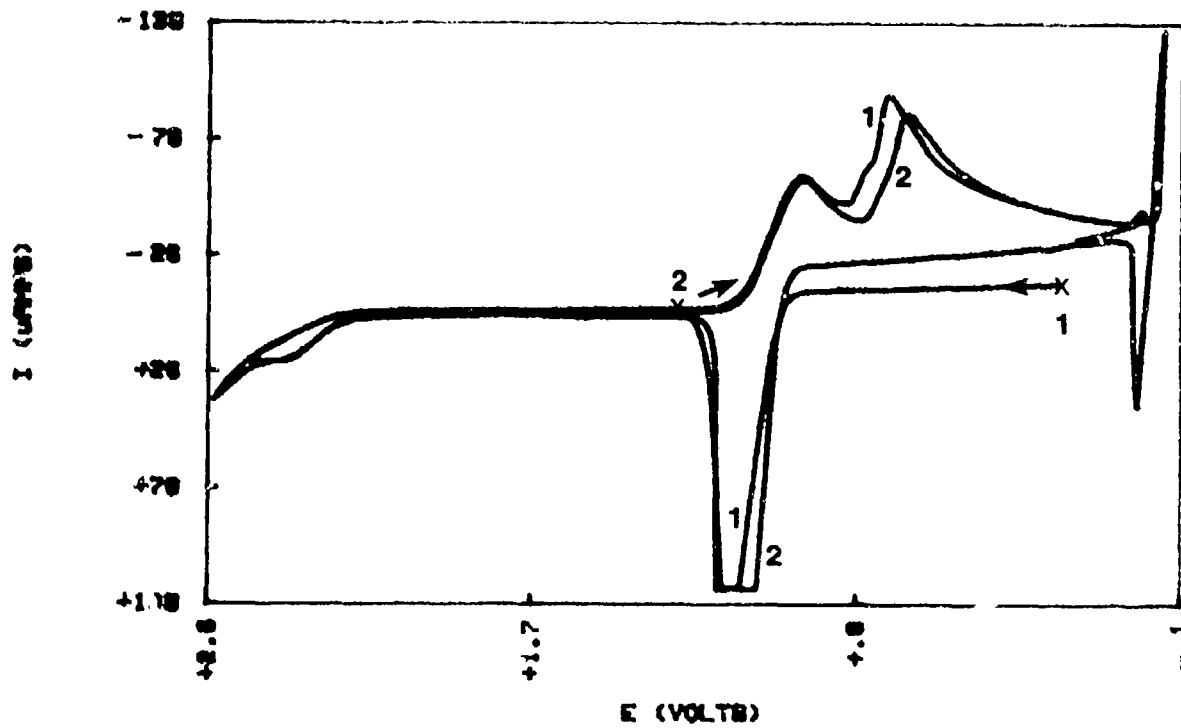


FIG 58 CV OF Hg(II) IN 0.4 MOLT

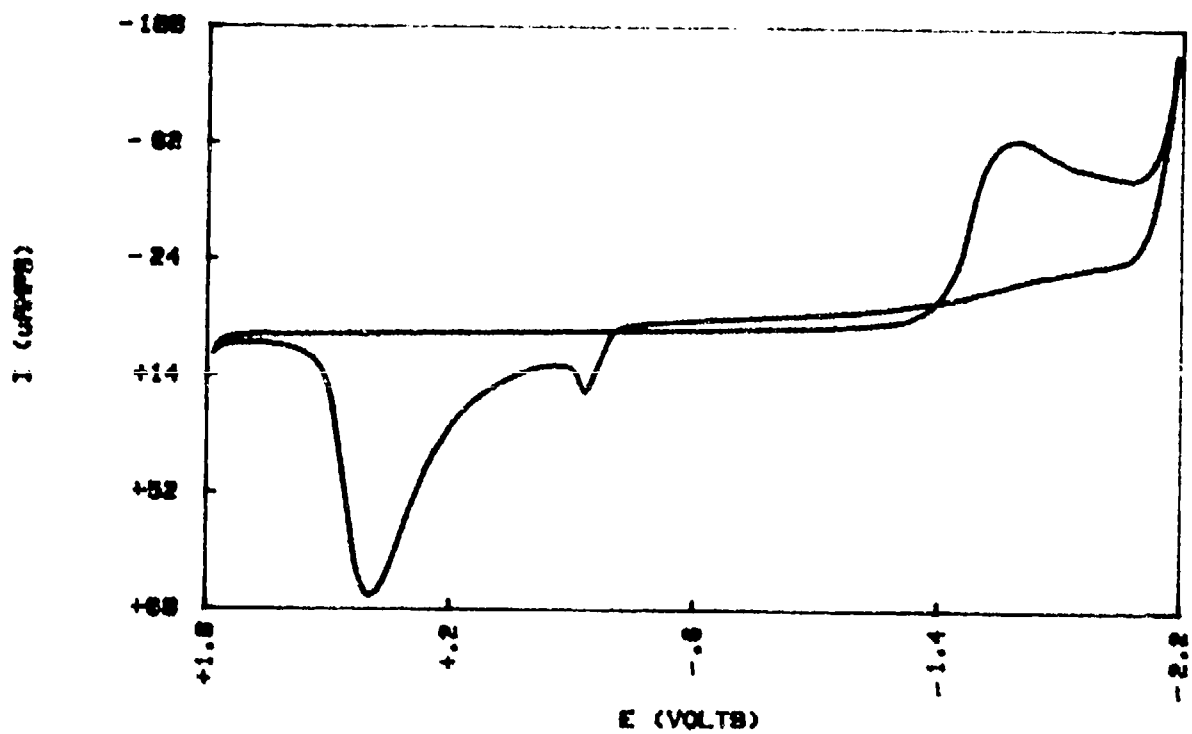


FIG 59 (a) CV OF Li(I) IN 8.4 MELT

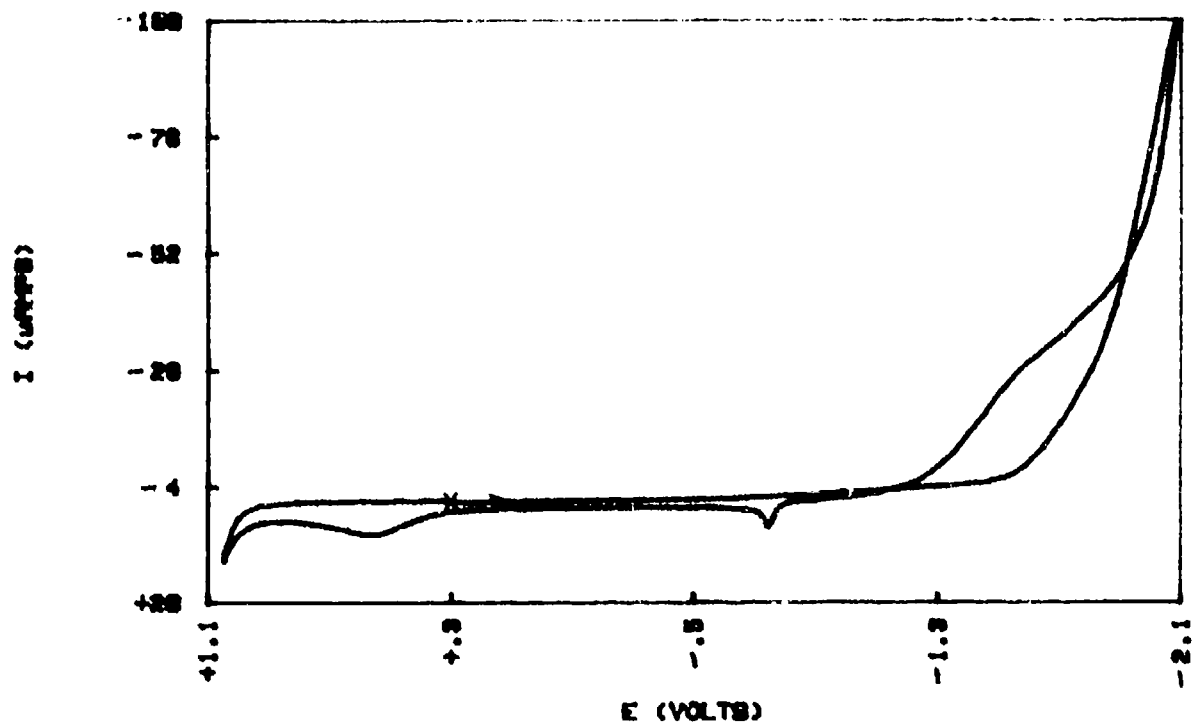


FIG 59 (b) CV OF Li(I) IN 8.8 MELT

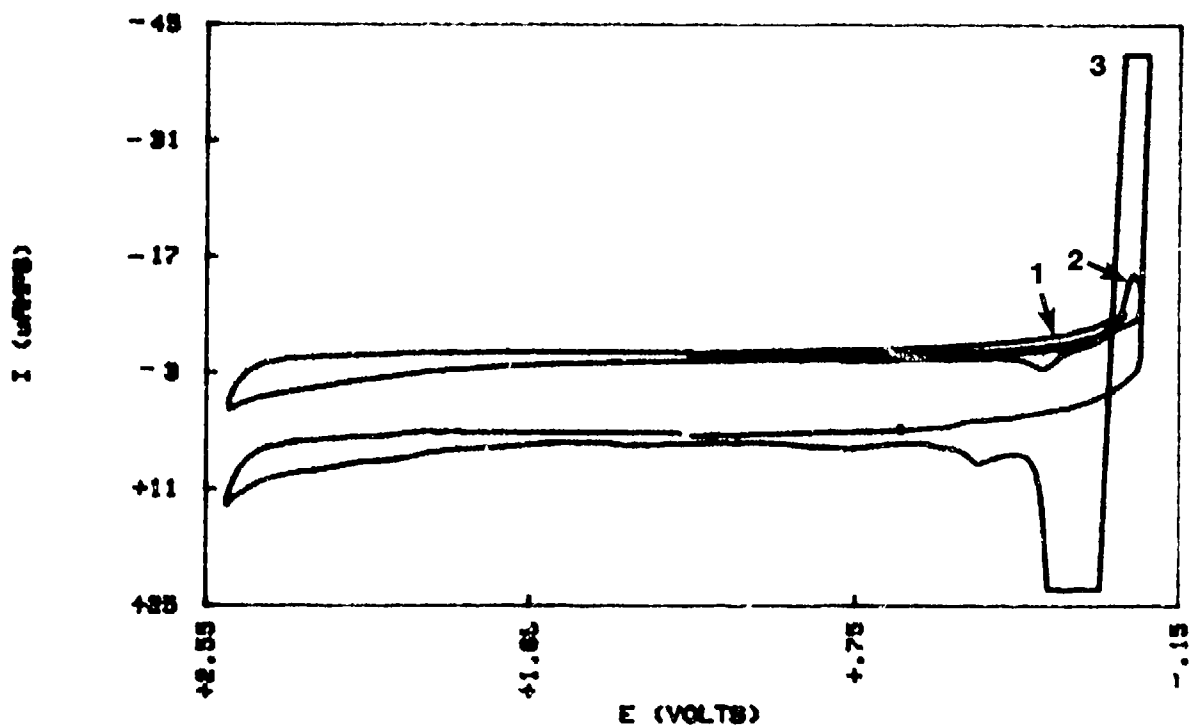


FIG 60 (a) CV OF Mn(II) IN 8.4 MELT

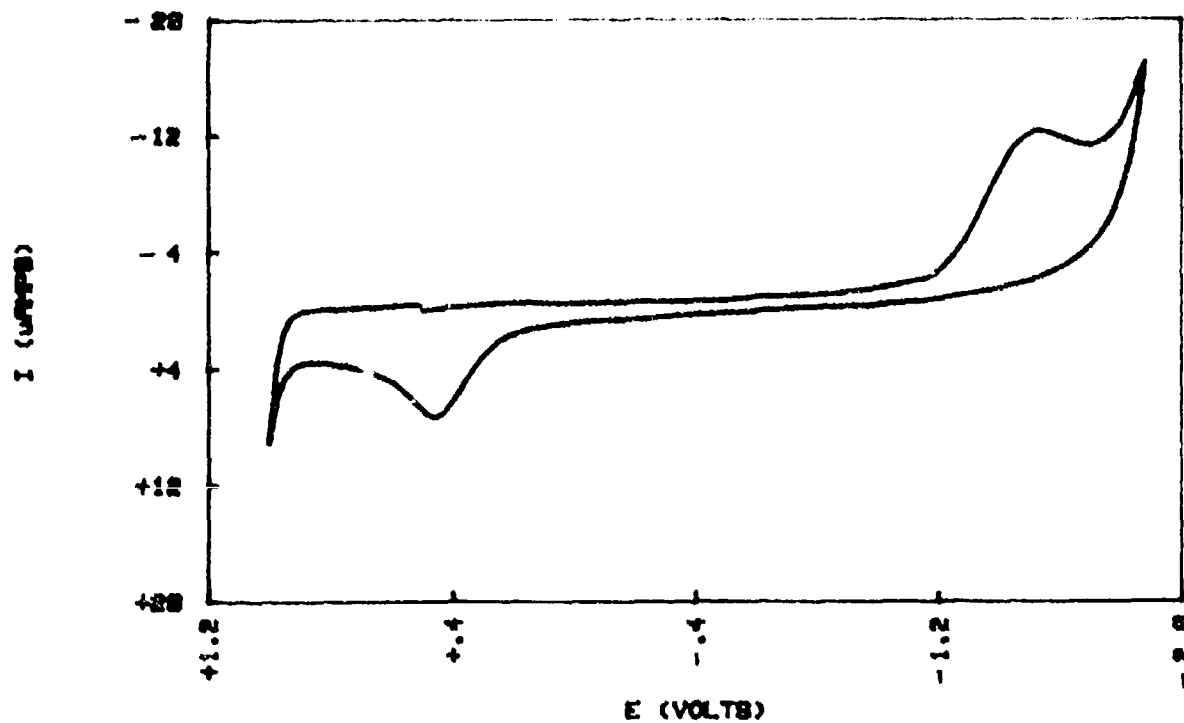


FIG 60 (b) CV OF Mn(II) IN 8.6 MELT

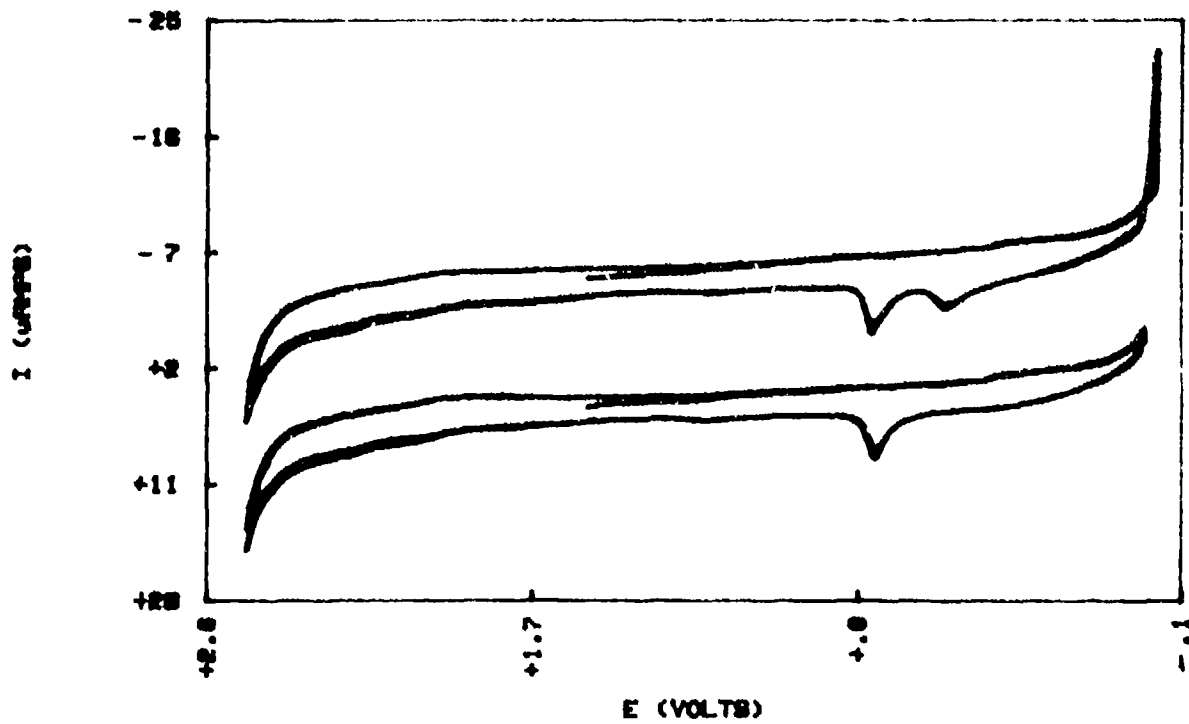


FIG 61 (a) CV OF Mo(III) IN 8.4 MELT

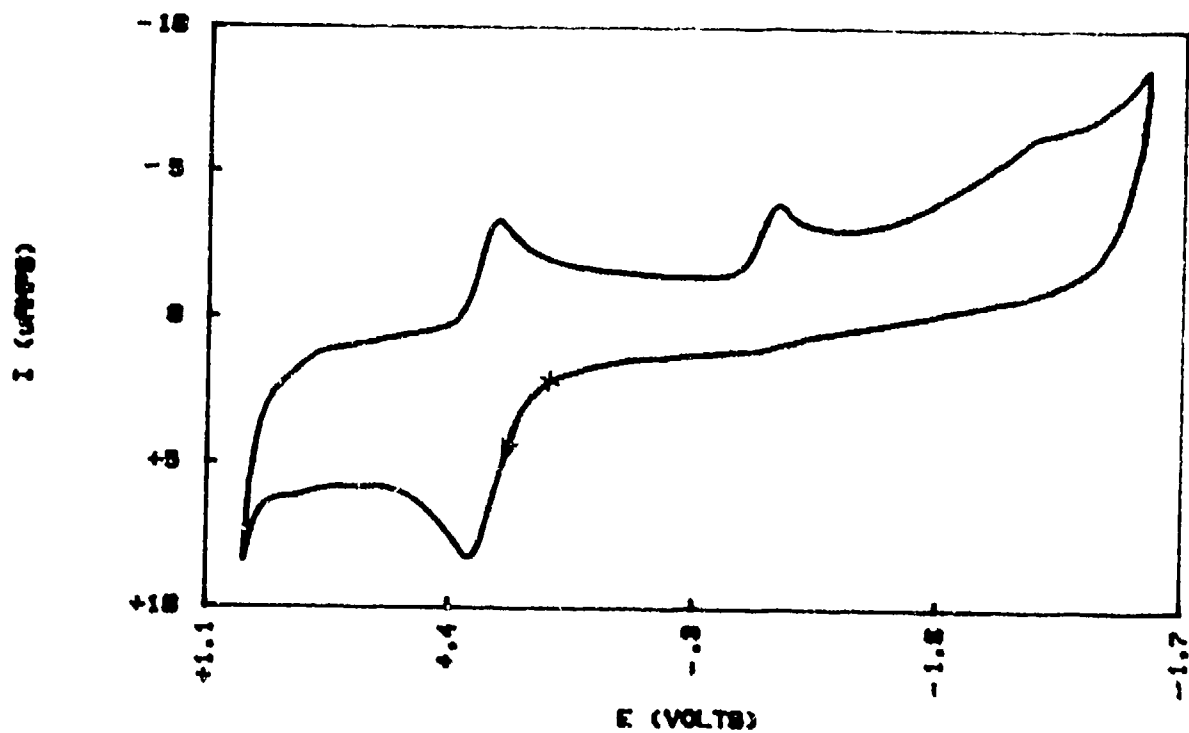


FIG 61 (b) CV OF Mo(III) IN 8.8 MELT

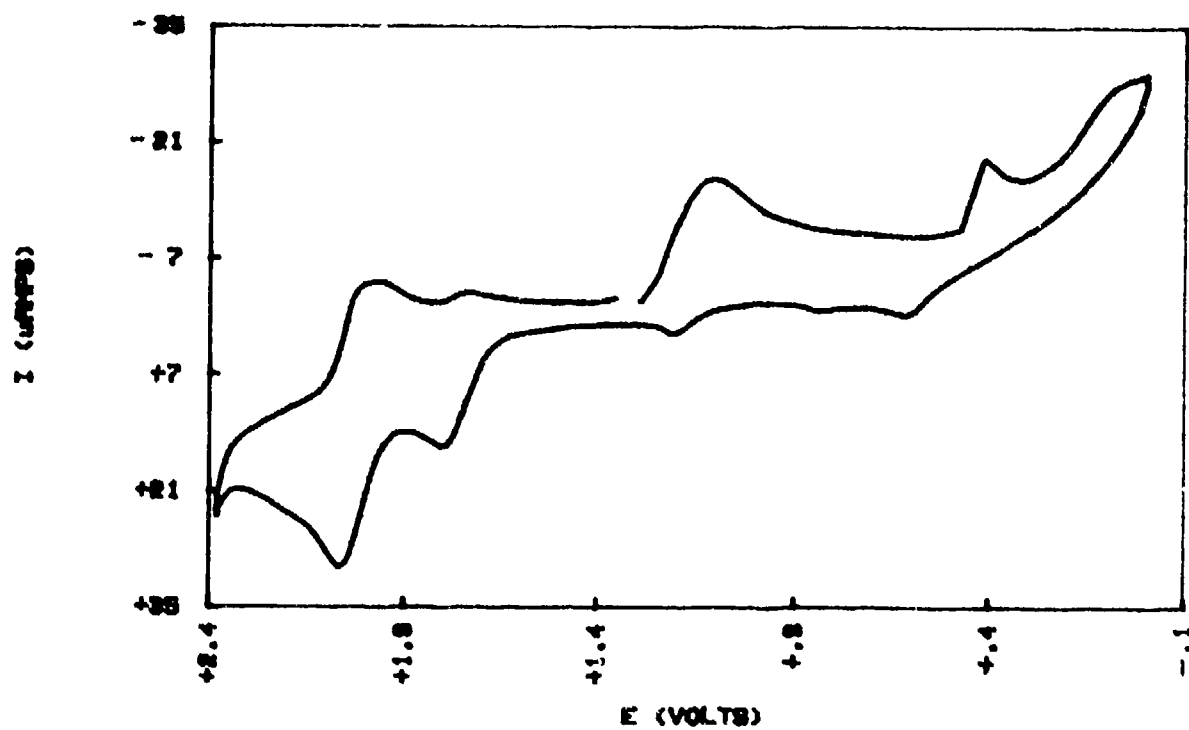


FIG 62 (a) CV OF Mo(IV) IN 0.4 MELT

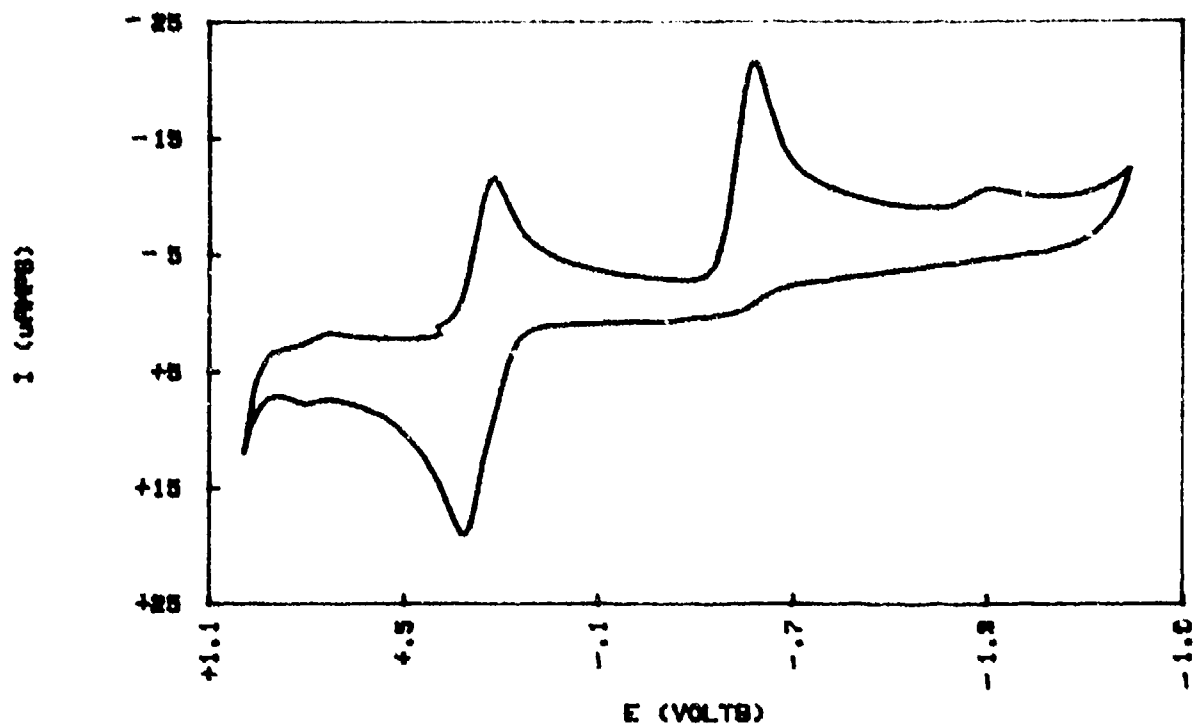


FIG 62 (b) CV OF Mo(IV) IN 0.6 MELT

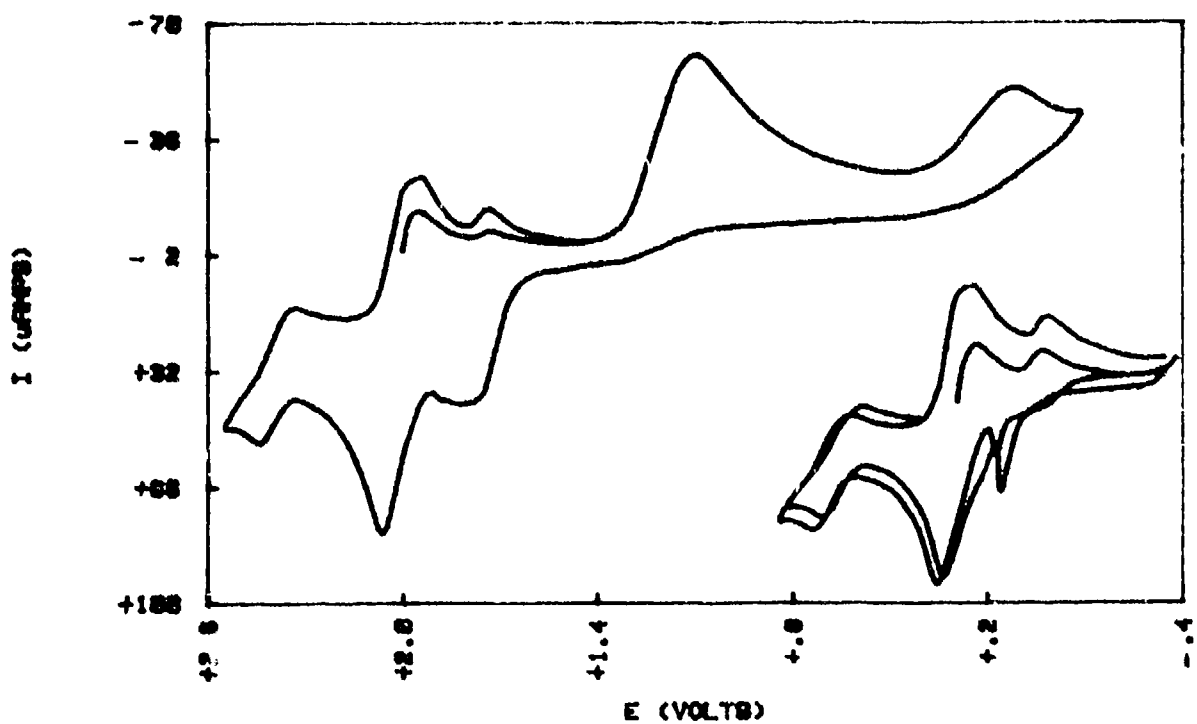


FIG 63 (a) CV OF Mo(V) IN 8.4 MELT

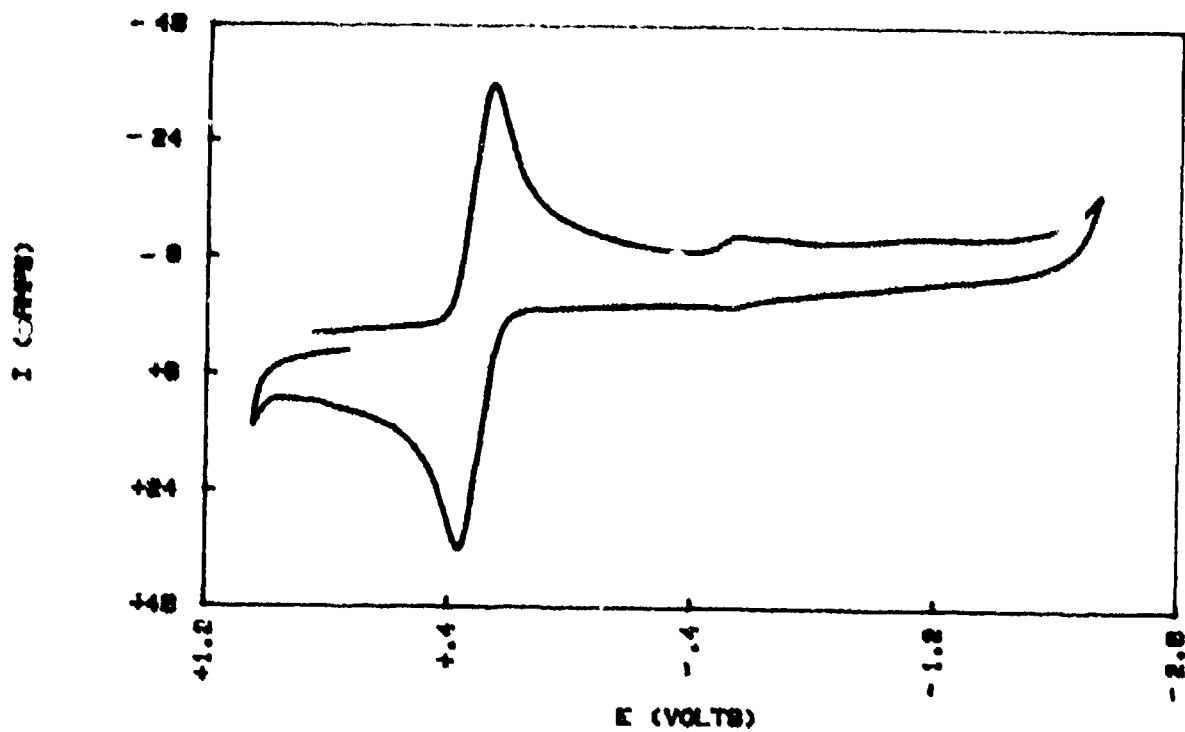


FIG 63 (b) CV OF Mo(V) IN 8.8 MELT

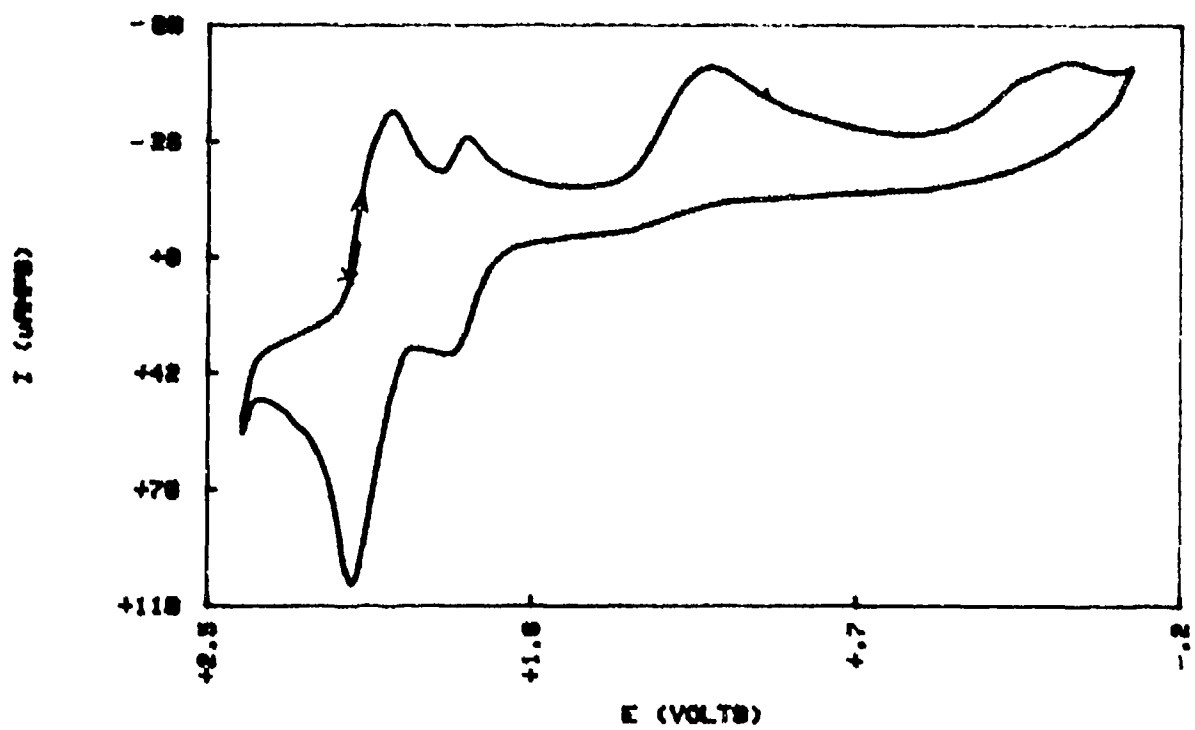


FIG 64 (a) CV OF oxide-free Mo(V) IN 0.6 MELT

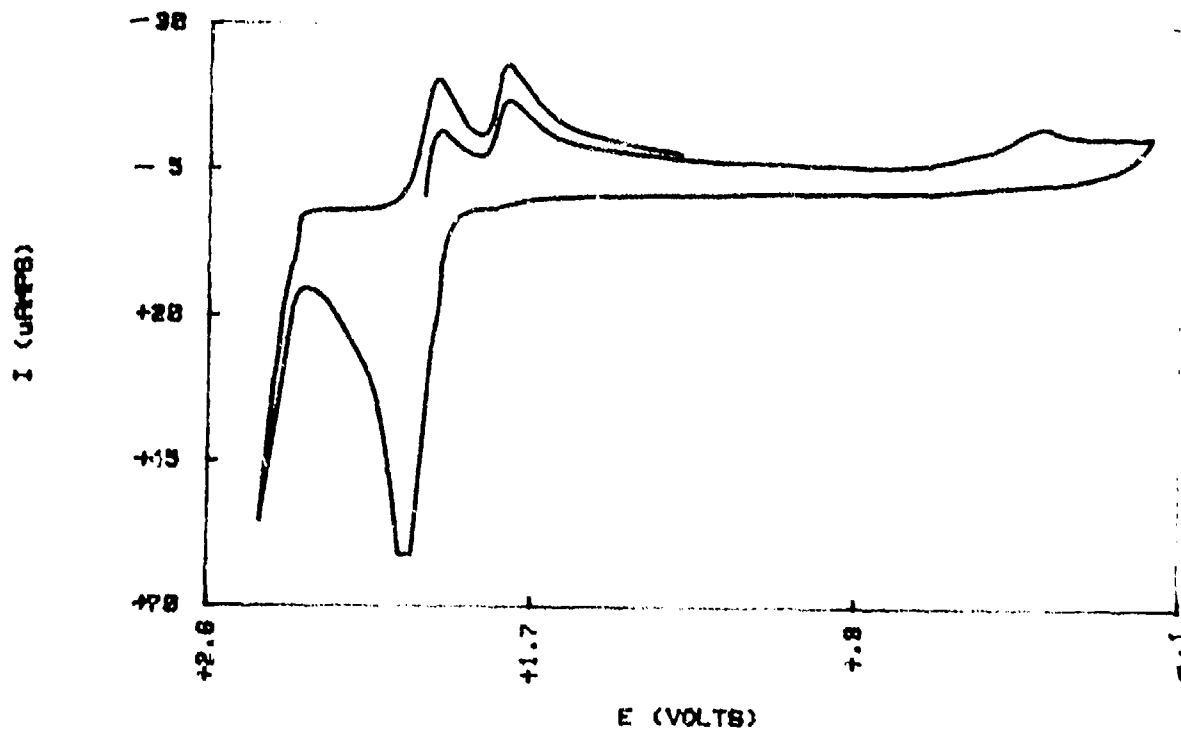


FIG 64 (b) CV OF Mo(V) IN 0.6 MELT

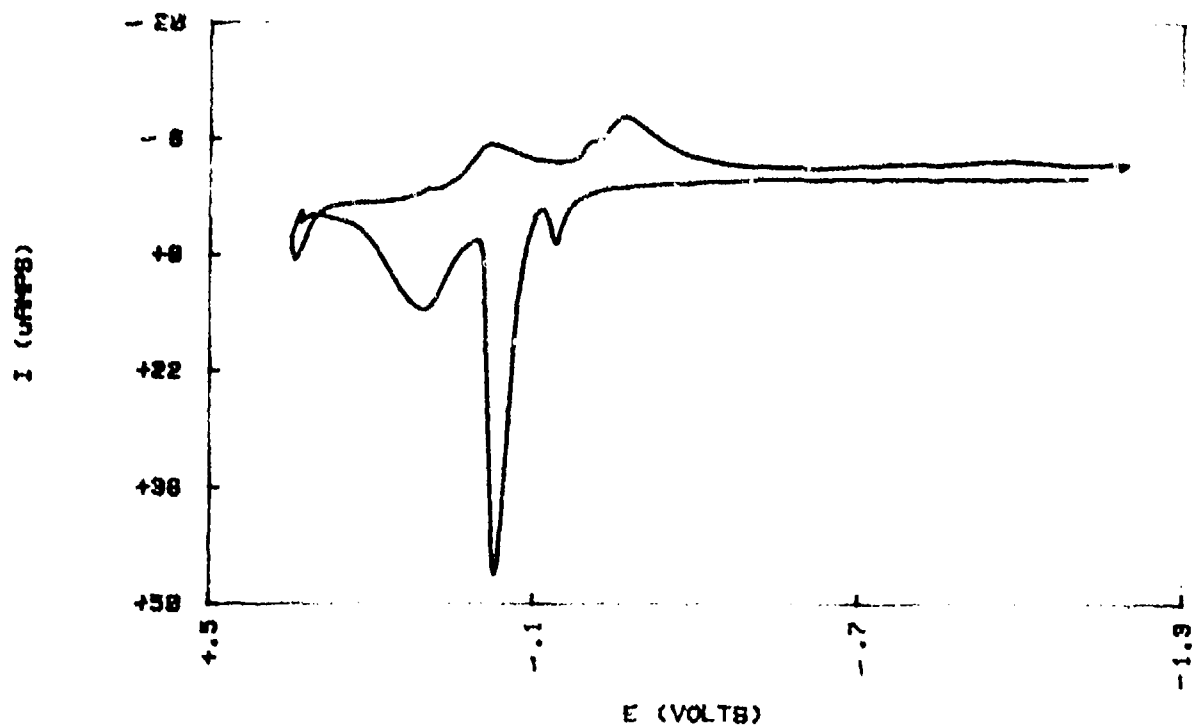


FIG 65 (a) CV OF Mo(V) IN 0.6 MELT

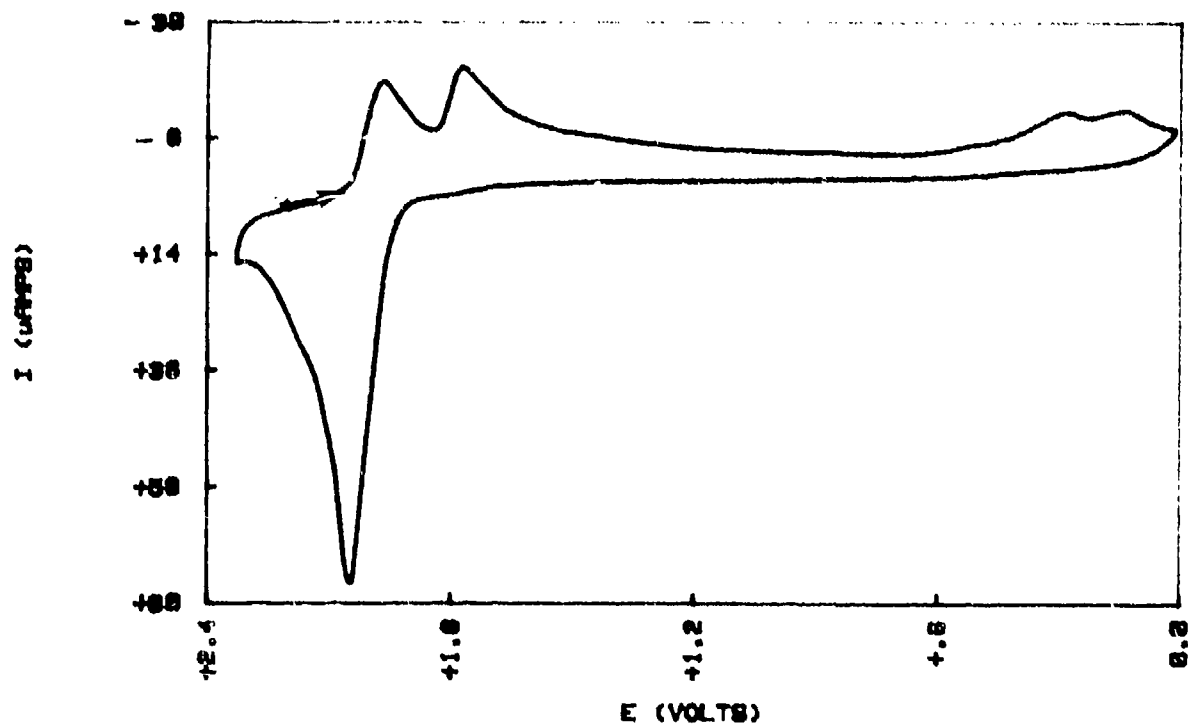


FIG 65 (b) CV OF Mo(V) IN 0.6 MELT

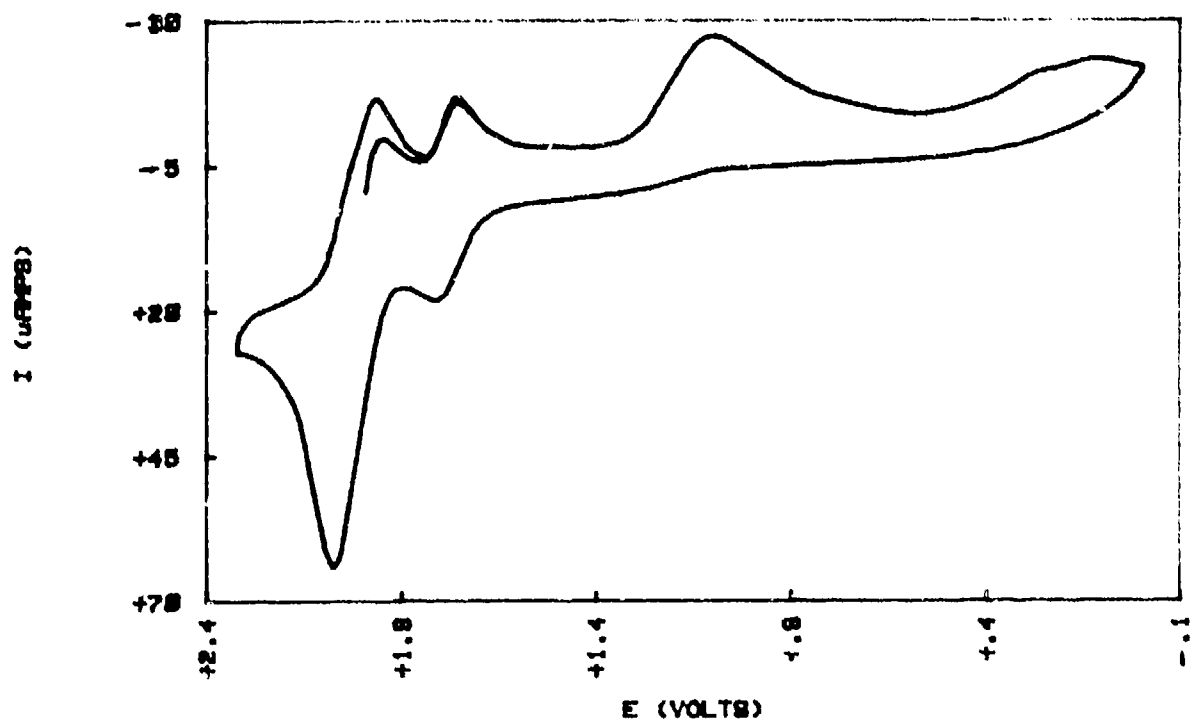


FIG 66 (a) CV OF MoO₂C12 IN 0.4 MELT

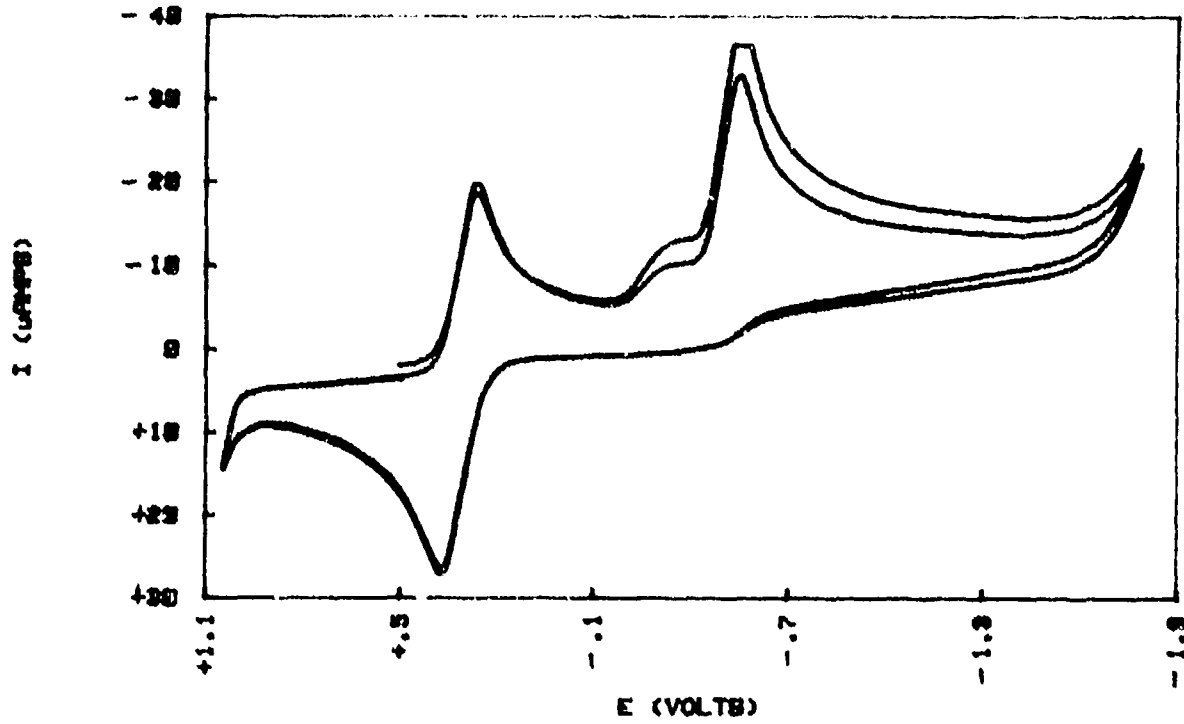


FIG 66 (b) CV OF MoO₂C12 IN 0.6 MELT

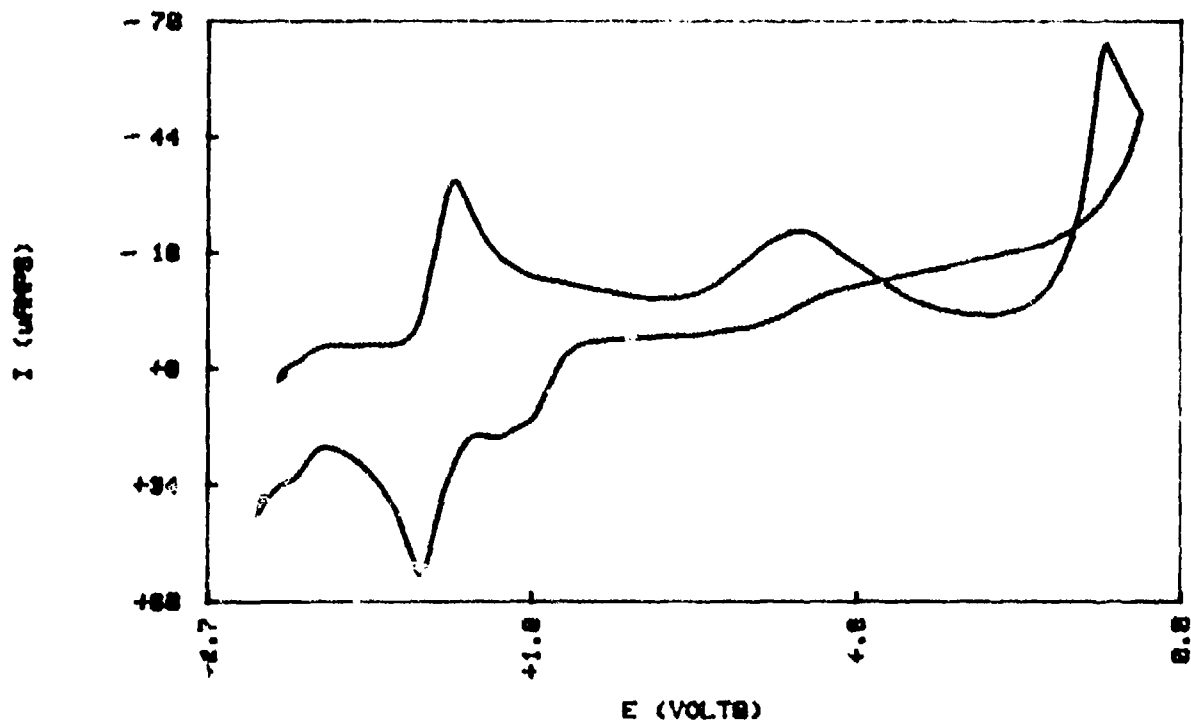


FIG 67 (a) CV OF MoO₂Cl₂ IN B.4 MELT

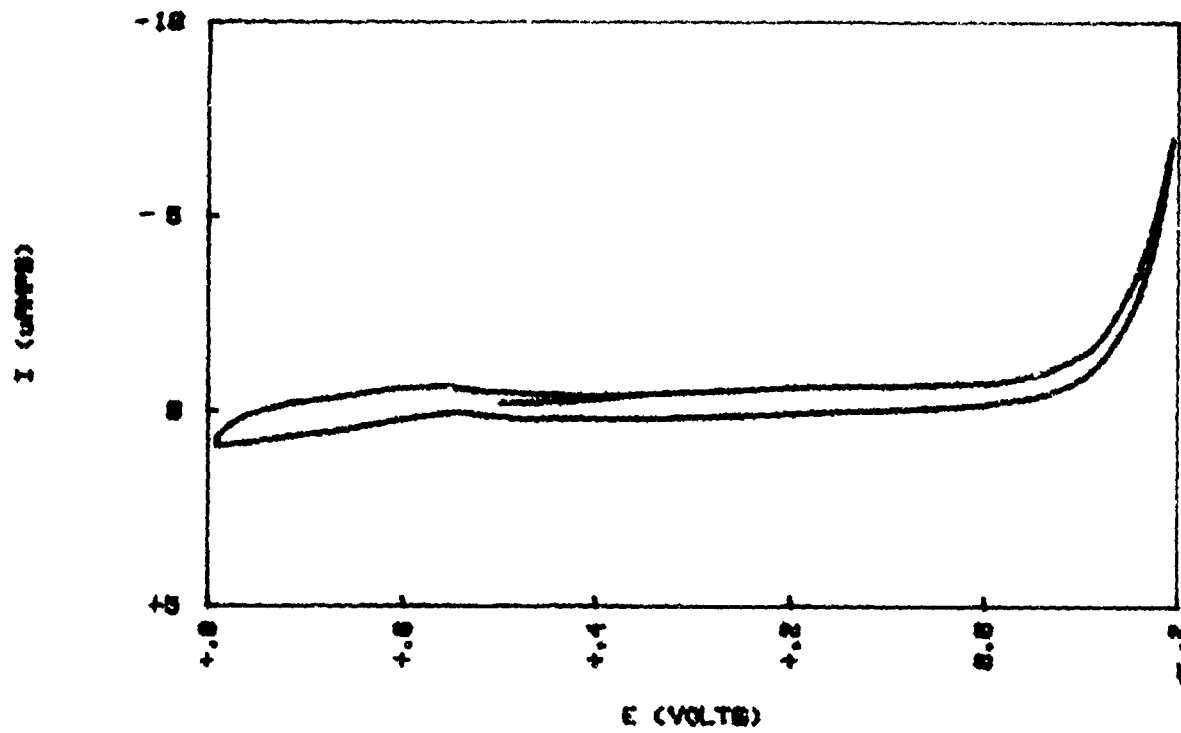


FIG 67 (b) CV OF MoO₂Cl₂ IN B.4 MELT

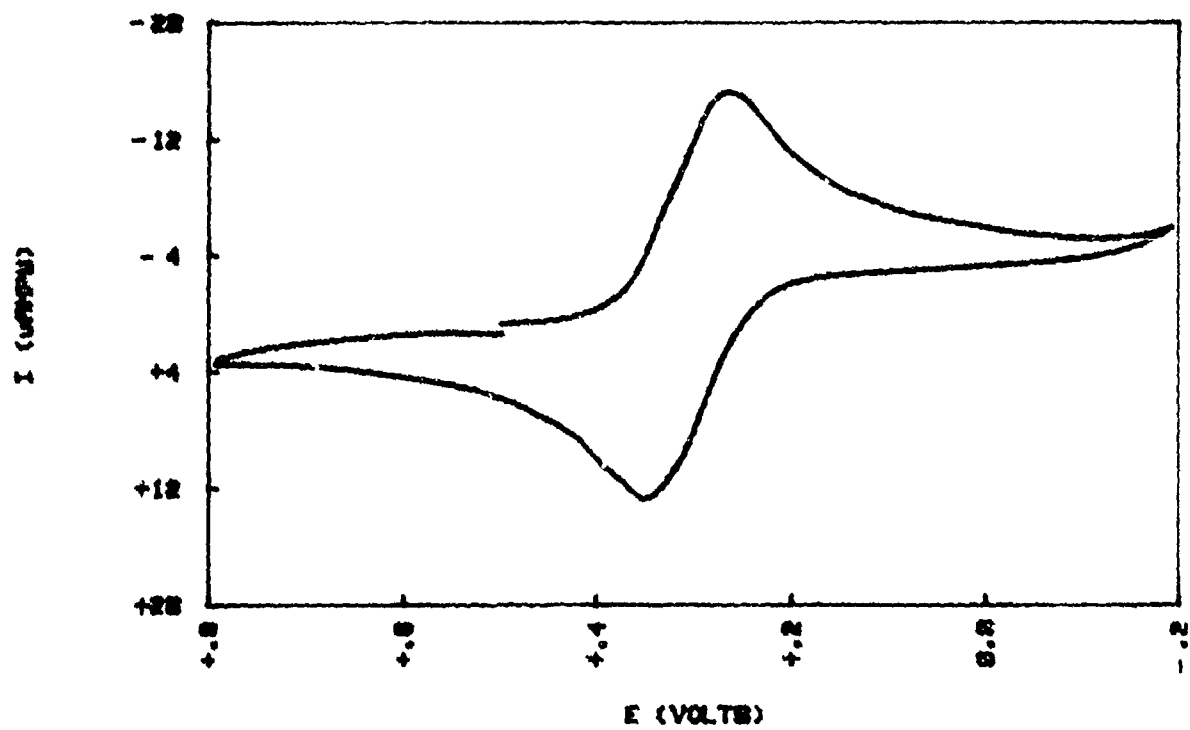


FIG 68 (a) CV OF MoO_2Cl_2 IN 0.6 MELT

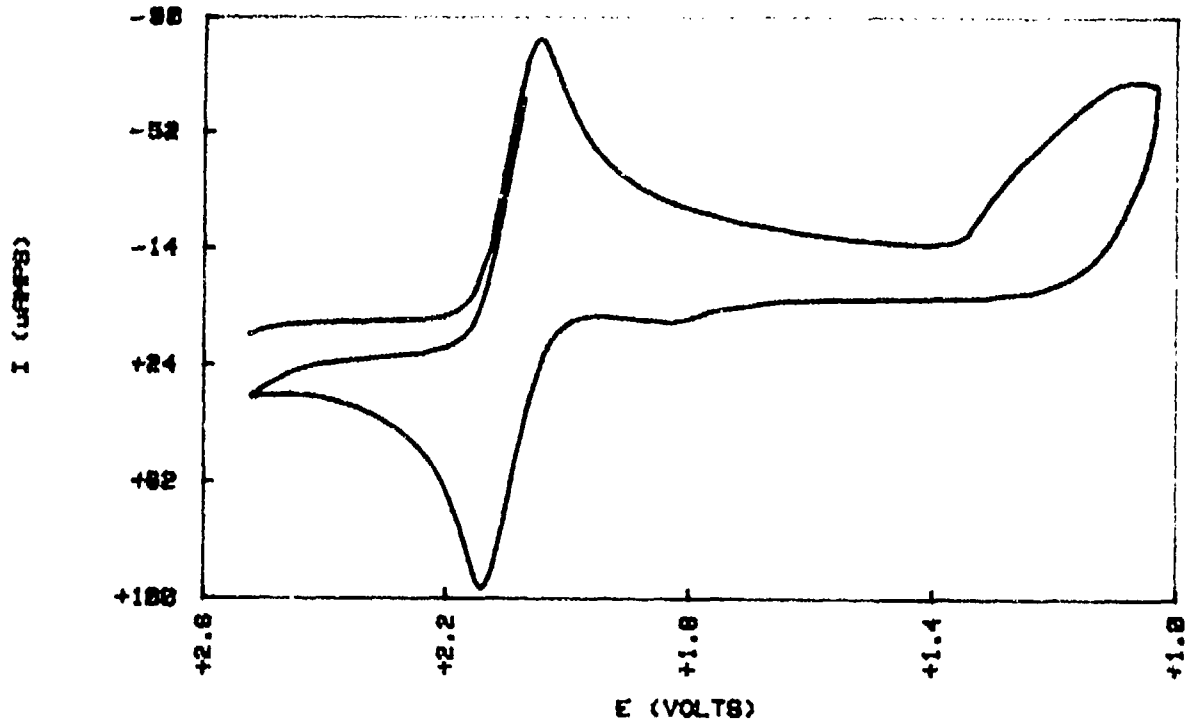


FIG 68 (b) CV OF MoO_2Cl_2 IN 0.6 MELT

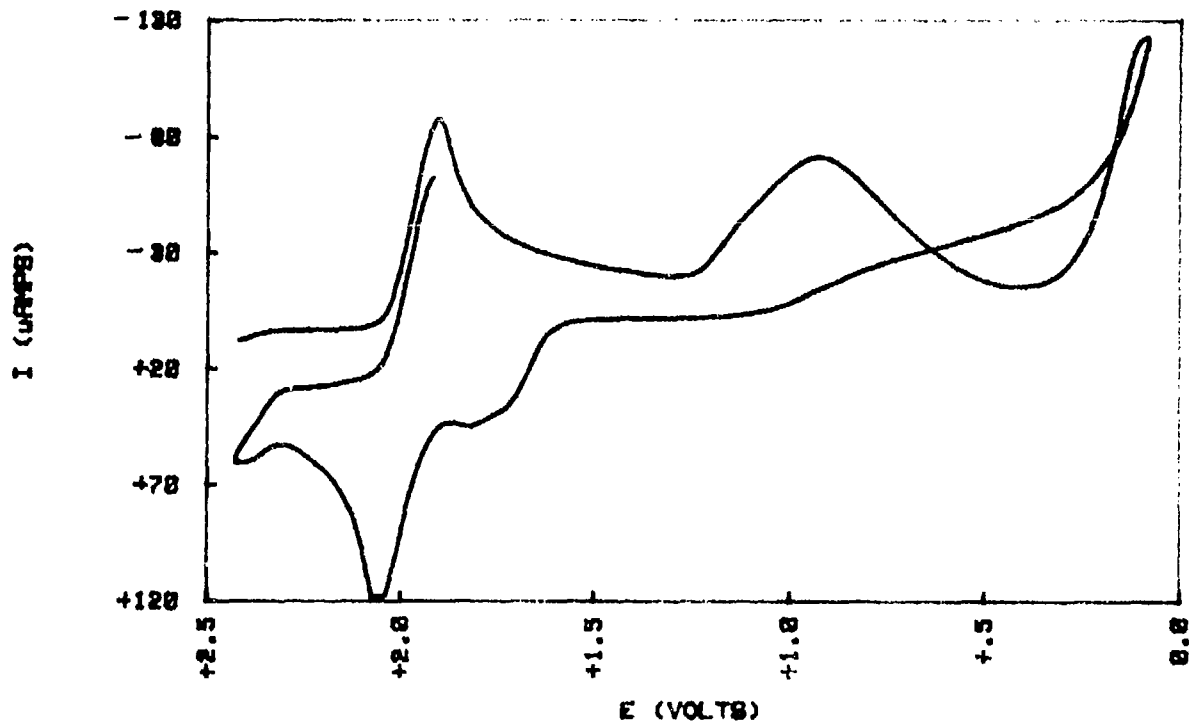


FIG 69 (a) CV OF Et4N MeCl8 IN 0.4 MELT

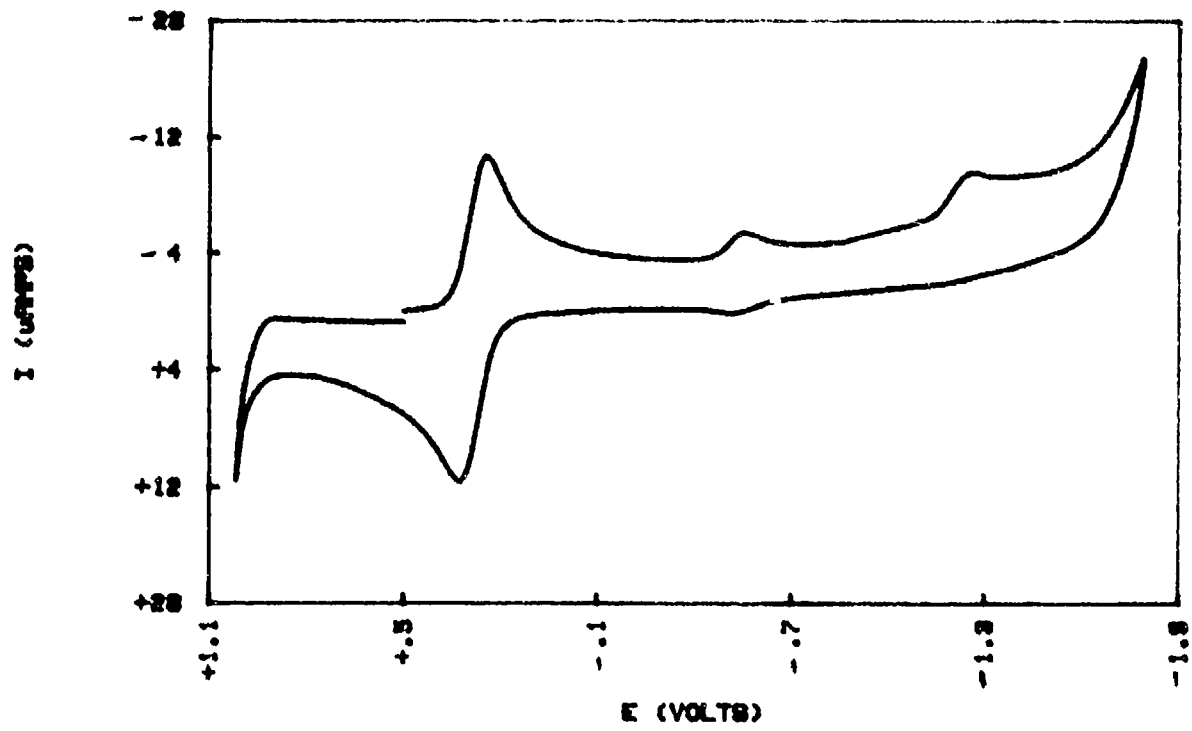


FIG 69 (b) CV OF Et4N MeCl8 IN 0.6 MELT

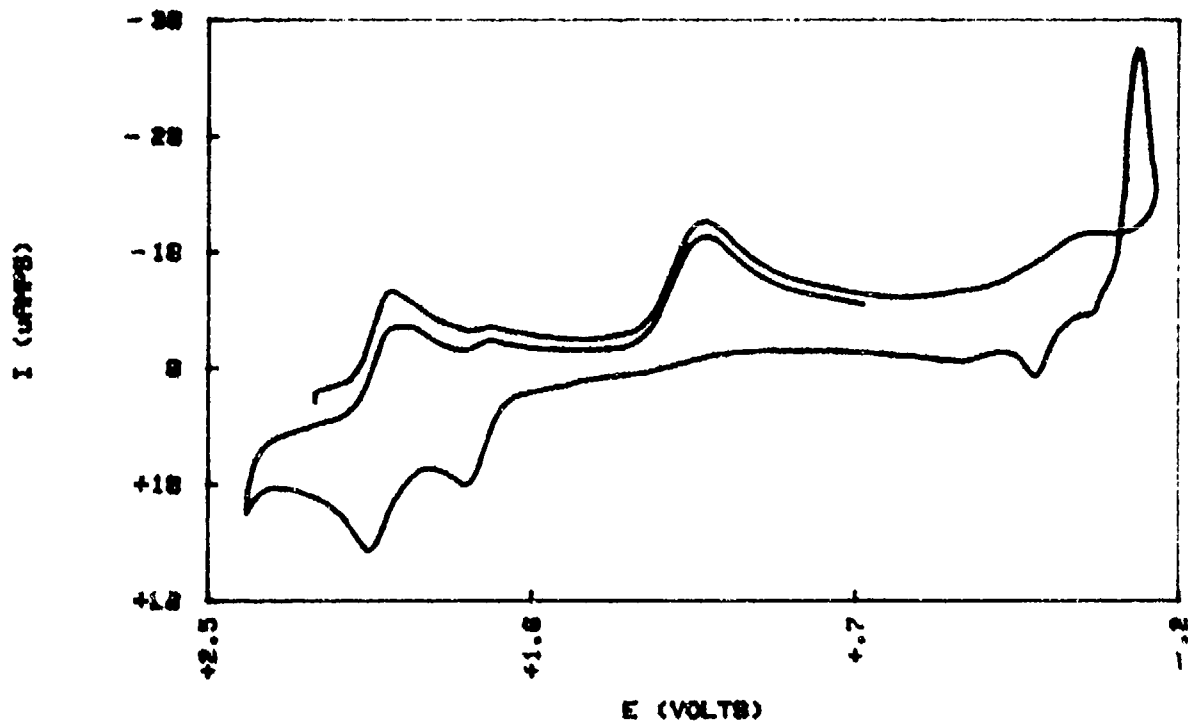


FIG 70 (a) CV OF Et₄N MoCl₆ IN 0.8 MELT

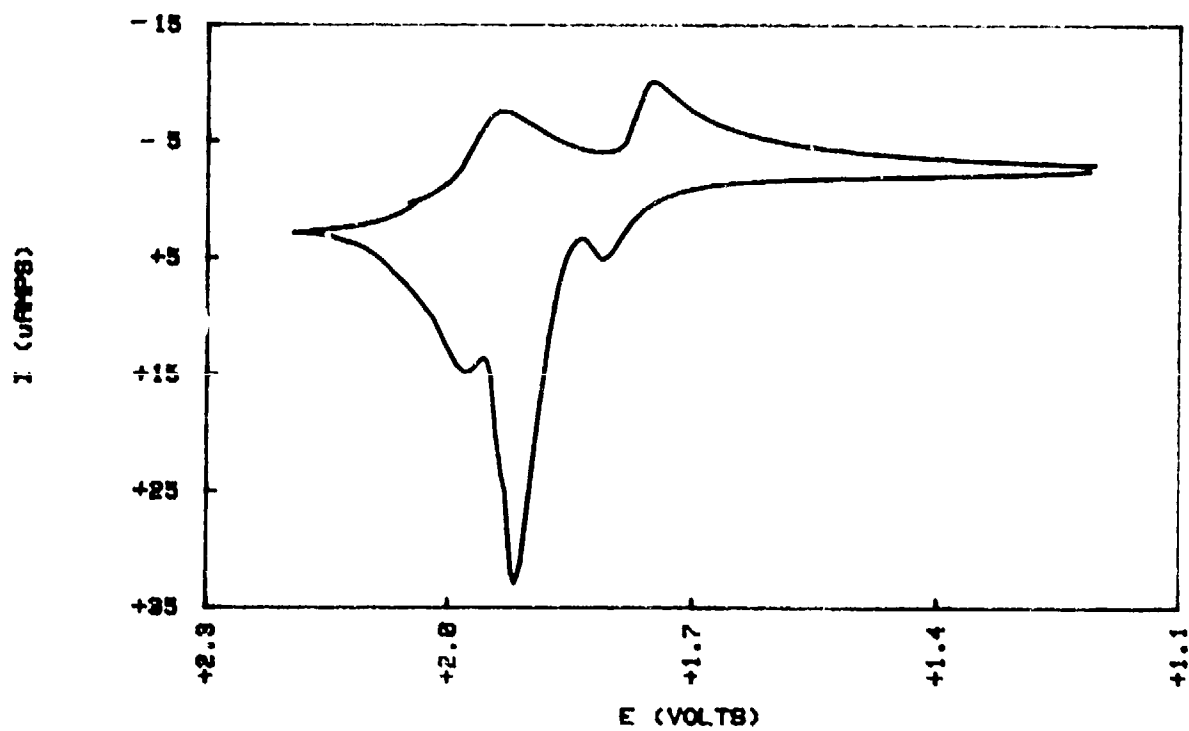


FIG 70 (b) CV OF Et₄N MoCl₆ IN 0.6 MELT

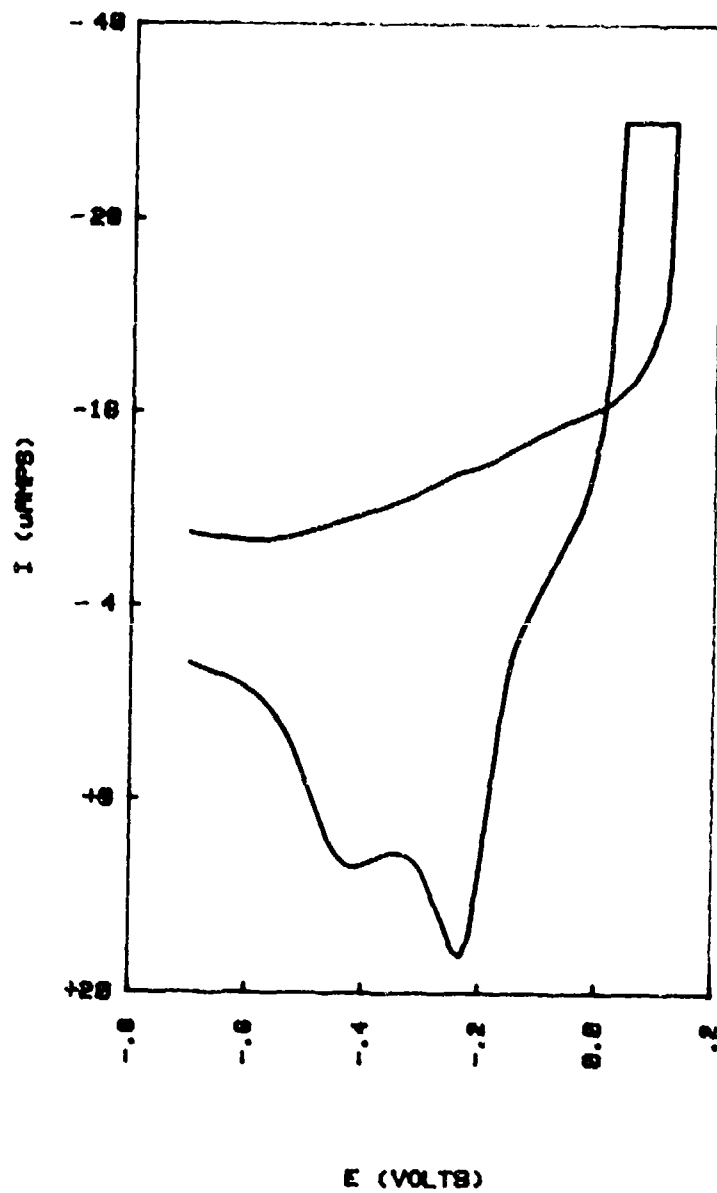


FIG 71 (a) CV OF Ni(II) IN 8.4 MELT

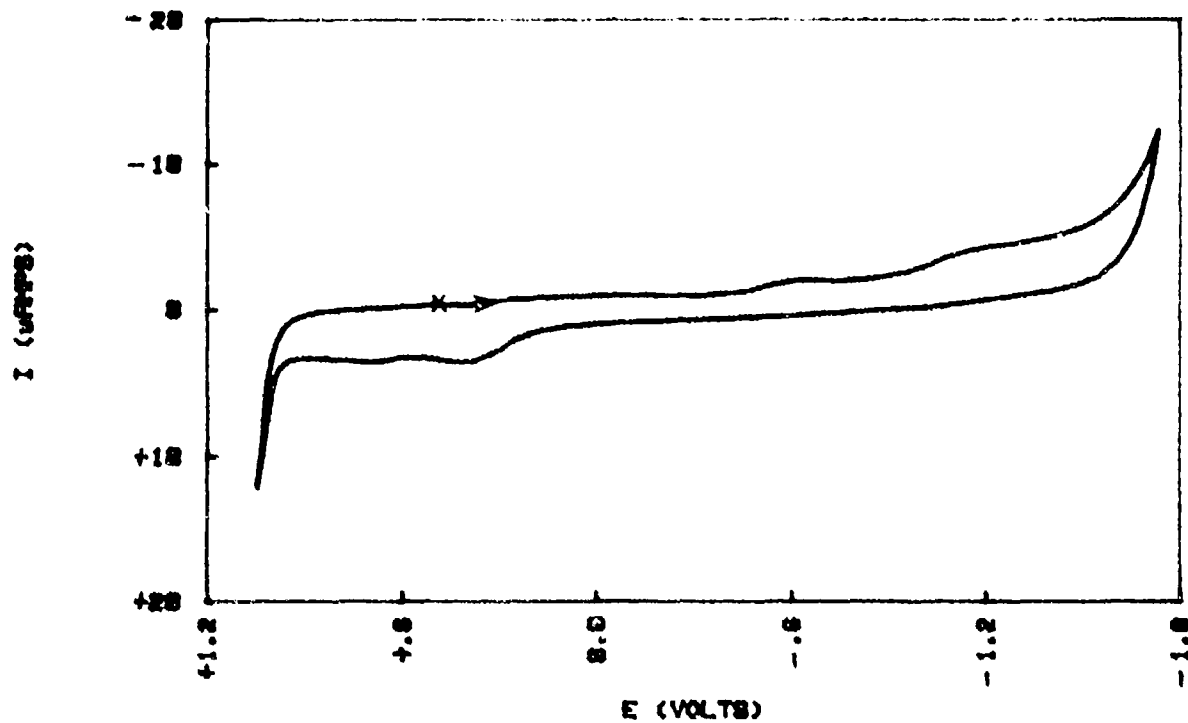


FIG 71 (b) CV OF Ni(II) IN 8.6 MELT

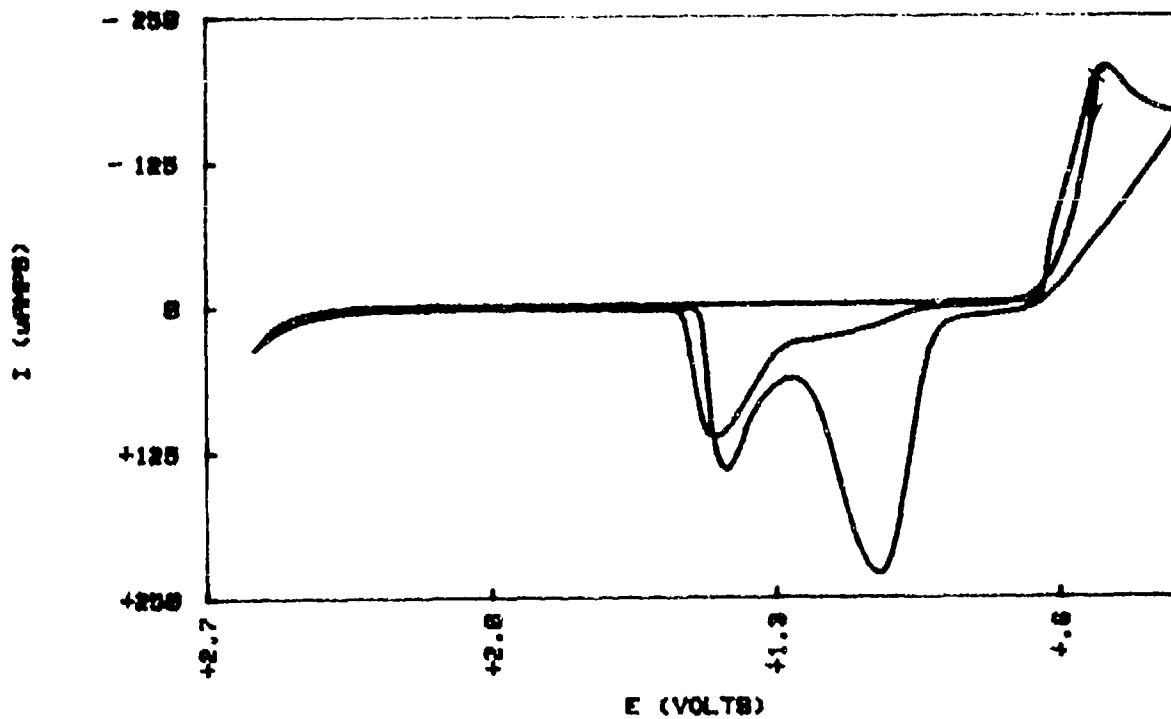


FIG 72 (a) CV OF Pb(II) IN 8.4 MELT

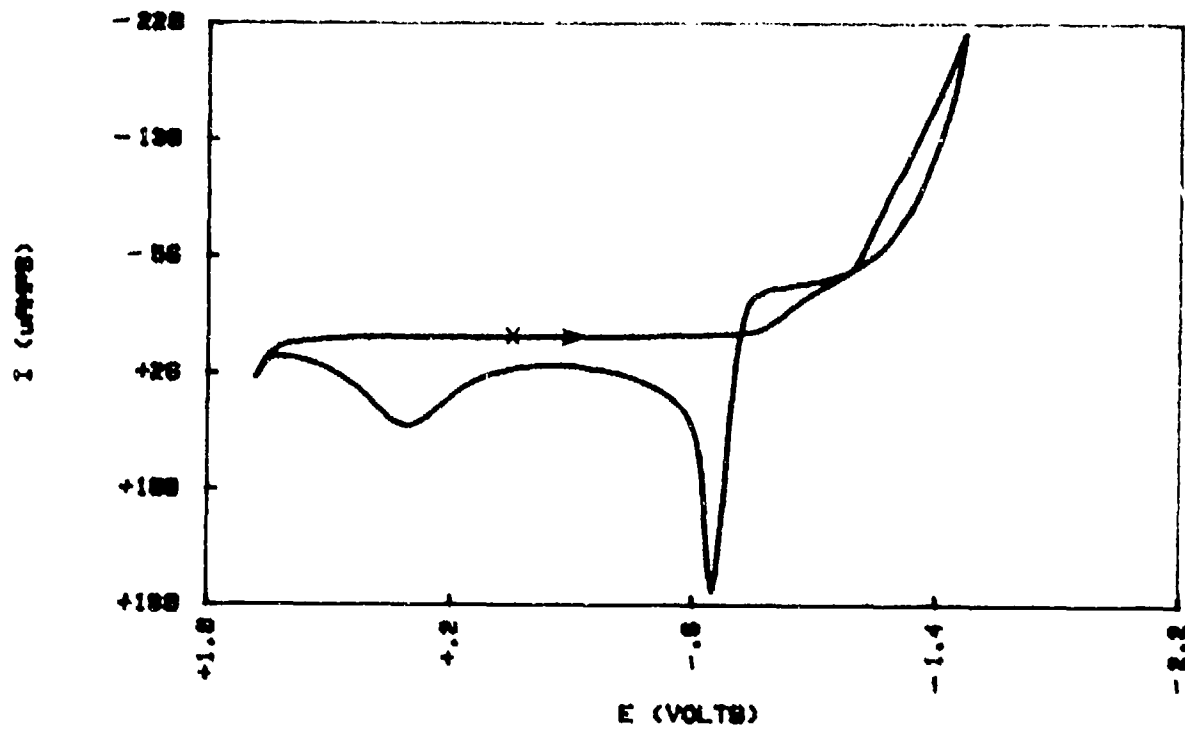


FIG 72 (b) CV OF Pb(II) IN 8.4 MELT

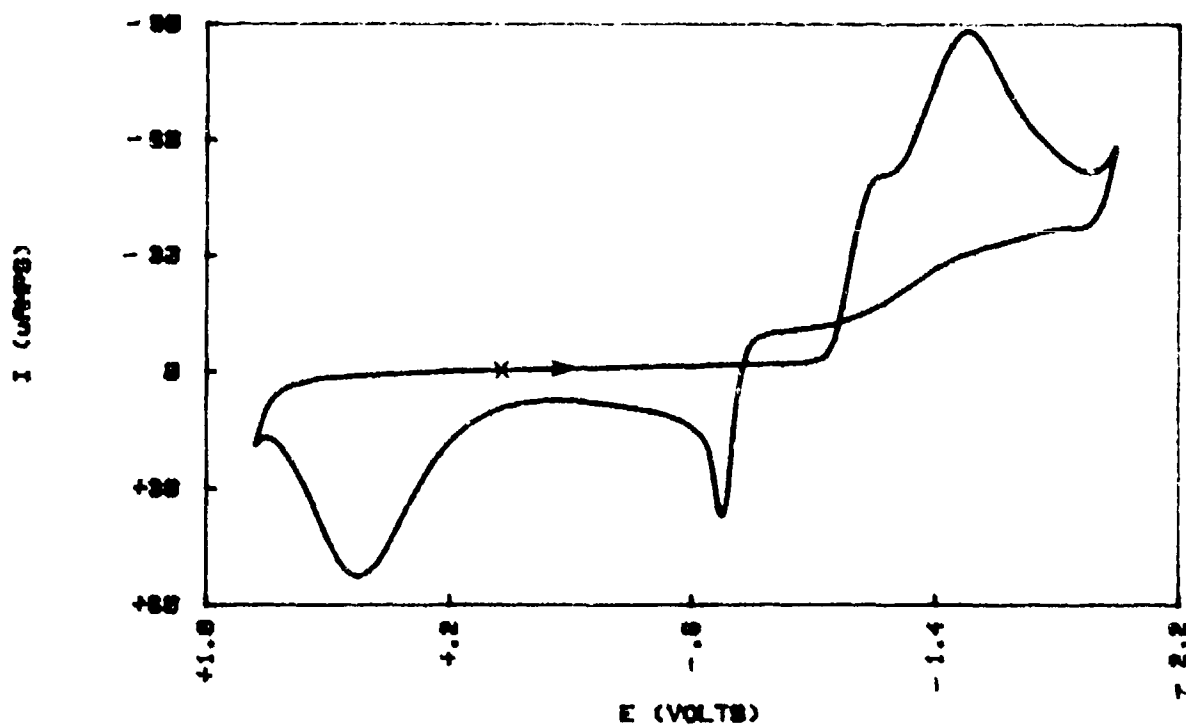


FIG 73(a) CV OF SULFUR IN 0.4 MELT

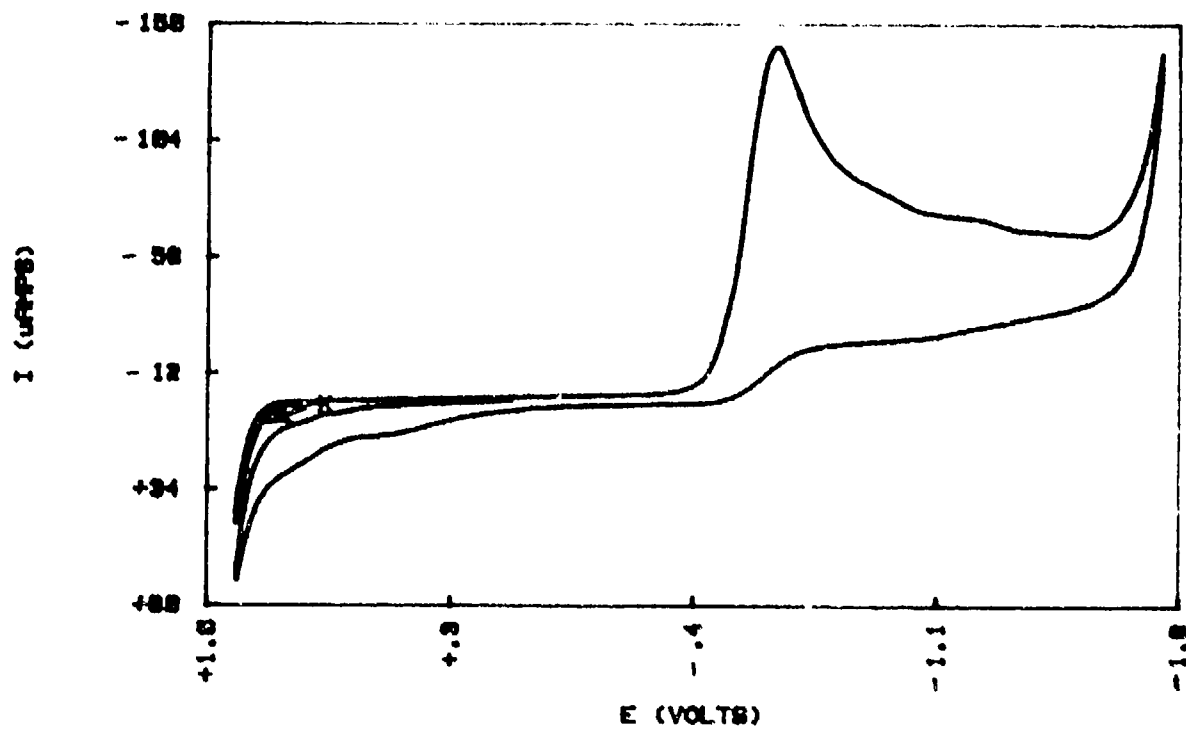


FIG 73(b) CV OF SULFUR IN 0.6 MELT

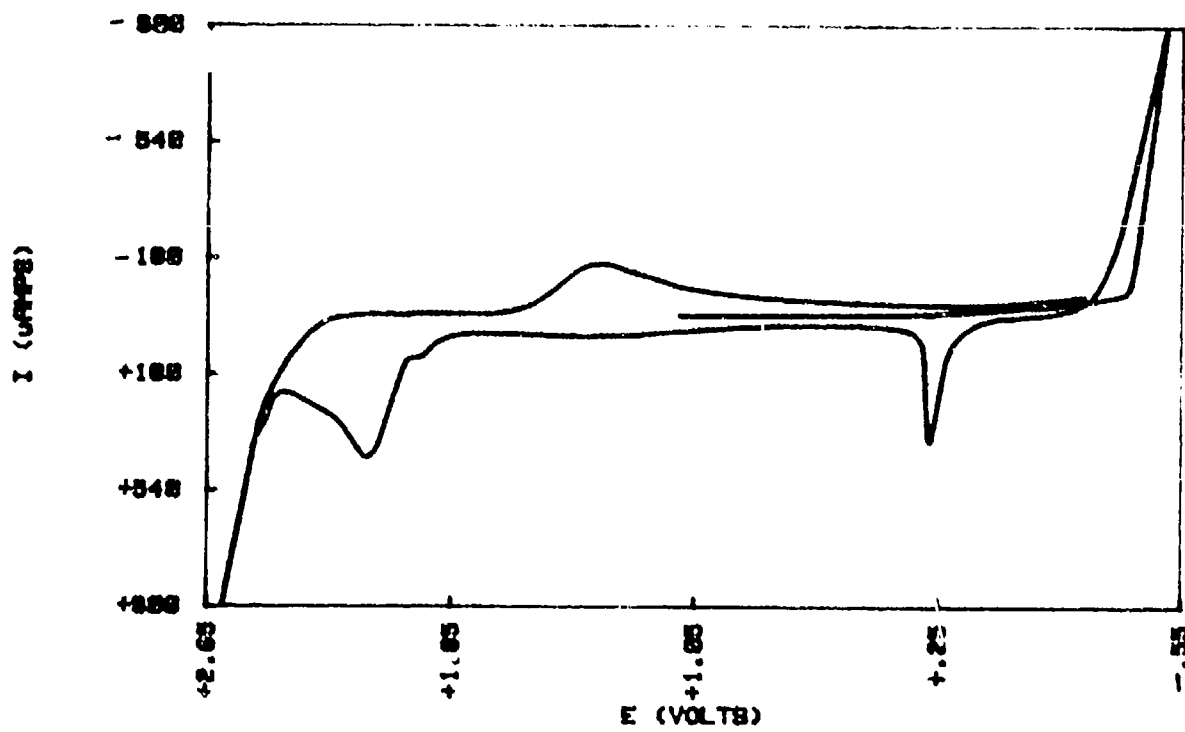


FIG 74 (a) CV OF SULFER IN 0.5 MELT

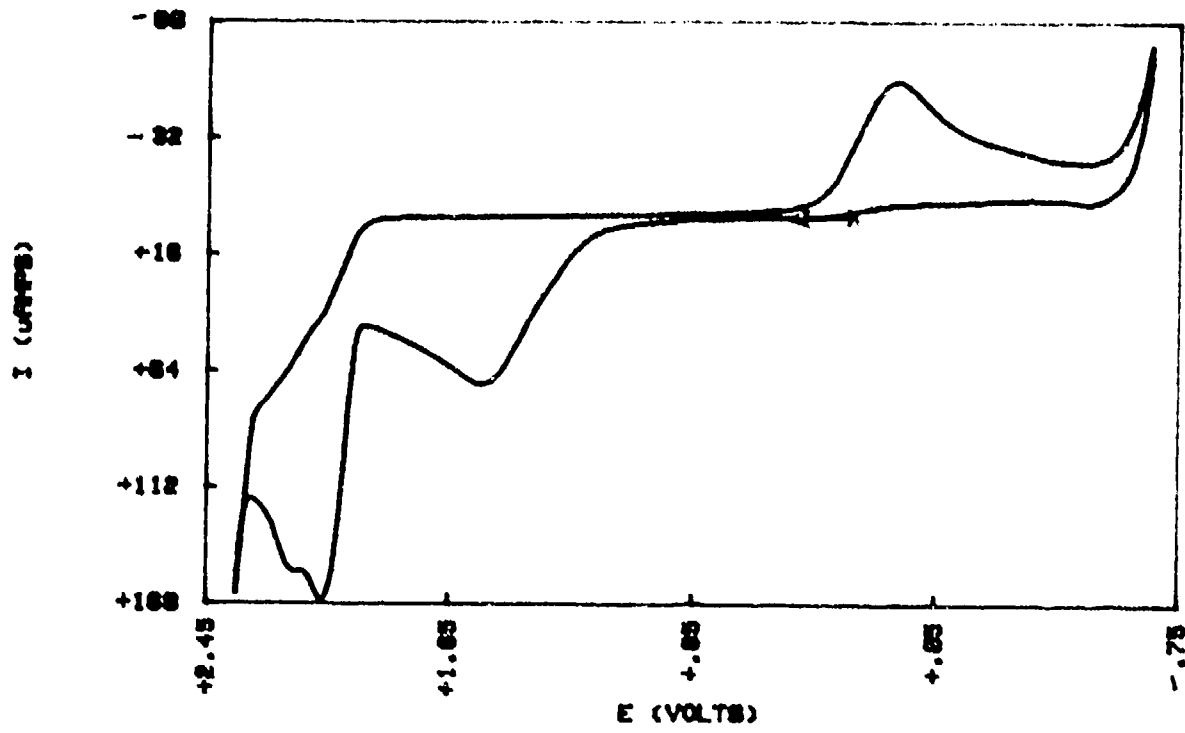


FIG 74 (b) CV OF 82C12 IN 0.5 MELT

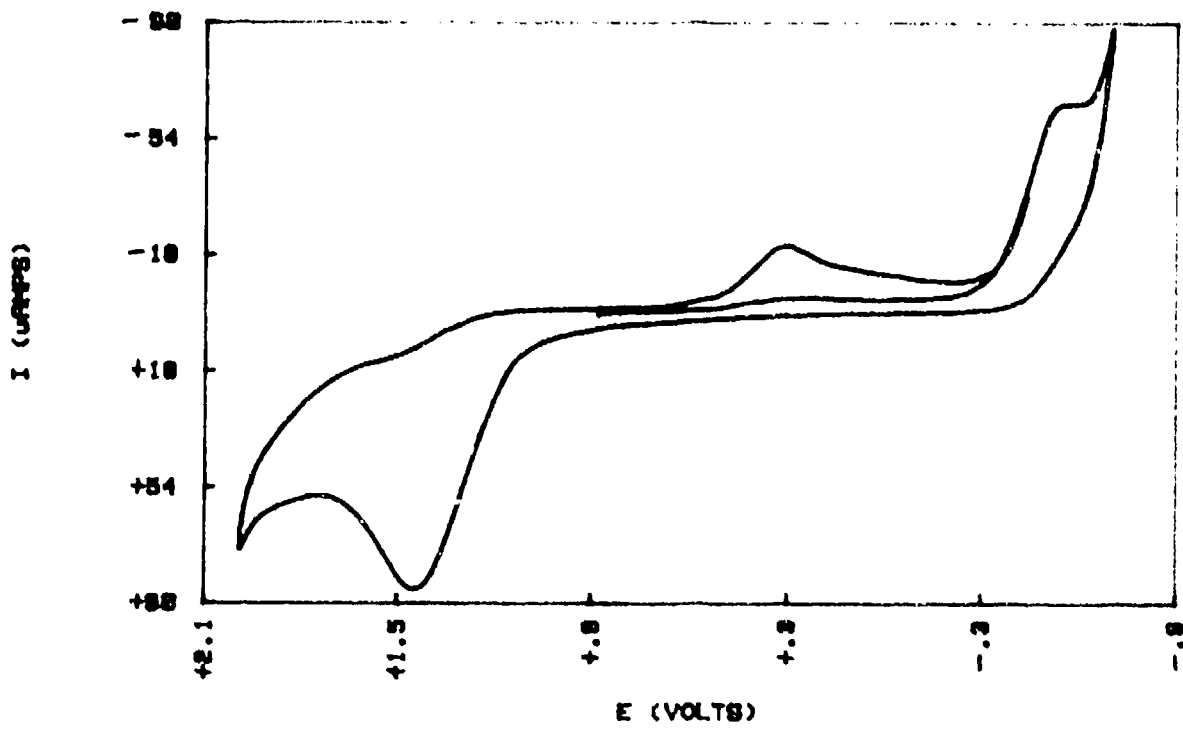


FIG 75 (a) CV OF S2C12 IN 8.4 MELT

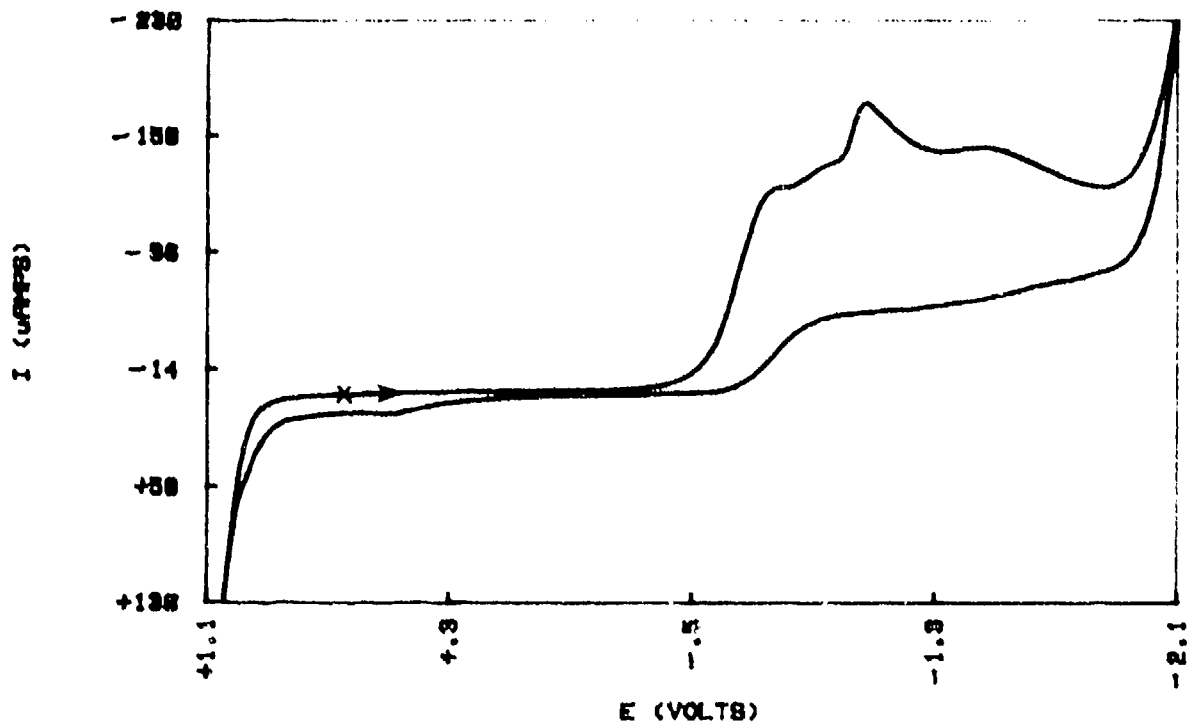


FIG 75 (b) CV OF S2C12 IN 8.8 MELT

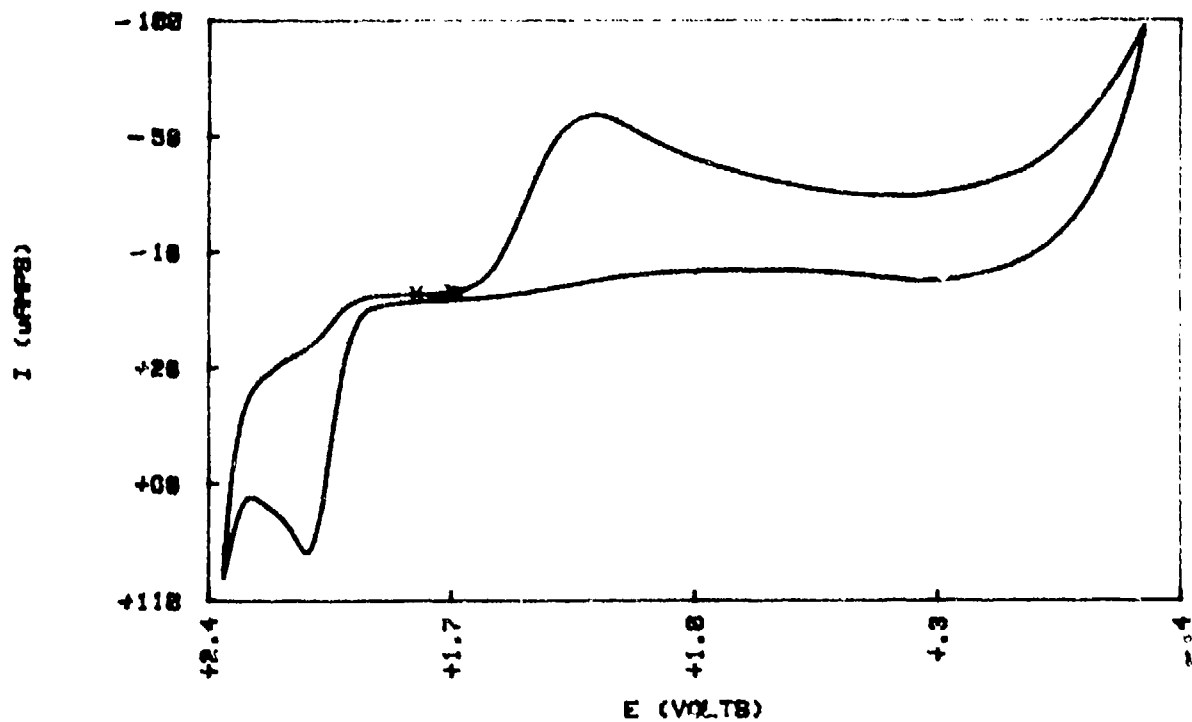


FIG 76 CV OF S2C12 IN 0.6 MELT

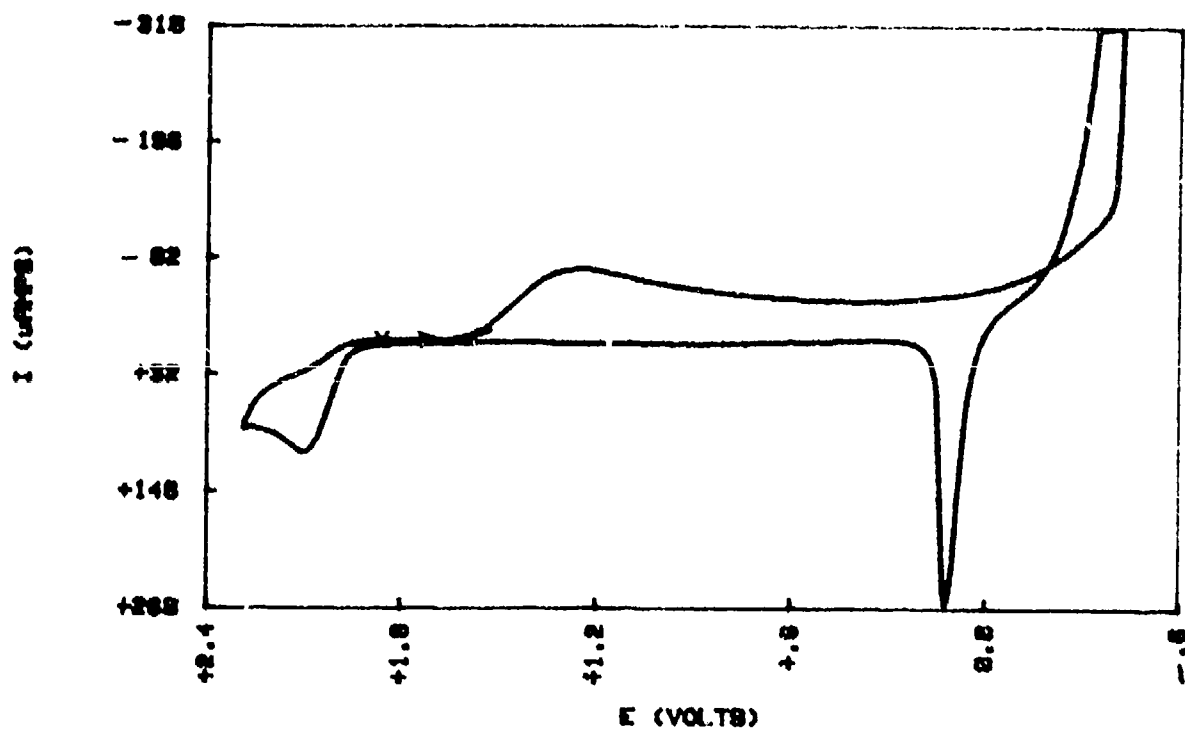


FIG 77 CV OF Sn(II) IN 0.4 MELT

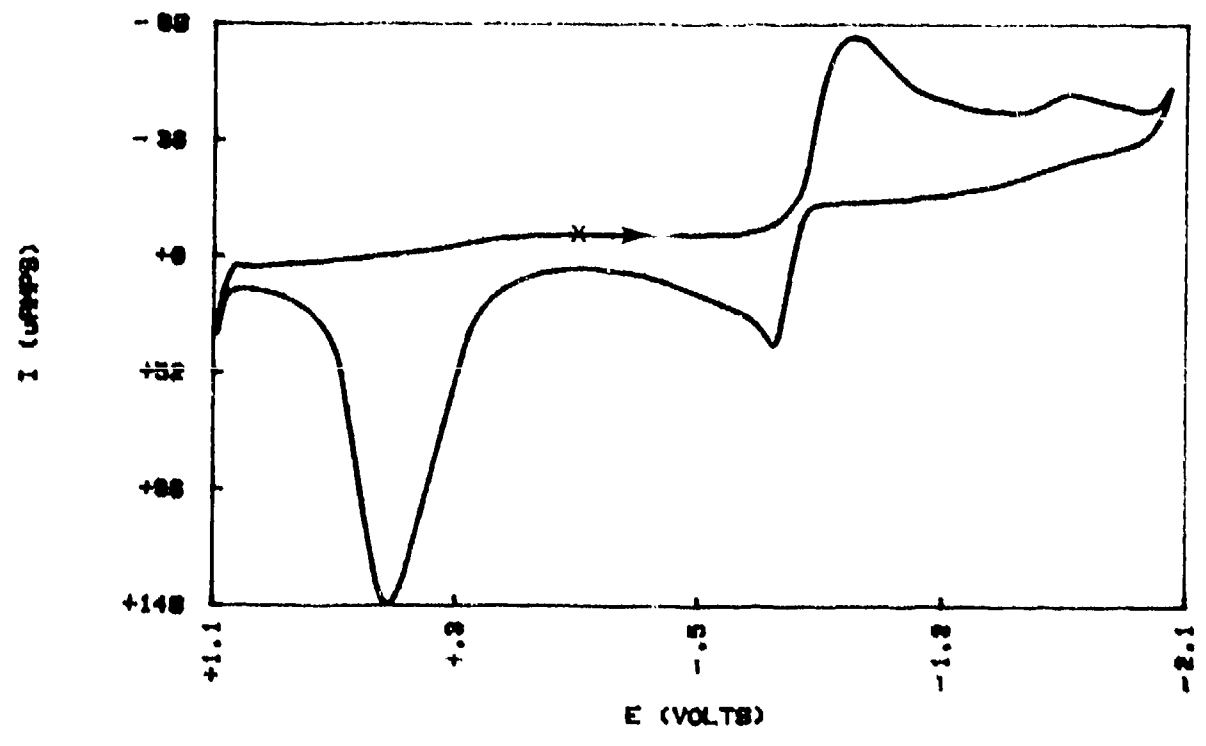


FIG 78 (a) CV OF Ta(V) IN 8.4 MELT

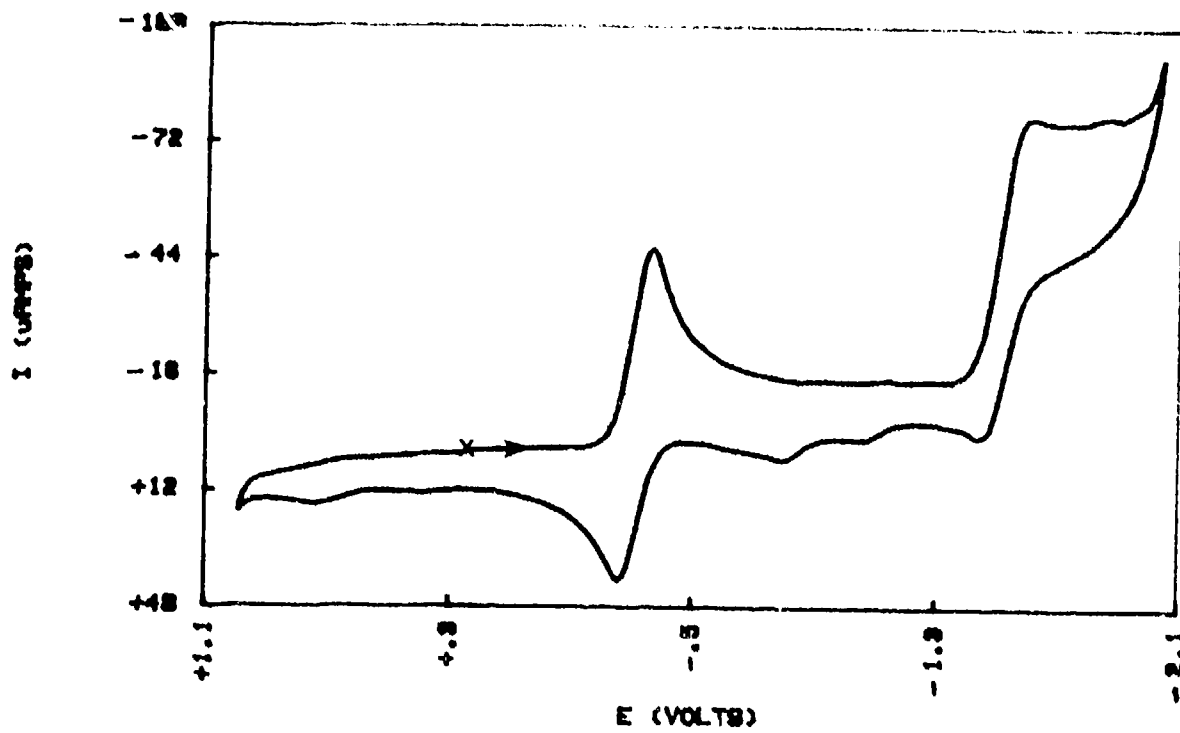


FIG 78 (b) CV OF Ta(V) IN 8.8 MELT

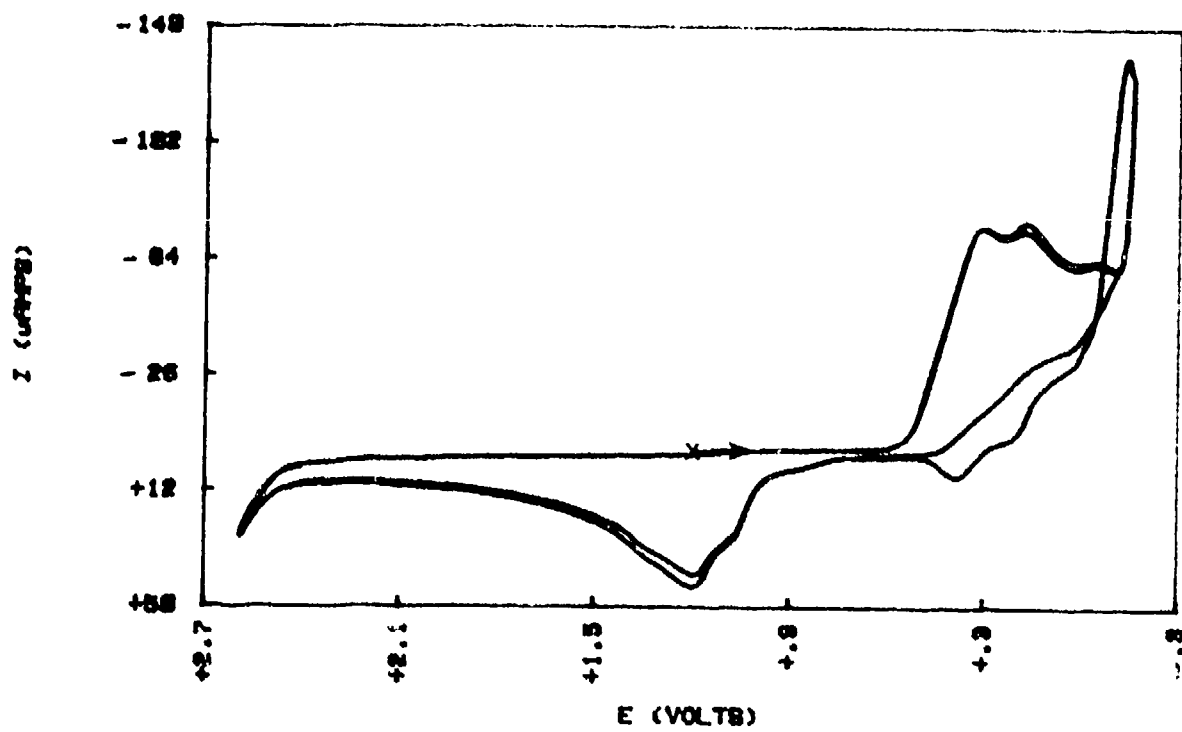


FIG 79 (a) CV OF Tl(IV) IN 0.4 MELT

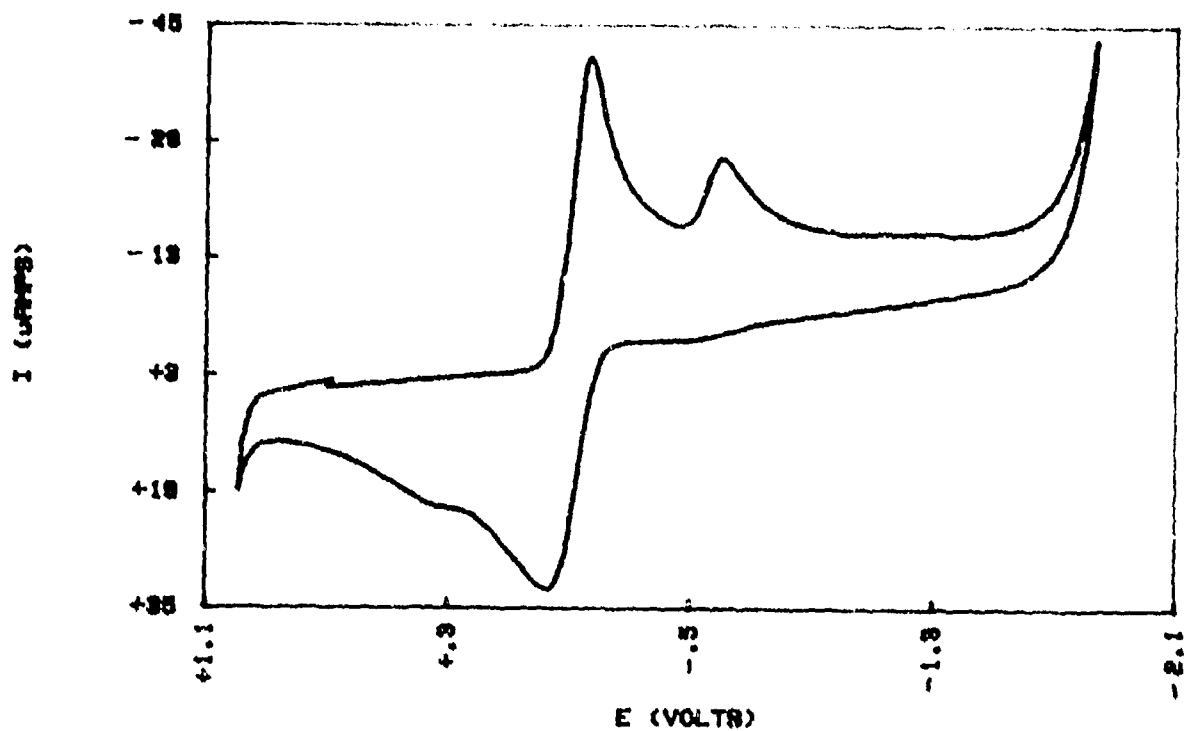


FIG 79 (b) CV OF Tl(IV) IN 0.8 MELT

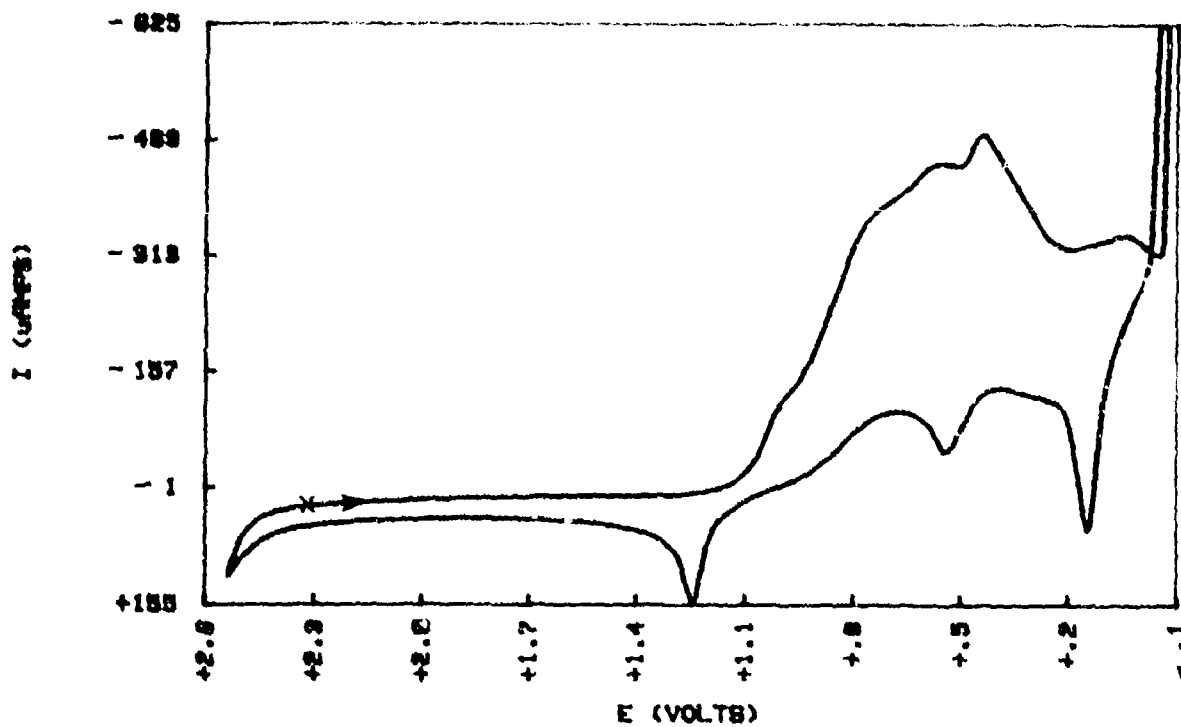


FIG 80 CV OF T1(IV) IN DMF

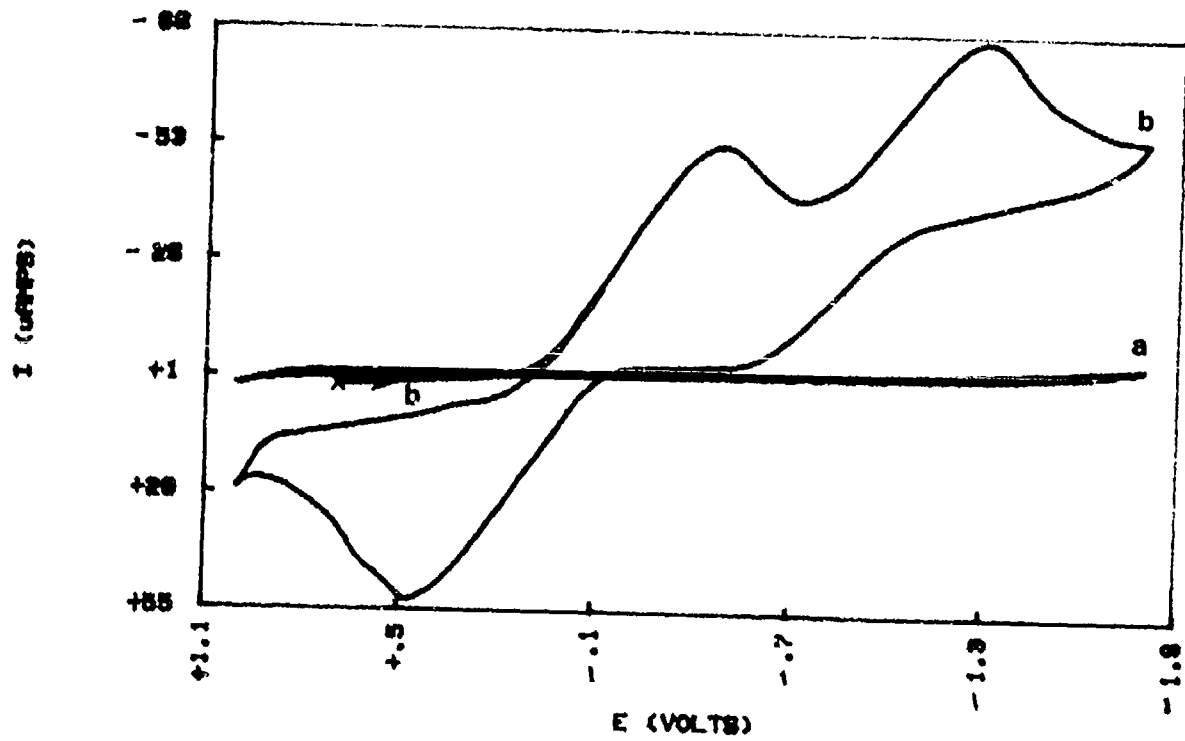


FIG 81 (a) CV OF W(VI) IN 8.4 MELT

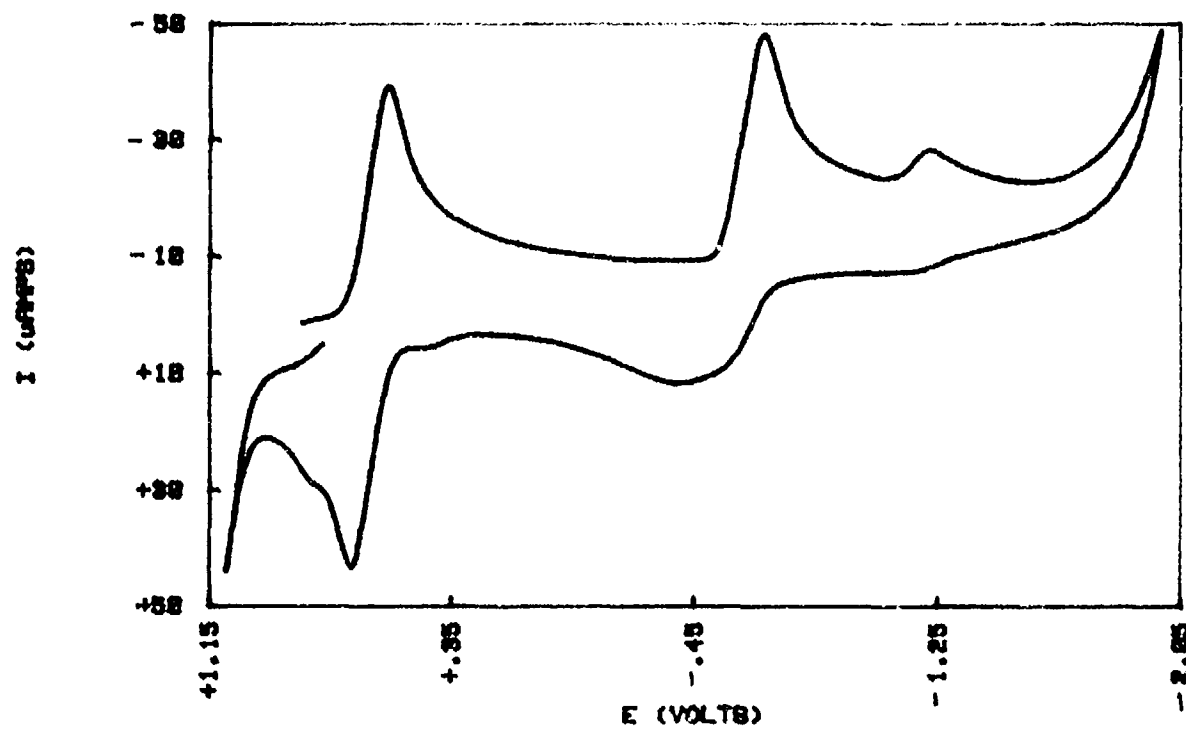


FIG 81 (b) CV OF W(VI) IN 8.8 MELT

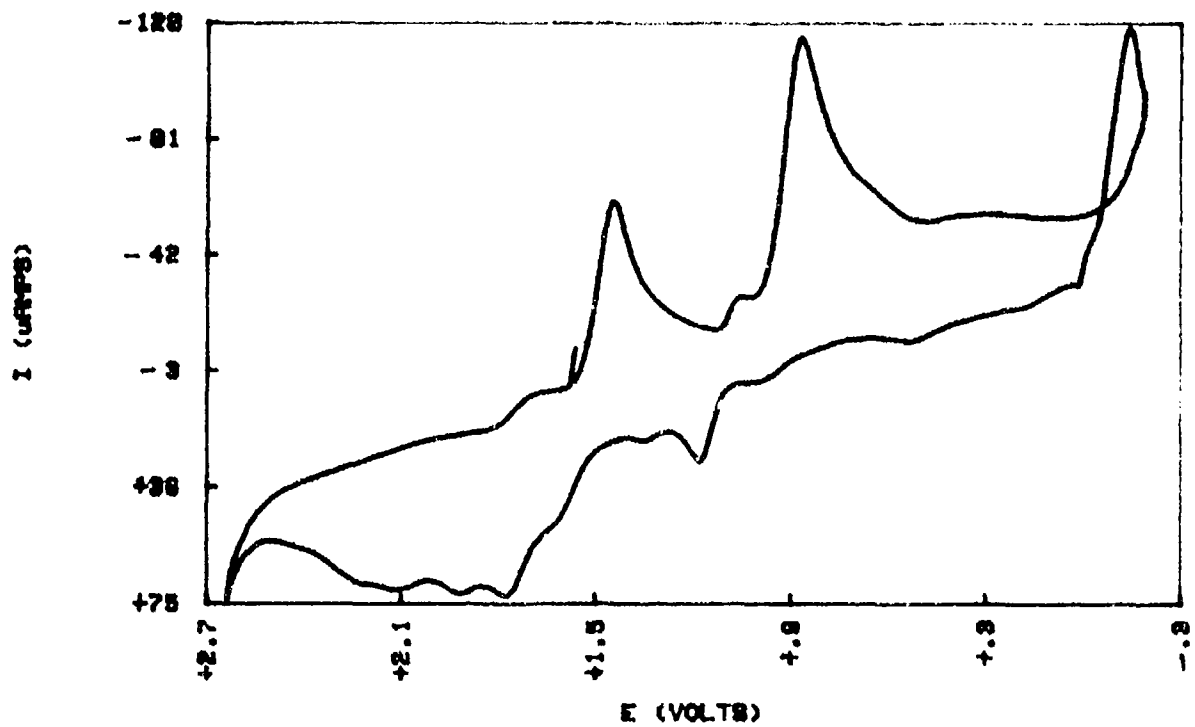


FIG 82 CV OF Zn(II) IN 8.4 MELT

